THE MECHANISM OF TRIPLET ENERGY TRANSFER IN SOLUTION: THE QUENCHING OF EXCITED-STATE BENZOPHENONE BY TRANSITION-METAL CHELATES

Thesis by

Robert Paul Foss

In Partial Fulfillment of the Requirements

For the Degree of

Doctor of Philosophy

California Institute of Technology

Pasadena, California

1963

For Nancy
and little Sandra Ellen

ACKNOWLEDGEMENTS

I wish to express my sincere gratitude to my research director, Dr. George S. Hammond, who has done his best to guide me in my work here at Caltech. His criticisms and advice have contributed greatly to my understanding of my research problem and to chemistry in general. It has been a great inspiration for me to work under him.

To the California Institute of Technology for granting me a tuition scholarship and a teaching assistantship for the years 1958-1962, I am very grateful.

I am very thankful to Dr. Chin-Hua Wu for supplying the "extra pure" chelates which were used in this study.

I also wish to thank the members of the Hammond research group for their assistance and criticisms of the present work. They were a great group of people with whom to work.

I would like to express my appreciation to Mrs. Lucille Lozoya, who spent many long hours and suffered many frustrations in the typing of this thesis.

I am deeply indebted to my parents for their faith, confidence and occasional bit of prodding which helped me in reaching this present goal.

Finally, I would like to express my thanks to my wife, Helen. Unfortunately, there are and will never be any words which can do this adequately.

ABSTRACT

The quenching of triplet-state benzophenone by transition-metal chelates of acetylacetone, dipivaloylmethane and dibenzoylmethane is studied in detail. Compounds with both diamagnetic and paramagnetic ground state configurations and with square planar and octahedral structural configurations are used in this investigation.

The most extensively studied chelates are the octahedrally complexed acetylacetonate and dipivaloylmethide complexes of iron, chromium, cobalt and aluminum. Detailed molecular orbital calculations considering the π-orbital interaction between the ligand π-orbital system and the d-atomic orbitals centered on the metal atom are performed on these chelates. The calculated spectra of the chelates agree well with the observed.

Quenching experiments show no correlation between the paramagnetic susceptibility of the chelates and their quenching efficiency. Furthermore, no correlation between quenching efficiencies and the energies of the low energy ligand field transitions is observed. A correlation is obtained, however, between the quenching efficiencies of the chelates and the calculated and observed π-π^* transition energies. A steric effect, introduced by the ligands, is observed between corresponding sets of dipivaloylmethide and acetylacetonate chelates. Both the energy correlation and the steric effect may be explained by

a general mechanism for triplet energy transfer in solution which is given in this thesis.

Quenching of singlet benzophenone by the dibenzoylmethide chelates of iron and chromium is also observed. A possible explanation of these results is given.

TABLE OF CONTENTS

TABLE OF CONTENTS (cont'd)

TABLE OF TABLES

TABLE OF FIGURES

TABLE OF FIGURES (Cont'd)

Appendix B

INTRODUCTION

The subject of energy transfer has received much attention in recent years. The mechanism is of considerable interest, not only from an academic point of view, but with respect to the understanding of biological systems. Molecular excited states are responsible for a large variety of chemical reactions. These include reductions, oxidations, isomerizations, additions, polymerizations, and others. In many systems the addition of trace amounts of certain impurities will quench the photochemical reactivity of the system by serving as energy sinks, deactivating the reactive excited molecules. In other systems energy is absorbed by sensitizors, then transferred to different molecular species, which then may undergo a chemical reaction. Thus the importance of understanding the mechanism of energy transfer becomes obvious.

Förster developed a theory for long range energy transfer which he called resonance transfer or inductive resonance (1, 2). His theory predicted that if the fluorescence transition of the donor and the absorption transition in the acceptor were strong electric dipole transitions, and the fluorescence spectrum of the donor overlapped the absorption spectrum of the acceptor, energy transfer could occur over distances which are considerably greater than ordinary molecular

collision diameters. These distances are in the neighborhood of 50 to 150 Angstroms. The efficiency of transfer depends on the degree to which the above conditions are satisfied.

The resonance transfer process is in competition with other modes of deactivation of the excited state. Therefore, if the lifetime of the excited state of the donor is sufficiently short, only transitions which give relatively large coupling interactions between it and acceptor states are important in this type of energy transfer process.

If spin interconversion is involved, as with singlet-triplet energy transfer, exchange terms in the transfer interaction matrix elements must be considered. This requires small distances for sufficient overlap between the orbital systems of the donor and acceptor molecules. Electron exchange allows energy transfer only under conservation of total spin multiplicity of the system. If sufficient dipole coupling is present, then energy transfer may still take place over distances in slight excess of ordinary collision diameters since exchange terms do not have to be large.

If the donor transition is further forbidden by symmetry, such as with an $n \rightarrow \pi^*$ transition, the dipole-dipole coupling interaction may be very small and higher order terms should be considered. When this is combined with spin interconversion requirements, transfer by inductive resonance will probably take place very slowly and give way to any other common yet faster mode of deactivation.

Terenin and Ermolaev (3) have measured phosphorescence spectra of several aromatic compounds using benzophenone and benzaldehyde as photosensitizers. The measurements were made in ethanol-ether glass at 77°K. As the concentration of acceptor in the glass was decreased, its characteristic emission also decreased while the donor phosphorescence increased. By assuming a completely random distribution of donor and acceptor molecules in the glass, Förster (2) has estimated from the results of Terenin that triplet energy was being transferred over a mean distance of about 14 Angstroms. This distance is in excess of ordinarily expected collision diameters. There is some question, however, as to whether a completely random distribution of donor and acceptor molecules actually exists in the glass. Prior to and during the cooling cycle, complexing between the two types of molecules may have resulted in the formation of molecular aggregates. However, the rate constants for energy transfer determined by Terenin (3) are several orders of magnitude smaller than the quenching constants normally encountered in solution.

Recently several workers have investigated triplet energy transfer in solution (4, 5, 6, 7, 8, 9). By observing the quenching of biacetyl phosphorescence, Bäckstrom and co-workers (4, 6) have measured rate constants for the deactivation of the lowest energy biacetyl triplet state by a number of compounds. Two types of quenchers were studied. The first were those which contained loosely

bound hydrogen atoms and quenched biacetyl triplets by reduction of the excited molecule through hydrogen transfer. The second group were molecules which did not contain any chemically reactive sites but which did have triplet state energies near that of biacetyl. Here, quenching was assumed to result from triplet energy transfer between biacetyl and quencher. Their (4, 6) results indicated that energy transfer was only taking place through molecular encounters. They also indicated that the apparent efficiency of the transfer process decreased as the energy of the acceptor increased toward that of biacetyl. At lower energies the effective rate of energy transfer approached that for a diffusion controlled process. Inefficient endothermic energy transfer was observed to occur along with a dependence on the sensitizer concentration.

Using a double-flash technique, Porter and co-workers (7, 8) have investigated the transfer of triplet energy between a number of donors and acceptors in solution. Their results are in accord with those obtained by Bäckstrom (4, 6). Quenchers with higher triplet energies than the donor were found to be poor, while those with lower energy were considerably more efficient. Again the maximum effective rate of energy transfer approached that for a diffusion controlled process.

In these laboratories the study of energy transfer has been undertaken using chemical techniques. These include the investigation

of the effect certain selected quenchers have on the photoreduction of benzophenone by benzhydrol and the study of the photosensitized isomerization of olefins. The former technique, which was developed by Moore (10, 11), has been used successfully by him and others (9, 12, 13) for measuring the quenching efficiencies of selected compounds.

Moore and Hammond (10, 11), and independently Bäckstrom and Sandros (5), have demonstrated that the chemically reactive excited state of benzophenone is the low-lying $n \rightarrow \pi^*$ triplet. The addition of trace amounts of quenchers reduce the quantum yield for the photoreduction of benzophenone by benzhydrol in a manner which is related to the effective deactivating ability of the quencher toward the chemically reactive ketone excited state.

Leermakers (9) has shown that compounds having triplet energies lower than that of benzophenone, in general, are good quenchers. Compounds having triplet state energies which are greater than that of benzophenone are either poor or altogether ineffective as quenchers. An unpublished study by Walsh (13), using the same benzophenone-benzhydrol system, has demonstrated a similar energetically selective quenching effect with a largely expanded collection of compounds. The results of Leermakers and Walsh are in accord with those obtained by Bäckstrom and co-workers (4, 6).

Saltiel (14) has employed the isomerization technique with stilbene. Through the use of selected sensitizers which have different triplet state energies, he has demonstrated the reversible nature of an energy transfer process involved in his system. The process is followed by observing changes effected in the steady state ratio of cis to trans stilbene in an inert solvent as a function of the triplet state energy of an added sensitizer. When the energy of the sensitizer is much higher than the triplet energies of both stilbene isomers, the steady state cis-trans ratio approaches and maintains a limiting value. This indicates that when energy transfer is largely exothermic it becomes equally efficient for both stilbene isomers. As the triplet state energy of the donor is decreased toward that of the high energy cis-stilbene isomer, the cis to trans ratio increases. The rate of increases does not reach a maximum value until after the energy of the sensitizer falls below that of the cis isomer.

As the sensitizer energy is continually decreased, the cis-trans ratio of stilbene isomers reaches a maximum value. This occurs when the triplet energy of the donor is somewhere between that of the two stilbene isomers. After passing the maximum the rate of change of the cis-trans ratio then decreases as the energy of the sensitizer approaches that of the low-energy trans-stilbene isomer, increasing to zero as the energy of the trans-isomer is passed. After the sensitizer energies fall below those of either stilbene isomer, much

longer periods of time are required to reach a steady state than when donor energies are higher than those of the stilbenes. Saltiel has explained his results by considering that the lifetime of the trans-stilbene triplet is sufficiently long that energy transfer from it to the ground state sensitizer serves as an effective mode of deactivation. The lifetime of the cis-isomer, however, is too short to allow this mode of deactivation to compete effectively with other non-radiative deactivation processes. These results indicate that reversible and endothermic energy transfer must occur. Turro (15) has also shown that a similar trend exists in the isomerization of piperylene.

In each of the cases cited above, effective quenchers were organic molecules which had a ground singlet state and an excited triplet state whose energy was close to but somewhat less than that of the donor being quenched. Other quenchers that were studied, but found to be less efficient, were molecules that either reacted chemically with the excited sensitizer or had triplet state energies which were higher than that of the donor.

In addition to those mentioned above, another class of molecules has been observed to quench excited triplet states. These are molecules which have unpaired electrons in their ground state configurations such as oxygen, nitrogen oxide, and paramagnetic transition metal ions. Deactivation of excited triplet state sensitizers by this

type of quencher has been investigated by several workers (7, 16, 17, 18, 19, 20). Bäckstrom (16) observed the quenching effect of oxygen and nitrogen oxide on the chemically active state of benzophenone. He proposed that quenching possibly resulted from the formation of a charge-transfer complex between quencher and the excited ketone. Strong chemical bonding could result due to the partial radical character of the excited donor and quencher. The charge transfer complex could decay to a lower energy state, decompose and regenerate the quencher.

Moore and Hammond (20) found that oxygen and ferric dipivaloylmethide quenched the triplet state of benzophenone. They proposed that since the ferric chelate apparently quenched as well as oxygen, bond formation of the type proposed by Bäckstrom (16) was not likely. Instead, they suggested that the mechanism involved was probably similar to that proposed by McConnell (21) to account for paramagnetic catalysis of the thermal isomerization of olefins.

Hammond, Baker and Moore (22) reported that the paramagnetic dipivaloylmethide chelates of iron(III), erbium, and samarium quenched the photoreduction of benzophenone by toluene. They also found that the diamagnetic dipivaloylmethide chelate of aluminum did not have a measurable effect on the reaction. It was concluded from these results that the quenching ability of the chelates was due to their paramagnetism.

Porter and co-workers (7, 20) observed quenching of triplet anthracene by molecular oxygen and nitrogen oxide. In addition, Porter and Wright (17) measured the rate of quenching anthracene triplets by transition metal ions in aqueous and alcoholic solutions. They also measured a self-quenching rate constant for anthracene triplets. It was found that only the paramagnetic ions which they studied were able to quench triplets appreciably. The diamagnetic ions that were studied had very little or no quenching ability.

Quenching rate constants were classified into three categories: The first included ions or molecules which have unpaired electrons localized in p-orbitals, such as oxygen and nitrogen oxide. The second were substances in which the unpaired electrons were located in d-orbitals, such as transition metal ions. The last category consisted of molecules in which the unpaired electrons were located in f-orbitals, such as rare earth ions. The quenching rates for substances in the first grouping were found to be in the neighborhood of ordinary diffusion controlled rates. The rates of quenching by molecules in the second group were about two orders of magnitude smaller than those of the first. Molecules classed in the final group exhibited quenching rates that were at least one order of magnitude smaller than those in the second. The quenching efficiencies showed no correlation with the magnetic susceptibilities of the ions. No correlation between the excited energy levels of the ions and their

quenching efficiencies was apparent. A theory was proposed to explain the results.

Since all of the paramagnetic ions and molecules that Porter and Wright (17) studied were able to quench anthracene triplets, and since no quenching was observed with solvated diamagnetic ions, they felt that the mechanism must be due to some effect associated with the spin multiplicities of the quenchers. A brief outline of their theory follows.

The process

$$A^*(S=x) + Q(S=y) \rightarrow A(S=x-1) + Q(S=y) \qquad (1)$$

is allowed by spin conservation rules when $x > 1$, if $y > 0$. The forbidden spin change of A from 1 to 0 becomes possible without the necessity of energy transfer to the quencher. However, solvent molecules must be present in order to absorb the energy released by A* when it decays to its ground state. The mechanism is distinct from any magnetic perturbation effect and therefore the reactivity of quenchers is not directly correlated with the magnitudes of their magnetic moments.

The process is considered to take place in two steps: (1) The formation of a collision complex, and (2) the dissociation of the complex. The quenching rate is expected to depend on (a) the spin-spin coupling between the donor and quencher in the complex, (b) the lifetime of the complex, and (c) a spin statistical factor.

By considering the statistical factor alone for the process given above, it is found that all paramagnetic molecules have an equal probability for the conversion of triplets to singlets. Therefore, the differences observed in the rates of quenching exhibited by the molecules studied were attributed to the lifetime of the collision complex and the spin-spin interactions between A and Q in the complex.

The above factors do not depend upon the paramagnetic susceptibility of the ions. They do, however, depend to some extent upon the degree of overlap between the orbitals containing the unpaired electrons in A and Q. The authors (17) stated that the degree of interaction expectedly decreased as the unpaired electrons became increasingly deep-seated while going from p- to d- to f-orbitals. The f-electrons of rare earth atoms only exhibit small interaction with solvent or other environment (23, 24). Since transition metal ions form complexes in solution, the d-orbitals are shielded, by the inner complexed solvent shell, from interacting with outside electronic systems. Porter also stated that according to the proposed mechanism, the radiationless transition probability is increased by the presence of a paramagnetic quencher only by an amount corresponding to the difference between a spin-forbidden and a spin-allowed radiative transition.

Linschiz and co-workers (18, 19, 25) have recently studied the quenching of anthracene triplets by solvated metal ions using a flash-

technique. Whereas Porter used water and alcohol mixtures as solvents, these investigators conducted their studies in pyridine solutions. Copper chloride was used primarily as the paramagnetic quencher. During the course of study, known quantities of ethylenediamine and ortho-phenanthroline were added to a mixture of anthracene and cupric chloride in pyridine. It was found that upon the addition of ethylenediamine, the quenching efficiency of the copper chloride decreased toward a limiting value which was lower than the value obtained with a solution free from ethylenediamine. Addition of ortho-phenanthroline resulted in an increase in the quenching efficiency of the copper chloride. The differences were accounted for by noting that conjugated systems are better "electron conductors" and thus can allow better electron exchange between the metal and the triplet state molecule than can be allowed by ethylenediamine. The authors felt that a charge transfer complex was formed between the excited molecule and the metal ion. The complex is then thought to undergo a rapid radiationless decay to its ground state. The forbidden spin conversion of the excited molecule was proposed to be catalyzed by a mechanism similar to that suggested by Porter (17).

The present investigation utilizes the technique of photoreduction of benzophenone by benzhydrol for the study of triplet state quenching by selected transition metal chelates. The results indicate

that a combination of several of the effects observed by others may be involved, and that earlier explanations are not complete.

EXPERIMENTAL

MATERIALS

Benzophenone

Benzophenone (Matheson, Coleman, and Bell, Reagent Grade) was recrystallized from a mixture of hot benzene and ligroin. The plates melted sharply at 50°.

Benzhydrol

Benzhydrol (Matheson, Coleman, and Bell, Reagent Grade) was recrystallized twice from a mixture of hot benzene and ligroin. Slow cooling yielded colorless, fine, light needles, m.p. 68°.

Benzene

Benzene (Mallinckrodt, Analytic Reagent Grade) was used without further purification after it was found that there was no effect upon experimental results after the benzene had been subjected to further purification. The purification consisted of washing the benzene with concentrated sulfuric acid, then distilling it over sodium. No darkening was observed upon the addition of sulfuric acid.

t-Butyl Alcohol

t-Butyl alcohol (Matheson, Coleman, and Bell, Reagent Grade) was redistilled; the fraction boiling from 82° to 83° was collected for use.

3-Methyl-2,4-pentandione

3-Methyl-2,4-pentandione was prepared by the method of Hauser and Adams (26). Acetic anhydride was reacted with 2-butanone using boron trifluoride as a catalyst. The product was distilled at 30 mm. pressure, and the fraction boiling in the range between 73° and 77° was collected for further use.

2-Acetylcyclohexanone

2-Acetylcyclohexanone (Eastman Kodak, White Label) was used directly without further purification.

Dibenzoylmethane

Dibenzoylmethane was obtained from Dr. Karl Kopecky (27). The compound melted at 79° and was used without further purification.

Chelates

Ferric dipivaloylmethide, chromium dipivaloylmethide, cobalt(III) dipivaloylmethide, aluminum dipivaloylmethide, ferric acetylacetonate, chromium acetylacetonate, cobalt acetylacetonate, aluminum acetylacetonate, cobalt(II) dipivaloylmethide, copper dipivaloylmethide, nickel(II) dipivaloylmethide, manganese dipivaloylmethide, lanthanum dipivaloylmethide, erbium dipivaloylmethide, and gadalinium dipivaloylmethide were obtained pure from Dr. Chin-Hua Wu (28a). The details of the synthesis of these chelates are given elsewhere (28b). The chelates were freshly sublimed before

use in quenching experiments. Physical details of these chelates are given in Table 1.

Ferric dibenzoylmethide and chromium dibenzoylmethide were prepared by the procedure given below. Metal chloride hexahydrate was dissolved in ethanol in which an excessive amount of sodium acetate had been added. A slight molar excess of dibenzoylmethane was dissolved in ethanol and the solution added to the chloride-acetate mixture. The reaction mixture was heated on a steam bath for a half hour and allowed to cool. During the heating period, the solution containing the iron compound quickly turned orange and then formed a blood-red precipitate. The solution containing the chromium chelate turned yellow-green in color. After cooling to room temperature, benzene was added and the mixture was extracted with water. The benzene layer was dried over anhydrous calcium chloride, then evaporated to dryness. The crude chelates were recrystallized three times from a benzene-ligroin mixture. The analytical data for these chelates are reported in Table 1.

Ferric and chromium 3-methylacetylacetonate, ferric and chromium acetylcyclohexanonate, ferric and chromium benzoylacetonate, ferric and chromium hydroxyacetophenonate, and ferric and chromium 8-hydroxyquinolate were prepared using the following general procedure. This method was also used for preparation of the previously described chelates and found equally effective for all.

Table I

Analytical Data from Chelate Synthesis

Metal	Abbreviation	M.P.	Carbon-Hydrogen Elemental Analysis % C Calc.	% C (found)	% H Calc.	% H (found)
Acetylacetonate Chelates						
Ferric	$Fe(AA)_3$	183				
Cobalt	$Co(AA)_3$					
Chromium	$Cr(AA)_3$					
Aluminum	$Al(AA)_3$	196				
Dipivaloylmethide Chelates						
Ferric	$Fe(DPM)_3$	163				
Chromium	$Cr(DPM)_3$	229				
Cobalt III	$Co(DPM)_3$	245				
Cobalt II	$Co(DPM)_2$	143				
Aluminum	$Al(DPM)_3$	264-5				
Copper II	$Cu(DPM)_2$	198				
Nickel II	$Ni(DPM)_2$	225				
Lanthanium	$La(DPM)_3$	148-9				
Erbium	$Er(DPM)_3$	153-4				
Manganese III	$Mn(DPM)_3$	165				
Dibenzoylmethide Chelates						
Ferric	$Fe(DBM)_3$	275	74.50	(73.85)	4.55	(4.50)
Chromium	$Cr(DBM)_3$	316	74.89	(74.20)	4.58	(4.49)
Ferric Acetylcyclohexonate	$Fe(AC)_3$	150	61.03	(60.32)	6.99	(6.87)
Ferric 3-Methylacetylacetonate	$Fe(MAA)_3$	145-8	54.70	(54.40)	6.84	(6.75)

Higher yields of the chromium chelates were generally obtained than are normally obtained by other procedures.

Metal chloride hexahydrate is dissolved in N,N-dimethylformamide. A slight molar excess of ligand is dissolved in additional N,N-dimethylformamide, and the two solutions are mixed. Excess sodium hydrogen carbonate is added and the flask is swirled until the mixture becomes homogeneous. The mixture is placed on a steam bath for a few minutes, removed, and allowed to stand until cool. Benzene is added, and the resulting solution is extracted with water. A small amount of ethyl ether had to be added in some instances to assist in the separation of the aqueous and organic layers. The organic layer containing the chelate is dried over anhydrous calcium chloride and evaporated to dryness. The crystalline residue is recrystallized twice from a benzene-ligroin mixture and sublimed if the melting point is sufficiently low.

The analytical data for the chelates are given in Table 1.

APPARATUS

The apparatus used for these experiments has been described in detail by Moore (11). The light source was a Westinghouse (SAH 800-c) 800 watt short arc, medium pressure, mercury lamp. The light was collected and collimated by specially constructed mirrors

so that a parallel beam of light would pass through a filter holder and cell holder mounted at the center of an optical bridge. The beam was sufficiently broad at the location of the cell holder that four 15 mm. tubes placed in a Beckman D.U. ultraviolet spectrophotometer cell holder could easily fit into the beam. The light beam was collected on a second mirror located behind the cell holder and focused on a thermopile (Eppley Laboratories). The output from the thermopile was measured by a Rubicon potentiometer. Output measurements from the thermopile were proportional to the light intensity. A diagram of the optics is given in figure I.

CELLS

Three types of cells were used in this investigation. Drawings of these cells are given in figure II. Early experiments were carried out in quartz cells of type I , which are described in detail by Moore (11). They were mounted in the apparatus by means of a cell holder set in a V-block and fitted with a 25.52 cm^2 diaphragm to insure a constant, incident light beam cross section. The second type of cell that was tried was formed by sealing a pyrex T-tube to the top of a quartz Beckman D. U. ultraviolet spectrophotometer cell. One end of the T-tube was attached to a 14/38 standard-taper, ground-glass joint. The other end was sealed. These tubes proved unsuccessful

Figure I. Optics

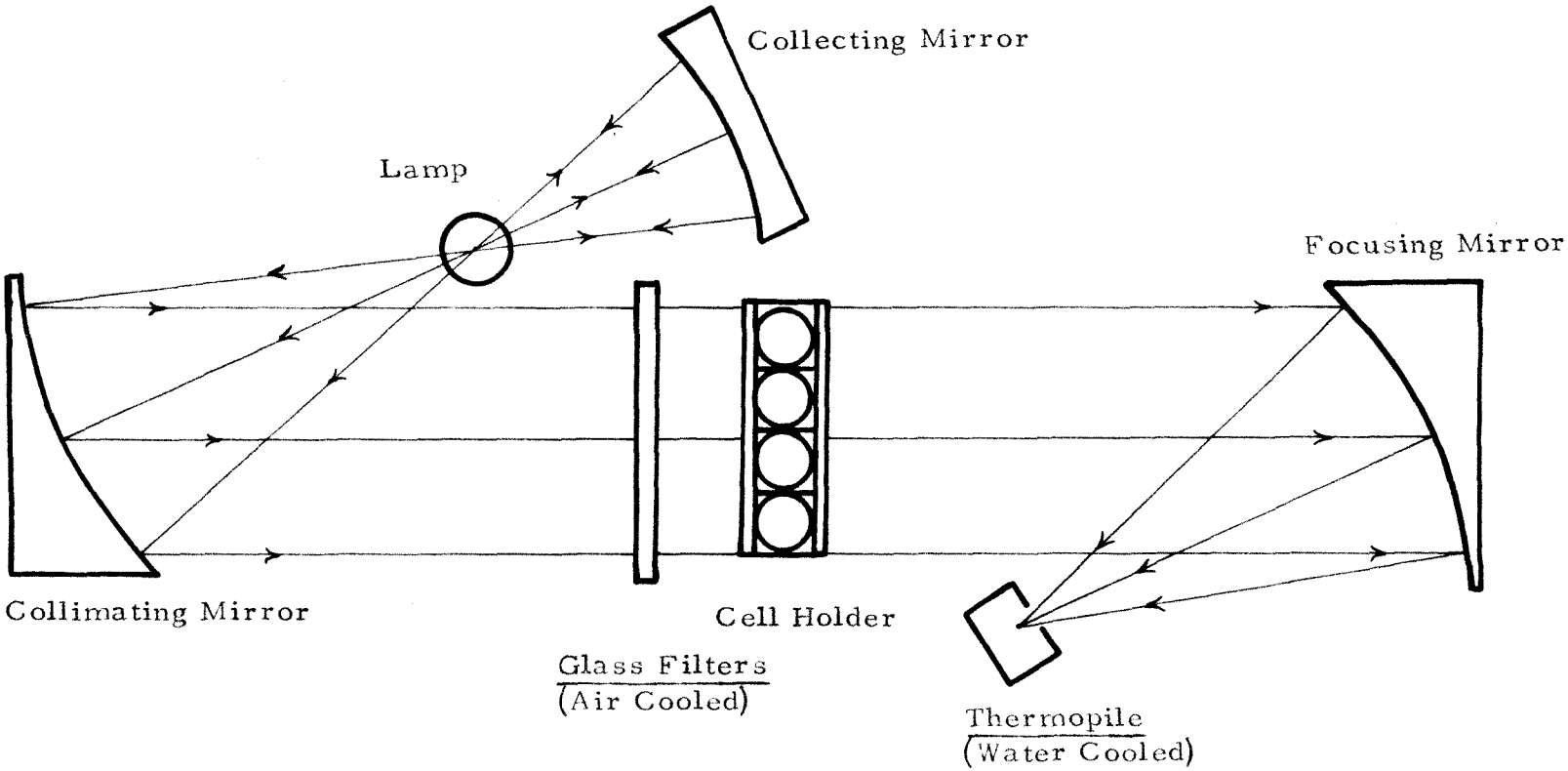

Figure II. Diagram of Cells Used for Photolysis Studies

Type I

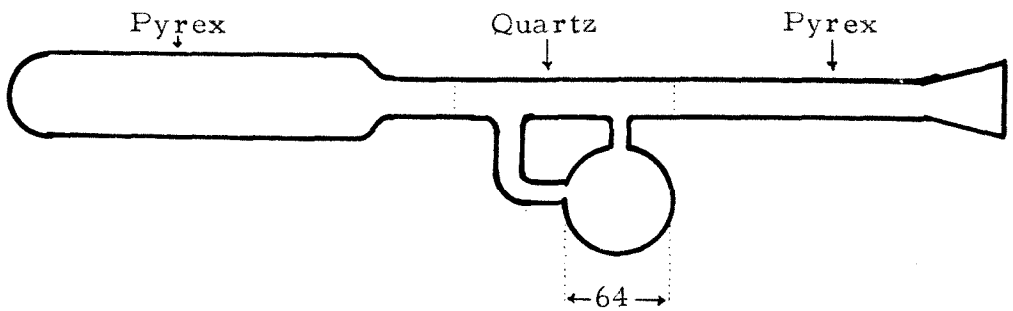

Volume = 75 ml.

Type II

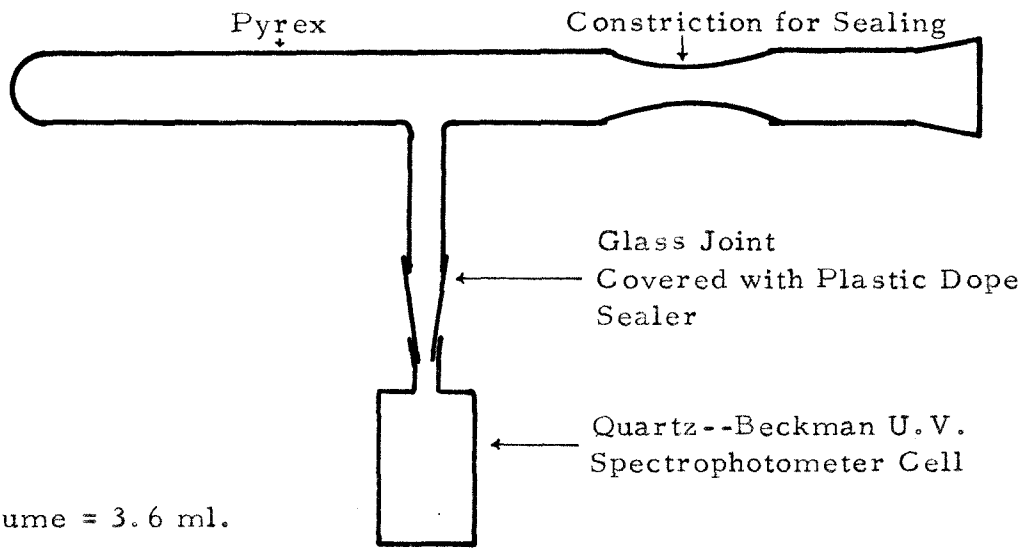

Volume = 3.6 ml.

Type III

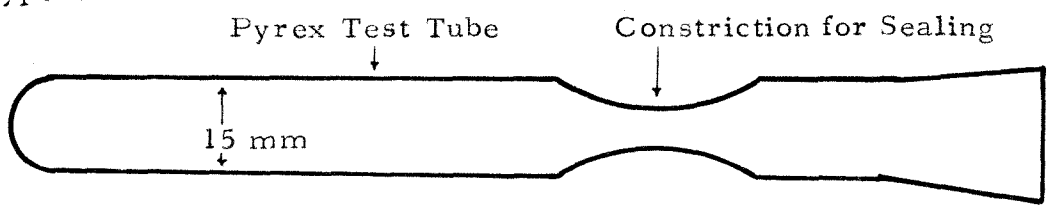

Volume = 4.0 ml.

due to continual leakage and difficulties in mixing. A third type of cell which was finally adapted for general use was made by sealing a 14/38 ground-glass joint to the top of a 15 mm. diameter pyrex test tube. The test tubes were matched for diameter and light transmission before use.

FILTER SYSTEM

The filter system that was used in this work consisted of a combination of Corning glass filters 0-52 and 7-60. This filter combination resulted in a narrow spectral band with a maximum transmission at 3700 Angstroms and a half-height width of 300 Angstroms. This completely eliminated the 3130 Å mercury line and allowed less than two percent of the 3450 Å and 4050 Å lines. The transmission at the maximum was 42 percent. Figure III is a representation of this system.

PROCEDURE AND ANALYSIS

All quenching experiments were conducted by using the same general procedure. Stock solutions of benzophenone, benzhydrol, and quencher were prepared. Samples consisting of the proper amount of each stock solution were placed in a flask and diluted with solvent.

Figure III. Filter System

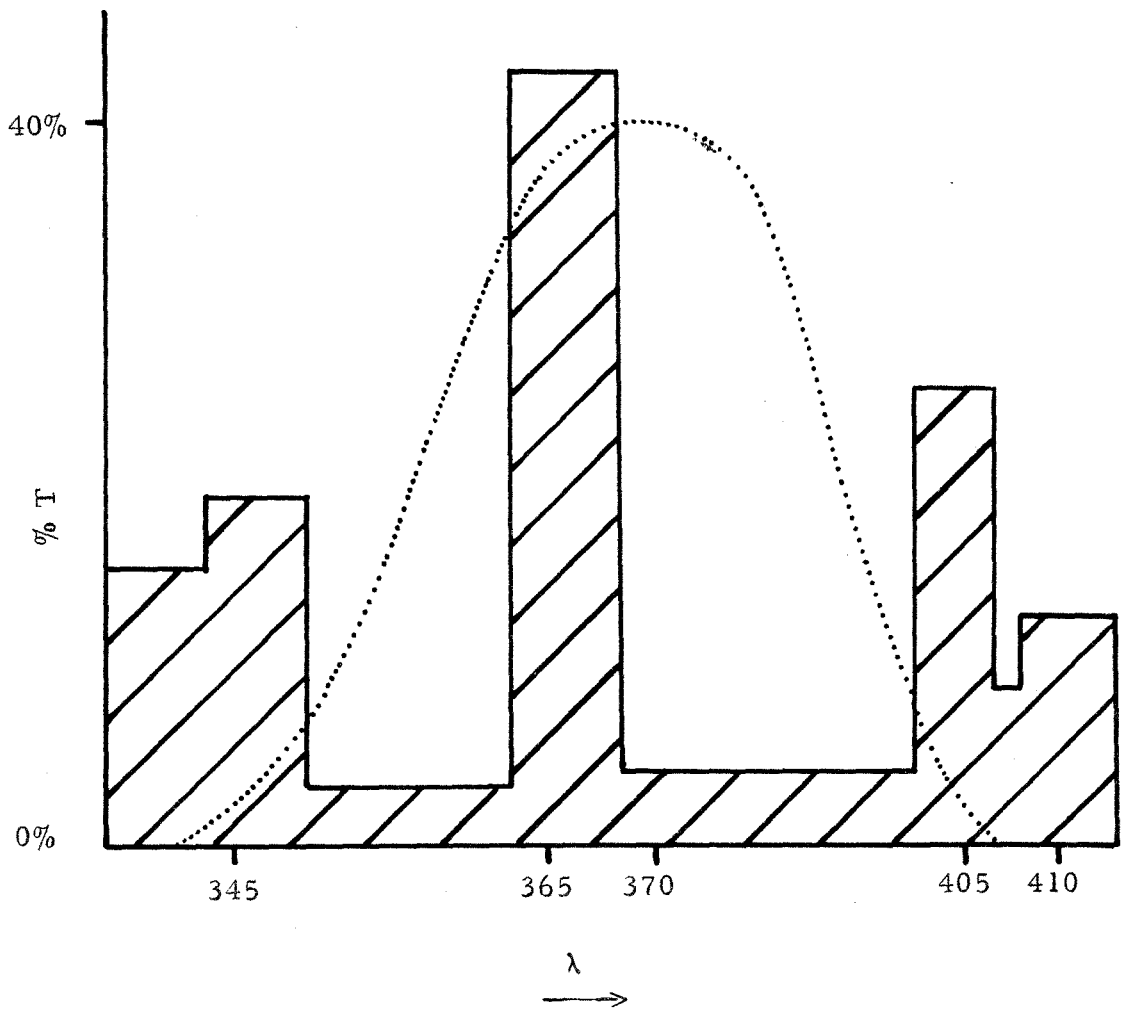

The cells were filled, then degassed three times to one micron pressure using a freeze-thaw cycle. After the final degassing cycle, the cells were sealed by torch. The large quartz cells (type I) held 75 ml. of solution. The small quartz cells (type II) and the pyrex tubes (type III) each held 4 ml. of solution. The smaller cells were filled with an automatic syringe set for the required volume. Precision in filling cells by this technique was found to be better than one part per thousand.

One large cell or four small cells could be placed in the light beam for each irradiation period. In every case in which small cells were used, one of the four contained only benzophenone and benzhydrol and was used for monitoring the light intensity. In all instances the initial benzophenone and benzhydrol concentrations in each of the four cells irradiated simultaneously were the same. In most cases, at regular intervals of 500 to 600 seconds during a run, the cells were mixed and rotated in their positions so that each cell spent an identical period of time in each cell location in the light beam. This insured an overall constant light intensity on each cell and sufficient mixing of the sample during the irradiation. It was found, however, that the cross-section intensity of the light beam was very constant.

Analysis was made by ultraviolet spectrophotometry. The fraction of benzophenone reacted was measured by comparing the optical density of the irradiated sample to that of the unreacted solution.

A twenty-fold dilution factor was normally used for benzophenone analysis. Analyses were usually made in benzene. (Methyl alcohol was used for making dilutions when the reactions were run in t-butyl alcohol.) Measurements were made at five millimicron intervals from 345 mμ to 365 mμ. The quantity of chelate destroyed during irradiation was determined by measuring the optical density of undiluted samples of irradiated and non-irradiated solutions, if possible, in regions where the chelate had a visible absorption not interfered with by benzophenone absorption.

The equipment used for analysis was a Beckman D. U. spectrophotometer and Cary Model 11 and Model 14 spectrophotometers.

ACTINOMETRY

Moore (11) used the photoreduction of benzophenone by isopropyl alcohol to measure the lamp intensity during his study of the photoreduction of benzophenone by benzhydrol. Benzophenone was dissolved in pure isopropyl alcohol and irradiated for different lengths of time. The lamp output was known to be constant as determined from thermopile measurements. Yet considerable variation in the rate of disappearance of benzophenone resulted when the reaction was allowed to proceed to different degrees of conversion. A fairly consistent value for the rate of benzophenone destruction was obtained

for runs in which the reaction was carried to about 20 percent conversion. This value was chosen as the standard rate of photoreduction of benzophenone by isopropyl alcohol at the constant light intensity where the photolyses were made.

Pitts et al. (29) showed that the quantum yield for the photoreduction of benzophenone by isopropyl alcohol was greater than one in degassed solutions and attributed the large quantum yield to the reaction:

$$CH_3\text{-}\overset{\overset{OH}{|}}{\underset{\cdot}{C}}\text{-}CH_3 + \varphi_2CO \longrightarrow CH_3\text{-}\overset{\overset{O}{||}}{C}\text{-}CH_3 + \varphi_2\dot{C}\text{-}OH \qquad (2)$$

Thus, for every benzophenone molecule photoreduced, a second could also be reduced by reaction 2.

Moore irradiated a sample of the ketone with a high concentration of benzhydrol present in benzene solvent. The rate of ketone disappearance obtained from this experiment closely approximated the rate determined for the benzophenone-isopropyl alcohol reaction when allowed to go to 20 percent conversion. It was decided that the secondary reaction proposed by Pitts (29) was not playing a significant role under the reaction conditions employed by Moore. This conclusion was reasonable because in the benzophenone-benzhydrol system the reaction corresponding to 2 would be an identity process. The quantum yield for the rate of disappearance of benzophenone in isopropyl alcohol

was concluded to be unity under Moore's reaction conditions.

Recent experiments have shown that the original conclusions drawn by Moore with respect to actinometry are probably not correct. The quantum yield for the destruction of benzophenone in isopropyl alcohol is actually greater than one under the conditions employed by him. Thus, this method for actinometry is no longer recommended.

A simple reaction sequence which accounts for the photoreduction of benzophenone by benzhydrol is

$$B \xrightarrow{eI_a} B^* \qquad (3)$$

$$B^* \xrightarrow{k_d} B + \text{Energy} \qquad (4)$$

$$B^* + BH_2 \xrightarrow{k_r} \text{Products} \qquad (5)$$

where $\underline{B}$ is ground state benzophenone, $\underline{B}^*$ is the chemically reactive excited triplet state benzophenone, $\underline{BH}_2$ is benzhydrol, $\underline{I}_a$ is the absolute intensity of the absorbed incident light, $\underline{e}$ is the efficiency factor for the formation of chemically reactive triplet molecules from those absorbing light, k_d is the rate constant for all first order deactivation processes both radiative and non-radiative, and k_r is the rate constant for the hydrogen abstraction step.

Two rate equations describing the sequence of reactions may be written. The first, used by Moore and later in this work, is

$$\frac{1}{\varphi} = \frac{1}{e} + \frac{k_d}{e k_r [BH_2]_{av}} \qquad (6)$$

where φ is the absolute quantum yield for the conversion of benzophenone and is defined as the number of moles of ketone reacted per Einstein of energy absorbed. The equation is appropriate when the benzhydrol concentration is moderately large and therefore remains nearly constant during the time interval of the reaction. The average benzhydrol concentration, rather than the initial concentration, is always used in calculating results from this equation.

The second equation is probably more precise and was used for the development of the actinometric procedure adopted for this work. Since for each benzophenone molecule reduced one benzhydrol is oxidized, the rate of disappearance of benzhydrol may be followed kinetically by following the rate of destruction of benzophenone.

Applying the steady state treatment to the triplet state benzophenone concentration one obtains:

$$[B^*] = \frac{e I_a}{k_d + k_r [BH_2]} \quad . \qquad (7)$$

The rate for the disappearance of benzhydrol is:

$$-\frac{d[BH_2]}{dt} = k_r [BH_2][B^*] \quad . \qquad (8)$$

Substitution of equation 7 into equation 8 gives:

$$- \frac{d[BH_2]}{dt} = k_r [BH_2] \left[\frac{e I_a}{k_d + k_r [BH_2]} \right] . \qquad (9)$$

After integration one obtains:

$$e I_a t = [BH_2]_o - [BH_2]_f + \frac{k_d}{k_r} \ln \frac{[BH_2]_o}{[BH_2]_f} , \qquad (10)$$

where t is time, $[BH_2]_o$ is the initial benzhydrol concentration, and $[BH_2]_f$ is final benzhydrol concentration.

There are two quantities which are unknown in equation 10. They are the effective intensity (eI_a) and the ratio of rate constants k_d/k_r. If for a series of samples the intensity remains constant, the value of the ratio k_d/k_r can be determined without knowledge of the intensity. Likewise, the effective intensity can be determined without knowledge of the value for k_d/k_r. This may be accomplished in the following manner by using data obtained from a series of experiments run simultaneously after making the substitutions

$$y_i = \frac{1}{t_i} \left[[BH_2]_f - [BH_2]_o \right]_i \qquad (11)$$

Substitution of equation 7 into equation 8 gives:

$$- \frac{d[BH_2]}{dt} = k_r [BH_2] \left[\frac{e I_a}{k_d + k_r [BH_2]} \right] . \qquad (9)$$

After integration one obtains:

$$e I_a t = [BH_2]_o - [BH_2]_f + \frac{k_d}{k_r} \ln \frac{[BH_2]_o}{[BH_2]_f} , \qquad (10)$$

where t is time, $[BH_2]_o$ is the initial benzhydrol concentration, and $[BH_2]_f$ is final benzhydrol concentration.

There are two quantities which are unknown in equation 10. They are the effective intensity (eI_a) and the ratio of rate constants k_d/k_r. If for a series of samples the intensity remains constant, the value of the ratio k_d/k_r can be determined without knowledge of the intensity. Likewise, the effective intensity can be determined without knowledge of the value for k_d/k_r. This may be accomplished in the following manner by using data obtained from a series of experiments run simultaneously after making the substitutions

$$y_i = \frac{1}{t_i} \left[[BH_2]_f - [BH_2]_o \right]_i \qquad (11)$$

$$x_i = \frac{1}{t_i}\left[\ln \frac{[BH_2]_o}{[BH_2]_f}\right]_i = \frac{1}{t_i}\left(2.303 \log_{10} \frac{[BH_2]_o}{[BH_2]_f}\right)_i \quad (12)$$

Equation 10 becomes

$$y_i = k_d/k_r\, x_i + eI_a$$

where the subscript $\underline{i}$ refers to data corresponding to the $\underline{i}^{th}$ run. The value for k_d/k_r may be determined from the slope of a plot of $\underline{y_i}$ against $\underline{x_i}$. The value for the effective light intensity (eI_a) encountered by these samples during the period of irradiation is given by the ordinate intercept of the plot described above.

Four experiments were run and the best possible fit of the data to equation 13 was effected by the method of least squares. The data from these experiments are given in Table 2. The value for the slope corresponding to k_d/k_r is given by the expression,

$$\frac{k_d}{k_r} = \frac{\sum_i^n y_i \sum_j^n x_j - n \sum_i^n x_i y_i}{\sum_i^n x_i \sum_j^n x_j - n \sum_i^n x_i^2} \quad (13)$$

The ordinate intercept corresponding to the effective intensity (eI_a) is given by the expression,

Table II

Experimental Data for Actinometry Development

Sample (n)	t_i (sec) (a)	$[BH_2]_o$	$[BH_2]_f$	y_i ($\times 10^6$)	x_i ($\times 10^5$)	$y_i x_i$ ($\times 10^{11}$)	x_i^2 ($\times 10^{10}$)
1	7200	0.1500	0.1314	-2.586	1.832	-4.74	3.36
2	7200	0.0600	0.0453	-2.041	3.900	-7.96	15.21
3	8000	0.0300	0.0192	-1.350	5.575	-7.53	31.10
4	9000	0.0900	0.0696	-2.243	2.853	-6.47	8.14
				Σy_i = -8.243 $\times 10^{-6}$	Σx_i = 1.416 $\times 10^{-4}$	$\Sigma y_i x_i$ = -2.670 $\times 10^{-10}$	Σx_i^2 = 5.781 $\times 10^{-9}$

(a) = interval between mixing equals 500 → 600 seconds

t_i = total photolysis time in seconds

$[BH_2]_o$ = initial benzhydrol concentration

$[BH_2]_f$ = final benzhydrol concentration

$$y_i = \frac{1}{t_i}\left[[BH_2]_f - [BH_2]_o \right]$$

$$x_i = \frac{1}{t_i}\left(2.303 \log_{10} \frac{[BH_2]_o}{[BH_2]_f}\right)$$

k_d/k_r = 0.0326 moles/liter

$e I_a$ = 3.19×10^{-6} Einsteins/liter second

$$eI_a = \frac{\sum_i^n x_i \sum_j^n x_j y_j - \sum_i^n x_i^2 \sum_j^n y_j}{\sum_i^n x_i \sum_j^n x_j - n \sum_i^n x_i^2} \qquad (14)$$

where n is the number of samples considered.

The value for k_d/k_r for the photoreduction of benzophenone by benzhydrol in benzene determined by the above procedure is 0.0326 moles/liter. The effective intensity of the incident light beam for this series of experiments is 3.19×10^{-6} Einsteins/liter·second. Using this effective intensity determined by equation 14, the effective quantum yields for the reduction of benzophenone for each benzhydrol concentration were calculated and are given in Table 3. The reciprocal of the effective quantum yield was plotted against the reciprocal average benzhydrol concentration according to equation 6. The slope of this plot, which corresponds to k_d/k_r is 0.0327 moles/liter. This value is in very close agreement with the value determined from the application of equation 10. The result of this argument is that equation 6 can now be written,

$$\frac{1}{\varphi'} = 1 + \frac{0.033}{[BH_2]_{av}} \qquad (15)$$

where φ' is the effective quantum yield and is defined by the expression

Table III

Quantum Yields for Actinometry Experiments

Sample	φ	$1/\varphi$	$1/[BH_2]_{av}$	k_d/k_r
1	0.805	1.242	7.15	0.0338
2	0.637	1.570	19.0	0.0300
3	0.421	2.379	40.7	0.0338
4	0.706	1.416	12.53	0.0332
			Average	0.0327

φ = quantum yield for the destruction of benzophenone.

1. The lamp intensity is 3.19×10^{-6} Einsteins/liter sec as determined by equation 14.

2. The values of k_d/k_r are determined from equation 6.

$$\varphi' = \frac{\varphi}{e} \tag{16}$$

Equation 15 may be used for measuring the effective light intensity as long as the reaction is not allowed to go to high conversion and the average value for the benzhydrol concentration is used.

The data obtained by Moore were recalculated using equation 10, and a value for k_d/k_r equal to 0.031 moles/liter was obtained. This value is in agreement with the value found in the present investigation. Two of Moore's points were eliminated from the calculations. One gave a very high value and the other gave the low value which led him to believe the quantum yield for the photoreduction of benzophenone by isopropyl alcohol to be unity. These experiments were repeated in the present work and found to give results in agreement with the present analysis.

It was of additional interest to determine the value of the efficiency factor (e) for the formation of reactive triplets from excited singlets. Several investigators have studied the radiative emission from solid solutions of benzophenone (3, 30, 31, 32). The quantum yield of phosphorescence from benzophenone in glasses at 77°K has been measured to be between 0.7 and 0.85 by different authors (3, 30, 31). In spite of the inconsistencies in reported phosphorescence quantum yields, a common observation is that there is no fluorescence observed. The lack of fluorescence indicates that the quantum yield for the

formation of triplet states must be very nearly one. The fact that the quantum yields of phosphorescence are less than one probably results from non-radiative decay of the triplet by some internal or thermal process before emission can take place.

To evaluate the efficiency factor (e), a number of experiments were run in which the intensity of the lamp was allowed to change between runs. Effective intensities were calculated by equation 15 for each run and are recorded in Table 4 with the corresponding thermopile readings. The method for measuring light intensities developed by Leighton and Forbes (33) through the use of uranyl oxylate was also used for measuring lamp intensities. The intensities calculated from these experiments are also recorded in Table 4.

The results obtained from the method of Leighton and Forbes are subject to doubt due to experimental difficulties which are inherent in the procedure. These difficulties were encountered while attempting to measure the percentage of light absorbed by the samples during irradiation and the uncertainty as to the exact value for the quantum yield of the uranyl oxylate decomposition. It was found that concentrations of reactants much higher than were used by Leighton and Forbes were needed in order to absorb all of the incident light. Using the suggested concentrations, only about 10 percent of the light was absorbed, thus requiring corrections for cell distortion, reflection, and absorption in order to estimate the exact amount of light absorbed

Table IV

Calculated Intensities with Corresponding Thermopile Readings

No.	Thermopile Reading (mv)	I_a ($\times 10^{-17}$ q/sec)	I_b ($\times 10^{-17}$ q/sec)	I_c ($\times 10^{-17}$ q/sec)
1	0.98	0.975	-	-
2	1.02	-	-	1.04
3	1.08	1.09	1.69	-
4	1.09	-	1.79	-
6	1.43	1.40 1.45	2.10	-
7	1.85	-	-	1.92
8	2.45	-	3.64	-
9	2.95	-	-	3.18

I_a = Intensity calculated from use of equation 15.

I_b = Intensity calculated from benzophenone-isopropyl alcohol system, assuming a quantum yield of unity.

I_c = Intensity calculated from uranyl oxylate system.

by the sample. In addition, the spectrum of the incident light was so broad that a range of quantum yields would be expected on the basis of the data of Leighton and Forbes. An average value of 0.53 was chosen for the quantum yield of the uranyl oxylate decomposition within the region of filter transmission.

The data from Table 4 are plotted in Figure IV. In spite of the difficulties encountered in the selection of a proper quantum yield for the decomposition of uranyl oxylate, the plot of intensity values determined by this procedure against corresponding thermopile readings lies on the same line as do the effective intensities determined from the benzophenone-benzhydrol system using equation 15 . If the uranyl oxylate results are correct, then the efficiency factor for the formation of reactive triplets from excited singlets for benzophenone must equal one.

It should be pointed out that for the present investigation it is not necessary that the efficiency factor be known, since the benzophenone-benzhydrol system has been used throughout and the efficiency factor always cancels when making quantum yield calculations.

Figure IV

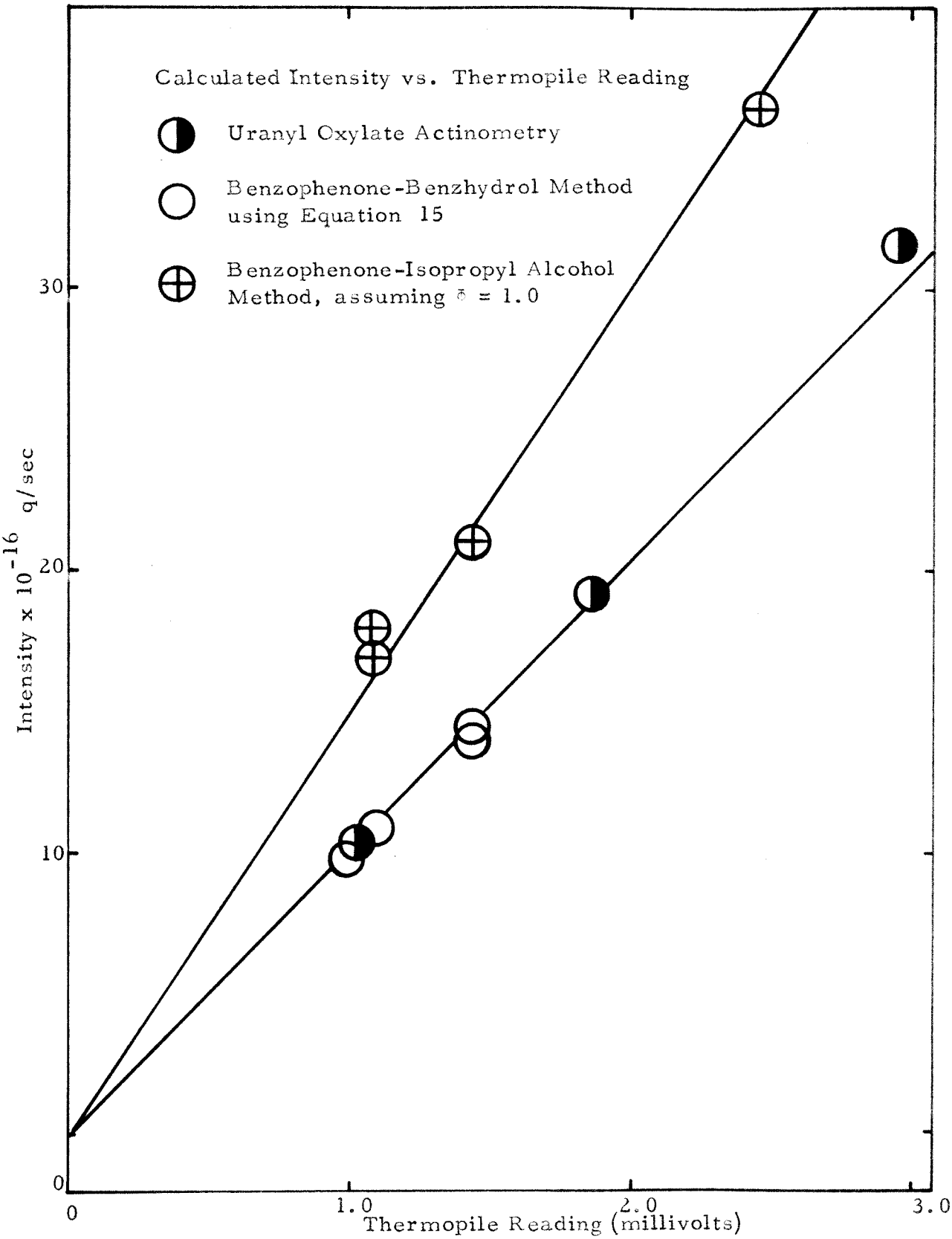
Calculated Intensity vs. Thermopile Reading
Uranyl Oxylate Actinometry
Benzophenone-Benzhydrol Method using Equation 15
Benzophenone-Isopropyl Alcohol Method, assuming Φ = 1.0
Intensity x 10^-16 q/sec
0
10
20
30
0
1.0
2.0
3.0
Thermopile Reading (millivolts)

RESULTS AND DISCUSSION

GENERAL

This investigation was initiated in order to determine the most probable mechanism for quenching of triplet benzophenone by transition metal chelates. It was presumed that the study might also cast some light on the overall mechanism of triplet energy transfer in solution. Several findings led to the initiation of the investigation, the most important of which are given below.

Moore used ferric dipivaloylmethide in his investigation of the mechanism for the photoreduction of benzophenone (11). In his studies he found that the quenching ability of this chelate was apparently comparable to that of oxygen. In addition, while studying the reaction between benzophenone and toluene (22), he found that chelates of erbium and samarium apparently also had small quenching effects on triplet benzophenone molecules, while diamagnetic aluminum dipivaloylmethide had no effect. The results were in accord with a mechanism involving paramagnetic catalysis. Porter has proposed such a mechanism (7). However, he had found that quenching of anthracene triplets by paramagnetic ions was about two orders of magnitude less efficient than quenching by oxygen. These observations implied that

something must be different between the quenching mechanism involving the chelates and the mechanism involving solvated transition-metal ions.

Further evidence for this conclusion was introduced by Leermakers (34). While studying the photoreduction of α-naphthaldehyde, he found that chromium dipivaloylmethide had no quenching effect on the excited aldehyde triplet. (Chromium dipivaloylmethide is paramagnetic, having three unpaired electrons.)

It is felt that the above investigators and others (18, 19, 25) have not considered the quenching mechanisms completely. Processes other than those considered may be involved. It is believed that the primary effect responsible for quenching by these and other chelates is energy transfer from the excited ketone to π-orbitals of the chelates. The transition metal d-orbitals interact with ligand orbitals in such a way that the energy levels of the ligand orbitals are shifted to a position favorable for accepting energy from excited sensitizor molecules.

The investigation was initiated in two directions: An experimental approach involved study of the quenching efficiencies of various selected chelates, and a theoretical approach where the energy levels of the chelates were estimated through molecular orbital calculations.

CHELATE MOLECULAR ORBITAL CALCULATIONS

Molecular orbital calculations were made in an attempt to help explain the quenching properties exhibited by a selected series of metal chelates. The chelate electronic states which are probably involved in energy transfer were determined. When combined with statistical arguments involving the conservation of electron spin for quencher and donor molecules, and the experimental observations, these calculations assist in the formulation of a possible mechanism for the quenching of excited triplet state molecules by transition metal chelates.

All chelates studied were composed of metal ions complexed by either two or three bidentate ligands. In general, the ligands were β-diketones. Those chelates with two ligands possess planar configurations and will be designated in following discussions by the abbreviation ML_2. Chelates with three ligands are octahedral and possess right- and left-hand "propeller" configurations. These chelates will be abbreviated as ML_3.

The solution of secular determinants corresponding to all electronic states of interest for each chelate was facilitated by use of an IBM 7090 computer. The program used allowed the evaluation

of eigenvalues, eigenvectors, charge distributions, and bond orders for any particular secular matrix.*

The most detailed calculations were made for the ML_3 acetylacetonate and dipivaloylmethide chelates of chromium, cobalt, iron, and aluminum. First approximation calculations were made for the ML_2 dipivaloylmethide chelates of cobalt, nickel, and copper. The σ- and π-molecular orbital systems were considered separately. The most precise calculations were made for ML_3 π-orbitals only. These calculations involved a reiterated solution of the secular determinant for ground and excited state configurations, until self-consistent electron distributions were obtained.

Selection of a Suitable Hamiltonian

The molecular orbitals were determined on the basis of an LCAO-MO approximation. Coulomb and resonance integrals, designated as $\underline{H}_{ii}$ and $\underline{H}_{ij}$, are derived from the operation of a modified one-electron Hamiltonian on linear combinations of normalized Slater atomic orbitals.

Given a problem containing N atomic orbitals, molecular wave functions may be expressed as

$$\psi_i = \sum_k a_{ik} \varphi_k \qquad (17)$$

where $\underline{\varphi}_k$ are atomic orbitals located on centers $\underline{k}$. The energy

*The program was obtained from Dr. Stanley Manatt of the Jet Propulsion Laboratory, California Institute of Technology.

corresponding to the orbital expressed by equation 17 is given by the operation of the Hamiltonian on the orbital wave function

$$\underline{H}\,\psi_i = E_i\,\psi_i \tag{18}$$

In general, the coefficients $\underline{a}_{ik}$ and the energies of the orbital functions are obtained from the solution of the matrix equation:

$$\det \left| H_{jk} - S_{jk}\,E \right| = 0 \tag{19}$$

where:

$$H_{jk} = \int \varphi_j \underline{H}\, \varphi_k \, d\tau \quad , \text{ for all j and k} \tag{20}$$

and:

$$S_{jk} = \int \varphi_j\, \varphi_k \, d\tau \quad , \text{ for all j and k .} \tag{21}$$

After making a Born-Oppenheimer assumption (37), considering inter-nuclear repulsions constant, and neglecting small second order terms, the general electronic Hamiltonian expressed in atomic units is:

$$\underline{H}_{elec} = \sum_n \left(-\tfrac{1}{2}\nabla_n^2 - \sum_k \frac{Z_k}{r_{nk}} \right) + \sum_{n \neq n'} \frac{1}{r_{nn'}} \tag{22}$$

Ignoring the electron-electron repulsion term

$$\sum_{n \neq n'} \frac{1}{r_{nn'}} \tag{23}$$

the Hamiltonian may be expressed as a sum of one electron Hamiltonians

$$\underline{H}_o = \sum_n \underline{H}_n^N = \sum_n \left(-\tfrac{1}{2}\nabla_n^2 - \sum_j \frac{Z_j}{r_{nj}} \right) \tag{24}$$

where $\underline{Z}_j$ is the nuclear charge on the j^{th} center.

Solutions of molecular problems which make use of the simple, one-electron-Hamiltonian approximation are, in general, not very accurate. Electron-electron repulsion terms are usually large and should be considered if possible.

A better approximation to the proper solution of a molecular problem results from the use of a self-consistent field (SCF) Hamiltonian. Equation 18 may be written as (38)

$$\left[H_1^N + \sum_j J_j - \sum_j{}' K_j \right] \psi_i(1) = E_i \psi_i(1) \tag{25}$$

where the terms J_j and K_j are defined as

$$J_j \psi_i(1) = \left(\int \psi_j^2(2) \frac{1}{r_{12}} d\tau_{12} \right) \psi_i(1) , \tag{26}$$

$$K_j \psi_i(1) = \left(\int \psi_j(2) \psi_i(2) \frac{1}{r_{12}} d\tau_{12} \right) \psi_j(1) . \tag{27}$$

The first term in the SCF Hamiltonian is the simple one electron Hamiltonian given by equation 24. The remaining two terms, J_j and K_j, account for electron-electron correlation. The value of these terms depends upon the molecular orbital wave function 17 which, in turn, depends upon coefficients $\underline{a}_{ik}$ determined from the evaluation of the secular determinant 19 .

The problem is solved by assuming reasonable initial values for the coefficients necessary for evaluation of $\underline{J}_j$ and $\underline{K}_j$. A new set of coefficients may then be obtained by solving the secular equation. The newly determined coefficients are then used for the evaluation of matrix elements in a second approximation matrix, which in turn yields a third set of coefficients. The process is reiterated until the coefficients obtained from the solution of the secular determinant are the same as those that went into the evaluation of the matrix elements. A major disadvantage encountered during this type of calculation is the necessity of evaluating a forbiddingly large number of integrals of type 26 and 27 during the reiteration processes.

A reduction of the number of terms requiring evaluation for each matrix element may be effected through the introduction of a core potential into the Hamiltonian (39). The σ-orbital system of a polyatomic molecule is considered to be sufficiently localized to allow the approximation that a specific σ-electron configuration is confined to given atoms within the molecule. The localized σ-electrons shield the nucleus from outer π-electrons. Therefore the π-electrons move in a coulombic field of shielded atomic nuclear charges. The Hamiltonian given by expression 25 may be altered by substituting effective nuclear charges for the actual ones. The problem is therefore reduced to making calculations for π-orbital systems only.

The effective nuclear charges remain constant throughout calculations of π-orbital energies and wave functions. The new SCF-Hamiltonian is

$$\underline{H} = \underline{H}_c + \sum_{j=1}^{n} J_j - \sum_{j=1}^{n} K_j \qquad (28)$$

and is similar to expression 25 but differs in that it is used only to operate on π-molecular orbitals.

Energies and wave functions for polymatomic molecules may also be determined by a perturbation treatment. The problem is first solved using a simple one-electron approximation. Electron-electron repulsion is then considered as a perturbation on the simple one-electron antisymmetrized state wave functions. New wave functions are built from linear combinations of the unperturbed state wave functions.

Both procedures described above for obtaining polyatomic molecular orbitals and calculation of the corresponding energy levels involve prohibitive amounts of arithmetic when considering large molecules. Chelates of the ML_3 type contain eighteen π-orbitals into which are placed an average of twenty-one electrons. In addition, there are electrons located in the chelate σ-bonds, as well as in non-bonding orbitals. A computer program necessary for the solution of these problems by the above methods was not available.

When a SCF Hamiltonian is used in evaluation of the

matrix elements for the secular determinant, the $\underline{K}_j$ and $\underline{J}_j$ integrals give rise to a series of terms represented by the general expression

$$(rs \mid tu) = \int \varphi_r(1)\, \varphi_s(1)\, \frac{1}{r_{12}}\, \varphi_t(2)\, \varphi_u(2)\, d\tau_1 d\tau_2 \qquad (29)$$

These terms are electron repulsive interactions between electron distributions on centers r, s, t, and u. The largest value for these integrals occurs when r=s=t=u (that is, when both electrons are located in atomic orbitals centered on the same atom). The second largest interaction results when the electrons are localized on adjacent atoms when $r=s \neq t=u$, and $r = t+1$ (39).

It has been shown, from studies of atomic systems, that repulsion between electrons localized on a given atom can be effectively approximated by the proper selection of nuclear shielding parameters (40). An effective nuclear charge so obtained is used in place of the actual unshielded charge in making calculations. The core potential used in making SCF calculations for π-orbital systems is an effective nuclear charge of this type; the nuclear shielding parameters arise from shielding by low-lying σ-electrons.

In order to make the simplifications which were necessary for solution of the chelate problems using the facilities available, a one-electron Hamiltonian was developed which had built into it a method of compensating for some electron-electron repulsion. The

Hamiltonian which was used differs from that defined by equation 24 in that effective nuclear charges are used in place of unshielded charges. The Hamiltonian is

$$\underline{H}_n^A = -\tfrac{1}{2}\nabla_n^2 - \sum_j \frac{Z_j^{eff}}{r_{nj}} \qquad (30)$$

where

$$Z_j^{eff} = Z_j - \sigma_{cj} - \sigma_{\pi j} \quad . \qquad (31)$$

Values for the effective nuclear charges, Z_j^{eff}, are determined from the unshielded atomic nuclear charges, Z_j, and two shielding parameters σ_{cj} and $\sigma_{\pi j}$. The parameter σ_c is essentially the one used for evaluating core potentials in standard SCF calculations and concerns low-energy non-bonding and σ-bonding electrons. The second parameter $\sigma_{\pi j}$ is concerned with nuclear shielding by π-electrons and is determined from the π-electron concentration on the center j.

An initial π-electron distribution is assumed which enables the evaluation of first order matrix elements for the molecular secular determinant. Solution of the determinant provides a new π-electron charge distribution. The new charge distribution is used to re-evaluate the matrix elements of the molecular determinant. The process is reiterated until the molecular electron distribution and state energy become self-consistent within given limits. This

calculation is conducted for ground and excited state electron configurations. The specific operations used in the evaluation of the shielding parameters and secular matrix elements are given in detail later.

Although this method has some shortcomings, it is able to include some electron correlation. In addition, the method simplifies calculations involving systems containing many hetero-atoms and d-p, π-bonding.

Determination of Effective Nuclear Charge Parameters

The method for evaluation of shielding parameters and effective nuclear charges described here was employed consistently throughout this series of calculations.

There are three possible cases for which contributions to shielding parameters must be evaluated. In the first, both atomic orbitals are centered on the atom whose effective nuclear charge is under consideration. In the second, one orbital is centered on the atom whose effective nuclear charge is being considered, while the other orbital is centered on an adjacent atom. These two cases are treated in the same manner.

In the third case, the atomic orbitals are centered on a nucleus or nuclei other than the one for which the effective nuclear charge is being evaluated. The method for determining the contribution

to the shielding parameter in this latter case will be outlined when the integrals in which they arise are discussed.

Slater's method for evaluating shielding parameters has been considerably successful in accounting for electron repulsion in atomic systems, thereby allowing the calculation of atomic ionization potentials with a fair degree of accuracy (40). In evaluation of shielding parameters for low energy core electrons, Slater's procedure is used with slight modifications.

In using this method, atomic orbitals are first combined into the groups

$$(1s),\ (2s, 2p),\ (3s, 3p),\ (3d),\ (4s, 4p),\ (4d),\ \cdots$$

The shielding parameter for a given electron is then determined as follows: A value of 0.35 is contributed to the shielding parameter for every other electron in the same group. When the electron under consideration is in an s- or p-orbital, a value of 0.85 is contributed to the shielding constant for each electron in the preceding group. If the electron under consideration is in a d-orbital, a value of 1.0 is contributed for each electron in the preceding group. A value of 1.0 per electron is assigned for all lower-lying electrons. Electrons in orbital groups succeeding the one being considered have no effect on the shielding constant.

Since low-angular momentum atomic orbitals may have radial distributions which penetrate closer to the nucleus than the radial distributions of high-angular momentum orbitals, it was felt that electrons in low-angular momentum orbitals in immediately succeeding groups should contribute to the shielding parameter of high-angular momentum orbitals. Therefore, to account for this effect, a modification of Slater's procedure was used in these calculations.

When calculating the shielding parameters for electrons in 3d-metal orbitals, a quantity of 0.15 was added for each electron in the 4s- and 4p-orbitals. The choice of 0.15 was motivated by an implication made in Slater's rules. Since the radial distributions of orbitals with principal quantum numbers greater than or equal to three do not differ considerably, the value of 0.15 is probably a lower limit for this contribution to the shielding parameter.

For the purposes of making molecular orbital calculations, atomic shells are grouped according to Slater's classification. The number of electrons assigned to each atom is determined as follows: All electrons localized in non-bonding atomic orbitals are assigned to the atom on which they are located. Electrons in specific σ-bonds are distributed between the two atoms connected by the bond according to the electronegativities of the two atoms. The number of π-electrons assigned is given by the π-electron concentration (on the atom under

consideration) as determined from the solution of the molecular determinant.

Since the molecular orbital calculations are conducted only on the π-orbital system, the non-bonding and σ-bonding electron distribution will remain constant for each atom while the π-electron distribution may vary. Therefore, shielding by the former is considered separately from the latter.

Following the classification of atomic orbitals, the shielding constants, σ_{cj} and $\sigma_{\pi j}$, are determined in the following manner. Non-bonding (n) and σ-electrons in atomic orbitals belonging to the same class as the atomic orbitals out of which the π-molecular orbitals are constructed each contribute a value of 0.35 to the shielding constant. If the atomic orbital contributing to the π-orbital system is p, a value of 0.85 is contributed for each n- or σ-electron in the preceding group. When the atomic orbital is d, a value of 1.0 is contributed for each n- or σ-electron in the preceding group. All electrons in groups lower than the immediately preceding group contribute a value of 1.0 to the shielding constant. Where the atomic orbital contributing to the π-system is 3d, a value of 0.15 is contributed to the shielding constant for each electron in the 4s and 4p atomic orbitals.

The two most commonly encountered situations for which shielding constants must be evaluated are for $2p^{\pi}$ and $3d^{\pi}$ electrons.

for $2p^{\pi}$ electrons the core-shielding parameter, $\sigma_{cj}(2p^{\pi})$, may be written as:

$$\sigma_{c_j}(2p^{\pi}) = 0.35\,(N) + 1.70 \qquad (32)$$

where N is the number of 2s and 2p non-bonding and σ-bonding electrons. The core shielding parameter for $3d^{\pi}$ electrons, $\sigma_{c_j}(3d^{\pi})$, may be written as:

$$\sigma_{c_j}(3d^{\pi}) = 0.35\,(M) + 0.15\,(R) + 18 \qquad (33)$$

where M is the number of non-bonding and σ-bonding 3d-electrons, and R is the number of 4s and 4p σ-electrons.

The problem of allocation of bonding pairs of σ-electrons to the two bonded nuclei is complicated somewhat if the two atoms are different. The method described here is felt to give the best possible distribution of electrons in non-symmetric σ-bonds.

Atomic electronegativities x_i obtained from Pauling's electronegativity table (41, 42) are related to the fraction of ionic character (P) in the σ bond between two atoms a and b by the expression (43)

$$P = 0.18\,|x_a - x_b|^{1.4} \quad . \qquad (34)$$

The electrons in a σ-bond with P ionic character are divided between the two bonded atoms as follows: The value of P

multiplied by the number of electrons in the bond is assigned to the most electronegative atom. The remaining fraction of electrons is considered to be in the covalent part of the bond and therefore is distributed evenly between the two atoms. Values for $\underline{P}$ obtained by the application of equation 34 to atom pairs forming bonds within the chelates studied are given in Table V .

Slater's method cannot be applied in the evaluation of the shielding parameters for delocalized π-electrons, σ_{π_i}. For this purpose the following method of evaluation was developed. When making calculations for atomic systems, electrons under consideration are located in orbitals localized on the same center. Each electron in the shell (or grouping of shells as defined by Slater's rules) under consideration is shielded from the nucleus by all other electrons in that shell. Therefore, it was analogously assumed that each π-electron located in a molecular system is shielded from the molecular core potential by all other electrons in the π-system.

That portion of an electron located at any time on a given center will be shielded by all other portions of π-electrons located on that center. In a large molecular system, the density of any one π-electron in a particular orbital on a given center will be small compared to the total π-electron density on that center. Therefore, it is <u>assumed</u> that the shielding parameter σ_{π_i} is proportional to the π-electron charge distribution at each atomic center. A numerical

TABLE V

Ionic Character of Chelate Atom Pairs

Atom Pair	Δx_{ij}	P_{ij}
Fe-O	2.05	0.480
Cr-O	2.45	0.630
Co-O	1.95	0.458
Al-O	2.35	0.593
Ni-O	1.95	0.458
Cu-O	1.75	0.394
O-C	1.10	0.205
C-C	0.00	0.000
C-H	0.50	0.067

x_i = electronegativity of atom i

$\Delta x_{ij} = |x_i - x_j|$

P_{ij} = fraction of ionic character in bond ij

value of 0.33 was chosen as the proportionality constant in making the calculations.

The charge distributions were calculated by solution of a secular determinant starting with a first order charge distribution assumed. Each new charge distribution was used to calculate new effective nuclear charges on each atomic center. These nuclear charges were then used for the evaluation of a new set of secular matrix elements. The process was reiterated until the π-electron charge distribution remained constant.

Coulomb, Resonance, and Overlap Integrals

Two basic types of atomic integrals result from the application of the Hamiltonian to molecular orbitals expressed as linear combinations of atomic orbitals. These are coulomb integrals

$$H_{ii} = \int \varphi_i \underline{H} \varphi_i \, d\tau = (\varphi_i \mid \underline{H} \mid \varphi_i) \tag{35}$$

and resonance integrals

$$H_{ij} = \int \varphi_i \underline{H} \varphi_j \, d\tau = (\varphi_i \mid \underline{H} \mid \varphi_j) \tag{36}$$

Substituting the value of the Hamiltonian into these equations, one obtains the expanded expressions

$$H_{ii} = (\varphi_i \mid -\tfrac{1}{2}\nabla^2 - \sum_k \frac{Z_k^{eff}}{r_k} \mid \varphi_i) \tag{37}$$

$$H_{ii} = (\varphi_i \mid -\tfrac{1}{2}\nabla^2 \mid \varphi_i) - (\varphi_i \mid \frac{Z_i^{eff}}{r_i} \mid \varphi_i) - \sum_{k \neq i} (\varphi_i \mid \frac{Z_k^{eff}}{r_k} \mid \varphi_i)$$

$$H_{ij} = (\varphi_i \mid -\tfrac{1}{2}\nabla^2 - \sum_k \frac{Z_k^{eff}}{r_k} \mid \varphi_j)$$

$$H_{ij} = (\varphi_i \mid -\tfrac{1}{2}\nabla^2 \mid \varphi_j) - (\varphi_i \mid \frac{Z_i^{eff}}{r_i} \mid \varphi_j) - (\varphi_i \mid \frac{Z_j^{eff}}{r_j} \mid \varphi_j) \tag{38}$$

$$- \sum_{k \neq i,j} (\varphi_i \mid \frac{Z_k^{eff}}{r_k} \mid \varphi_j)$$

Orbitals $\underline{\varphi}_j$ are Slater atomic orbitals (40) and are defined as

$$\varphi_j(\underline{n}, \underline{\ell}, \underline{m}) = \frac{(2\zeta_j)^{n+\frac{1}{2}}}{\sqrt{(2n)!}} r^{n-1} e^{-\zeta_j r} S_{\ell,m}(\theta, \varphi) , \tag{39}$$

where

$$\zeta_j = \frac{Z_j^{eff}}{\underline{n}} , \tag{40}$$

$\underline{n}$ is the principal quantum number, $\underline{l}$ is the orbital angular momentum quantum number, $\underline{m}$ is the magnetic quantum number, and $S_{\ell,m}(\theta, \varphi)$ are the normalized real spherical harmonics of hydrogen-like wave functions. The one and two center integrals in expressions 37 and 38 may be evaluated directly. The three center integrals, on the other hand, cannot, but can be approximated by terms which may be

directly evaluated. Such an approximation (44) is

$$(\varphi_j \mid \frac{Z_p}{r_p} \mid \varphi_k) \simeq \tfrac{1}{2}\left[(\varphi_j \mid \frac{Z_p}{r_p} \mid \varphi_j) + (\varphi_k \mid \frac{Z_p}{r_p} \mid \varphi_k)\right](\varphi_j \mid \varphi_k) . \quad (41)$$

In the present series of calculations, integrals of the three center variety were found to make no significant contributions to the values of the resonance integrals (H_{ij}). They were, therefore, neglected.

Expressions 37 and 38 contain two classes of integrals which need to be evaluated. They are kinetic energy integrals

$$(\varphi_a(n,\ell,m) \mid -\tfrac{1}{2}\nabla^2 \mid \varphi_b(n',\ell',m)) = \int \varphi_a(-\tfrac{1}{2}\nabla^2)\varphi_b \, d\tau \quad (42)$$

and two types of nuclear attraction integrals

$$(\varphi_a(n,\ell,m) \mid \frac{Z_a}{r_a} \mid \varphi_b(n',\ell',m)) = Z_a \int \varphi_a \frac{1}{r_a} \varphi_b \, d\tau \quad (43)$$

and

$$(\varphi_a(n,\ell,m) \mid \frac{Z_b}{r_b} \mid \varphi_a(n,\ell,m)) = Z_b \int \varphi_a \frac{1}{r_b} \varphi_a \, d\tau \quad . \quad (44)$$

The kinetic energy integrals may be expressed in terms of ordinary- and quasi-overlap integrals by the expression (45)

$$(\varphi_a(n,\ell,m) \mid -\tfrac{1}{2}\nabla^2 \mid \varphi_b(n',\ell',m)) = (-\tfrac{1}{2}\nabla^2\varphi_a(n,\ell,m) \mid \varphi_b(n',\ell',m))$$

$$= -\tfrac{1}{2}\zeta_a^2\left[(\varphi_a(n,\ell,m) \mid \varphi_b(n',\ell',m)) - 2(2n)^{\frac{1}{2}}(2n-1)^{-\frac{1}{2}}(\varphi_a(n-1,\ell,m) \mid \varphi_b(n,\ell',m))\right.$$

$$\left. + \frac{4(n+\ell)(n-\ell-1)}{[2n(2n-1)(2n-2)(2n-3)]^{\frac{1}{2}}} (\varphi_a(n-2,\ell,m) \mid \varphi_b(n',\ell',m))\right] . \quad (45)$$

Of the two types of nuclear attraction integrals, those defined by equation 43 may be expressed, in terms of overlap integrals, by

$$\left(\varphi_a(n,\ell,m) \left| \frac{Z_a}{r_a} \right| \varphi_b(n',\ell',m) \right) =$$

$$= \frac{2Z_a\zeta_a}{[2n(2n-1)]^{\frac{1}{2}}} \left(\varphi_a(n-1,\ell,m) \mid \varphi_b(n',\ell',m)\right) . \qquad (46)$$

Nuclear attraction integrals of type 44 may be evaluated directly without reduction to functions of overlap integrals. These integrals describe interactions between electrons localized on one center and a shielded nuclear charge on another. Only cases of adjacent atoms were considered here. If the atomic orbitals on the first center are pure $\underline{p}_\pi$, they cannot penetrate to the second center because the second center lies in a nodal plane of these orbitals. These nuclear attraction integrals are very similar to the coulombic repulsion integrals of the type described by equation 29, when $r = s \neq t = u$. As mentioned previously, these coulombic repulsion integrals have the second largest magnitude of the repulsion integrals encountered. Since there is little or no penetration to the positive center of the second atom by orbitals localized on the first, and since a large coulombic repulsion exists between electrons localized on the two centers, a nuclear-charge shielding parameter (necessary for evaluating the effective nuclear charge, $\underline{Z}_j^{eff}$, of the second atom) was

chosen as the product of 1.00 times the number of π-electrons located on that center. This may result in either a negative or a positive contribution from these integrals in the value of the matrix elements $\underline{H}_{ii}$. The magnitude of the effective nuclear charge on the isolated center calculated in the manner described is usually small. In addition, it was found that the values resulting from the solution of the "integral part" of expression 44 are generally small. Therefore, the contribution to the numerical value of the matrix element $\underline{H}_{ii}$ by the total integral 44 is usually not very significant.

Treatment of the integrals 42, 43, and 44 as described leads to a good approximation for the opposing effects of neighboring nuclear attraction and electron repulsion which are normally considered by standard self-consistent field calculations.

In order to arrive at numerical values for the matrix elements $\underline{H}_{ii}$ and $\underline{H}_{ij}$, a number of ordinary- and quasi-overlap integrals $(\varphi_a | \varphi_b)$ must be evaluated. The general procedure for making these calculations will be given below.

Slater atomic orbitals (40) are given in terms of spherical-polar coordinates. One center integrals may be solved in this coordinate system while two center integrals require prolate spheroidal coordinates for solution. The atomic orbitals are placed in the spheroidal coordinate system in the following manner: One atom is

placed in a left-handed, and the other is placed in a right-handed cartesian coordinate system. The positive $\underline{z}$-axis (where $\underline{\theta} = 0$) for each atom is chosen to point toward the other atomic center. A point in the spheroidal coordinate system is located in terms of the spherical coordinates by:

$$\xi = (r_a + r_b)\frac{1}{R}\,, \quad \eta = (r_a - r_b)\frac{1}{R}\,, \text{ and } \varphi = \varphi_a = \varphi_b\,, \tag{47}$$

where $\underline{r}_a$ and $\underline{r}_b$ are the radial distances of the point from the centers $\underline{a}$ and $\underline{b}$, respectively, and $\underline{R}$ is the internuclear distance expressed in units of Bohr radii. Expressions given in spherical polar coordinates are related to prolate spheroidal coordinates by

$$r_a = \tfrac{1}{2}(\xi + \eta)\, R$$

$$r_b = \tfrac{1}{2}(\xi + \eta)\, R$$

$$\cos\theta_a = (1 - \xi\eta)/(\xi + \eta)$$

$$\cos\theta_b = (1 + \xi\eta)/(\xi - \eta)$$

$$\sin\theta_a = [(\xi^2 - 1)(1 - \eta^2)]^{\frac{1}{2}}/(\xi + \eta)$$

and

$$\sin\theta_b = [(\xi^2 - 1)(1 - \eta^2)]^{\frac{1}{2}}/(\xi - \eta) \tag{48}$$

The integration volume element is given by the expression

$$d\tau = \frac{R^3}{8}(\xi^2 - \eta^2)\, d\xi\, d\eta\, d\varphi \tag{49}$$

The limits of integration are:

$$0 \le \varphi \le 2\pi, \quad -1 \le \eta \le 1 \text{ and } 1 \le \xi \le \infty\,. \tag{50}$$

Overlap integrals are functions of parameters ζ_a, ζ_b, and $\underline{R}$. In order to facilitate the solution of the integrals, these terms are replaced by new parameters defined by

$$\bar{\zeta} = \tfrac{1}{2}(\zeta_a + \zeta_b) \ ,$$

$$\tau = (\zeta_a - \zeta_b) \ / \ (\zeta_a + \zeta_b) \ ,$$

$$\rho = \bar{\zeta} R \qquad (51)$$

After making all necessary substitutions, the overlap integrals may be expanded in terms of incomplete γ-functions given by

$$A_k(\rho) \equiv \int_1^{\infty} \xi^k e^{-\rho\xi} d\xi = e^{-\rho} \sum_{\mu=1}^{k+1} [k! \ / \ e^{\mu}(k-\mu+1)!] \qquad (52)$$

$$B_k(\tau\rho) \equiv \int_{-1}^{1} \eta^k e^{-\tau\rho\eta} d\eta = -A_k(\tau\rho) + (-1)^k A_k(-\tau\rho) \qquad (53)$$

$B_k(0) = 2/k+1$ for k even; $= 0$ for k odd.

These functions have been tabulated for many values of $(\underline{\rho})$ and $(\tau\rho)$ (46, 47). Unfortunately, these tables are usually not very complete.

From the available values of $A_k(\rho)$ and $B_k(\tau\rho)$, the overlap integrals were evaluated. The values were plotted against (ρ). These plots yielded by interpolation values for all overlap integrals in the regions of interest. In addition, Mullikan has evaluated some overlap integrals involving 1s, 2s, 2p, 3s, 3p, 5s, and 5p orbitals, for both σ- and π-bonds (48). When possible, values were taken from his tables.

Evaluation of the overlap integrals is greatly simplified when $\zeta_a = \zeta_b$ and thus $\tau = 0$. Therefore, when $\bar{\zeta}$ can be used in place of ζ_a and ζ_b, a great deal of arithmetic involved in the calculation of matrix elements is eliminated. When both atomic centers are identical, or have nearly the same effective nuclear charge, the substitution of $\bar{\zeta}$ in place of the other terms is undoubtedly valid. For evaluation of the integrals of interest in the chelate calculations, it was found that this approximation served very well even when the values of ζ_a and ζ_b were considerably different.

In many cases rather large approximations were necessary to obtain the value of the integrals 45 and 46 when using ζ_a and ζ_b. These approximations were necessary because of the inadequacy of the tables of incomplete γ-functions. When using $\bar{\zeta}$, the necessity of making these approximations was eliminated. Therefore, since numerical values determined for the resonance integrals, H_{ij}, using either approximation were very similar, they were taken to be identical.

The same corresponding bond lengths were used throughout the series of chelate calculations. Crystal structures of most of the compounds studied here have not been determined. Ferric acetylacetonate is the only ML_3 chelate whose crystal structure has been studied in detail (49). The bond-lengths found for this chelate are 1.95 Å for the Fe–O bonds, 1.28 Å for the O–C bonds, 1.39 Å for

the C=C bonds, and 1.53 Å for the C—C bonds. In addition to the bond lengths given above, metal-oxygen bond lengths have been measured for other complexes between various metals and ligands (50). When the ligands are α-diketones, β-diketones, oxylate esters, and similar compounds, the metal-oxygen bonds vary consistently between 1.95 Å and 2.05 Å with the majority measuring about 2.00 Å . Therefore, the metal-oxygen bond length chosen for the purposes of these calculations was 2.00 Å. The carbon-oxygen and ring carbon-carbon distances that were used are those given above for ferric acetylacetonate.

Important kinetic-energy and nuclear-attraction integrals, evaluated in terms of overlap integrals for specific atomic orbitals, are given in Appendix A. Specific regular- and quasi-overlap integrals evaluated in terms of the incomplete γ- functions $A_k(\rho)$ and $B_k(\tau\rho)$ are also reported in Appendix A. The second type of nuclear attraction integrals (given by equation 44) are functions of two parameters ζ_a and the internuclear distance R. These integrals may be evaluated directly in terms of the incomplete γ-functions $A_k(\zeta_a R)$ and $B_k(\zeta_a R)$. Some nuclear attraction integrals of this type are also evaluated and reported in Appendix A.

ML_3 Chelate Molecular Orbitals

Metal-ligand σ-bonds are considered to be formed by interactions between sp^2 hybrid oxygen orbitals and 4s, 4p, and 3d or 4d transition-metal atomic orbitals. Neglecting strain or distortion resulting from the ligands, oxygen atoms are arranged about the central metal atom with octahedral symmetry. This is a valid assumption on the basis of the crystal studies on ferric acetylacetonate (49). The σ-molecular orbitals should, therefore, transform like representations of the O_h symmetry group.

The atoms may be placed in a cartesian coordinate system with the metal atom located at the origin and oxygen atoms lying equidistant from the origin along the x, y, and z axes. Linear combinations of individual oxygen atomic orbitals can be taken which may be classified by various symmetry classes of the O_h group. In addition, the metal atomic orbitals may also be classified according to symmetry classes of this group. Only orbitals with exactly matching symmetry may interact to form bonding and antibonding molecular orbitals. Table VI shows the classification of metal and isolated ligand atomic orbitals according to the symmetry classes of the O_h group.

The oxygen sp^2 hybrid orbitals may be represented as

$$x_{sp^2} = \frac{1}{\sqrt{3}} S + \frac{2}{3} p_\sigma \qquad (54)$$

where p_σ is directed along the internuclear axis.

Chelate σ-molecular orbitals may be written as

$$\psi_{\sigma} = N_c ({}_M\varphi_c + \epsilon \Gamma_c) \qquad (55)$$

where N_c is the normalization factor, subscript c refers to the symmetry class. The constant ϵ is either positive or negative, depending upon whether the orbital is bonding or antibonding, and has a magnitude which depends upon the degree of interaction between the metal orbital ${}_M\varphi_c$ and the ligand orbital Γ_c.

Only the lowest energy $\pi \rightarrow \pi^*$ transitions were of interest in this study. These transitions will be described in detail later. The chelate π-molecular orbitals which are involved in these low-energy transitions were, in all cases, lower in energy than the isolated 4s-, 4p-, and 4d-orbitals of the metals. They were also all higher in energy than the isolated atomic orbitals of oxygen. Chelate orbitals resulting from interaction between pairs of these isolated atomic orbitals may have either lower energy, if they are bonding, or higher energy, if they are antibonding, than the lowest or highest energy isolated atomic orbitals from which they are constructed.

Since the A_{1g} and T_{1u} σ-orbitals of the ML_3 chelates arise from combinations of metal 4s- and 4p-atomic orbitals with localized oxygen orbitals, numerical calculations were unnecessary for these bonds because their energies would be higher and lower than those of the π-orbitals of interest. It was necessary, however, to

calculate the energies resulting from interactions of metal $3d_{z^2}$ and $3d_{x^2-y^2}$ with oxygen atomic σ-combinations belonging to the E_g symmetry class. In general, these energies were intermediate with respect to the π-orbital energies of interest. The numerical values resulting from first order calculations for these molecular orbitals are reported in conjunction with the results from the π-orbital calculations.

The π-orbitals of the ML_3 chelates are considered in the same cartesian coordinate system as the σ-orbitals. They are formed by interactions between $3d_{xy}$, $3d_{xz}$, and $3d_{yz}$ metal atomic orbitals and p^{π} atomic orbitals of atoms comprising the ligands. The general secular determinant used for the evaluation of the π-orbital energies and wave functions is given in Figure Va. The matrix elements were determined by the methods outlined in pages 41 through 63. The calculated energies of the lowest electronic states of the iron, chromium, cobalt, and aluminum chelates of acetylacetone and dipivaloylmethane are given in Figure VI.

The ground state π-orbital system of the ML_3 chelates has D_3 symmetry, and therefore the orbitals may be classified by representations of that group. Representative energy levels of the orbitals obtained from the solution of a ground state molecular determinant are shown in the orbital diagram given in Figure VII. This diagram denotes a general situation and does not refer to any specific chelate. The orbital symmetries are recorded along with their degeneracies.

Figure Va. General ML_3 π-Orbital Matrix (Upper-half Diagonal)

	1	2	3	4	5	6	7	8	9	10	11	12	13	14	15	16	17	18
1	(M^2)	(M,O)																$-(O,M)$
2		(O^2)	(O,C)			$(O,O)^{\pi}$												$-(O,O)^{\sigma}$
3			(C_1^2)	(C_1,C_2)														
4				(C_2^2)	(C_1,C_2)													
5					(C_1^2)	(O,C_1)												
6						(O^2)	$-(O,M)$	$-(O,O)^{\sigma}$										
7							(M^2)	(M,O)										
8		$(a^2) = (a\|H\|a) - E$						(O^2)	(O,C_1)			$(O,O)^{\pi}$						
9		$(a,b) = (a\|H\|b) - (a\|b)E$							(C_1^2)	(C_1,C_2)								
10		$M = M^{\sigma}3d$								(C_2^2)	(C_1,C_2)							
11											(C_1^2)	(O,C_1)						
12		$O = O^{\sigma}2p$										(O^2)	$-(O,M)$	$-(O,O)^{\sigma}$				
13		$C_i = C_i^{\sigma}2p$											(M^2)	(O,M)				
14														(O^2)	(O,C_1)			$(O,O)^{\pi}$
15															(C_1^2)	(C_1,C_2)		
16																(C_2^2)	(C_1,C_2)	
17																	(C_1^2)	$(O,C_1$
18																		(O^2)

Consideration given to nearest neighbor interaction only with exception of $(O,O)^{\pi}$ $(O,O)^{\sigma}$.

Figure Vb. General ML_2 D_{2h}, π-Orbital Matrix (Upper-half Diagonal)

	1	2	3	4	5	6	7	8	9	10	11	12	13
1	(M_p^2)		$(M,O)^p$				$(M,O)^p$		$(M,O)^p$				$(M,O)^p$
2		(M_d^2)	$(M,O)^d$										$-(M,O)^d$
3			(O^2)	(O,C)			$(O,O)^\pi$		$(O,O)^\pi$				
4				(C_1^2)	(C_1,C_2)								
5					(C_2^2)	(C_1,C_2)							
6						(C_1^2)	(O,C_1)						
7							(O^2)	$(M,O)^d$					$(O,O)^\pi$
8								(M_d^2)	$-(M,O)^d$				
9									(O^2)	(O,C)			$(O,O)^\pi$
10										(C_1^2)	(C_1,C_2)		
11											(C_2^2)	(C_1,C_2)	
12												(C_1^2)	(O,C_1)
13													(O^2)

$(a^2) = (a|H|a) - E$

$(a,b) = (a|H|b) - (a|b)E$

$M_p = \varphi_{M,4p_z}$

$M_d = \varphi_{M,3d}$

Consideration given to nearest neighbor interaction only with exception of $(O,O)^\pi$

Since there are a number of $\underline{a}_1$, $\underline{a}_2$- and $\underline{e}$-orbitals, superscripts in parentheses are added in order to give more specific designations to the individual orbitals for the purpose of clarity and reference.

Of the eighteen chelate π-orbitals, the lowest nine are filled by the eighteen electrons contributed to the π-system by the three ligands. The next highest energy π-orbitals are occupied by electrons contributed by the metal ion. Both iron and chromium contribute three electrons to the π-system, cobalt contributes six, and aluminum contributes none. The number of electrons contributed to the π-system by the metal is determined from the number of $\underline{3d}$ electrons contained on each metal ion when isolated from the ligands, and by reference to the results from paramagnetic susceptibility measurements made on the chelates.

Magnetic measurements have been made on iron(III), cobalt(III), and chromium(III) acetylacetonate chelates at liquid helium temperature (51, 52, 53). These measurements indicate that the ground states of the iron(III) and chromium(III) chelates have five and three unpaired electrons, respectively. Cobalt(III) acetylacetonate, on the other hand, is diamagnetic, indicating that an inner $\underline{d}$-complex is formed. The aluminum dipivaloylmethide and acetylacetonate chelates are diamagnetic

The dipivaloylmethide chelates are assumed to have the same magnetic susceptibility in their ground states as the corresponding acetylacetonate chelates. Even though magnetic measurements have not been made on these chelates, available experimental evidence supports this conclusion. Nuclear magnetic resonance spectra were obtained for both the dipivaloylmethide and acetylacetonate chelates of cobalt(III) and aluminum, while none could be obtained for either the chromium or iron chelates (54, 28). In the latter two cases, both chelates have an odd number of electrons and therefore must be paramagnetic, thus accounting for the inability to obtain spectra. The fact that spectra could be obtained in the first two cases indicates that both chelates are probably diamagnetic. The NMR results, however, do not show whether the iron and chromium chelates are electronically identical to their acetylacetonate counterparts. The strongest evidence for a close relationship comes from the similarity of their ultraviolet and visible spectra. Corresponding acetylacetonate and dipivaloylmethide chelates have spectra which are practically superimposable. In addition, molecular orbital calculations predict identical electronic structures for corresponding chelates.

Two of the five unpaired electrons in the ground state configuration of the iron chelates are considered to be located in e_g nonbonding or σ-antibonding orbitals. The three remaining unpaired electrons are therefore located in the π-system. All three of the

unpaired electrons in the ground state of the chromium chelate are considered to be located in the π-orbital system, thereby making the π-systems of the iron and chromium chelates isoelectronic.

Since the σ- and π-orbital systems belong to different symmetry species, they were considered separately in these calculations. The lowest energy configuration of the σ part of the chromium chelate has an even number of paired electrons and is therefore hypothetically a singlet. On the other hand, the two unpaired electrons in the σ part of the iron chelates can give either singlet or triplet hypothetical states. The "triplet" will have lower energy than the "singlets," and therefore is considered to be the "ground state" of the σ electronic system of the iron chelates. The possible σ states may exist for all possible "π"-states. The degree to which the σ- and π- states are mixed is unknown; however, it is felt that the mixing is not large.

The lowest energy π-states of the FeL_3 and CrL_3 chelates are quartet states where the total π-electron spin angular momentum quantum number is 3/2, and where each of the three electrons contributed by the metal to the π-system singularly occupies one of the three lowest energy unfilled π-orbitals. These molecular orbitals are a singly degenerate $\underline{a}_1^{(2)}$ orbital and a degenerate pair of somewhat higher energy $\underline{e}^{(4)}$ orbitals. This electronic configuration gives an electron distribution which is symmetric about the central metal atom.

Combination of the quartet π-electron ground state configurations for the chromium and iron chelates with the proper σ-configurations gives the total ground state electron configurations for the chelate molecules. The σ- and π-orbital parts of the cobalt(III) and aluminum chelates do not contain any unpaired electrons and therefore allow only singlet ground state configurations.

Only energies for the lowest excited states were calculated. These excited states may result from $\underline{n}$-π^*, π-n*, π-σ^*, σ-π^*, or π-π^* transitions. The ones of primary interest in this study involve σ-σ^* and π-σ^* or π-n* transitions. In general, the π-π^* transitions lie at such short wavelength that they were not considered (see page 65).

First, consideration is given to the low energy π-σ^* or π-n* transitions, which are similar to the transitions occurring in an ordinary, ionic crystal field (55). These transitions are between the lowest unfilled σ^*-orbitals and the highest energy occupied π-orbitals and are symmetry forbidden.

It is observed from the results of the molecular orbital calculations that the highest energy occupied π-orbitals contain considerable $\underline{d}$ character. The $\underline{d}_{xy}$-, $\underline{d}_{xz}$-, and $\underline{d}_{yz}$-orbitals, when considered in the same coordinate system as the chelate σ-orbitals, belong to the T_{2g} symmetry class of the O_h group. The lowest energy available σ^* or metal non-bonding orbitals belong to the E_g symmetry class. Transitions between t_{2g} and e_g orbitals are symmetry forbidden.

For the cobalt(III), iron(III), and chromium(III) chelates, these transitions occur in the visible region of the spectrum and have normal extinction coefficients of about 10^2. Specific transition assignments will be made later for each chelate under consideration.

The π-π^* transitions are of particular interest because they are probably the ones responsible for the quenching of benzophenone triplets (see page 40). The calculated π-states and transition energies for the chromium and iron chelates will be discussed first. A discussion of the cobalt(III) and aluminum chelates will follow.

Since the π-electronic systems of the chromium and iron chelates are isoelectronic, they will be discussed in terms of the spin multiplicities of the π-electronic states only. It must be remembered that while a specific spin multiplicity of a π-state of a chromium chelate corresponds to the spin multiplicity of the complete chelate, this is not true for the iron chelates. As a result of there being two unpaired non-bonding electrons on the metal ion, the total spin multiplicity of the iron chelates will be two greater than that reported for the π-system alone. In other words, a quartet π-state will correspond to a sextet chelate state and a doublet π-state will correspond to a chelate quartet state for the iron chelates. As mentioned on page 69, the lowest energy ground π-state configurations for the iron and chromium chelates are quartet states (Q_0), where one of the three unpaired electrons is located in the $\underline{a}_{-1}^{(2)}$ orbital and two electrons

are each located in separate degenerate $\underline{e}^{(4)}$ orbitals. In both chelates, a pair of nearly degenerate low energy doublet states exist (D_1) which are slightly higher in energy than the ground quartet. These doublets have two electrons in the $\underline{a}_1^{(2)}$ orbital and one electron in an $\underline{e}^{(4)}$ orbital. The energies of these two low energy doublet states are probably sufficiently close to the ground quartet state to allow considerable occupation of the higher doublet states at room temperature. At liquid helium temperature , exclusive occupation of the lower quartet state may be effected, thus providing a high spin measurement at this temperature. Experimental evidence supporting this hypothesis will be given later.

The next lowest energy $\pi \rightarrow \pi^*$ excited state is a doublet (D_2) and has the same orbital composition as the ground state quartet. This doublet is followed in energy by another nearly degenerate pair of doublets (D_3) which have one electron in the $\underline{a}_1^{(2)}$ orbital and two paired electrons occupying one of the two $\underline{e}^{(4)}$ orbitals. The two $\underline{e}^{(4)}$ orbitals are degenerate for the symmetric ground state electron distribution as shown in Figure VII. However, in this latter pair of D_3 doublet excited states and in the lowest energy D_1 doublets, the electron distribution is not symmetric about the central metal atom. The chelate no longer possesses exact D_3 symmetry when in these excited states. The distortion is not large, but is sufficient to cause a removal of the degeneracy of the $\underline{e}$ orbitals.

Following the doublet states described above are the lowest excited quartet states Q_1. There are four states which would be degenerate if it were not for the removal of the $\underline{e}$ orbital degeneracy through the formation of unsymmetrical charge distributions in the excited states. The separation of the orbital degeneracies here is greater than encountered in the case of the doublet states mentioned above.

Still higher in energy is a singularly degenerate quartet state Q_2, formed by the excitation of an $a_2^{(2)}$ electron to the $a_1^{(2)}$ orbital. One electron is contained in each $\underline{e}^{(4)}$ orbital and the excited molecule retains its D_3 symmetry in its excited state. Above this state is another nearly degenerate doublet pair D_4 which contains three electrons in the two $\underline{e}^{(4)}$ orbitals. These states have unsymmetrical charge distributions and are therefore not expected to be degenerate.

The procedure used for making molecular orbital calculations is unable to distinguish between states of different spin multiplicity. However, the calculations do yield relative energy separations of electronic states of identical multiplicity. Therefore, it was necessary to find some method by which the energies of electronic states with identical space parts but different spin functions could be established relative to each other. By assuming that the Q_0 quartet and D_1 doublet π-states of the CrL_3 and the FeL_3 chelates were sufficiently

close that significant occupation of the higher energy D_1 states was possible at room temperature, the ultraviolet and visible spectra of the chelates could be predicted with reasonable accuracy.

Observing Figures VI and VIII, it is seen that the calculated transition energies follow the same energetic trend as is demonstrated by the ultraviolet spectra of the chelates. Table VII shows the relationship between calculated transition energies and the spectrally observed transition energies. The calculated transition energies were determined by assuming that the calculated energy separations were proportional to the wave number of the transition. A single calculated transition energy was assigned a wave number corresponding to an observed transition to which it was believed that the calculated transition belonged. All other transition energies for all chelates were then estimated by using the first assigned transition as reference. This reference transition is designated in Table VII.

The assumption that the Q_0 and D_1 states are close in energy alone is not enough. Moderate occupation of both states is required if the optical transitions have been properly assigned. According to Table VII, the lowest energy $\pi \rightarrow \pi^*$ transitions result from the excitation of an electron from some low energy "ground" state to the D_2 and D_3 doublets. If all of the molecules are in the ground quartet state (Q_0), then these lowest $\pi \rightarrow \pi^*$ transitions would be multiplicity forbidden. A spin orbit perturbation may allow a small transition

Table VII

Calculated and Observed $\pi \rightarrow \pi^*$ Transition Energies and Spectra

Chelate	Transition	Transition Energy (eu)	Transition Energy (cm^{-1})	Calc. Wavelength ($m\mu$)	Obs. λ_{max} ($m\mu$)	Remarks
FeL_3	$Q_0 \rightarrow Q_1$	0.2855	28550	354	380	Broad absorption, no separation of bands- $\varepsilon \sim 5 \times 10^3$
		0.2868	28680	349	↑(350	
		0.2889	28890	346	↓max)	
		0.2902	29020	344	330	
	$Q_0 \rightarrow Q_2$	0.4637	46370	226	270	$\varepsilon \sim 30000$
	$D_1 \rightarrow D_2$	0.2225	22250	450	550	Very broad peak, no separation of bands. $\varepsilon \sim 4 \times 10^3$. $\pi \rightarrow \sigma^*$ transitions also occur in this region $\varepsilon \sim 10^2$
		0.2232	22320	448	↑	
		0.2524	25240	396	(435	
		0.2531	25310	395	max)	
		0.2531	25310	395	↓	
		0.2538	25380	394	380	
	$D_1 \rightarrow D_4$	0.4756	47560	210	235	$\varepsilon \sim 15000$
		0.4763	47630	210		
		0.4763	47630	210		
		0.4770	47700	210		
CrL_3	$Q_0 \rightarrow Q_1$	0.3428	34280	300	350	Strong absorption $\varepsilon = 2 \times 10^4$, sharp peaks some indications of more than one band.
		0.3444	34440	298	↑(330	
		0.3450	34500	297	↓max)	
		0.3466	34660	296	300	
	$Q_0 \rightarrow Q_2$	0.4762	47620	221	242	$\varepsilon \sim 10^4$
	$D_1 \rightarrow D_2$	0.2336	23360	428	440(430)	Broad band with $\varepsilon \sim 10^3$. Separation of band observed into maxima given in parentheses.
		0.2353	23530	425	↑ (410)	
	$D_1 \rightarrow D_3$	0.2633	26330	380	(390)	
		0.2650*	26500*	378	(380)	
		0.2650*	26500*	378	↓ (380)	
		0.2667	26670	375	365(375)	
	$D_1 \rightarrow D_4$	0.4969	49690	202	220	($\pi \rightarrow \sigma^*$ transition at 5600 Å, $\varepsilon \sim 10^2$)
		0.4986	49860	201		
		0.4986	49860	200		
		0.5003	50030	200		

*Used as wave no. reference (.2650 eu=26500 cm^{-1})

Table VII (continued)

Chelate	Transition	Transition Energy (eu)	Transition Energy (cm^{-1})	Calc. Wavelength (mμ)	Obs. λ_{max} (mμ)	Remarks
CoL_3	$S_0 \rightarrow S_1$	0.3472	34720	290	less	$\pi \rightarrow \sigma^*$ transition
		0.3507	35070	286	than	observed at 600
		0.3606	36060	277	360,	mμ, $\epsilon \sim 200$
		0.3641	36410	274	$\epsilon > 10^3$	
	$S_0 \rightarrow S_2$	0.5510	55100	181	257	$\epsilon \sim 32000$
		0.5620	56200	178		very broad
	$S_0 \rightarrow S_3$	0.8830	88300	113	228	$\epsilon \sim 34000$
		0.8890	88900	114		very broad
	$S_0 \rightarrow T_1$	0.2625	26250	382		
		0.2660	26600	376		
		0.2759	27590	363		
		0.2794	27940	358		
	$S_0 \rightarrow T_2$	0.2837	28370	352		
AlL_3	$S_0 \rightarrow S_1$	0.7947	79470	126		
	$S_0 \rightarrow S_2$	0.8134	81340	123	270	
		0.8140	81400	123		
	$S_0 \rightarrow T_1$	0.5407	54070	185		
	$S_0 \rightarrow T_2$	0.6677	66770	150		
		0.6683	66830	150		

probability. However, the extinction coefficients observed for these transitions for both FeL_3 and CrL_3 chelates are of the order of 10^3. The extinction coefficients for the iron chelates are larger than that for the chromium chelates by a factor of five. The only way in which the high transition probabilities may arise is that the transition be multiplicity allowed. This can only occur if there is significant occupation of the D_1 doublet states at room temperature. Some additional evidence supporting this assumption was obtained experimentally and will be described following the discussion of the electronic spectra of these chelates.

Consideration is given first to the spectra of the CrL_3 chelates. An absorption observed at 5600 Å with an extinction coefficient of 10^2 is considered to correspond to a $\pi \rightarrow \sigma^*$ transition of the type described on page 70. The grouping of four or possibly five absorption bands which lie together between 3700 Å and 4200 Å are felt to correspond to the $D_1 \rightarrow D_2$ and $D_1 \rightarrow D_3$ transitions. The separate maxima of these peaks are distinguishable and are reported in Table VII. The extinction coefficients of these transition maxima are about 10^3. The very intense absorption band observed at 3370 Å is assigned to the $Q_0 \rightarrow Q_1$ transitions. The molecular orbital calculations indicate that there should be four closely spaced transitions in this region. All four are felt to lie under the same absorption peak. This absorption band has

an extinction coefficient that is twenty-five times greater than the $D_1 \rightarrow D_2$ and $D_1 \rightarrow D_3$ absorption bands.

No separate $\pi \rightarrow \sigma^*$ absorption bands are observable with the iron chelates, in contrast to the case of the chromium chelates. It is felt that these transitions, of which there are several, lie under the low energy $\pi \rightarrow \pi^*$ doublet-doublet absorption bands. These latter bands are found in the region between 3750 Å and 5250 Å. There is no apparent separation between various component absorption bands within this particular grouping as observed in the chromium chelates. This may be accounted for by the increased number of transitions which may occur within the same wavelength region, and the fact that the transition energies are not as greatly separated in the case of iron as in the chromium chelates. The observed composite absorption band exhibits no fine structure and has a maximum extinction coefficient of about 5×10^3 at 4300 Å.

The higher energy $\pi \rightarrow \pi^*$, $Q_0 \rightarrow Q_1$ bands are found in the region between 3250 Å and 3850 Å and have an observed maximum extinction coefficient of about 5×10^3 at room temperature in benzene. The molecular orbital calculations predict that there should be four transitions in this grouping; however, the energies of these transitions are apparently so close together that no separation may be expected to be observed.

Returning now to the assumption that the pair of D_1 π-states are close to the ground quartet state, it is apparent that unless all of these states have exactly the same energy, the spectra should be subject to variations corresponding to changes in temperature. These states cannot have the same energy since magnetic measurements indicate that $Fe(AA)_3$ and $Cr(AA)_3$ have five and three unpaired electrons at 10°K. (51). Experiments concerning a possible temperature effect were attempted and the predicted variation was observed. Since the lowest $\pi \rightarrow \pi^*$ multiplicity allowed transitions probably originate from D_1 doublets, a decrease in temperature should and did bring about a decrease in the ratio of these lowest energy absorption bands to the higher energy bands assigned to the $Q_0 \rightarrow Q_1$ transitions. An increase in temperature, on the other hand, should and did induce an increase in the ratio of band intensities. Unfortunately, however, the results were not as definitive as had been hoped.

Spectra were taken of the chelates at room temperature and at the temperature of a slush made from Dry-ice and isopropyl alcohol. The solvent used was 60-70 ligroin. This solvent was chosen because it is non-polar and does not significantly complex or exchange with ligands of the chelate. It also does not freeze or solidify at the temperatures where the spectra were made.

The spectra of a particular chelate taken at the two different temperatures were very similar. There was no shift in the peak maxima or shape. The only variation observed was in the relative intensities of the two composite bands. It was impossible to determine absolute changes in the separate extinction coefficients since cooling produced a decrease in volume of the solvent and therefore produced an increase in the chelate concentration.

The chromium chelates presented the greatest difficulty in observing a temperature effect. Since the $Q_0 \rightarrow Q_1$ absorption bands are twenty-five times greater than the lower energy bands originating from the D_1 doublet states, it became quite difficult to measure accurately relative changes in peak maxima produced by lowering the temperature. However, a definite decrease in the ratio corresponding to a decrease in the temperature was observed.

The iron chelates present a quite different picture from the chromium chelates. In ligroin the ratio of the two absorption bands of interest have equal extinction coefficients of 5×10^3 at room temperature. The main difficulty encountered here is that the temperature effect is not large. By assuming that the temperature difference between the sample at room temperature and at the temperature of a slush of Dry-ice and isopropyl alcohol is 100°, the difference in energy between the ground Q_0 quartet and the D_1 doublet states could be estimated from the Boltzmann factor relating the population of the higher to lower energy states at the two temperatures.

The results from these experiments concerning both chelates are given in Table VIII. The energy separation (ΔE) in ligroin solvent for the iron chelate is 102 cal./mole. Using this energy value, the relative absolute extinction coefficients for the upper to lower states (ϵ_u/ϵ_ℓ) can be estimated. This ratio is 1.19 for the iron chelate in ligroin. Using the value for ΔE given above, the relative population of the upper to lower states was estimated for various temperatures between 4° and 20° K. It is seen that almost exclusive occupation of the ground Q_0, π-states is attained at temperatures less than 20° K.

The value of ΔE for the chromium chelates is subject to more doubt than for the iron chelates because of the large differences in the extinction coefficients of the two absorption bands. By assuming that the ratio of absolute extinction coefficients, ϵ_u/ϵ_ℓ, for the two transitions is the same as for the iron chelates, ΔE may be calculated at a single temperature. This value so obtained is 800 cal./mole. However, using the best approximation for the change in the ratio between the two temperatures, ΔE is 580 cal./mole, and ϵ_u/ϵ_ℓ is 0.5.

In addition to the above temperature effect, the spectra are subject to a variation with solvent as well. No shifts in the wavelength maxima of the absorption bands were observed; however, the extinction coefficients underwent a considerable change. The most significant variation was observed for the iron chelates, where the relative intensities of the two bands are similar. In ligroin the ratio of peak

Table VIII

Temperature Effects on the Electronic Spectra of the $Fe(AA)_3$ and $Cr(AA)_3$ Chelates

Chelate	Temp. (°K)	R_o	$\frac{\epsilon_u}{\epsilon_\ell}$	ΔE (cal./mole)	Remarks
$Fe(AA)_3$	300	1.0 L	--	--)	Used for calculating ΔE and ϵ_u/ϵ_ℓ for this chelate in ligroin
	200	0.91 L	1.19	102)	
	20	0.084	1.19	102	
	14	0.031	1.19	102	
	10	0.007	1.19	102	Calculated assuming ΔE = 109 cal./mole and ϵ_u/ϵ_ℓ = 1.19
	4	0.000+	1.19	102	
$Fe(AA)_3$	300	0.75 A	--	--)	Used for calculating ΔE and ϵ_u/ϵ_ℓ for this chelate in ethanol
	200	0.69 A	1.11	102)	
$Cr(AA)_3$	300	0.055L	0.5	--	Calculated directly assuming temp. variation of R accurate. (Subject to much doubt)
	200	<0.027L	0.5	580	
$Cr(AA)_3$	300	0.055L	1.19	800	ΔE calculated assuming ϵ_u/ϵ_ℓ = 1.19

1. $R_o = \frac{OD_u}{OD_\ell} = \frac{\epsilon_u C_u}{\epsilon_\ell C_\ell}$

2. D_u = optical density of the $D_1 \rightarrow D_2, D_3$ transitions.

3. OD_ℓ = optical density of the $Q_0 \rightarrow Q_1$ transitions.

4. ϵ_i = extinction coefficient for the transition involving the i^{th} ground state.

5. C_i = concentration of molecules in the i^{th} ground state.

6. $R_o = \frac{\epsilon_u}{\epsilon_\ell} e^{-\frac{\Delta E}{RT}}$

7. $\Delta E = 2.303 \frac{RT_1T_2}{T_1 - T_2} \log R_o$

8. ΔE = difference of energy between the Q_0 and D_1 states.

9. T = Temp. (° K)

10. L = ligroin solvent
A = alcohol solvent

maxima is 1.0, while in ethanol the ratio drops to 0.75 at room temperature. The temperature variation in both solvents is the same (see table VIII), therefore yielding the same value for the energy difference (ΔE) between the two "ground" states. The difference observed between the two solvents therefore probably results from an effect on the absolute extinction coefficients of the absorption bands by the solvent. The polar solvent apparently decreases the transition dipoles by different amounts. In non-polar solvent (such as ligroin) the extinction coefficients for both transitions at room temperature are 5×10^3, while in ethanol the extinction coefficients are 4.4×10^3 and 3.3×10^3 for the $Q_0 \rightarrow Q_1$ and the $D_1 \rightarrow D_2$, D_3 transitions respectively.

The ground states of both the CoL_3 and the AlL_3 chelates are singlets (S_0). The $a_1^{(2)}$ and $e^{(4)}$ orbitals of the cobalt chelates are filled, while they are vacant in the aluminum chelates. The ground states of both sets of chelates have symmetric electron distributions about the central metal atom and therefore possess D_3 symmetry.

The lowest energy excited singlet states (S_1) and corresponding triplet states (T_1) of the cobalt chelates result from the excitation of an $\underline{e}^{(4)}$ electron to one of the two $\underline{e}^{(5)}$ orbitals. There are four possible combinations of $\underline{e}$ orbitals which can lead to four states for each possible spin multiplicity. The energies of the excited states are close

together but not degenerate due to their unsymmetrical charge distributions.

The next highest energy singlet and triplet π-states result from the excitation of an $\underline{a}_1^{(2)}$ electron to an $\underline{e}^{(5)}$ orbital. Disregarding spin, two possible states resulting from this type of excitation can be formed. The highest energy singlet and corresponding triplet states on which calculations were made for the cobalt chelates result from the excitation of an $\underline{e}^{(4)}$ electron to an $a_1^{(3)}$ orbital. Here also there are two possible states for each spin multiplicity.

The cobalt chelates exhibit two types of visible and near ultraviolet transitions. A strong $S_0 \rightarrow S_1$, $\pi \rightarrow \pi^*$ transition is observed in the region of 3300 Å with a maximum extinction coefficient of 10^4. A weak transition, with a maximum extinction coefficient of about 10^2 at 6000 Å, is observed to occur between 5100 Å and 6900 Å. This latter transition is assigned to low energy $\pi \rightarrow \sigma^*$ transitions.

The lowest energy excited singlet (S_1) and corresponding triplet states T_1 of the aluminum chelates result from the promotion of an $\underline{a}_2^{(2)}$ electron to an $\underline{a}_1^{(2)}$ orbital. Since both orbitals are singularly degenerate, there is only one singlet and one corresponding triplet with this excited orbital configuration. The next highest singlet (S_2) and corresponding triplet states (T_2) result from the excitation of an $\underline{a}_2^{(2)}$ electron to one of the $\underline{e}^{(4)}$ orbitals. Both triplet states described for the aluminum chelates are probably of sufficiently high energy that

they are unable to accept excitation energy from the triplet state of benzophenone.

The aluminum chelates exhibit no visible absorption spectra and none is predicted on the basis of the molecular orbital calculations. The maximum of the lowest energy absorption band is observed at 260 mμ.

As will be shown later, the results from the quenching experiments run with these acetylacetonate and dipivaloylmethide chelates support the assignment of electronic states made here. The ability of the chelates to quench triplet benzophenone parallels the predicted availability of $\pi \rightarrow \pi^*$ electronic states and shows no correlation with the energies of $\pi \rightarrow \sigma^*$ transitions. This is in accord with an observation made by Porter (17), who found no correlation between the transition energies of solvated transition metal ions and their abilities to quench anthracene triplets. More will be said in this connection in following sections.

It should be emphasized that the assignment of excited states made here is based on the results of the present molecular orbital calculations and several experimental observations. Therefore, they may be subject to change when better calculations are made and additional experimental observations are made.

ML_2 Chelate Molecular Orbitals

Only brief consideration was given to the ML_2 chelates. The dipivaloylmethide chelates of cobalt(II), nickel(II), and copper(II) are planar (54, 56, 57, 58). The cobalt and copper chelates are paramagnetic, and the nickel chelate is diamagnetic.

The ML_2 σ-orbitals may be classified by representations of the D_{4h} symmetry group. The symmetry classification of isolated ligand oxygen and metal atomic orbitals are given in Table IX.

The π-orbitals may be classified by representations of the D_{2h} symmetry group. Metal atomic orbitals that are unable to interact with oxygen atoms to form σ bonds and which may interact with ligand π-orbitals are reclassified according to the D_{2h} group. The $3d_{xy}$ and the $3d_{z^2}$ metal orbitals do not interact with the ligand in either the σ- or π-orbital systems. These orbitals are thus non-bonding in the chelates. The $4p_z$-, $3d_{xz}$-, and $3d_{yz}$- orbitals do interact with ligand π-orbitals. In all three cases considered, transitions between b_{2g} and b_{1u} chelate π-orbitals are lowest in energy. These transitions are symmetry allowed. This low energy transition involves an electron shift from the ligands to the metal $4p_z$-orbital. This causes a general lowering of total π-energy of the excited state with respect to that estimated from the separation of the b_{2g}- and b_{1u}-orbitals obtained from the ground state calculation.

TABLE IX

Symmetry Classification of Metal-atomic and Ligand-atomic Orbitals Constituting the σ-Orbital System of the ML_2 Chelates According to the D_{4h} Symmetry Group.

Symmetry Class	Metal Atomic	Ligand Atomic
A_{1g}	φ_s	$\Gamma_{a_{1g}} = \frac{1}{2}(x_1 + x_2 + x_3 + x_4)$
E_u	φ_{px}	$\Gamma_{e_u,x} = \frac{1}{\sqrt{2}}(x_1 - x_2)$
	φ_{py}	$\Gamma_{e_u,y} = \frac{1}{\sqrt{2}}(x_3 - x_4)$
B_{1g}	$\varphi_{dx^2-y^2}$	$\Gamma_{b_{1g},x^2-y^2} = \frac{1}{2}(x_1 + x_2 - x_3 - x_4)$
A_{1g}	φ_{dz^2}	
A_{2u}	φ_{pz}	
B_{2g}	φ_{dxy}	
E_g	$\varphi_{dxz}, \varphi_{dyz}$	

x_i are localized oxygen atomic orbitals and described by equation 55.

The oxygen atoms are numbered as shown below.

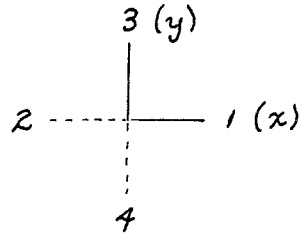

Figure IX is a diagrammatic representation of the b_{1g}-σ-, and π-orbitals of the ML_2 chelates. As with the ML_3 diagram, the orbitals shown do not represent those for any specific chelate, but rather describe the general relative energy locations of these orbitals for this particular class of chelates. The corresponding orbital symmetries are given.

Only values for lowest energy transitions were computed. These values were determined from a single reiterated computation, whereas six or seven reiterations were normally performed in estimation of the levels of ML_3 states. π-σ^* transitions were not considered in the actual numerical calculations. The results indicated that the cobalt(II), nickel(II), and copper(II) dipivaloylmethide chelates, which are all planar, have low energy $\pi \rightarrow \pi^*$ electronic states. The energies of these transitions are all close to the lowest energy iron and chromium $\pi \rightarrow \pi^*$ transitions. The calculations predict that all three chelates should probably be approximately equally efficient quenchers of triplet benzophenone.

QUENCHING OF TRIPLET BENZOPHENONE

The reaction system used in this investigation was the photoreduction of benzophenone by benzhydrol in benzene. A simple reaction sequence which describes the overall photochemical process in the absence of oxygen or other quencher was given in the discussion on actinometry. Following is a more complete reaction sequence than the one given earlier.

$$\varphi_2CO + h\nu \longrightarrow \varphi_2CO^{*S} \tag{56}$$

$$\varphi_2CO^{*S} \xrightarrow{k_f} \varphi_2CO + E \tag{57}$$

$$\varphi_2CO^{*S} \xrightarrow{k_{is}} \varphi_2CO^{*T} \tag{58}$$

$$\varphi_2CO^{*S} + Q \xrightarrow{k_{sq}} \varphi_2CO + Q^{*} \tag{59}$$

$$\varphi_2CO^{*S} + \varphi_2CHOH \xrightarrow{k_{sr}} 2\varphi_2\dot{C}OH \tag{60}$$

$$\varphi_2CO^{*T} \xrightarrow{k_d} \varphi_2CO + E \tag{61}$$

$$\varphi_2CO^{*T} + Q \xrightarrow{k_q} \varphi_2CO + Q^{*} \tag{62}$$

$$\varphi_2CO^{*T} + \varphi_2CHOH \xrightarrow{k_r} 2\varphi_2\dot{C}OH \tag{63}$$

$$2\varphi_2\dot{C}OH \xrightarrow{k_c'} HOC\varphi_2C\varphi_2OH \tag{64}$$

$$2\varphi_2\dot{C}OH \xrightarrow{k_p} \varphi_2CO + \varphi_2CHOH \tag{65}$$

Reaction 56 describes the formation of excited singlet benzophenone through the absorption of light. Equations 57, 58, 59, and 60 describe the fate of singlet benzophenone. Application of the steady-state treatment to the singlet benzophenone concentration yields the expression for the rate of formation of triplet benzophenone;

$$\frac{d[\varphi_2 CO^{*T}]}{dt} = \frac{k_{is} I_a}{k_{is} + k_f + k_{sq}[Q] + k_{sr}[\varphi_2 CHOH]} \quad . \qquad (66)$$

I_a, as before, is the intensity of absorbed radiation in Einsteins/sec., k_{is} is the rate constant for intersystem crossing between excited singlet and triplet states, k_f is the rate constant for radiative and non-radiative first order decay of the singlet state, k_{sq} is the rate constant for deactivation of the excited singlet by a specific quencher through some non-radiative process, k_{rs} is the rate constant for the abstraction of hydrogen from benzhydrol by the excited singlet benzophenone, and $[Q]$ is the quencher concentration.

The efficiency factor (e) for the formation of chemically reactive excited states is given by

$$e = \frac{k_{is}}{k_{is} + k_f + k_{sq}[Q] + k_{sr}[\varphi_2 CHOH]} \quad . \qquad (67)$$

If

$$k_{is} \gg k_f + k_{sq}[Q] + k_{sr}[\varphi_2 CHOH] , \qquad (68)$$

the efficiency factor for the formation of triplets will be very close to one. It is known that $k_{is} >> k_f$ from the observation that fluorescence is absent from the emission spectrum of benzophenone in either glass at liquid nitrogen temperature or in solution. It is also apparent from the observation that intensities calculated using uranyl oxylate actinometry correspond to the effective intensities calculated from the benzophenone-benzhydrol procedure. The latter also suggests that the value of $k_{sr}[\varphi_2CHOH]$ is insignificantly small for the benzhydrol concentrations used.

The value for $k_{sq}[Q]$ may be significant in certain instances. This value depends upon the efficiency of a quencher toward the deactivation of the excited singlet state of benzophenone. The quenching mechanism may be similar to that proposed by Förster (35). If conditions are right, coupling between the electronic states of benzophenone and quencher may be sufficient to allow long range energy transfer.

In order for the term $k_{sq}[Q]$ to be measurable, it must be about the same order of magnitude as the rate of intersystem crossing. Moore (11,36) has estimated the rate constant for fluorescent decay of the lowest singlet state of benzophenone, k_f, to be approximately $10^6 sec^{-1}$. Therefore, the rate constant

k_{is} must be very large (at least of the order of 10^8) in order for this process to compete effectively with fluorescent decay. Since the quencher concentration was kept very small (on the order of 10^{-4} molar) during the course of study, the singlet-quenching constant k_{sq} must be extremely large (on the order of 10^{12}) for the quenching term, $k_{sq}[Q]$ to be significant. Therefore, an extremely strong dipole coupling interaction must be involved. The only cases where singlet quenching apparently occurred were in experiments in which ferric and chromium dibenzoylmethides were used as quenchers. More will be said about these experiments later.

Equations 61, 62, and 63 describe the fate of benzophenone triplets. Step 61 is the reaction accounting for all first order radiative and non-radiative decay processes excluding catalytic effects produced by added quencher. Reaction 62 describes the deactivation of the triplet state through energy transfer to a quencher or through a catalyzed deactivation by a specific quencher. Step 63 describes the reaction of triplet benzophenone with benzhydrol and accounts for the destruction of benzophenone. Reactions 64 and 65 describe the fate of the ketyl radicals produced from reaction 63. Reaction 65 probably plays an insignificant role in the overall reaction scheme. It corresponds to a non-radiative decay process of triplet benzophenone catalyzed by benzhydrol. The reaction is felt to be insignificant because the ordinate intercept of a plot of $1/\varphi$ against $1/[BH_2]$ is apparently 1.0. If this reaction was significant then the intercept would be greater than 1.0.

Considering the triplet benzophenone concentration by the steady state treatment, one obtains for its concentration the expression

$$[\varphi_2 CO^{*T}] = \frac{e I_a}{k_r[\varphi_2 CHOH] + k_d + k_q[Q]} \tag{69}$$

The rate of the disappearance of benzophenone is therefore

$$-\frac{d[\varphi_2 CO]}{dt} = \frac{k_r e I_a [\varphi_2 CHOH]}{k_r[\varphi_2 CHOH] + k_d + k_q[Q]} \tag{70}$$

Substituting the value for the effective quantum yield described by equation 16 into equation 70, the following rate law is obtained:

$$\frac{1}{\varphi'} = 1 + \frac{k_d + k_q[Q]}{k_r[\varphi_2 CHOH]_{av}} \tag{71}$$

This equation is the same as equation 6 except that a term for deactivation by a known quencher has been added. As long as benzhydrol concentrations are kept between 0.15 and 0.03 molar, the equation is appropriate.

Equation 71 was used for the treatment of all experimental data with regard to quenching experiments. Since the value for k_d/k_r is known, the data can be plotted in the following manner. The quantity $1/\varphi' - 0.033/(\varphi_2 CHOH)_{av}$ is plotted as ordinate against $(Q)/(\varphi_2 CHOH)_{av}$ as abscissa. The slope of the line obtained will be the value for the ratio of rate constants, k_q/k_r. The primary advantage for plotting data in this manner is that it is possible for the same point

on a curve to be determined with a number of different benzhydrol and quencher concentrations. This enables one to observe peculiar effects associated with variation in the concentrations of quenchers. These effects may include quenching of singlet benzophenone, as may be exhibited by the DBM chelates, effects resulting from improper compensation for internal filtering by chelates, and effects resulting from the decomposition of chelates during irradiation. More will be said about these effects later when the experimental results are discussed in detail.

The data for quantum yields for disappearance of benzophenone in quenching experiments are reported in Table X. The results are plotted according to equation 71 in Figures X through XVIII.

It was of primary importance to know whether or not the chelates were stable during irradiation. Moore (36) observed the formation of a green precipitate when $Fe(DPM)_3$ was irradiated with benzophenone and toluene. He also observed a lightening in the color of the solution due to $Fe(DPM)_3$ when a sample was irradiated in the presence of benzophenone and benzhydrol. The latter observation was also made in this investigation when irradiation was conducted over extended periods of time. When the sealed sample was opened and its contents exposed to the air, the color of $Fe(DPM)_3$ returned, and in the toluene solution, the green precipitate disappeared. A possible sequence of reactions to account for these phenomena is:

Table X

Experimental Data Concerning the Quenching of Triplet Benzophenone by Transition Metal Chelates

No.	Quencher	Quencher Concen. $[Q]\times 10^4$	$\frac{1}{\varphi'}$	$\frac{1}{\varphi'} - \frac{0.033}{[BH_2]_{av}}$	$\frac{[Q]}{[BH_2]}\times 10^4$	$[\varphi_2CHOH]_{av}$ (mol./liter)
1	$Fe(DPM)_3$	1.107	1.594	1.120	15.91	0.080
2	"	1.165	1.890	1.236	23.07	0.060
3	"	1.132	1.500	1.147	12.11	0.100
4	"	1.132	1.634	1.174	15.80	0.080
5	$Cr(DPM)_3$	1.329	1.579	1.104	19.12	0.080
6	"	1.329	1.769	1.104	26.66	0.060
7	"	1.124	1.560	1.096	15.80	0.080
8	"	1.130	1.420	1.019	13.73	0.090
9	$Fe(AA)_3$	1.020	2.225	1.770	14.06	0.080
10	"	1.700	2.298	1.951	17.84	0.100
11	"	1.700	3.253	2.662	30.47	0.060
12	"	1.000	1.950	1.505	10.44	0.100
13	$Cr(AA)_3$	1.529	2.302	1.849	21.01	0.080
14	"	1.529	2.601	1.980	28.79	0.060
15	"	1.349	1.904	1.553	14.35	0.100
16	"	1.349	2.558	1.956	24.62	0.060
17	$Co(DPM)_3$	1.00	1.243	1.008	7.110	0.150
18	"	0.987	1.530	0.936	17.78	0.060
19	"	1.033	1.440	0.983	14.84	0.080
20	"	2.066	1.420	0.958	28.90	0.080
21	$Co(AA)_3$	1.222	1.500	1.035	17.21	0.080
22	"	2.444	1.640	1.188	33.50	0.080
23	"	1.222	1.418	1.066	13.18	0.100

Table X (continued)(2)

No.	Quencher	Quencher Concen. $[Q] \times 10^4$	$\frac{1}{\varphi'}$	$\frac{1}{\varphi'} - \frac{0.033}{[BH_2]_{av}}$	$\frac{[Q]}{[BH_2]} \times 10^4$	$[Q_2CHOH]_{av}$ (mol./liter)
24	$Al(DPM)_3$	1.014	1.441	0.970	14.45	0.080
25	"	2.028	1.533	1.070	28.50	0.080
26	"	1.014	1.350	0.998	13.18	0.090
27	$Al(AA)_3$	1.454	1.698	0.984	24.16	0.080
28	"	1.454	3.395	0.990	47.35	0.040
29	"	1.454	1.354	1.002	13.20	0.120
30	$Fe(MAA)_3$	1.190	2.385	1.933	16.29	0.08
31	"	1.190	2.805	2.189	22.20	0.06
32	"	1.448	2.398	2.054	15.08	0.10
33	"	1.122	1.979	1.520	15.60	0.08
34	$Fe(AC)_3$	1.057	2.960	2.516	14.20	0.08
35	"	1.057	3.590	2.990	19.21	0.06
36	"	0.547	1.653	1.310	5.68	0.100
37	"	1.093	2.140	1.801	11.25	0.100
38	"	1.640	2.520	2.181	16.80	0.100
39	$Gd(DPM)_3$	1.028	1.440	1.039	12.49	0.09
40	$La(DPM)_3$	1.087	2.326	1.026	42.83	0.04
41	"	1.00	2.500	1.206	39.20	0.03
42	"	2.00	1.462	1.116	21.00	0.10
43	"	2.00	1.772	1.040	44.34	0.05
44	"	0.913	1.500	1.114	10.67	0.10
45	$Er(DPM)_3$	1.085	1.433	1.032	13.18	0.09
46	"	1.00	1.430	1.027	12.20	0.09
47	"	1.00	2.430	1.136	39.20	0.03

Table X (continued) (3)

No.	Quencher	Quencher Concen. $[Q] \times 10^4$	$\frac{1}{\varphi'}$	$\frac{1}{\varphi'} - \frac{0.033}{[BH_2]_{av}}$	$\frac{[Q]}{[BH_2]} \times 10^4$	$[Q_2CHOH]_{av}$ (mol./liter)
48	$Mn(DPM)_3$	1.00	1.690	1.071	18.75	0.06
49	"	1.00	1.418	1.015	12.20	0.09
50	$Co(DPM)_2$	1.00	1.720	1.333	11.72	0.09
51	"	1.07	2.190	1.606	18.94	0.06
52	"	1.00	1.718	1.322	12.00	0.09
53	$Ni(DPM)_3$	1.00	2.063	1.458	18.35	0.06
54	"	2.00	1.995	1.598	24.06	0.09
55	"	2.00	2.374	1.765	36.90	0.06
56	"	1.00	1.700	1.309	11.85	0.09
57	"	1.00	1.637	1.288	10.57	0.100
58	"	1.00	2.286	1.560	22.00	0.05
59	$Cu(DPM)_2$	1.116	1.610	1.225	13.01	0.09
60	"	1.163	1.445	1.098	12.25	0.10
61	$FeCl_3$	1.231	1.694	0.972	13.97	$0.10^{(t)}$
62	"	1.231	2.327	0.890	28.73	$0.050^{(t)}$
63	"	1.231	1.956	1.027	18.55	$0.075^{(t)}$
64	$Fe(DPM)_3$	1.041	1.937	1.250	11.62	$0.10^{(t)}$
65	"	1.041	2.400	1.493	15.32	$0.075^{(t)}$
66	"	1.041	2.869	1.476	23.55	$0.050^{(t)}$
67	DPM	1.876	1.587	1.125	26.24	0.080
68	"	4.690	1.606	1.145	65.50	0.080
69	AA	2.080	1.524	1.060	29.23	0.080
70	"	4.160	1.650	1.185	57.94	0.080

Table X (continued) (4)

No.	Quencher	Quencher Concen. $[Q] \times 10^4$	$\frac{1}{\varphi'}$	$\frac{1}{\varphi'} - \frac{0.033}{[BH_2]_{av}}$	$\frac{[Q]}{[BH_2]} \times 10^4$	$[Q_2CHOH]_{av}$ (mol./liter)
71	DBM	1.295	2.326	1.881	17.45	0.080
72	"	2.590	3.457	3.030	33.46	0.080
73	AC	1.601	2.091	1.643	21.77	0.080
74	"	3.203	2.846	2.407	42.56	0.080
75	MAA	1.754	1.895	1.350	23.70	0.080
76	"	3.509	2.028	1.578	87.84	0.080

a. The initial benzophenone concentration in all of the experiments listed above is 0.10 molar.

b. The solvent used for all experiments listed here was benzene with the exception of those designated by (t) where t-butylalcohol was used.

c. Initial benzhydrol concentrations are listed for each experiment.

d. φ' is the effective quantum yield and is defined by equation 16.

$$\varphi_2\dot{C}OH + Fe(DPM)_3 \longrightarrow \varphi_2\overset{+}{C}OH + Fe(DPM)_3^- \longrightarrow \varphi_2CO + Fe(DPM)_2 + HDPM$$

$$\varphi\text{-}\dot{C}H_2 + Fe(DPM)_3 \longrightarrow [\varphi_2\text{-}\overset{+}{C}H_2 \cdots Fe(DPM)_3^-] \qquad (72)$$

In addition to chelate destruction described above, the chelate concentration was also observed to decrease slowly in the presence of alcohols. Destruction was much more rapid with benzpinacol than with benzhydrol. The half-life of the most rapid exchange process measured for any chelate was greater than forty hours in the dark at room temperature.

A common observation which was made during the course of the present investigation was that all chelates capable of quenching triplet benzophenone were observed to be decomposed irreversibly to some extent during irradiation. This situation differs from that described by equation 72, which should be reversed upon exposure to oxygen. Irreversible decomposition is believed to occur as a result of the dissipation of energy accepted from the excited ketone during the quenching step. This process will be discussed in detail later.

After lengthy investigation, experimental conditions were determined such that no significant decomposition of the dipivaloylmethide and acetylacetonate chelates of iron, cobalt, chromium, and aluminum occurred. The experimental conditions were also selected

such that internal filtering by the chelates was not significant. In addition to the chelates described above, decomposition of other chelates was followed and minimized when possible.

Figures X, XI, XII, and XIII show the results obtained from quenching experiments conducted with added quantities of ferric, chromium, cobalt and aluminum acetylacetonates and dipivaloylmethides. The results demonstrate two effects. The first shows how the different transition metal atoms influence the quenching ability of the general ML_3 chelate. The quenching efficiency of the chelates decreases as one goes from FeL_3, to CrL_3, to CoL_3, to AlL_3. The trend parallels the availability of low-energy chelate $\pi \rightarrow \pi^*$ orbitals which are energetically and statistically available for interaction with the excited donor.

The second result obtained for this series of chelates demonstrates an apparent steric effect which is exhibited by the dipivaloylmethide chelates toward interaction with the triplet ketone. The acetylacetonate and dipivaloylmethide chelates having the same central metal atom have equivalent excitation energies , as shown by both molecular orbital calculations and comparison of absorption spectra. However, in all pairs of chelates studied, it was observed that the dipivaloylmethide chelate was consistently less effective as a quencher than the corresponding acetylacetonate chelate. A difference in diffusion rates for these chelates resulting from differences in molecular sizes may account for

some of the observed variation in quenching rates, but it is felt that the effect found is larger than may be expected purely on this basis.

Both the chromium and cobalt chelates have low energy $\pi - \sigma^*$ transitions that are moderately separated from π-π^* transitions. These π-σ^* electronic states have sufficiently low energy that they should be very favorable for accepting energy from triplet benzophenone. However, the quenching efficiencies of these chelates do not correlate with the energies of these transitions. On the other hand, a correlation between the quenching efficiencies and the predicted and observed π-π^* transition energies is obtained. From the above experiments, it was reasonably felt that, at least in these situations, the low energy chelate π-orbitals were those which were primarily involved in the energy transfer process. The chelate π-molecular orbitals are distributed throughout the ligands and offer maximum opportunity for interaction with the π-orbital system of a donor molecule. The low energy chelate E_g σ-antibonding and nonbonding orbitals are localized well within the interior of the chelate and are thus shielded effectively from direct interaction with the excited donor orbital system by the ligands.

In order to demonstrate the importance of chelate π-orbitals for the quenching of triplet benzophenone, experiments were run using t-butyl alcohol as solvent and where known amounts of $FeCl_3$ and $Fe(DPM)_3$ were added. The results are shown in Figure XVII. The samples containing $FeCl_3$ showed no quenching effect, even though the

fact that the solution is yellow guarantees that the solvated metal ion has low energy transitions. It was assumed that the ferric ion was octahedrally complexed by t-butyl alcohol. Some Cl^- ions may also be directly attached to the metal ion. The visible transitions probably result from ordinary ligand field splittings of ion d-orbitals into T_{2g} and E_g sets. The t-butyl groups prevent effective interaction of these orbitals with the ketone orbital system which is necessary to effect energy and electron exchange. For this reason no apparent quenching occurred. The above transitions in $Fe(t\text{-}buOH)_6Cl_3$ probably correspond to low energy π-σ^* transitions in the chelates. $Fe(DPM)_3$, which has available low-energy π-orbitals, did effectively quench triplet benzophenone in the t-butyl alcohol solution.

Of the four pairs of chelates studied in the acetylacetonate-dipivaloylmethide series, two were paramagnetic and two diamagnetic. An important result found in these experiments was that the diamagnetic chelate of cobalt acetylacetonate was able to quench benzophenone triplets, thus demonstrating that paramagnetism is not necessary for quenching by the chelate. Unfortunately, the quenching efficiency of the cobalt chelate is not large.

Since diamagnetic $La(DPM)_3$ had been reported to quench 1-naphthaldehyde triplets (34), it was used here in an attempt to find an additional case of quenching of triplet benzophenone by a diamagnetic chelate. However, rough consideration of the type of π-bonding interactions that one might expect between metal and ligand indicates that

there should not be any low-energy π-π^* electronic states available for accepting energy from the excited donor. This seemed to be verified by the spectra of this chelate. Spectroscopic studies made on selected rare earth chelates by Crosby (24) indicate that the lowest energy π-π^* triplet should be somewhat higher than that of benzophenone for a rare earth chelate with ordinary β-diketone ligands.

In addition to those conducted on $La(DPM)_3$, experiments were carried out with the dipivaloylmethide chelates of erbium, gadolinium, and samarium. The results of the experiments performed with $La(DPM)_3$ and $Er(DPM)_3$ are given in Figure XV.

All four rare earth chelates were found to be very poor quenchers. They were found to be stable with respect to decomposition during irradiation. Their quenching efficiencies are all very nearly identical and within experimental error of having a nul quenching efficiency. These results are in some disagreement with those reported earlier (34). With the exception of the lanthanum chelate, the other two are paramagnetic substances statistically capable of quenching by their ground state, but do not have π-orbitals in the ligand available for accepting energy from the donor.

Manganese (III) dipivaloylmethide may be expected to have electronic transitions somewhere between those of the iron and chromium chelates. Therefore, this compound was also expected to possess an intermediate quenching efficiency. The experimental results shown in

Figure XIV indicate that the chelate apparently is a poor quencher; however, it was found to be very unstable during irradiation. A black precipitate was observed to form which did not disappear when the sample was exposed to air afterwards. Some slow precipitation was observed in the solution even in the dark. Destruction of the chelate, therefore, makes the results inconclusive.

Chelates containing other ligands of varying steric requirements were used in an attempt to extend this phase of the study. To accomplish this, iron acetylcyclohexanonate and iron 3-methylacetylacetonate were prepared. Their ultraviolet spectra are very similar to those of the iron acetylacetonate and dipivaloylmethidechelates. (See Figure VIII.) Both chelates were found apparently to be good quenchers, as shown in Figure XIV , but the data are quite inconclusive. During irradiation, the chelates were destroyed very rapidly, even though their stability in the dark was good. Chelate destruction ran as high as fifty percent for some runs.

It has been found that β-diketones with groups larger than methyl or methylene in the 3 - position are usually unable to form chelates. In many instances, organometallic polymers result when chelation is attempted. In addition, chelates containing those ligands which have groups other than hydrogen in the 3-position are usually more unstable thermally than their hydrogen counterparts. The probable mechanism for the destruction of these chelates will be discussed in detail later.

When destruction of the chelate occurs, such as was observed here, it is not known what species is actually performing the quenching operation. It might be a combination of both ligand and chelate, or fractional chelate. If both ligand and "chelate" quench, the concentration of quencher used for calculating quenching efficiencies will not be the value corresponding to the actual quenchers present. In this instance, the calculated results will be higher than the actual value expected for the particular chelate in question. The plot of points in Figure XIV showed no unique pattern with respect to initial quencher concentration that would indicate the occurrence of a quenching process different than expected as a result of chelate decomposition.

As a further check, quenching efficiencies of each ligand were determined. The results from these experiments are given in Figure XVIII . It was found that acetylcyclohexanone and 3-methylacetylacetone are moderately active quenchers, while acetylacetone and dipivaloylmethane are not. The quenching efficiencies of the former are significant when compared to the k_q/k_r values obtained for the chelates. Since chelate destruction does occur, and the ligands are observed to be moderate quenchers, the experimental results concerning these chelates are inconclusive.

The planar dipivaloylmethide chelates which were studied are believed to quench benzophenone triplets by the same mechanism as the ML_3 chelates. $Ni(DPM)_2$ has been shown to be diamagnetic over a large

temperature range. The corresponding $Ni(AA)_2$ chelate, on the other hand, is paramagnetic (58). This difference is not a result of a difference in the ligand's electronic capability toward bonding, but is due to the formation of a nickel acetylacetone trimer. Each nickel atom within the trimer is octahedrally complexed. The electronic structures of the two chelates are entirely different. Dipivaloylmethide chelates cannot form the trimer because of steric hindrance offered by the t-butyl groups.

The planar chelates of $Co(DPM)_2$ and $Ni(DPM)_2$ have paramagnetic ground states which are required by an uneven number of electrons in the chelate. Molecular orbital calculations indicate that all three chelates have low-energy transitions which may be involved in energy transfer. The results of quenching experiments using these chelates are shown in Figure XVI . It is seen that diamagnetic $Ni(DPM)_2$ is as efficient a quencher as the two paramagnetic chelates.

It is observed that the quenching efficiencies of these chelates lie intermediate in value between those of the acetylacetonate and dipivaloylmethide chelates of iron and chromium. Planar chelates may offer less steric hindrance to the approach of benzophenone than the $M(DPM)_3$ chelates. The intermediate values of the quenching constants may arise from an intermediate steric effect as well as the availability of suitable electronic states. Approach of benzophenone to the chelate

is hindered by the t-butyl groups when this approach is made in or near the plane of the chelate. Hindrance is similar to that encountered for the $M(DPM)_3$ chelates. However, when approach is made from above or below the plane, much less hindrance is encountered. The interaction of the excited ketone with the ML_3 acetylacetonates is approximately independent of orientation. A more critical discussion of the nature of the "steric effect" will be given in a following section as a part of the general theory of energy transfer in solution.

Destruction of all three chelates occurs to different degrees during irradiation. $Ni(DPM)_2$ and $Co(DPM)_2$ are relatively stable, and experimental conditions were selected such that decomposition of these chelates was insignificant during the reaction period. $Cu(DPM)_2$, on the other hand, was found to be quite unstable, forming a black precipitate upon exposure to light. Compensation for the decomposition of this chelate was impossible.

In the dark, decomposition of the nickel and cobalt chelates can occur but may be eliminated. $Ni(DPM)_2$ may absorb water and form an octahedral hydrated complex. Sublimation before use and storage within a dessicator prevented this from occurring. The $Co(DPM)_2$ is oxidized at a moderate rate when dissolved in aerated benzene. Oxidation was minimized by flushing the solvent with nitrogen and by adding the chelate to the solvent under a nitrogen atmosphere at the last moment before degassing.

It is concluded from the results with planar chelates that, at least in this situation, the diamagnetic and paramagnetic chelates are equally efficient as triplet energy sinks.

The question arises as to what happens to the excited chelate and how energy is dissipated after energy transfer. In general, there are two processes possible. The first involves interaction with other specific molecules either chemically or physically. Chemical reaction results in the destruction of the specific quencher. Physical interaction consists of transferring excitation energy to another molecule. The second method covers unimolecular decay processes involving emission of the energy by either fluorescence or phosphorescence, or non-radiative decay to ground state by intersystem-crossing and thermal relaxation. The relative importance of each process in the dissipation of energy depends upon the nature of the molecules and excited states involved, and may differ considerably as one varies quenchers.

Not much is known about the chemical reactivity of excited chelates toward other molecules, but it is felt that any bimolecular process of this type is slow with respect to other modes of deactivation within the systems studied. Since the electronic states of the chelates studied here are lower than the triplet state energies of all other molecules present, it is felt that transfer of electronic energy from an excited chelate to other molecules in the reaction system is ruled out as a possible mode of deactivation. This leaves radiative emission and thermal relaxation as the most probable mechanisms of deactivation.

Diamagnetic chelates require the formation of an excited triplet state upon absorbing energy from triplet benzophenone. Therefore, phosphorescence might be expected from these chelates in the absence of any faster deactivation process. Paramagnetic chelates, on the other hand, form excited states which have no multiplicity restrictions against transitions from excited to ground states. Since allowed transitions may occur in the paramagnetic chelates, observation of induced fluorescence might be expected.

No sensitized emission was observed from any samples containing chelate and benzophenone at room temperature. A slight blue emission was observed in benzene solutions containing benzophenone, which may be due to benzophenone phosphorescence or fluorescence. This emission was quenched by the addition of $Fe(DBM)_3$, and no new emission was observed. In addition, no emission was observed from samples of chelates dissolved in ethanol-ether glass at 77° K. This indicates that deactivation of the excited state of the chelates is probably proceeding through an internal non-radiative process.

The molecular-orbital calculations indicate that the lowest excited state bond orders are altered only slightly from those of the ground state. The molecules should be distorted somewhat from their original D_3 symmetry when in their lowest energy excited states. It seems reasonable to expect a large amount of vibronic overlap between excited and ground states, thus making internal conversion favorable and rapid.

Evidence to support the above hypothesis that non-radiative decay accounts for the loss of excitation energy comes from the experimental observation that only chelates which actively quenched triplet benzophenone were susceptible to decomposition during photolysis. In addition to the possible reaction involving a reversible reduction of chelate as shown on page 95 , thermal destruction resulting from the internal dissipation of large energies may ensue. Chelates which bear a hydrogen atom at the 3-position of the ligand are very much more stable during irradiation than those chelates which have methyl or methylene groups in this position. Introduction of these groups into the 3-position results in substantially weakening the metal-ligand bonds. Therefore, these bonds are more likely to be broken in the vibrationally excited ground state molecules which are formed by decay of excited electronic states.

Decomposition through excited vibrational levels of excited electronic states may also be possible when these states are formed during energy transfer. When donor and acceptor transition energies are close, the probability of the formation of an excited vibronic state capable of decomposing directly is small if the potential energy surface for the excited electronic state is relatively deep. Since molecular orbital calculations indicate that the bond orders in the excited states involved in energy transfer are not altered greatly from those of the ground state, it seems likely that their potential energy surfaces should

be similar. The stability of the metal-ligand bonds depends on the structure of the ligands and may be fairly poor for ligands with hindering groups in the 3-position. In this case, decomposition from excited as well as ground electronic states may be significant.

A summary of results from the quenching experiments is tabulated in Table XI. Values for the ratio of rate constants k_q/k_r for each chelate were obtained from the plots given in Figures X-XVIII. No great precision can be claimed for values of k_q/k_r less than 30. As described earlier, all good quenchers underwent photodecomposition at rates which varied considerably from case to case. Values derived from runs in which decomposition was extensive are indicated in Table XI as approximate (~) or as a lower limit (<).

Several things are immediately apparent from observing the results given in Table XI. First, it is evident that there is no correlation between the magnetic properties of the ground state of a compound and its quenching efficiency. The six diamagnetic chelates studied exhibited considerably different quenching efficiencies. $Ni(DPM)_2$ is almost half as efficient a quencher as paramagnetic $Fe(AA)_3$, the best quencher studied here. $Co(AA)_3$ is about five times less efficient than the nickel chelate, while the remaining diamagnetic chelates $La(DPM)_3$, $Co(DPM)_3$, $Al(DPM)_3$, and $Al(AA)_3$ do not exhibit any significant quenching ability.

Table XI

Summary of Experimental Results Regarding the Quenching of Triplet Benzophenone by Transition Metal Chelates

No.	Quencher	k_q/k_r	No.	Quencher	k_q/k_r
1	$Fe(AA)_3$	540	15	$Co(DPM)_2$	296
2	$Fe(DPM)_3$	100	16	$Ni(DPM)_2$	246
3	$Cr(AA)_3$	380	17	$Cu(DPM)_2$	>130
4	$Cr(DPM)_3$	45	18	H DBM	577
5	$Co(AA)_3$	47	19	H AC	320
6	$Co(DPM)_3$	0	20	H MAA	128
7	$Al(AA)_3$	10	21	H DPM	27
8	$Al(DPM)_3$	0	22	H AA	27
9	$Fe(AC)_3$	~860	23	$FeCl_3$(t-buOH)	0
10	$Fe(MAA)_3$	~550			
11	$Mn(DPM)_3$	> 32			
12	$La(DPM)_3$	~ 28			
13	$Er(DPM)_3$	30			
14	$Gd(DPM)_3$	~ 31			

AA = acetylacetonate

DPM = dipivaloylmethide

MAA = 3-methyl-acetylacetonate

AC = 2-acetylcyclohexanonate

DBM = dibenzoylmethide

The paramagnetic chelates also show considerable variation with respect to their quenching efficiencies. The best chelate quencher accurately known, and reported in Table XI, is $Fe(AA)_3$. (This compound probably quenches benzophenone triplets at a rate that is near diffusion controlled.) The poorest paramagnetic quenchers are $Cr(DPM)_3$, $Er(DPM)_3$, and $Gd(DPM)_3$, the latter two showing no effective quenching ability.

The second general observation made from Table XI is that the ML_3 dipivaloylmethide chelates are consistently less effective as quenchers than the corresponding acetylacetonate chelates, thus suggesting some type of steric effect. Finally, the quenching ability of the series of ML_3 acetylacetonate and dipivaloylmethide chelates is seen to correlate with the calculated energies of their lowest $\pi \rightarrow \pi^*$ transitions.

Any mechanism for the quenching of triplet benzophenone by the chelates reported here must be able to explain all of the above observations satisfactorily. In addition to satisfying these results, the mechanism should be in agreement with all available information regarding triplet energy transfer in solution.

QUENCHING OF SINGLET BENZOPHENONE

Quenching by Dibenzoylmethide Chelates

Variations of the central metal atoms of the chelates described previously have a marked bearing on their quenching abilities. Steric effects were also apparent for different ligands which had identical electronic structures. The existence of energetically, statistically, and sterically available electronic states involving chelate π-orbitals is apparently necessary for quenching of triplet benzophenone. Therefore, alteration of the electronic structure of the ligands was expected to effect the quenching ability of the chelates.

The dibenzoylmethide chelates of iron and chromium were chosen in an effort to demonstrate any effect of the type expected by altering the ligand π-orbital systems. It was felt that these chelates would offer a larger number of favorable low energy π-orbitals necessary for quenching than their acetylacetonate counterparts. Their ultraviolet spectra are very similar to corresponding acetylacetonate and dipivaloylmethide chelates but are shifted in their entirety to longer wavelengths.

Experiments indeed showed that these chelates were very efficient quenchers, more so than any other quencher thus far

examined. Treatment of the experimental data by equation 71, as done for all other chelates investigated, gave the results shown in Figure XIX. The experimental points appear very scattered and inconsistent. Mean slopes which best fit the experimental points and which correspond to the k_q/k_r values were found for both chelates to be about an order of magnitude greater than the largest value obtained for any other quencher. The maximum value found for any triplet quencher apparently is from 580 to 650 for the benzophenone-benzhydrol system in benzene. These values are assumed to correspond to ordinary diffusion-controlled processes. If the mean slopes calculated from the experimental data as plotted in Figure XIX are correct, the triplet quenching rates resulting from these chelates must be faster than diffusion-controlled by an order of magnitude. Long range triplet energy transfer does not seem reasonable because conditions necessary for electron exchange are not satisfied. Quenching of singlet states is possible over large distances because the spin conservation requirement does not have to be satisfied through a bimolecular interaction. Therefore, the possibility that quenching of the benzophenone excited singlet state was occurring was investigated.

Closer inspection of the data represented in Figure XIX reveals a unique dependence on the quencher concentration. Lines drawn through points obtained with the same initial quencher

concentration give ordinate intercepts differing from unity and from each other.

Returning to the kinetic discussion given on page 87 , the assumption was made that the rate of intersystem crossing, k_{is}, is much larger than all other terms in the efficiency factor (e) for most quenchers studied. This assumption implies that the efficiency factor approaches 1.0 and leads to the rate equation 71 normally used for treatment of the experimental data. If, however, the value for $k_{sq}(Q)$ is not negligible when compared to k_{is}, then the efficiency factors for the control runs as actinometers are greater than those for the samples containing the quencher.

Equation 70 may be rewritten as:

$$-\frac{d[\varphi_2CO]}{dt} = \frac{k_{is}\, k_r\, I_a\, [\varphi_2CHOH]}{(k_{is} + k_{sq}[Q])(k_d + k_q[Q] + k_r[\varphi_2CHOH]} \qquad (73)$$

The proper expression for quantum yield becomes:

$$\frac{1}{\varphi} = \left[1 + \frac{k_{sq}}{k_{is}}[Q]\right]\left[1 + \frac{k_d + k_q[Q]}{k_r\,[\varphi_2CHOH]}\right] \qquad (74)$$

A plot of $1/\varphi$ versus $1/(\varphi_2CHOH)_{av}$ should yield straight lines for each separate quencher concentration. The ordinate intercepts are given by the term

$$\text{intercept} = 1 + \frac{k_{sq}[Q]}{k_{is}} \qquad (75)$$

Their slopes will be

$$\left[1 + \frac{k_{sq}[Q]}{k_{is}}\right]\left[\frac{k_d + k_q[Q]}{k_r}\right] \qquad (76)$$

If a first order dependence on quencher concentration really exists, then a plot of intercept against quencher concentration should give a straight line with an ordinate intercept of one and a slope given by k_{sq}/k_{is}.

A plot of $1/\varphi$ versus $1/(BH_2)$, as suggested by equation 74, was made for the $Fe(DBM)_3$ and $Cr(DBM)_3$ experiments for each different quencher concentration. These results are given in Figures XX and XXI. A plot of intercept versus the quencher concentration yields lines which have slopes corresponding to k_{sq}/k_{is}, of 4×10^4 and 1.2×10^4 for iron and chromium dibenzoylmethide, respectively.

Förster's theory (35) of singlet exciton transfer or resonance transport is based on the assumption that two molecules capable of interaction are isolated from one another at a mutual distance R. Coupling between electric dipoles of donor emission and acceptor absorption are responsible for the interaction necessary for energy transfer.

In most molecules, due to the broadness of their spectra, there is usually always some degree of spectral overlap between donor and acceptor. In an ideal case, the acceptor will have an

Table XII

Experimental Data Concerning the Quenching of Singlet Benzophenone by the Dibenzoylmethide Chelates of Iron and Chromium.

No.	Quencher	$[Q]\times10^4$	$\frac{1}{\varphi}$	$\frac{1}{[BH_2]}$	$\frac{1/\varphi - 0.033}{[BH_2]}$	$\frac{[Q]}{[BH_2]}\times10^4$	A	$B\times10^4$	K
77	$Fe(DBM)_3$	0.1812	2.240	13.77	1.786	2.495	0.061	4.31	1.725
78	"	0.2719	2.750	13.44	2.307	3.660	0.219	7.65	2.088
79	"	0.1812	2.287	19.18	1.654	3.478	-0.071	6.00	1.725
80	"	0.2719	2.940	18.55	2.330	5.050	0.242	10.55	2.088
81	"	0.554	3.525	10.38	3.183	5.750	-0.035	17.95	3.218
82	"	0.554	4.035	21.50	3.325	11.91	0.107	37.30	3.218
83	"	0.1812	2.0767	10.50	1.730	1.901	0.005	3.28	1.725
84	$Cr(DBM)_3$	0.452	2.550	13.61	2.101	6.146	0.558	9.48	1.543
85	$Cr(DBM)_3$	0.452	2.459	18.98	1.833	8.571	0.290	13.22	1.543
86	"	0.226	1.696	10.38	1.354	2.346	0.082	2.98	1.272
87	"	0.226	1.830	13.95	1.370	3.153	0.098	4.00	1.272
88	"	0.515	2.210	10.60	1.860	5.459	0.242	8.83	1.618
89	"	0.515	2.830	22.22	2.097	11.443	0.379	18.5	1.618
90	"	0.452	2.308	10.51	1.961	4.753	0.418	7.34	1.543

$$A = \frac{1}{\varphi} - \frac{0.033}{[BH_2]_{av}} - K$$

$$B = K\frac{[Q]}{[BH_2]}$$

$$K = 1 + \frac{k_{sq}[Q]}{k_{is}}$$

The initial benzophenone concentration used in the experiments listed above was 0.10 molar. The solvent was benzene.

absorption band moderately displaced to the red with respect to the first absorption band of the donor . The fluorescence spectrum of benzophenone has never been observed but is expected to be the inverse of its absorption spectrum. Both dibenzoylmethide chelates have large absorptions in this region, whereas the other chelates studied do not. (See Fig. VIII.)

The coupling is strongest if the corresponding optical transitions of both molecules are electric dipole radiation. These transitions are coupled not only with the radiation field, but also with each other. Interaction energies are of a dipole-dipole nature and depend upon the inverse third power of the intermolecular distance. Since the probability of energy transfer is proportional to the square of the interaction energy matrix element, the probability is thus proportional to the square of the dipole-dipole interaction and decreases as the sixth power of the distance (35).

The first order rate constant for energy transfer of this type may be described by the simple equation

$$k_o(\text{sec}^{-1}) = \frac{1}{\tau_s} \left(\frac{R_o}{R} \right)^6 \qquad (77)$$

Here R_o is defined as the critical distance for which exciton transfer and spontaneous deactivation of the sensitizer are of equal probability. This parameter is dependent upon the magnitude of the dipole coupling.

R_o values of 50 to 150 Å have been measured(1). R is the distance between donor and acceptor. τ_s is the actual mean lifetime of the excited sensitizer and is related to the intrinsic or radiative lifetime τ_s^o by the expression

$$\tau_s = \varphi_s^o \tau_s^o \tag{78}$$

where φ_s^o is the quantum yield of the sensitizer fluorescence without transfer.

The range of quencher concentrations used for the study of the dibenzoylmethide chelates was confined to values less than or approximately equal to 5×10^{-5} molar. In general, these concentrations were a factor of 2 to 10 less than those used for other chelates. The choice of these lower concentrations was necessitated because of the extremely large quenching efficiencies encountered and to reduce internal filtering problems.

Assuming that quenching proceeds by a mechanism similar to that proposed by Förster, a value for R_o may be determined by equation 77 after making the proper substitutions. The actual mean lifetime of the singlet state τ_s may be written as

$$\tau_s = \frac{1}{k_f} \left(\frac{k_f}{k_{is} + k_{sq}[Q]} \right) \tag{79}$$

Substitution of 79 into equation 77 gives the expression

$$k_{sq}[Q] = \left[k_{is} + k_{sq}[Q] \right] \left(\frac{R_o}{R} \right)^6 \qquad (80)$$

Considering the situation where the efficiency factor $\underline{e}$ is 0.5 or when $k_{is} = k_{sq}(Q)$, then

$$\frac{1}{2} = \left(\frac{R_o}{R} \right)^6 \qquad (81)$$

From Figure XX , the quencher concentration which corresponds to an efficiency factor of 0.5 for $Fe(DBM)_3$ is 2.5×10^{-5} molar. Assuming a complete random distribution of quencher molecules throughout the solution, the average distance between molecules $\underline{R}$ is calculated to be 202 Å . Substituting this value into equation 81, $\underline{R_o}$ is found to be 178 Å .

This estimate is larger than would normally be expected, since the largest values found for other molecules usually never exceed 100 Å (35). These values are obtained for dye molecules where extremely strong electric dipole transitions are involved.

Only the lowest energy $\underline{n} \rightarrow \pi^*$ singlet state is populated in benzophenone under the reaction conditions. Since $\underline{n} \rightarrow \pi^*$ transitions are symmetry forbidden, there can be no strong dipole coupling between this and the $\pi \rightarrow \pi^*$ transition in the chelate. Vibrational

mixing, however, will allow some. Therefore, a small value for R_o might be expected in this system. Granted that the experimental results are by no means sufficiently complete to place definite confidence in the values determined, the largest variation that can be introduced into the results from the available data still requires that the R_o value calculated by Förster's formula must be greater than 150 Å.

A further discrepancy found, with respect to the application of Förster's theory to this problem, involves the inverse sixth power dependence on intermolecular distance. This dependence implies that the rate of energy transfer should vary as the square of the quencher concentration. A linear dependence is indicated experimentally.

The dipolar interaction that Förster considers is between molecules isolated from each other at a distance R, in either a solid matrix of inert gas, a crystal, or in solutions where interaction between solvent and donor or acceptor is negligible. The present reaction system may be somewhat different. It is felt that interaction between sensitizer and acceptor may involve coupling with excited states of the solvent.

The dibenzoylmethide chelates are unique with respect to other chelates studied in that each ligand contains two phenyl groups. Benzene is found to be a very good solvent for these chelates, probably

because of π-interaction with the ligands. In addition, benzophenone is a carbonyl compound containing two phenyl groups. Coupling of the dibenzoylmethide chelate states with those of benzophenone through solvent may account for the large quenching effects. Interaction with the environment may lead to the first order dependence on quencher concentration that is found experimentally. If solvent interaction is important, a large solvent effect on the quenching rates may be expected. Unfortunately, no experiments of this type have yet been conducted.

The discussion thus far has ignored the possibility that the predominate contribution to the rate of singlet energy transfer here may result from dipole coupling between benzophenone and quencher under resonance conditions. These conditions result when the energies of the excited electronic states of both donor and acceptor are identical. Under these conditions, the rate for energy transfer is directly proportional to the dipole coupling matrix element. Therefore, the rate of energy transfer should be directly proportional to quencher concentration. This possibility for singlet transfer will be discussed more completely in the following section where possible mechanisms for both singlet and triplet energy transfer are considered.

The slopes of the lines plotted in Figures XX and XXI which correspond to expression 76 depend on the period of the mixing cycles to which the cells are exposed during irradiation. A discussion of diffusion effects and their results as applied to these experiments are given in Appendix B.

DISQUISITION

Introduction

Two similar and closely related mechanisms for energy transfer will be considered here. The first (a) involves a process whereby the electronically excited donor and unexcited acceptor interact with a weak perturbation. The interaction is considered of such a type whereby the two distinguishable particles, D (donor) and A (acceptor), may retain their physical individuality during the time of the interaction. Each molecule is considered to have its own characteristic 3N degrees of freedom, where N is the number of atoms in each molecule.

The second mechanism (b) concerns a process where the interaction between two molecules is of the type and magnitude such that an exchange complex is formed. The complex may be extremely short-lived. However, formation of a complex requires that the number of separable molecular particles in the system decreases by one from the number contained in the system prior to complex formation. This in turn requires that the system alter 12 degrees of freedom upon the formation of the complex. The three translational, three rotational, and 3N-6 vibrational degrees of freedom of the individual molecules D and A must be replaced by three translational, three rotational, and $3N_D + 3N_A - 6$ vibrational degrees of freedom of the complex as a whole.

Each mechanism described above will be discussed in detail and the cases where each process applies will be given.

All evidence concerning the rates of triplet energy transfer in solution which has been obtained in these and other laboratories indicates that the maximum rate approaches that which corresponds to a diffusion-controlled process (4-20, 22, 34). This observation implies that bimolecular contact, or very near contact, is necessary for efficient energy transfer. These observations are also in accord with the requirement that electron exchange is necessary in order to conserve spin in the overall transfer process.

Exchange interaction removes the distinguishability between the electron systems of donor and acceptor. Therefore, the intermediate particle composed of interacting donor and acceptor may be considered distinguishable from both the donor and acceptor molecules. This intermediate corresponds to an exchange complex of the type described above and is necessary for triplet energy transfer. Further evidence supporting a mechanism involving a complex intermediate for triplet energy transfer is obtained from results contained in this thesis.

Mechanism (a) may be applied to energy transfer processes where spin conservation requirements can be satisfied without electron exchange. Some processes which satisfy these requirements are (1) intersystem crossing, internal conversion, and vibrational relaxation within a single molecule located in a fluid environment; (2) singlet

energy transfer in fluid and crystalline media; and (3) the absorption and emission of radiation.

Qualitative Discussion of the Mechanism for Triplet Energy Transfer in Solution

The general mechanism involving a complex intermediate may be written as

$$D^* + A \underset{k_{-1}}{\overset{k_1}{\rightleftharpoons}} (DA)^*_i \tag{82}$$

$$(DA)^*_i \underset{k_{-2}}{\overset{k_2}{\rightleftharpoons}} (DA)^*_{fa} + \Delta E_{i,fa} \tag{83}$$

$$(DA)^*_{fa} \underset{k'_{-2}}{\overset{k'_2}{\rightleftharpoons}} (DA)^*_{fb} + \Delta E_{fa,fb} \tag{84}$$

$$(DA)^*_{fn} \underset{k_{-3}}{\overset{k_3}{\rightleftharpoons}} D + A^* \tag{85}$$

Equation 82 shows the formation of a complex between D* and A which may be considered to be in an initial electronic state $(DA)^*_i$. In the absence of any strong long-range electrostatic effects, the rate at which the two reacting molecules can diffuse together and apart will depend on the factors that normally effect diffusion rates in fluid media. In general, these factors include molecular sizes, fluid viscosities, and

temperature. In the systems which are of interest here, the second order collision rates are of the order of 10^9 liters/mole/sec. In the absence of any interaction between them, D* and A should remain within close proximity of one another for about 10^{-9} seconds.

Equation 83 represents an internal conversion and vibrational relaxation process between an initial complex electronic state $(DA)^*_i$ with energy close to that for D* + A, and a second electronic state of the complex $(DA)^*_{fa}$, which has energy that may be close to the energy of D + A*. This process is expected to be very fast when the energy differences between electronic states are small. There may be more than one final electronic state to which the initial state may be directly converted. In addition, all of these final states may be interconvertible, as shown by equation 84.

Finally, the energy transfer products, D + A*, are formed from the decomposition of the weak complex,as shown by equation 85. The rate at which the complex may decompose depends on the amount of bonding between D and A* in the complex. For very weak bonding, the rate of decomposition should correspond to the rate at which the complex partners diffuse apart. This will be shown later.

All processes shown in equations 82-85 are considered to be reversible. However, it should be noted that complex formation and decomposition may be able to proceed by several paths, some being favored for decomposition and others for formation. A discussion of

the different reaction paths that may be followed will be given in a following section.

Thus far in the discussion concerning the complex transfer mechanism, the spins of D*, A, D, A*, and the complex (DA)* have not been specified. It has been stated, however, that the mechanism chosen for a particular mode of energy transfer must contain within it a means for satisfying the spin conservation requirement. It is now of particular interest to see what that spin requirement is for systems that are of experimental interest here.

From time to time the term "triplet energy transfer" has been and will be referred to. In general, this term will be used when considering any process where an excited triplet state donor is involved and in which the triplet donor is converted to its ground singlet state during the transfer reaction.

The following processes are allowed by spin conservation rules under the specific conditions listed:

$$D^*(x) + A(y) \rightarrow (DA)^* \rightarrow D(x) + A^*(y); \quad x \geq 0, \; y \geq 0 \tag{86a}$$

$$D^*(x) + A(y) \rightarrow (DA)^* \rightarrow D(x - 1) + A^*(y + 1); \quad x \geq 1, \; y \geq 0 \tag{86b}$$

$$D^*(x) + A(y) \rightarrow (DA)^* \rightarrow D(x - 1) + A^*(y); \quad x \geq 1, \; y \geq \tfrac{1}{2} \tag{86c}$$

$$D^*(x) + A(y) \rightarrow (DA)^* \rightarrow D(x - 1) + A^*(y - 1); \quad x \geq 1, \; y \geq 1 \tag{86d}$$

In the above expressions, $\underline{x}$ and $\underline{y}$ refer to the total spin $\underline{S}$ of the molecular wave functions of $\underline{D}$ and $\underline{A}$. ($\underline{S}$ is determined from the operation of the $\underset{\sim}{S}^2$ operator on the particle wave functions.)

In the absence of any energetic effects which may influence the rates of product formation, the statistical probabilities for each of the above processes depend upon the specific values of $\underline{x}$ and $\underline{y}$. Of particular interest here are the cases where $\underline{x} = 1$, for the triplet state of the donor molecule, and $\underline{y}$ takes values from 0 to 5/2. Table XIII represents the statistical probability for each process for specific values of $\underline{x}$ and $\underline{y}$ which are of interest.

The probabilities of processes 86a through 86d occurring are determined as follows: Molecules $\underline{D}^*$ and $\underline{A}$ of spin $\underline{x}$ and $\underline{y}$ may combine to form a complex $(DA)^*$ with spin $\underline{S}$ equal to

$$x + y,\ x + y - 1,\ x + y - 2,\ \ldots,\ y - x \text{ for } y > x \quad \ldots,\ x - y \text{ for } x > y \tag{87}$$

The statistical weight for each of these complex spin states is given by

$$g_i = 2S_i + 1 \tag{88}$$

The total statistical weight for the formation of complex with all possible spin combinations will be the sum of statistical weights of the complexes with spin functions given in equation 87. Therefore, the total statistical weight of all complexes will be:

$$g_t = \sum_i g_i = 2(x + y) + 1 + 2(x + y - 1) + 1 + \ldots + 2(y - x) + 1; \quad y > x$$
$$\ldots + 2(x - y) + 1; \quad y < x \tag{89}$$

Table XIII

Spin Statistical Factors for Formation and Decomposition of Collision Complexes Requiring the Conservation of Total Spin.

(y)	(x)	Process 1	Process 2	Process 3	Process 4
0	0	1	-	-	-
y> 0	0	1	-	-	-
0	1	-	1	-	-
$\frac{1}{2}$	1	-	$\frac{2}{3}$	$\frac{1}{3}$	-
1	1	-	5/9	$\frac{1}{3}$	1/9
3/2	1	-	$\frac{1}{2}$	$\frac{1}{3}$	1/6
2	1	-	7/15	$\frac{1}{3}$	1/5
5/2	1	-	4/9	$\frac{1}{3}$	2/9

Process 86a $B(x)^* + Q(y) \rightarrow B(x) + Q(y)^*$; $x \geq 0$, $y \geq 0$

Process 86b $B(x)^* + Q(y) \rightarrow B(x-1) + Q(y+1)^*$; $x \geq 1$, $y \geq 0$

Process 86c $B(x)^* + Q(y) \rightarrow B(x-1) + Q(y)^*$; $x \geq 1$, $y \geq \frac{1}{2}$

Process 86d $B(x)^* + Q(y) \rightarrow B(x-1) + Q(y-1)^*$; $x \geq 1$, $y \geq 1$

Only spin factors are considered in above processes.

For each process only complexes which have spins given by

$$\begin{aligned}
&\text{Process 86a.} \quad x + y,\ x + y - 1,\ \ldots,\ x - y;\ x > y \\
&\text{Process 86b.} \quad x + y,\ x + y - 1,\ \ldots,\ x - y;\ x > y \\
&\text{Process 86c.} \quad y + x - 1,\ y + x - 2,\ \ldots,\ y - x + 1;\ y > x \\
&\text{Process 86d.} \quad y + x - 2,\ y + x - 3,\ \ldots,\ y - x;\ y > x
\end{aligned} \tag{90}$$

can decompose to give products with proper spin. These complexes will be referred to as deactivating complexes.

Since the spins of D and A do not change during the energy transfer process described by equation 86a, an exchange complex is not required as a reaction intermediate. Energy transfer involving this process may, however, proceed by either or both mechanisms introduced on page 119. Whichever mechanism takes precedence over the other depends on the magnitude and type of interaction between particles and on the physical nature of the system involved.

Triplet energy transfer may be described by equations 86b, 86c, and 86d, where $x = 1$. With the exception of experiments with paramagnetic substances, such as certain transition metal chelates and solvated paramagnetic ions, most triplet state quenching studies have been carried out using diamagnetic quenchers (usually pure organic compounds) which have available low-lying triplet states that can be coupled with the occupied triplet state of the excited donor. These reactions proceed exclusively by process 86b, where $x = 1$ and $y = 0$.

As seen from Table XIII, this process has a spin statistical factor of one, indicating that every complex formed may decompose into product. Therefore, the primary factors which may influence the rate of energy transfer by this process arise from the energetics involved in the formation, internal conversion, and subsequent decomposition of the complex.

Paramagnetic substances may quench a triplet state donor by any or all of the processes described by equations 86b, 86c, and 86d, subject to the initial spin constraints given for each process. The spin statistical factor for each reaction is given in Table XIII for all initial quencher states with spins ranging from 1/2 to 5/2. The rates of energy transfer through each of the different reaction paths for a given quencher depend on the interaction energies between donor and quencher and the separation of the electronic states of the donor and quencher which are involved in the transfer process.

Observing the spin statistical factors reported in Table XIII for paramagnetic substances, it becomes apparent that only a fractional number of the complexes formed by each process (86b-86d) are able to decompose into product. These complexes are the ones that satisfy the spin requirements shown in expression 90. The complex spin states which do not satisfy the decomposition requirements are excited states of complexes that do. These excited complex states have different spin multiplicities than the "deactivating" complex states. However, they

may be converted to "deactivating" states through intersystem crossing. The probability that the necessary interconversion can occur during the lifetime of the complex depends on the magnitude of the spin-orbit perturbation that mixes the different spin states. The spin-orbit perturbation may be quite large in systems containing heavy metals such as in transition metal chelates.

The lifetime of the excited complexes may also be dependent on the rate of intersystem crossing between an excited complex state and the "deactivating" state. This may result when the energy of the final electronic state of improper spin for product decomposition is sufficiently low that reverse decomposition into reactants becomes unfavorable. In this case, the complex would be trapped in a semi-stable state until converted by spin-orbit interaction to a final spin state capable of decomposition into product. If this is true, then the quenching efficiencies of the paramagnetic chelates should correlate directly with the energies of their electronic states and not with their spin statistical factors. Experimental evidence contained in this thesis indicates that a process of the type described here probably does occur in some systems studied.

Introduction to the Semiquantitative Discussion of the Mechanism of Triplet Energy Transfer

A precise time-dependent quantum mechanical treatment of the mechanistic processes involved in triplet energy transfer is too complicated and difficult to consider here. It is possible, however, to consider the mechanism in a semiquantitative manner under certain limiting conditions. Much valuable information can be obtained from a treatment of this type. It is doubtful whether a more complete treatment will be of any additional benefit, since most triplet energy transfer reactions in solution are expected to proceed under the limiting conditions where the approximate treatment applies.

In following sections, a discussion of the time-dependent quantum mechanics involved in the partitioning of energy between possible states of macroscopic systems will be given. This will be followed by a brief discussion of the factors governing the rates of internal conversion, intersystem crossing and vibrational relaxation in these systems.

Electronic interactions between specific pairs of molecules will be considered under two conditions. The first is where exchange interaction is unnecessary for the transfer of energy and the other where it is necessary. Consideration of the first process leads to a general mechanism for singlet energy transfer in solution. According to this mechanism, energy may be transferred over distances in excess of

ordinary collision diameters. Consideration of the second condition leads to a general mechanism for triplet energy transfer in solution.

In the final section each of the steps composing the proposed mechanism for triplet energy transfer in solution will be considered in a semiquantitative manner. The factors that influence the overall rate of the transfer process will be discussed, and a simple expression for the rate constant, k_q, will be given. The equation will be applied to experimental data obtained in these and other laboratories. The results obtained are very gratifying.

Time-Dependent Quantum Mechanics for the System

First let us consider a system that consists of a specific molecule, M, located in an environment of solvent molecules, S. The entire system is considered to be isolated from its external environment. Under this condition energy is conserved within the system.

The lowest excited electronic states of the solvent molecules are considered to be significantly higher than the excited electronic states of M which are of physical interest in this discussion. Furthermore, all electronic states of the solvent S are considered to be of sufficiently high energy that there is no significant occupation of these states when the system is at thermal equilibrium at room temperature. (This restriction is not placed on the electronic states of M.) Also, at this temperature, the difference in energy between vibrational states,

ΔE_{vib}, for most molecules at thermal equilibrium with their environment, is large compared to $\underline{kT}$. ($\underline{k}$ is Boltzmann's constant, and $\underline{T}$ is temperature.) Therefore, most of the molecules in the system described will be in their lowest vibrational states when at thermal equilibrium at room temperature. Under these conditions, thermal energy is primarily distributed throughout translational and rotational modes of excitation.

Finally, all molecules composing the system are considered to move in the weak coulombic field produced by all other particles in the system. Motion of the molecular particles is perturbed only slightly except when in very near contact with other molecules of the system. The major type of interaction encountered between pairs of molecules is, in general, of a repulsive electrostatic nature. Exchange interaction between molecules is considered negligible in this sytem.

The wave-function , $\Psi(p_i, q_i, t)$, describing our knowledge of the system at any instant, must be a function of the conjugate momenta $\underline{p_i}$ and coordinates $\underline{q_i}$ of all particles composing the system. The complicated function, however may be simplified by expansion in a Taylor series about the set of molecular coordinates which produce the minimum potential field for the system.

Since no exchange interaction is considered significant here, and since the repulsive interactions between molecules are considered very small except when in near contact with one another, only the first term in the series expansion is significant. The wave-function for this

configuration may be represented approximately as a product wave-function for each separate molecular particle in the system. This instantaneous zero-order stationary-state wave-function may be written as

$$\Psi_k^{\,o} = (M)_i \, v_{i,n} \, R_{i,r} \, T_t \, \varphi_j \, e^{-i/\hbar \, E_k^{\,o} t} \tag{91}$$

where $(M)_i$ is the electronic wave-function for the $\underline{i}^{th}$ electronic state of molecule $\underline{M}$, $v_{i,n}$ represents the vibrational wave-function of $\underline{M}$ corresponding to the $\underline{n}^{th}$ vibrational state of the $\underline{i}^{th}$ electronic state, $R_{i,r}$ is the rotational wave-function for $\underline{M}$ corresponding to the $\underline{r}^{th}$ rotational state of the $\underline{i}^{th}$ electronic state, and T_t is the translational wave-function for the $\underline{t}^{th}$ translational state of $\underline{M}$. Finally, φ_j is a composite environmental wave-function which includes electronic, vibrational, rotational and translational wave-functions for all molecular particles making up the environment. The total energy for the state represented by $\Psi_k^{\,o}$ is $E_k^{\,o}$.

The wave-functions described by equation 91 are solutions of the time-dependent Schrodinger equation

$$\underset{\sim}{H}^{o} \Psi_k^{\,o} = -\frac{\hbar}{i} \frac{\partial \Psi_k^{\,o}}{\partial t} \tag{92}$$

where $\underset{\sim}{H}^{o}$ represents the total energy of the system when it is in its minimum potential energy configuration. In general, for every E^o there are a very large number of isoenergetic or nearly isoenergetic

states for the system. Each of these states is represented by a wave-function, Ψ_k^o, defined by a $\underline{k}^{th}$ set of quantum numbers.

The total Hamiltonian for the system, $\underset{\sim}{H}$, contains in addition to $\underset{\sim}{H}^o$ an additional term, $\underset{\sim}{H}'$, which accounts for changes in potential energy corresponding to changes in the molecular coordinates of the particles composing the system. The total Hamiltonian may be written as

$$\underset{\sim}{H} = \underset{\sim}{H}^o + \underset{\sim}{H}' \tag{93}$$

The most significant contributions to $\underset{\sim}{H}'$ in the present system correspond to the repulsive and distortive interactions exerted between pairs of molecules during an encounter. This interaction is able to convert the system from certain initial states represented by Ψ_i^o to certain final states represented by Ψ_f^o.

At any time $\underline{t}$, the complete wave-function for the system under the action of the total Hamiltonian (93) may be expressed as a linear combination of functions of type 91 as

$$\Psi(t) = \sum_k a_k(H', t)\, \Psi_k^o(t) \tag{94}$$

The coefficients $a_k(t)$ may be determined in the following manner. Replacing Ψ_k^o by $\Psi(t)$ and $\underset{\sim}{H}^o$ by $\underset{\sim}{H}$ in equation 92, multiplying on the left by Ψ_j^{o*}, and integrating over all configuration space, one obtains a set of simultaneous differential equations in $a_j(t)$ written as

$$\frac{da_j(t)}{dt} = -\frac{i}{\hbar} \sum_k a_k(t) \int \Psi_j^{o*} \underset{\sim}{H'} \Psi_k^{o} \, d\tau \tag{95}$$

This set of equations may be more conveniently written in matrix form as

$$\frac{d}{dt} \begin{bmatrix} a_1 \\ a_2 \\ a_3 \\ \vdots \end{bmatrix} = -\frac{i}{\hbar} \begin{bmatrix} H'_{11} & H'_{12} & H'_{13} & \cdots \\ H'^{*}_{12} & H'_{22} & H'_{23} & \cdots \\ H'^{*}_{13} & H'^{*}_{23} & H'_{33} & \cdots \\ \vdots & \vdots & \vdots & \end{bmatrix} \begin{bmatrix} a_1 \\ a_2 \\ a_3 \\ \vdots \end{bmatrix} \tag{96}$$

where

$$H'_{jk} = \int \Psi_j^{o*} \underset{\sim}{H'} \Psi_k^{o} \, d\tau \tag{97}$$

If the system is known to be in some particular initial state, Ψ_o^{o}, at time $t = 0$, equation 96 describes the change of the system to final states, Ψ_f^{o}, as a function of time. The probability that the system will be in a particular state at $t = t'$ is given by the quantity $a_p(t')^* a_p(t')$. When the system reaches thermodynamic equilibrium, a statistical distribution of final states is obtained. The rate of change of the probability that the system will be in a particular final state at some later time approaches zero, and the total wave-function becomes stationary. This stationary-state wave-function describes the system at any time after equilibrium is established until the system is subjected to a new perturbation which destroys the equilibrium.

The stationary-state wave-function describing the system at thermodynamic equilibrium may be written as

$$\Psi^{s}_{eq}(t) = \sum_{j} a'_{eq,j} \Psi_{j}^{o}(t) \qquad (98)$$

where the $a'_{eq,j}$'s are time-independent. (In following sections all time-independent coefficients will be primed, such as a'_{j}.) Equation 98, representing the distribution of states at equilibrium, is only one specific wave-function of the complete set of stationary-state wave-functions corresponding to all possible configurations of states for the system with total energy equal to E^{o}. This set of stationary-state functions may be represented as

$$\Psi^{s}_{m} = \sum_{j} a'_{m,j} \Psi_{j}^{o} \qquad (99)$$

where $a'_{m,j}$'s are constants which describe the $\underline{m}^{th}$ configuration of system stationary states Ψ_{j}^{o}.

Substituting 91 into 98 and rearranging the terms according to states of molecule $\underline{M}$, one obtains for the wave-function describing the system at equilibrium the expression

$$\Psi^{s}_{eq}(t) = \left[\sum_{k} b'_{eq,k} (M)_{i} v_{i,n} R_{i,r} T_{t} \sum_{j} c'_{eq,j} \varphi_{j,\epsilon_{k}} \right] e^{-i/\hbar E_{s} t} \qquad (100)$$

which may be rewritten as

$$\Psi^{s}_{eq}(t) = \sum_{k} b'_{eq,k} (M)_i \, v_{i,n} R_{i,r} T_t \, \Phi_{eq,\epsilon_k} e^{-i/\hbar(E_{M_k} + \epsilon_k)t} \qquad (101)$$

In equations 100 and 101, the coefficients $b'_{eq,k}$ describe the equilibrium occupation of the $\underline{k}^{th}$ set of states for $\underline{M}$ where $k = k(i,n,r,t)$. Φ_{eq,ϵ_k} is one of the complete set of environmental stationary states

$$\Phi_{\sigma,\epsilon_k} = \sum_{j} c'_{\sigma,j} \varphi_{j,\epsilon_k} \qquad (102)$$

that corresponds to the equilibrium distribution with energy equal to ϵ_k. This set of functions represents all possible isoenergetic stationary configurations of the environment.

The amount of energy partitioned between states of $\underline{M}$ which are defined by the $\underline{k}^{th}$ set of quantum numbers is E_{M_k}. The total energy for the system at equilibrium is E_s. Therefore, the difference $E_s - E_{M_k} = \epsilon_k$ is the energy that is partitioned between different states of the environment for each $\underline{k}$.

Internal Conversion, Intersystem Crossing, and Vibrational Relaxation

Now let us assume that ΔE_{elec} between the ground electronic state of $\underline{M}$, $(M)_o$ and all excited electronic states $(M)_u$ is large. Also, let us assume that ΔE_{vib} between two vibrational states of $\underline{M}$ is large compared to $\underline{kT}$. Under these conditions, equation 101 may be written as

$$\Psi^{s}_{eq} = (M)_{o}\, v_{o,o}\, \Phi''_{eq,\varepsilon_o}\, e^{-i/\hbar E_o t} \tag{103}$$

where $\Phi''_{eq,\varepsilon_o}$ is the same as $\Phi_{eq,\varepsilon}$, except that the rotational and translational wave-functions for $\underline{M}$ have been included with the environmental wave-functions.

Now if at some time $t = t_o$, $\underline{M}$ is excited from its ground state to an excited electronic state, say $(M)_a$, the system may undergo internal conversion and vibrational relaxation until thermodynamic equilibrium is reestablished. The wave-function describing the system at any time during this period may be given by a function of the type described by equation 94 as

$$\Psi_{(t)} = a_o(t)(M)_a\, v_{a,n}\, \Phi''_{eq,\varepsilon_o}\, e^{-i/\hbar(E_o + \Delta E_{a,o})t}$$

$$+ \sum_{j \neq o} a_j(t)(M)_i\, v_{i,m}\, \Phi''_{\sigma,\varepsilon_k}\, e^{-i/\hbar(E_{M_k} + \varepsilon''_k)t} \tag{104}$$

In equation 104, the $\Phi_{\sigma,\varepsilon_k}$'s are all members of a complete set of environmental states similar to those defined by equation 102 with energy of ε''_k. These terms differ from the set shown by expression 102 in that the rotational and translational wave-functions of $\underline{M}$ have been included. Subscript $j=j(k,\sigma)$, and designates the $\underline{k}^{th}$ set of electronic and vibrational quantum numbers for $\underline{M}$ and the σ^{th} distribution of environmental states represented by $\Phi''_{\sigma,\varepsilon_k}$. For each $\underline{k}$ there is

a complete set of environmental states, $\Phi''_{\sigma,\varepsilon_k}$.

Only final states with total energy equal to or very nearly equal to the energy of the initial state will contribute significantly to the time-dependent wave-function for the system. Therefore, $(E_o + \Delta E_{a,o}) \simeq (E_{M_k} + \varepsilon''_k)$ where $E_o = (E_{M_o} + \varepsilon''_o)$. E_o is the energy of the system prior to excitation. In spite of this restriction, in general, there remains a very large number of final states that may be coupled directly to the initial state of the system.

The coefficients for equation 94 may be determined from the solution of a matrix equation of type 96 with the initial condition that $a_o(t_o) = 1$. If one considers only isoenergetic states for the system or assumes that the total energy for any state of the system can be approximated accurately by the average energy $\bar{E}$ of all possible states of the total system, then the solutions for equation 96 are

$$a_k(t) = \sum_{\underline{n}} u_{nk}\, u^*_{n1}\, e^{-i/\hbar\, \lambda_n t} \tag{105}$$

Here λ_n are the $\underline{n}$ eigenvalues for the Hermetian matrix $\bar{H}_{ij}$. u_{nk} are the $\underline{k}^{th}$ terms of the eigenvectors $\bar{u}_n$ corresponding to the $\underline{n}^{th}$ eigenvalue for the Hermetian matrix. These terms are the elements of the unitary matrix that diagonalizes $\bar{H}_{ij}$. u^*_{n1} are the complex conjugates of the first terms in the eigenvectors for each eigenvalue of the matrix and arise from the initial condition that $a_o(t_o) = 1$. The probability,

$w(t')$, that the system will be in any final state at $t = t'$ is

$$w(t') = 1 - |a_o(t')|^2 = \sum_{k \neq o} |a_k(t')|^2 \qquad (106)$$

Transmission of energy from $\underline{M}$ into its environment accompanies the conversion of $\underline{M}$ from high to low electronic states. Absorption of energy from the environment must accompany the formation of electronic states of $\underline{M}$ that are higher energy than the initial state $(M)_a$. When higher electronic states have energy that is close to the initial state, there may be expected a significant probability of thermal excitation to these higher states. At moderate to large energy separation between upper states, only conversion to lower electronic states is significant.

It is of interest to investigate briefly the types of matrix elements that constitute the Hermetian matrix of equation 96. These elements represent the interactions between particles of the system which are responsible for the conversion of the system from initial to final stationary-state configurations.

The perturbation Hamiltonian $\underset{\sim}{H}'$ may be effectively separated into parts

$$\underset{\sim}{H}' = \underset{\sim}{H}'_{elec,s} + \underset{\sim}{H}'_{vib,s} + \underset{\sim}{H}'_{s,s} \qquad (107)$$

In equation 107, $\underset{\sim}{H}'_{elec,s}$ represents the distortive electrostatic interaction between $\underline{M}$ and particles composing the environment. These interactions are responsible for the mixing of different electronic states

of molecule $\underline{M}$. $\underset{\sim}{H}'_{vib,s}$ represents the interaction between $\underline{M}$ and the environment which converts vibrational energy of $\underline{M}$ into translational, rotational, and vibrational energy of the environment. $\underset{\sim}{H}'_{s,s}$ represents the interaction energy between particles in the environment which converts the system from one environmental state to another.

The diagonal matrix elements

$$H'_{k_i k_i} = (\Psi^s_k |\underset{\sim}{H}'| \Psi^s_k) = ((M)_i \, v_{i,n} \, \Phi''_{\sigma,\varepsilon_k} |\underset{\sim}{H}'| (M)_i \, v_{i,n} \, \Phi''_{\sigma,\varepsilon_k}) \quad (108)$$

represent the effect of the perturbation on each of the stationary-state functions Ψ^s_k making up the total time-dependent wave-function of the system. These terms do not contribute to the rates of conversion between possible states of the system.

There are three types of off-diagonal matrix elements for this problem. The first represents mixing between electronic states of $\underline{M}$ as a function of the interactions with the environment. These interactions are responsible for internal conversion and intersystem crossing between the different electronic states of $\underline{M}$. The matrix elements may be written as

$$H'_{k_i k_j}(\text{elec}) = ((M)_i \, \Phi''_{\sigma_i} |\underset{\sim}{H}'_{\text{elec},s}| (M)_j \, \Phi''_{\sigma_j})(v_{i,n} | v_{j,m}) e^{-i/\hbar \Delta E t}$$

$$= \beta_{\text{elec}_{ij}} (v_{i,n} | v_{j,m}) e^{-i/\hbar \Delta E t} \quad (109)$$

Here, $\beta_{elec_{ij}}$ represents the direct mixing between the $\underline{i}^{th}$ and $\underline{j}^{th}$ electronic states of $\underline{M}$. ΔE is the difference in energy between the two states of the system coupled by this matrix element. $(v_{i,n}|v_{j,m})$ is the vibrational overlap factor representing the amount of overlap between the $\underline{n}^{th}$ vibrational state of the $\underline{i}^{th}$ electronic state of $\underline{M}$ with the $\underline{m}^{th}$ vibrational state of the $\underline{j}^{th}$ electronic state of $\underline{M}$. The subscripts k_i and k_j represent the sets of parameters (i,σ_i,n) and (j,σ_j,m) that designate the two states that are coupled by the matrix element, $H'_{k_i k_j}(elec)$.

The infinite number of possible terms of type 109 may be restricted to a large finite number by considering that only system states, Ψ_k^s, which are in resonance or very near resonance ($\Delta E \simeq 0$), contribute significantly to the total wave-function for the system. The magnitude of these matrix elements depends on the magnitude of $\beta_{elec_{ij}}$ for any pair of electronic states that are coupled through interaction with the environment, and on the magnitude of the vibrational overlap factor $(v_{i,n}|v_{j,m})$.

Internal conversion between two electronic states of $\underline{M}$ can occur at any vibrational level of the initial state subject to the condition that excitation of $\underline{M}$ results in the population of that vibrational state. When the final electronic state has energy that is close to that of the initial state, large overlap between vibrational states of the initial and final electronic states is usually possible. This results in relatively

large coupling matrix elements of type 109. For large energy separations between electronic states, the vibrational overlap factors for isoenergetic system states may be expected to become quite small. In this case, direct coupling between non-isoenergetic states may be significant. However, the importance of this coupling rapidly diminishes as the energy separation ΔE between the initial and final states increases. Robinson (59) has discussed vibrational overlap factors in considerable detail, and so no further discussion along this line will be pursued here.

In the above discussion, no restriction was placed on the spin multiplicities of the states whose coupling is described by electronic matrix elements of type 109. Due to the action of an inherent spin-orbit perturbation, which is characteristic of all molecules, each complete electronic wave-function is expected to contain contributions from unperturbed electronic wave-functions with different spins. If the spin-orbit interaction is very small compared to other interactions described by the total Hamiltonian for the molecule, complete electronic stationary-state wave-functions may be written approximately according to first order perturbation theory as

$$(M)_i^{\bar{s}_1} = (M)_i^{s_1} + \sum_{s'} \frac{H'(s.o.)}{\Delta E_{s_1 s'_1}} (M)_i^{s'_1} \qquad (110)$$

where $\underline{s}_1 \neq \underline{s}'_1$. Here $\underline{s}_1$ is the spin of the principal unperturbed state wave-function, and s'_1 is the spin of other possible states with the $\underline{i}^{th}$

orbital configuration which are weakly mixed with the principal state through the action of the spin-orbit perturbation $\underset{\sim}{H}'(s.o.)$. $\Delta E_{s_1 s'_1}$ is the energy separation between the electronic states with spins s_1 and s'_1. When $\Delta E_{s_1 s'_1}$ is very small or when the spin-orbit interaction energy $H'(s.o.)$ is very large, then expression 110 is not accurate and must be properly normalized. It is most convenient, however, to consider the condition where expression 110 does apply satisfactorily.

Substituting 110 into 109, one obtains for the time-independent part of the electronic coupling matrix element, $H'_{k_i k_j}(elec)$, the expression

$$H'_{k_i k_j}(elec) = ((M)_i^{\bar{s}_1} \Phi''_{\sigma_i} | \underset{\sim}{H}'_{elec,s} | (M)_j^{\bar{s}_2} \Phi''_{\sigma_j})(v_{i,n} | v_{j,m})$$

$$= \beta_{elec_{ij}}(v_{i,n} | v_{j,m}) \left[\delta_{s_1 s_2} + \sum_{s'_1} \frac{H'(s.o.)}{\Delta E_{s_1 s'_1}} \delta_{s'_1 s_2} \right.$$

$$\left. + \sum_{s'_2} \frac{H'(s.o.)}{\Delta E_{s_2 s'_2}} \delta_{s_1 s'_2} + \cdots \right] \qquad (111)$$

where δ_{ab} is the Kronecker delta. Only the most significant first order terms have been included in expression 111. $(M)_i^{\bar{s}_1}$ and $(M)_j^{\bar{s}_2}$ are functions described by expression 110 with principal spins of s_1 and s_2. Expression 111 is general for all electronic coupling matrix elements in equation 96 and describes both internal conversion between states with identical spin (e.g., $s_1 = s_2$) and intersystem crossing between states

with different principal spin (e.g., $s_1 \neq s_2$ but some $s'_1 = s_2$ or $s_1 = s'_2$).

The remaining two kinds of off-diagonal matrix elements for equation 96 are (1) elements that represent the coupling between different vibrational states of $\underline{M}$ through interaction with the environment and (2) elements that represent coupling between different environmental states of the system. The first of these terms representing the conversion of $\underline{M}$ from vibrational state v_{i,n_1} to state v_{i,n_2} may be written as

$$H'_{vib,s} = (v_{i,n_1}\Phi''_{\sigma_a}|\underset{\sim}{H}_{vib,s}|v_{i,n_2}\Phi''_{\sigma_b})\, e^{-i/\hbar\,\Delta E t}$$

$$= \alpha^{\sigma_a\sigma_b}_{n_1 n_2}\, e^{-i/\hbar\,\Delta E t} \qquad (112)$$

where σ_a and σ_b represent possible stationary distributions of environmental states, φ''_{j,ϵ_k}, constituting the general environmental state $\Phi''_{\sigma,\epsilon_k}$. Elements that describe coupling between different environmental states may be written as

$$H'_{s,s} = \gamma_{\sigma_a\sigma_b} = (\Phi''_{\sigma_a}|\underset{\sim}{H'}_{s,s}|\Phi''_{\sigma_b})\, e^{-i/\hbar\,\Delta E t} \qquad (113)$$

It is of interest to consider briefly special cases for which simple solutions of equation 96 may be obtained. Fortunately, these special cases correspond to physically important situations whose understanding will greatly assist in the discussion concerning the quenching mechanism that is to follow.

First consider the possibility that the energies of two electronic states of $\underline{M}$ with the same spins are identical (e.g., $E_{(M)_a} = E_{(M)_b}$). Further consider that during the time interval $t_o < t < t'$, conversion of the system to all possible electronic states other than the two mentioned is negligible. Finally, assume that the system is known to be in electronic state $(M)_a$ and vibrational state $v_{a,o}$ at $t = t_o$. In addition, consider that a perturbation, $\underset{\sim}{H}'$, capable of mixing the electronic states, acts during the same time interval. Under these ideal conditions no transfer of energy from $\underline{M}$ into the environment through vibrational relaxation is possible. A wave-function describing the system during this time interval may be written as

$$\Psi(t) = \left[e^{-i/\hbar H'_{aa} t} \cos \frac{H'_{ab} t}{\hbar} \right] \Psi_a^s + \left[i e^{-i/\hbar H'_{aa} t} \sin \frac{H'_{ab} t}{\hbar} \right] \Psi_b^s \qquad (114)$$

under the assumption that $H'_{aa} = H'_{bb}$. The coefficients $a_a(t)$ and $a_b(t)$ were determined directly from equation 105. The probability that the molecule will be in either electronic state $(M)_a$ or $(M)_b$ at time $\underline{t}$ is

$$|a_a|^2 = \cos^2 \frac{H'_{ab} t}{\hbar}$$

$$|a_b|^2 = \sin^2 \frac{H'_{ab} t}{\hbar} \qquad (115)$$

The time necessary for the system to be converted from the initial to the final state is $t = \frac{h}{4 H'_{ab}}$. In an equivalent length of time, the system will be converted back to its initial state if H'_{ab} is constant. The rate of conversion of the system between the initial and final state is therefore

$$k_t = t^{-1} = \frac{4 \beta_{ab}(v_{a,o} | v_{b,o})}{h} \tag{116}$$

It should be noted, however, that H'_{ab} is not expected to remain uniform for any real system during the time interval between measurements on the system as required for expression 115 to hold true. Furthermore, there is expected to be an intrinsic error introduced as a result of making measurements on the system. The exact time intervals required for the measurement are also subject to small fluctuations. The above results in an uncertainty of finding the system in a particular state at a specific time $\underline{t}$. Due to the uncertainty in H'_{ab}, the probability of finding the system in either state at some time after $t = t_o$ rapidly approaches 1/2 as shown by the expression

$$\overline{|a_b(t)|^2} = \tfrac{1}{2} - \frac{\hbar}{2t\Delta H'} \cos\left(\frac{2 H'_{ab}}{\hbar}\right) \sin\left(\frac{\Delta H' t}{\hbar}\right) \tag{117}$$

Equation 117 shows that the probability approaches 1/2 in an oscillatory manner as both $\underline{t}$ and the variation in H'_{ab} , $\Delta H'$, increase. When the limiting value of 1/2 for the probability for finding the system in either

state at any time is achieved, then the wave-function for the system becomes stationary with the energy partitioned equally between the two possible states.

The second and most important limiting case where a solution for the time-dependent problem for internal conversion and vibrational relaxation may be obtained, is when the energy separations between electronic states of $\underline{M}$ are very large and where the time necessary for internal conversion between electronic states, τ_{el} is slow compared to the time necessary for vibrational relaxation τ_{vib}. To best describe this process, it is convenient to write the following reaction sequence:

$$[(M)_a\, v_{a,o}] \xrightarrow{k_{ic}} [(M)_b\, v_{b,n}] \qquad (118)$$

$$[(M)_b\, v_{b,n}] \xrightarrow{k_v} [(M)_b\, v_{b,m}] \qquad (119)$$

k_{ic} is the rate constant for internal conversion and k_v is the rate constant for vibrational relaxation. Under the initial restriction for this problem, $k_v >> k_{ic}$. The rate constant for the overall decay process described by equations 118 and 119 is k_d.

The molecule $\underline{M}$ is considered to be initially in an excited electronic state $(M)_a$ which has energy $\Delta E_{a,b}$ greater than a final electronic state $(M)_b$. The initial vibronic state of the system $(M)_a v_{a,o}$ may be coupled directly to a number of final vibronic states $(M)_b v_{b,m}$

by a set of electronic matrix elements of the type 111. Each final vibrationally-excited state, $v_{b,m}$, may in turn be coupled to lower vibrational states, $v_{b,p}$, by sets of matrix elements of type 112. The most significant coupling elements of this type correspond to conversions involving the loss of only a single quantum of vibrational energy (e.g., $p = m - 1$). Finally, sets of excited environmental states are coupled with other environmental states by matrix elements of type 113.

Due to the excessive number of final vibronic and environmental states for the system, the transmission of energy from $\underline{M}$ into the environment becomes essentially irreversible when the energy gap between the initial and final electronic states is large. Robinson (59, 60) has considered the above problem in detail for nonradiative relaxation in the solid phase. His treatment leads to the following expression for the rate constant for the first order decay of the initial excited electronic state of $\underline{M}$:

$$k_d = \frac{w(t)}{t} = \frac{2\tau_{vib}}{\hbar^2} \sum_{k_j} H'^2_{k_o k_j}(\text{elec}) \qquad (120)$$

In the derivation of equation 120, the assumption is made that the initial state is linearly coupled to a single final state by the electronic matrix element $H'_{k_o k_j}(\text{elec})$. This final state is then linearly coupled to a second final state by an average vibrational-environmental matrix element $\bar{\gamma} = \bar{\alpha} \simeq \frac{\hbar}{\tau_{vib}}$. A somewhat complicated expression for the rate

of decay of the initial electronic state results directly from the treatment, but it reduces to expression 120 for cases of physical importance where the number of linearly-coupled final states is large.

The problem may also be treated by assuming that a continuum of final states are directly coupled to the initial state by an average electronic matrix element $\bar{H}'_{k_o k_j}$. This treatment may be expected to be somewhat more applicable to the decay process in solution than the treatment mentioned above. However, the result obtained using this model only differs from equation 120 by a factor of π. The result, therefore, is essentially identical by either approach (60).

The summation in 120 is taken over all final vibronic states of $\underline{M}$, $[(M)_b v_{b,m}]$, that are directly coupled to the initial state by an electronic matrix element $H'_{k_o k_j}$. Observing the form of $H'_{k_o k_j}$, it is noted that it contains a vibrational overlap factor, $(v_{a,o}|v_{b,m})$, between the vibrational state $v_{a,o}$ of the initial electronic state and the excited vibrational state $v_{b,m}$ of the final electronic state. For small energy separations between electronic states, this factor may approach unity (depending on differences in nuclear coordinates and potential energy surfaces for the two electronic states). However, for large energy separations, these factors may become very small ($\sim 10^{-6}$). Since the rate of conversion from initial to final states depends on the squares of these terms, they become very important in determining the

magnitude of k_d. A decrease in the vibrational overlap factors as well as in $\beta_{elec_{ab}}$, resulting from an increase in the energy difference between the upper and lower electronic states of M, produces a decrease in the rate of conversion between these states. For very large energy separations, radiative modes of deactivation of the excited state may become competitive with the rate of non-radiative internal conversion and relaxation described by 120. However, for small energy separations between electronic states, non-radiative partitioning of energy may become extremely fast compared to the rates of radiative deactivation.

Electronic Energy Transfer Between Specific Pairs of Molecules

It is now of interest to consider a system which contains two specific molecules D and A, which are situated in a fluid environment. Excited electronic state energies of the solvent molecules S are considered to be significantly higher than the lowest excited electronic states of D and A which are of physical interest here. Therefore, no significant electronic interaction between either the molecules D or A with environmental molecules is possible. This type of restriction is not placed on the excited state energies of D and A however. As a result, significant electronic interaction between these two molecules may be possible. The system thus described is very similar to the one used for the discussion of the non-radiative conversion of a single molecule M from excited to ground electronic states.

The processes of internal conversion, intersystem crossing, and vibrational relaxation within D and A, which results from the interaction between these molecules and their environment, has been discussed earlier. The transfer of electronic energy between D and A will now be considered as an additional mode of excited-state deactivation which is in competition with the internal decay processes.

In the following discussion, D will always refer to the donor molecule. Initially at time $t = t_o$, this molecule will always be considered to be in an initial excited electronic state. The ground state of D will always be considered as a singlet unless otherwise stated. Electronic energy transfer is considered to proceed from D to an unexcited acceptor A. If the lifetime of the excited electronic state of D is sufficiently long, then a condition of pseudo-equilibrium may be established among the various vibrational, rotational, and translational states of the system. This pseudo-equilibrium condition will remain until it is upset following the transfer of electronic energy to A, or upon internal conversion or intersystem crossing to the ground electronic state of D.

There are two general types of transfer processes that may be considered. The first involves a transfer mechanism that does not require electron exchange between D and A in order to conserve the spin multiplicity of the overall transfer process. The second mechanism does require this condition to be met. Even though the bulk of this

discussion will be concerned with the second type of transfer process, it is advisable to briefly consider the first mechanism, since it involves the process of singlet energy transfer in dilute solutions, glasses and crystals. This transfer process may be greatly affected by the ability of the solvent to interact electronically with the donor and acceptor.

(1) Singlet Energy Transfer

Robinson has considered the problem of singlet energy transfer in detail with special emphasis placed on transfer in dilute glasses and crystals (59). The results of his treatment are expected to be equally applicable to systems involving dilute solutions. Therefore, it is unnecessary to go into the details regarding the theoretical treatment of the problem. It suffices to mention that the treatment very closely follows the treatment described earlier concerning internal conversion and vibrational relaxation. The only difference lies in the fact that the specific weak electronic interaction between excited donor and unexcited acceptor has been included.

The only cases that are of physical interest are those in which the energy transfer process competes effectively with internal modes of deactivation of the excited donor. Therefore, the weak environmental perturbations which mix electronic states of the donor in the absence of a specific interaction with acceptor are neglected. This assumption is perfectly valid for this problem.

As in the previous discussion, two solutions to the problem may be obtained. The first applies to a non-resonance condition where the electronic energy for the system before transfer is significantly greater than the electronic energy of the system after transfer. This results when the principally coupled electronic state of the acceptor has lower energy than the initial excited electronic state of the donor.

The second solution for this problem results when a resonance condition is involved. This is expected to apply to exciton migration among identical molecules. This may also be significant in situations where the donor and acceptor are not identical, but where the excited electronic states of the acceptor, capable of significant coupling with $\underline{D}^*$, have energies that are very near that of the initial excited state of the donor.

The solution to the problem for the rate of energy transfer from excited donor $\underline{D}^*$ to $\underline{A}$ under non-resonance conditions ($\Delta E_{el} >> \alpha >> \beta$) is the same as given in equation 120 :

$$k_{sq} = \frac{w(t)}{t} = \frac{2\tau_{vib}}{\hbar^2} \sum_{f,\upsilon} \left[H'_{DA_{f,\upsilon}}\right]^2 \qquad (121)$$

where

$$H'_{DA_{f,\upsilon}} = \left((D)_1(A)_0 \left| \underset{\sim}{H}'_{DA} \right| (D)_0(A)_f\right)\left(v_1^D \mid v_0^D\right)_\upsilon \left(v_0^A \mid v_f^A\right)_\upsilon \qquad (122)$$

The rate of energy transfer described by equation 121 is proportional to the sum of the squares of electronic coupling matrix elements defined

by 122. The summation is taken over all directly coupled final electronic states of $\underline{A}$, $(A)_f$, and all υ^{th} combinations of corresponding final vibrational states of the system which satisfy the energy conservation requirement for the transfer process.

Usually, significant coupling occurs only between a single final electronic state and the initial electronic state of the system. For each final electronic state which is directly coupled to the initial state, there is a set of υ combinations of final vibrational states of $\underline{D}$ and $\underline{A}$ which conserve energy in the overall transfer step. Each of these final vibrational combinations of the complete set has its own Franck-Condon overlap factor, $(v_1^D | v_0^D)_\upsilon$ and $(v_0^A | v_f^A)_\upsilon$, with the initial vibrational states for the system. The magnitudes of the matrix elements $H'_{DA_{f,\upsilon}}$ are strongly dependent on these vibrational overlap factors. For large energy gaps between initial and final electronic states of the system, these terms may become very small ($\sim 10^{-6}$) (59). Therefore, as a result, the rate of energy transfer is expected to decrease with an increase in the energy difference between electronic states of $\underline{D}$ and $\underline{A}$.

Finally, the electronic coupling matrix element for the transition, $((D)_1(A)_0 | \underset{\sim}{H}'_{DA} | (D)_0(A)_f)$, is of great importance in considering the overall rate of energy transfer. In the case of no interaction with the environment, the most significant contribution to the perturbation Hamiltonian may be expected to be dipole-dipole coupling between the respective radiative emission and absorption transition dipoles in $\underline{D}$

and A. Consideration of this contribution alone leads to Förster's equation for singlet energy transfer (35). Since the dipole perturbation Hamiltonian varies as $1/R^3$, the rate is expected to have a $1/R^6$ dependence on the intermolecular distance between D and A during the transfer process. This result is expected to apply most significantly to dilute fluid systems with non-interacting solvent.

In dilute crystalline and glassy systems, association between donor and acceptor molecules may be such that molecular aggregates may be formed during the cooling cycle. True random distributions of molecules are not necessarily expected under these conditions. Therefore, accurate intermolecular distances cannot be estimated under these circumstances. In addition, short-range interaction differing from the dipole-dipole interaction may also be expected. Under these conditions, experimental results may be expected not to agree with those predicted by Förster's theory.

Significant contributions to the perturbation Hamiltonian from higher multipole interactions between the electronic systems of donor and acceptor molecules may also be expected to bring about a situation where Förster's equation for singlet transfer does not apply. This has been pointed out carefully by Robinson (59).

When excited states of the solvent are able to interact significantly with excited states of the donor and acceptor, the mechanism for energy transfer may be altered considerably. In this case, entirely

different dependences on the internuclear distances between $\underline{D}^*$ and $\underline{A}$ may be expected than are predicted purely on the basis of electric dipole coupling.

The solution to the problem under resonance conditions (e.g., $\Delta E_{el} \simeq 0$) is similar to equation 116. It is

$$k_{sq} = \frac{4}{h} \left((D)_1(A)_0 \left| \underset{\sim}{H'}_{DA} \right| (D)_0(A)_f\right)\left(v_1^D \middle| v_0^D\right)_0\left(v_0^A \middle| v_f^A\right)_0 \quad (123)$$

Here, the vibrational overlap factors $\left(v_1^D \middle| v_0^D\right)_0$ and $\left(v_0^A \middle| v_f^A\right)_0$ represent the overlap between the zeroth or first vibrational states of the corresponding upper and lower electronic states of $\underline{D}$ and $\underline{A}$ which are coupled by $\underset{\sim}{H'}_{DA}$. The magnitude of these terms is strongly dependent on changes in the nuclear coordinates of each molecule during the respective electronic transitions. For large molecules, the Franck-Condon overlap between these vibrational states may be expected to become quite large. In fact, values as large as 0.1 to 1.0 are possible.

It is seen from equation 123 that the transfer rate constant is directly proportional to the purely electronic matrix element for the coupled transitions in $\underline{D}$ and $\underline{A}$, $\left((D)_1(A)_0 \left| \underset{\sim}{H'}_{DA} \right| (D)_0(A)_f\right)$. If the coupling perturbation is primarily electric dipole in nature, then the rate constant k_{sq} should vary as $1/R^3$, where R is the intermolecular distance between $\underline{D}$ and $\underline{A}$. This radial dependency would predict a linear dependence of the rate constant $\underline{k}_{sq}$ on the concentration of the acceptor present in the solution.

Experimental evidence contained in this thesis indicates that ferric dibenzoylmethide and chromium dibenzoylmethide are able to quench singlet benzophenone. The available experimental results indicate that the quenching rate is directly proportional to the concentration of the added quencher rather than on the square of the quencher concentration as expected on the basis of Förster's theory (35), which is related to equation 121. Energy transfer under near-resonance conditions as described above may account for the first order concentration dependence found experimentally, if the interaction between donor and acceptor is primarily electric dipole in nature.

The conditions for the quenching experiments conducted on the DBM chelates were such that only the lowest energy n-π^* excited singlet state of benzophenone was formed by absorption of filtered radiation. The fluorescent transition in this compound, therefore, is not expected to have a strong electric dipole associated with it, even though some is expected to be introduced through vibrations. However, it is seen from 123 that the electric dipole coupling matrix element $((D)_1(A)_0|\underset{\sim}{H}'_{DA}|(D)_0(A)_f)$ may be very small and yet account for significant energy transfer if the vibrational overlap terms are large.

The concentration of benzophenone used in these experiments was usually maintained at a moderately high level (0.1 molar). Under these concentration conditions, each benzophenone molecule may be expected to be somewhere in the immediate neighborhood of another

benzophenone molecule. Singlet energy migration, under resonance conditions, may possibly occur between several benzophenone molecules before final transfer to a DBM chelate.

Internal radiative and non-radiative modes of deactivation of the excited singlet state of any molecule will be in competition with the rate of singlet energy transfer. Within benzophenone, the most prominent deactivation process is expected to be the conversion of the singlet to the corresponding triplet. This triplet state is no longer expected to be able to transfer energy in the same manner as the singlets. In the chelates, deactivation may be expected to result from rapid internal conversion or radiative emission to lower electronic states, thus making these molecules good energy sinks for the migrating electronic energy.

It should be noted that the part which the solvent plays in the overall transfer process in the DBM chelate systems is presently unknown. The type of concentration dependence that one might expect as a result of significant solvent interaction is questionable. However, if singlet energy transfer in these systems is strongly dependent on coupling with excited environmental electronic states, it seems reasonable to expect a significant solvent effect on both the overall rate of singlet transfer and on the concentration dependency of the quencher as well. On the other hand, if the transfer process observed takes place under near-resonance conditions as described above, it is felt that the observed rate and concentration dependences should be nearly independent

of solvent as long as the solvents used do not have sufficiently low energy excited states capable of coupling significantly with donor and quencher.

(2) Triplet Energy Transfer

Until now, the type of coulombic interaction exerted between separate molecules in the reaction systems has been considered to be basically similar to the type described by equation 44 on page 57. This type of interaction represents the electrostatic effect that the nuclear and electronic system of one molecule exerts on the isolated electronic system of another.

The bimolecular interaction represented by coulombic matrix elements similar to those given by equation 43 describes the energy of stabilization resulting from the movement of electrons in an electronic system common to both molecular cores. This exchange interaction is related to the overlap of the electronic systems of the two molecules which has heretofore been considered negligible.

Exchange interaction between $\underline{D}^*$ and the solvent or between $\underline{A}^*$ and the solvent may be considered unimportant, if the populated excited-state energies of $\underline{D}^*$ and $\underline{A}^*$ are significantly lower than the lowest excited-state energies of the solvent. In the systems considered here, this energy restriction is satisfied. Exchange interaction between $\underline{D}^*$ and $\underline{A}$ may not be neglected, however, if it is required in order to satisfy spin conservation requirement for triplet energy transfer.

For the following discussion of the mechanism for triplet energy transfer involving a complex intermediate, the most common triplet transfer process will be considered. This reaction is the quenching of an excited triplet state donor by a singlet quencher. The conclusions obtained from this treatment may be extended to systems involving paramagnetic quenchers of the chelate type where energy transfer rather than some other possible quenching mechanism is involved.

In order to simplify the discussion, it will be assumed that the lifetimes of the lowest-energy triplet states of molecules in the system are long compared both to the times necessary for internal conversion and vibrational relaxation between states of identical spin, and the times necessary for molecules to diffuse together and apart in the solvent used. As a result of these restrictions, a pseudo-equilibrium condition may be established within the system.

The pseudo-equilibrium condition referred to here applies to a system where the lifetimes of the excited triplet states of molecules contained in the system are long compared to the times necessary for thermal equilibrium to be established among the possible environmental states. This condition may not be exactly met in all cases in actual laboratory systems; however, in most circumstances, it is felt that equilibrium may be closely approached.

Deactivation processes which involve changes in the total spin multiplicity of the system will not have to be considered simultaneously

with the energy transfer process discussed here, since the triplet state lifetimes are considered long. It should be noted, however, that internal non-radiative decay and phosphorescent emission are expected to be in competition with the energy transfer process for the deactivation of $\underline{D}^*$. The significance of these decay processes will be described whenever appropriate.

Only the lowest excited triplet states, $(D)_1^T$ and $(A)_1^T$, and ground singlet states, $(D)_0^S$ and $(A)_0^S$, of $\underline{D}$ and $\underline{A}$ will be considered important in this discussion. The energy separations between these singlet and triplet states are considered to be such that there is no significant occupation of the higher-energy state when the system is at true thermal equilibrium at room temperature.

Pseudo-equilibrium stationary-state wave-functions which describe the system before and after energy transfer and in the absence of any significant exchange interaction between $\underline{D}$ and $\underline{A}$ may be written as

(1) prior and energy transfer

$$\Psi^S_{init} = \left[(D)_1^T (A)_0^S \sum_k a'_{eq,k} \left| v^D_{1,n} \right| v^A_{o,m} \left| R^D_r \right| R^A_{r'} \left| T^D_t \right| T^A_{t'} \right| \Phi_{\sigma_{eq}, \epsilon_k} \Big] e^{-i/\hbar E_S t} \tag{124}$$

and (2) after energy transfer

$$\Psi^S_{final} = \left[(D)_0^S (A)_1^T \sum_{k'} a'_{eq,k'} \left| v^D_{0,n'} \right| v^A_{1,m'} \left| R^D_r \right| R^A_{r'} \left| T^D_t \right| T^A_{t'} \right| \Phi_{\sigma_{eq}, \epsilon_{k'}} \Big] e^{-i/\hbar E_S t} \tag{125}$$

These wave-functions may be expected to adequately describe the system when D and A are separated by distances that are in slight excess of ordinary collision diameters.

The pseudo-equilibrium stationary-state wave-functions described above are similar to the equilibrium function for a single molecule M in a solvent environment given by equation 101. The only difference between these functions and equation 101 is that here the electronic, vibrational, rotational, and translational wave-functions for both D and A are included. Notation is the same as before, except for the following changes: (1) The superscripts T and S indicate that the corresponding electronic wave-functions for D and A with molecular orbital configuration designated by the subscripts 1 and 0 have been anti-symmetrized as triplets and singlets, respectively. (2) The summations are taken over all k or k' configurations of system states defined by the k^{th} or k'^{th} set of quantum numbers, n, m, r, r', t, and t', for the system before energy transfer and n', m', r, r', t, and t', for the system after energy transfer. The time-independent coefficients $a'_{eq,k}$ correspond to the equilibrium distribution of states with total energy E_S.

When a collision between D* and A occurs, electronic exchange interaction between these two molecules may be expected to remove the individuality of their electronic systems. During the time that this exchange interaction is in effect, D and A are considered to be combined in an excited triplet state complex (DA)*. A time-dependent wave-

function similar to 104 , which describes the system during this period may be constructed from stationary-state wave-functions of the type

$$\Psi_c^S = (DA)_i^T \left| v_{i,n}^{DA^*} \right| R_r^{DA^*} \left| T_t^{DA^*} \right| \bar{\Phi}_{\sigma,e_k} e^{-i/\hbar E_S t} \qquad (126)$$

where $k = k(i,n,r,t)$. $(DA)_i^T$ is an electronic triplet state wave-function for the exchange complex (DA)* with the $\underline{i}^{th}$ orbital configuration. There are four possible triplet states of the complex which may be formed as a result of the weak interaction between $\underline{D}^*$ and $\underline{A}$. Two of the four are bonding, while the other two are antibonding. These electronic wave-functions will be described more completely below. $v_{i,n}^{DA^*}$ is the vibrational wave-function for the complex corresponding to the $\underline{n}^{th}$ vibrational level of the $\underline{i}^{th}$ electronic state, $R_r^{DA^*}$ and $T_t^{DA^*}$ are the rotational and translational wave-functions for the complex.

If the interaction energy between $\underline{D}^*$ and $\underline{A}$ in the complex is small compared to the total electronic energy of $\underline{D}^*$ and $\underline{A}$ when isolated from each other, then the electronic interaction between them may be treated as a weak perturbation. This assumption seems reasonably valid in situations considered here.

The electronic Hamiltonian for the complex may be written as

$$\underset{\sim}{H}_{elec} = \underset{\sim}{H}_D^0 + \underset{\sim}{H}_A^0 + \underset{\sim}{H'}_{DA} = \underset{\sim}{H}^0 + \underset{\sim}{H'}_{DA} \qquad (127)$$

where $\underset{\sim}{H}_D^0$ and $\underset{\sim}{H}_A^0$ are the electronic Hamiltonians for $\underline{D}$ and $\underline{A}$, and $\underset{\sim}{H'}_{DA}$ is the perturbation Hamiltonian which describes the interaction between $\underline{D}$ and $\underline{A}$ in the complex. $\underset{\sim}{H'}_{DA}$ may be roughly expressed as

$$\underset{\sim}{H'}_{DA} = \left.\frac{q'_D}{r_D}\right|_A + \left.\frac{q'_A}{r_A}\right|_D \tag{128}$$

where $\left.\frac{q'_D}{r_D}\right|_A$ and $\left.\frac{q'_A}{r_A}\right|_D$ describe the effect of the coulombic fields of each molecule, $\underline{D}$ and $\underline{A}$, on the electronic systems of the other.

By using a perturbation treatment, the electronic wave-functions for the complex $(DA)^*$ may be written as linear combinations of unperturbed electronic wave-functions for the system before and after energy transfer as

$$(DA)_j^T = [C_{1j}(D)_1(A)_0 + C_{2j}(D)_0(A)_1]^T \tag{129}$$

The energies and coefficients for these complex wave-functions may be obtained from the solution of a secular determinant for the problem with the electronic matrix elements given by

$$H_{11} = ((D)_1(A)_0|\underset{\sim}{H}^0 + \underset{\sim}{H'}_{DA}|(D)_1(A)_0) = E^0_{D_1A_0} + \zeta H'_{11} - H'' \tag{130}$$

$$H_{22} = ((D)_0(A)_1|\underset{\sim}{H}^0 + \underset{\sim}{H'}_{DA}|(D)_0(A)_1) = E^0_{D_0A_1} + \zeta H'_{22} - H'' \tag{131}$$

$$= E^0_{D_1A_0} - \Delta E^* + \zeta H'_{22} - H''$$

$$H_{12} = H_{21} = ((D)_0(A)_1 | \underset{\sim}{H}^0 + \underset{\sim}{H}'_{DA} | (D)_1(A)_0) = \zeta H'_{12} \qquad (132)$$

where $\zeta = +1$ when the complex states being considered are bonding, and $\zeta = -1$ when considering antibonding states. The $\underline{H}''$ terms represent the purely electrostatic interactions exerted between the electronic systems and nuclear cores of the opposing molecules, and vary as $1/R^3$ where R is the intermolecular distance. The integrals representing this type of interaction are similar to those described by equation 44 for pairs of atoms. $E^0_{D_1A_0}$ and $E^0_{D_0A_1}$ are the electronic energies of the system before and after energy transfer in the absence of any perturbation interaction between the two molecules $\underline{D}$ and $\underline{A}$, and are given by: $E^0_{D_1A_0} = E^0_{D_1} + E^0_{A_0}$ and $E^0_{D_0A_1} = E^0_{D_0} + E^0_{A_1}$. ΔE^* is the difference in energy between these two unperturbed states of the system. H'_{11}, H'_{22} and H'_{12} represent the exchange or "resonance" interaction between the two molecules during an encounter. These terms are related to the overlap between the electronic systems of $\underline{D}$ and $\underline{A}$ in the complex. In order to simplify the calculations, it is convenient and reasonable to assume here that $H'_{11} \simeq H'_{22} \simeq H'_{12} \simeq H'$. The energy terms E^0, H' and H'' in equations 130, 131, and 132 are treated as negative quantities.

The energies of the electronic states of the complex are

$$E = E^{0}_{D_1A_0} - H'' - \frac{\Delta E^*}{2} + \zeta H' \pm \frac{\zeta H'}{2}\sqrt{\left[\frac{\Delta E^*}{H'}\right]^2 + 4} \qquad (133)$$

The coefficients for the wave-functions described by equation 129 are

$$c_1 = \frac{x}{\sqrt{x^2 + 1}} \qquad (134)$$

and

$$c_2 = \frac{-1}{\sqrt{x^2 + 1}} \qquad (135)$$

where

$$x = -\left|\frac{\Delta E^*}{2\zeta H'}\right| \pm \tfrac{1}{2}\sqrt{\left|\frac{\Delta E^*}{H'}\right|^2 + 4} \qquad (136)$$

Figure XXII contains energy-level diagrams representing the energy profile of the electronic states for three possible complexes which may be formed as reaction intermediates. The energies of the complex states are plotted as functions of the intermolecular distance between $\underline{D}$ and $\underline{A}$. The energies of the respective states are given for each situation.

Considering the case where the triplet state energy of the donor is significantly higher than the triplet state energy of the acceptor, it is found that one bonding and one antibonding electronic state of the complex (Figure XXIIc) has energy that is close to $\underline{D}^*$ plus $\underline{A}$, while the other pair of complex electronic states have energy that is close to $\underline{D}$ plus $\underline{A}^*$. One of the upper electronic states of the complex may be

formed initially upon the introduction of the interaction between $\underline{D}^*$ and $\underline{A}$. This upper state may then undergo rapid internal conversion and vibrational relaxation to lower states of the complex with identical spin. These processes have been described in detail between pages 136 and 150 . The lower electronic states of the complex may then decompose into products $\underline{D}$ and $\underline{A}^*$.

In competition with the internal conversion and vibrational relaxation processes is the rate of dissociation of the complex. If the lifetime of the complex is sufficiently long, then a condition of pseudo-equilibrium within the system containing the complex may be established. Under this condition the rate of change of the coefficients in the time-dependent wave-function becomes stationary. A pseudo-equilibrium stationary-state wave-function for the system containing the complex may be written as

$$\Psi^S_{(DA)^*} = \sum_k a'_{eq,k} (DA)_i^T \left| v_{i,n}^{DA} \right| R_r^{DA} \left| T_t^{DA} \right| \Phi_{\sigma_{eq}, \epsilon_k} e^{-i/\hbar E_S t} \quad (137)$$

The arguments concerning the establishment of equilibrium in competition with the decomposition of the complex when ΔE^* between the upper and lower unperturbed states of the system is large also apply to the system when the energy separation between electronic states becomes very small, as shown in figures XXIIa and XXIIb. As the

energy separation between upper and lower electronic states of the complex decreases, the rate of the establishment of the equilibrium condition is expected to increase as predicted by equation 120.

Kinetics for Triplet Energy Transfer Involving a Complex Intermediate

The kinetics for triplet energy transfer involving a complex intermediate of the type proposed can most easily be discussed by considering the reactions involved under selected limiting conditions. The limiting cases that will be described apply to both non-equilibrium and to equilibrium situations. Each process will be described in detail below.

Case 1. ΔE^* Large; Rate of Partitioning of Energy between Complex States Slow Compared to Diffusion Rates

It is convenient to first consider the case where non-radiative partitioning of energy between electronic states of the complex is slow compared to the lifetime of the complex. This non-equilibrium condition may be expected to become significant when the energy difference between $\underline{D}^*$ and $\underline{A}^*$, and correspondingly the upper and lower electronic states of the complex, is very large. Decomposition of the complex into reactants ($\underline{D}^*$ and $\underline{A}$) may greatly compete with the rate of internal conversion to lower states of the complex, even though non-reversible conversion to lower electronic states is energetically possible.

A reaction sequence which describes the transfer process under these conditions is

$$D^* + A \underset{k_{-1}}{\overset{k_1}{\rightleftharpoons}} (D^*A) \tag{138}$$

$$(D^*A) \xrightarrow{k_d} (DA^*) \tag{139}$$

$$(DA^*) \xrightarrow{k_\rho} D + A^* \tag{140}$$

Equation 138 describes the formation and decomposition of an excited-state complex with energy equal to E_{i1} or E_{i2}, as shown in Figure XXIIc . The excited complex (D*A) can decompose directly by the reverse of reaction 138 or may decay to a lower electronic state by process 139. This latter reaction is considered irreversible under the condition that ΔE^* is very large. Once formed, a complex in a lower electronic state may decompose into product by reaction 140.

The rate of formation of transfer products ($\underline{D} + \underline{A}^*$) by the reactions described above, may be written as

$$\text{rate} = \frac{k_1 k_d}{k_{-1} + k_d} [D^*][A] \tag{141}$$

Under the condition that $k_{-1} >> k_d$ (that is, the complex is not significantly stable in its upper electronic state), then

$$\text{rate} = \frac{k_1}{k_{-1}} k_d [D^*][A] \xrightarrow[k_{-1} \to k_1]{} k_d [D^*][A] \tag{142}$$

The rate constant for the decay of the upper electronic states of the complex, k_d, is given by equation 120. The factors which influence the magnitude of this term have been described in the section regarding internal conversion and vibrational relaxation.

Case 2: ΔE^* Large; Rate of Partitioning of Energy between Complex States Fast Compared to Diffusion Rates

The situation considered here applies to systems where the difference in energy between electronic levels of the complex is large as in Case 1. However, the rate of internal decay from upper to lower electronic states of the complex is fast compared to the rates at which $\underline{D}^*$ and $\underline{A}$ can diffuse together and apart.

The reaction sequence described by equations 138, 139, and 140 may be used here to describe the process involved. It is seen from equation 141 that when $k_d >> k_{-1}$, as is the case in point, the rate of the overall process becomes

$$\text{rate} = k_1 [D^*][A] \tag{143}$$

Under the reaction conditions described, $k_1 \rightarrow k_\delta$ where k_δ is the mean diffusion rate constant for $\underline{D}^*$ and $\underline{A}$ in the fluid environment.

By assuming a rigid sphere model as an approximation to the description of $\underline{D}$ and $\underline{A}$ in the solvent environment, the diffusion rate constant k_δ may be written as

$$k_{\delta} = \frac{No}{1000} \frac{kT}{3\eta} \frac{(r_D + r_A)^2}{r_D r_A} \qquad (144)$$

where r_D and r_A are the molecular radii of D and A, respectively, and η is the viscosity of the solvent. No is Avogadro's number, and k is Boltzmann's constant.

Case 3: No Restriction on ΔE^*; Partitioning of Energy between Complex States Fast Compared to Diffusion Rates

The final set of conditions for energy transfer by the proposed mechanism is more general than those described for Case (1) and Case (2). Here, the rate of partitioning of energy between possible states of the complex system is considered fast compared to rates of diffusion for particles in the reaction environment. No restriction is placed on the separation of possible electronic states of the complex.

The rate equation for triplet energy transfer derived under this final set of conditions should be applicable to a large segment of the spectrum of triplet transfer reactions in solution. The equation is expected to describe both endothermic and exothermic energy transfer. For large exothermic processes, the rate will approach the limiting value described by equation 144. The present treatment is expected to break down under the extreme non-equilibrium conditions encountered in Case 1.

The overall transfer process may be best described by the following sequence of reactions:

$$D^* + A \underset{k_\delta}{\overset{k_\delta}{\rightleftharpoons}} D^* | A \qquad (145)$$

$$D^* | A \underset{k_{-c}}{\overset{k_c}{\rightleftharpoons}} (DA)^* \qquad (146)$$

$$(DA)^* \xrightarrow{k_\rho} D + A^* \qquad (147)$$

Reaction 145 describes the diffusion of D* and A from separate points in the environment to neighboring positions. Both molecules are considered to retain their electronic individuality until this point is reached. When a neighboring position is obtained, the two molecules may interact to form a complex as shown by reaction 146, or diffuse apart by the reverse of reaction 145. Finally, the complex may decompose into product as shown by equation 147.

A rate equation for the above process under the conditions set forth for this problem (e.g., k_c, $k_{-c} \gg k_\delta$, k_ρ) may be written as

$$\text{rate} = \frac{k_\rho K [D^*][A]}{1 + \frac{k_\rho}{k_\delta} K} \qquad (148)$$

or

$$\text{rate} = \frac{a K k_\delta [D^*][A]}{1 + aK} \qquad (149)$$

in 149, a is the fraction of complexes which may decompose directly into product D + A*. The decomposition of these complexes is felt to

proceed at a diffusion-controlled rate; therefore, the substitution $k_\rho = ak_\delta$ was made in equation 148 in order to obtain 149. K is the rate constant for the formation of the complex from D* and A and is equal to k_c/k_{-c}.

It is seen from equations 148 and 149 that when a $K \gg 1$, the rate of the formation of transfer product approaches the rate corresponding to a diffusion-controlled process.

$$\text{rate} = k_\delta [D^*] [A] \tag{150}$$

On the other hand, when a $K \ll 1$, the rate for the energy transfer process becomes

$$\text{rate} = aK k_\delta [D^*] [A] \tag{151}$$

It is now of interest to consider the quantities a and K which are found in equations 149 and 151. The efficiency factor, a, for the formation of product from the decomposition of complexes, will be considered first. The problem will be considered under two conditions. The first condition is where the resonance interaction between the two partners in the complex is very weak. Under this condition, the steady-state concentration of complex formed during the transfer reaction is expected to be negligible. The second condition to be considered is where strong complexing between D* and A is possible. In this case the steady-state concentration of complexes may become sufficiently high that specific spectroscopic measurements made on the system may indicate the existence of the intermediate transient specie.

In the following treatment, it is assumed that the total environmental energy of the system in which the energy transfer reaction takes place is large compared to the quantum of excitation energy interconverted with thermal energy during the overall transfer process. This condition is nearly always satisfied in actual laboratory systems through thermostating and through the sheer bulk of the systems.

The complex is assumed to have electronic state energies given by equation 133. Energy level diagrams for representative complexes have been given in Figure XXII . It is observed from this figure that two of the states, $(DA)_{f_1}$ and $(DA)_{f_2}$, decompose directly into product, while the other two, $(DA)_{i_1}$ and $(DA)_{i_2}$, decompose into reactant. Under very weak bonding conditions, it may be assumed, to the first approximation, that both the final bonding and final antibonding states ($(DA)_{f_1}$ and $(DA)_{f_2}$) of the complex have an equal probability of decomposing at a diffusion-controlled rate. The two initial electronic states of the complex, however, are not considered to be able to decompose into product but must return to $\underline{D}^* + \underline{A}$.

With these assumptions, the efficiency factor $\underline{a}$ may be written as

$$a = \frac{\sum_{j'=f_1,f_2} e^{-E_{j'}/RT}}{\sum_{j=i_1,i_2,f_1,f_2} e^{-E_j/RT}} \qquad (152)$$

where $\underline{E}_j$ is the energy of the $\underline{j}^{th}$ electronic state of the complex.

It is seen from equation 133 that when $\underline{H}' << \Delta E^*$, the energies of the initial and final electronic states of the complex may be written as shown in Figure XXIIc . Under the conditions considered here, the electronic state energies may be effectively represented by these values except in the small region where $|\Delta E^*| \simeq |H'|$. Substituting these energy values into equation 152, $\underline{a}$ may be written as

$$a = \frac{e^{\Delta E^*/RT}}{e^{\Delta E^*/RT} + 1} \qquad (153)$$

It is now of interest to consider the equilibrium constant $\underline{K}$. The rate of partitioning of energy between states of the complex system is considered here to be fast compared to the rate of diffusion of $\underline{D}$ and $\underline{A}$ through the environment and compared to the rate of decomposition of the complex. Therefore, the equilibrium constant, $\underline{K}$, for the formation of the complex may be determined from the ratio of partition functions which describe the complete system at equilibrium with its environment immediately before and after formation of the complex. The equilibrium wave-functions for the system before and after complex formation are given by equations 124 and 137. The corresponding partition functions may be represented as a product of the single-particle partition functions for $\underline{D}^*$, $\underline{A}$ or the complex $\underline{DA}^*$ and the canonical partition function for the environment. In the ratio of partition functions

under the present conditions, the environmental partition functions cancel, leaving only those corresponding to D, A, and (DA*). The equilibrium constant K may therefore be written as

$$K = \frac{Q_{(DA)*}}{Q_{D*} Q_A} \tag{154}$$

For the present problem, the total molecular partition functions in equation 154 may be written as

$$Q_{(DA)*} = g_{(DA)*} Q^T_{(DA)*} \sum_{j=i_1, i_2, f_1, f_2} Q^R_{(DA)*_j} \; Q^V_{(DA)*_j} \; e^{-E_j/RT} \tag{155}$$

for the complex, and

$$Q_{D*} = Q^T_{D*} \; Q^R_{D*} \; Q^V_{D*} \; g_{D*} \; e^{-E_{(D)_1}{}^T/RT} \tag{156}$$

$$Q_A = Q^T_A \; Q^R_A \; Q^V_A \; g_A \; e^{-E_{(A)_o}{}^S/RT} \tag{157}$$

for D* and A, respectively. E_j are the energies of the j^{th} electronic states of the complex. Q^T, Q^R, and Q^V are the translational, rotational, and vibrational partition functions for each respective particle. $E_{(D)_1}{}^T$ and $E_{(A)_o}{}^S$ are the energies of the occupied electronic states of D and A, and $E_{(D)_1}{}^T + E_{(A)_o}{}^S = E^O_{D_1, A_o}$. It has been assumed that the energies of all other electronic states of D and A with proper spin multiplicity, g, are sufficiently separated from these

states that they do not contribute significantly to the electronic partition function for these molecules.

The total partition function for the complex may be further simplified under the conditions that bonding between partners in the complex is weak and that large molecules are involved in the energy transfer reaction. It may be assumed that all rotational, and similarly all vibrational, partition functions for the j electronic triplet states of the complex are approximately equal, and therefore may be factored from the right side of the summation sign in 155.

Substituting the values for the total partition functions of D^*, A, and $(DA)^*$ into equation 154, and assuming H'' is negligible for the complex while in its minimum energy configuration, the equilibrium constant K is

$$K = 2\Re \cosh \frac{|H'|}{RT} \left(1 + e^{\Delta E^*/RT}\right) \tag{158}$$

where

$$\Re = \frac{Q^T_{(DA)^*} Q^R_{(DA)^*} Q^V_{(DA)^*}}{Q^T_{D^*} Q^T_A Q^R_{D^*} Q^R_A Q^V_{D^*} Q^V_A} \tag{159}$$

The product aK, therefore, is simply

$$aK = 2\Re \cosh \frac{|H'|}{RT} e^{\Delta E^*/RT} \tag{160}$$

The problem is now reduced to the evaluation of the set of partition functions in expression 159. Partition functions derived for molecules in the gas phase are totally inapplicable to molecules in solution, and so may not be used here. No special attempt will be made to evaluate the partition functions exactly for the molecules in solution. However, some consideration will be given to factors contributing to the magnitude of each type of function.

The translational partition functions, $\underline{Q}^{T}$, are concerned with the three translational degrees of freedom for each molecule or complex. In order to obtain an idea as to the order of magnitude of the energy separations between translational quantum levels, the molecular particles may be considered to move in a small three-dimensional box with lengths of sides equal to the average distance between solvent molecules. The approximate total partition function may be represented as a product of three identical functions for the particle moving in a one-dimensional box, each representing a single translational degree of freedom. The potential field in which the molecules move may be approximated by a square well with infinite potential barriers. The simple quantum mechanical solution to this problem (61) indicates that from three to thirty translational energy levels may exist within the energy gap equal to $\underline{kT}$, depending on the mass of the molecular particles. T is taken here to be 300°K. For this small number of states within $\underline{kT}$, it is evident that the partition function must be obtained by summation rather than

integration over the range of possible translational states. An estimate as to the magnitude of the total translational partition function with a mass of 10^2 to 5×10^2 is about 10^2 to 10^4.

The rotational partition functions, Q^R, describe the external rotations of the molecules as a whole in the environment. Even though there is expected to be some hindrance to rotation resulting from interaction with the environment, the energy levels for rotational states may be obtained approximately by considering the molecules as three-dimensional rigid rotors, each with three rotational degrees of freedom (61). Again here, summation rather than integration is necessary for the evaluation of the partition function. The order of magnitude of these functions is about the same as for translations ($\sim 10^3$).

The energy level separation between possible rotational states of $\underline{D}^*$, $\underline{A}$, and $(\underline{DA})^*$ is inversely proportional to the moments of inertia for each molecule. Therefore, the corresponding rotational partition functions are strongly dependent on the magnitude of these terms. The moments of inertia are dependent on both the masses of the interacting molecules and on their sizes. Variations in the moments of inertia of $\underline{D}^*$ and $\underline{A}$ and of the complex $(\underline{DA})^*$ may account for a significant part of the "steric" effect observed in the rate of energy transfer which may be observed in systems containing varying steric and mass requirements and which have identical electronic systems. An effect of this

type has been observed in quenching experiments using transition metal chelates and was reported earlier in this thesis. More will be said about the "steric" effect with respect to the proposed mechanism later.

Finally, partition functions describing vibrations within the molecules $\underline{D}^*$, $\underline{A}$, and $(\underline{DA})^*$ should be considered. As with translations and external rotations, vibrations are strongly influenced by the environment. However, the potential exerted on the molecule by the environment may be considered complementary to that already exerted by the bonds directed along the normal coordinates of vibration. The total vibrational wave-function may be represented approximately as a product of partition functions for individual vibrations along the normal coordinates of each molecule. There are 3N-6 vibrational and internal rotational degrees of freedom that must be considered here for each molecule, where $\underline{N}$ is the number of atoms in the molecule. Normally the energy separation between vibrational states is large or on the order of $\underline{kT}$. Therefore, the corresponding partition functions for each individual vibration are relatively small $(10^0 - 10^1)$. Functions describing internal rotations, however, may be somewhat larger, depending on the potential barriers to rotation.

There is one very important vibrational function for the complex that should receive special attention. This function describes vibrations directed along the weak bond formed between partners in the complex. For very weak bonding, these vibrations correspond to translations

of the partners in the complex in opposite directions leading to decomposition. These opposite translations of complex partners will be referred to in the future as the internal translation of the complex. Therefore, in the case considered here, this particular vibrational partition function is replaced by a one-dimension translational partition function describing the motion of the complex along the reaction coordinate leading to decomposition. However, this translational partition function differs from other translational functions for the complex in that the reduced mass rather than the total mass for the complex is used. This is done because the motion of partners in the complex is opposite and relative to each other.

Using appropriate values for the corresponding approximate partition functions of donor, acceptor, and complex with masses equal to 10^2 for $\underline{D}^*$ and $\underline{A}$ and 2×10^2 for $(\underline{DA})^*$, $\Re \simeq 10^{-3} - 10^{-4}$. The value of $\Re$ given here can only be expected to be a very rough estimate in the light of the gross simplifications made in evaluating the approximate partition functions. However, this does give one an idea as to the order of magnitude that one might normally expect for a typical ratio $\Re$.

When $H' << RT$, then $\cosh \frac{|H'|}{RT} \simeq 1$, and the rate equation for triplet energy transfer becomes

$$\text{rate} = \frac{2 k_{\delta} \Re e^{\Delta E^*/RT}}{1 + 2\Re e^{\Delta E^*/RT}} [D^*][A] \qquad (161)$$

Equation 161 has been derived for the condition that bonding between partners in the complex is sufficiently weak that decomposition of the complex from all electronic states is diffusion-controlled. This may be true for most experimental cases. However, strong bonding may very well result in some situations. Under these circumstances, a build-up in the stationary-state concentration of the complex to a significant level may occur during the irradiation period.

Strong bonding may be expected to be most significant in systems containing planar donors and acceptors with very similar triplet state energies. Identical planar molecules may be expected to exhibit the most significant bonding. Radiative emission from transient species has been observed in certain systems of this type and is in accord with this mechanism (62). These transients have been called eximers.

In the strong bonding case, as in the weak bonding case, when $\Delta E^* >> H'$, the electronic energy levels for the complex may be given approximately by those reported in Figure XXIIc . Even under these simplifying conditions, expressions for $\underline{a}$ and $\underline{K}$ in the rate law for energy transfer in systems where strong bonding is possible are considerably more complicated than given by equations 153 and 158.

For weak bonding, the partition function describing internal translations of the complex along the reaction coordinate leading to decomposition was considered to be identical for all electronic states of the complex. This assumption may not be used where strong bonding is involved. The potential energy affecting these internal translations of the complex may differ significantly between bonding and antibonding states.

The assumption can be made that all antibonding complexes may decompose at a diffusion-controlled rate. However, only bonding complexes with internal translation energies greater than $\underline{H'}$ (in the limiting case) may decompose. The above assumptions lead to the following expressions for the efficiency factor $\underline{a}$:

$$a = \frac{e^{\Delta E^*/RT}\left(e^{H'/RT} + \beta e^{-H'/RT}\right)}{2\cosh\frac{|H'|}{RT}\left(1 + e^{\Delta E^*/RT}\right)} \qquad (162)$$

where

$$\beta = \frac{\sum_t e^{-(E_t > H')/RT}}{Q^T_{int(b)}} \qquad (163)$$

The $\underline{E_t}$'s are the energies of the internal translational states of the bonded complex. $Q^T_{int}(b)$ is the internal translational partition function for the bonding state of the complex.

The constant $\underline{K}$ may be evaluated in a manner similar to the approach given to the evaluation of expression 158. However, here the internal translational partition function for each state of the complex cannot be factored from the right of the summation sign in expression 155 as was done in the weak bonding case.

As $\underline{\beta}$ (given above) approaches unity, the expression for the corresponding rate law approaches that given by equation 161. Since very little is known about the partition functions or the magnitude of the bonding interaction H', it is both convenient and advisable to treat most experimental data by equation 161.

A plot of the logarithm of the quenching rate constant, $\underline{k}_q$, against the difference in triplet state energy of donor and acceptor, ΔE^*, for a similar series of compounds, should resemble the plot given in Figure XXIII . The figure is divided into three regions where rate expressions for the limiting cases (142, 143, and 151) apply. The curve in regions 2 and 3 is described by

$$\log k_q = \frac{\Delta E^*}{2.3RT} + \log 2k_\delta \Re - \log(1 - 2\Re e^{-\Delta E^*/RT}) \qquad (164)$$

In region 1 of Figure XXIII , the rate of energy transfer is expected to fall below the diffusion-controlled maximum and approach zero as a limit. It is in this region where the rate of partitioning of energy between possible states of the complex becomes slow compared

to diffusion rates. In region 2, the rate of energy transfer is diffusion-controlled. In region 3, the rate of energy transfer is expected to again fall below the rate for a diffusion-controlled process. The plot of log $\underline{k}_q$ versus ΔE^* should ideally approach linearity as ΔE^* decreases, obtain a slope equal to $+\frac{1}{2.3RT}$ and have a $\Delta E^* = 0$ intercept equal to log $2\underline{k}_\delta \Re$.

The results obtained from experiments using transition metal chelates as quenchers may be adequately explained by the proposed mechanism. The apparent steric effect which is observed between corresponding dipivaloylmethide and acetylacetonate chelates is probably due in part to several different factors. Each of these contributes some unknown amount to the final observed quenching efficiency of the compound. First, the larger $M(DPM)_3$ chelates are expected to have somewhat slower diffusion rates in the solvent than the corresponding $M(AA)_3$ chelates as shown by equation 144.

Secondly, the translational (both internal and external) and rotational partition functions for the systems containing corresponding chelates are expected to vary according to the differences in the masses and in the moments of inertia of the quenchers and corresponding complexes as described earlier. An increase in both mass and moment of inertia produces an increase in the magnitude of the corresponding partition functions in which these quantities occur. The changes produced in the partition functions alter the value for $\Re$ in the rate equation

161. An increase in the mass and moment of inertia of the quencher and complex is expected to produce a decrease in $\underline{k}_q$.

The interactions between A and (DA)* with the environment have effects on the partition functions for both the quencher and complex. Increased hindrance to translational, rotational and vibrational motion of the more bulky DPM chelates over that offered to the smaller compounds may be expected. These interactions should result in a decrease in the order of magnitude of the partition functions for A and (DA)* as their molecular sizes increase.

Finally, the mixing between upper and lower states of the complex by interaction with the environment (which accounts for internal non-radiative decay) is strongly dependent on the magnitudes of $\underline{H}'$ and $\underline{H}''$. The first term, $\underline{H}'$, describes the exchange interaction, and is related to the overlap between the electronic systems of the donor and quencher molecules. Therefore, the magnitude of this term should be subject to the hindrance of electronic overlap offered between donor and quencher by the ligands. The second term, $\underline{H}''$, describes the dipole and higher multipole interactions between partners in the complex. This term is small for symmetry-forbidden transitions in $\underline{D}$ or $\underline{A}$, or in both, except at very close distances between the complex partners. Negligible interaction between the internal σ-system of the chelates with the electronic system of the donor accounts for the correlation of quenching efficiencies with the π-π^* state energies.

All four of the effects mentioned above lead to the expectation of a significant steric effect in the rate of quenching by DPM and AA chelates.

Plots of the logarithm of k_q/k_r against the calculated π-state energies for these chelates are given in Figure XXIV . The slopes of the plots for DPM and AA chelates are not necessarily expected to agree with the predicted slope of $+\frac{1}{2.3RT}$ in section 3 of the graph. This lack of agreement may result, since only approximate calculated energies for the chelates have been used for the plot. Furthermore, more than one final electronic state of the chelate may be mixed significantly with triplet state of the donor. This is most certainly expected, especially with the paramagnetic chelates studied. As a result of this, the efficiency factor a is uncertain. Rapid partitioning of energy between some complex electronic states, while slow partitioning among others, may be involved, thus making the problem extremely complicated. However, it is apparent from Figure XXIV that there is a direct correlation between the calculated energies of the π-states and the quenching efficiencies of the chelates. In addition, there is also an apparent correlation between the quenching ability and the mass and size of corresponding acetylacetonate and dipivaloylmethide chelates.

Further support for the proposed mechanism for triplet energy transfer may be obtained from the consideration of experimental data other than that reported in this thesis. Backstrom (6) has conducted

a very detailed investigation into the quenching of triplet state biacetyl by a large number of acceptors. The second order quenching rate constants, $\underline{k}_q$, obtained by him for a series of quenchers with similar masses and sizes, are reported in Table XIII , with corresponding quencher triplet state energies. The logarithms of the quenching constants are plotted against the energies of the triplet states in Figure XXV . The resulting plot is seen to correspond to the type expected for regions 2 and 3 of the total spectrum of quenching rate constants shown in Figure XXIII .

The slope of the region 1 plot which corresponds to $+\frac{1}{2.303RT}$ is equal to $+0.745 \times 10^{-3}$ moles/cal. The value for the temperature determined from this slope is 292°K. The actual temperature at which the experiments were conducted was 293°K. The diffusion-controlled rate constant $\underline{k}_\delta$ for this set of systems is obtained from the region 2 plot and is approximately 8×10^9 liter/mole/sec. The $\Delta E^* = 0$ intercept for the region 1 plot, which corresponds to $\log 2\Re k_\delta$, is 7.0. The average partition function ratio $\Re$, therefore, is 6.3×10^{-4} for this set of reaction systems. This ratio is in very good agreement with the roughly estimated value of $10^{-3} - 10^{-4}$ described earlier on page 181. As seen here, the results obtained by Bäckstrom are in excellent agreement with those predicted on the basis of the proposed complex mechanism.

Table XIII

Quenching of Biacetyl Phosphorescence by Selected Quenchers in Benzene at 20°C (Bäckstrom)

Quencher	k_q (1/mole/sec)	E_T (cm^{-1})
Phenanthrene	2.3×10^3	21600
Naphthalene	3.8×10^3	21246
Nitrobenzene	1.4×10^4	21100
Methyl β-naphthyl ketone	8.5×10^4	20700
1-Chloronaphthalene	5.9×10^4	20645
1-Bromonaphthalene	1.0×10^5	20652
2-Nitrofluorene	1.4×10^6	20600
4,4'-Dinitrobiphenyl	3.6×10^6	20200
2,2'-Dinaphthyl	9.7×10^6	19560
1-Nitronaphthalene	1.1×10^8	19250
Coronene	2.0×10^8	19040
trans-Stilbene	4.4×10^9	17750
Pyrene	7.5×10^9	16930
1,2-Benzanthracene	7.0×10^9	16520
Anthracene	8.1×10^9	14927
3,4-Benzpyrene	8.2×10^9	14670
Biacetyl	---	19700

SUMMARY

To satisfy spin conservation, triplet energy transfer must be accompanied by electron exchange between sensitizer and acceptor molecules. In the absence of exchange requirements, such as those involved in multiplicity forbidden transitions, the rates of energy transfer may exceed those for ordinary diffusion-controlled processes. A theory developed by Förster (35), assuming that the donor and quencher are isolated from each other at a distance R, predicts that transition probabilities should vary as the square of the dipole coupling between their optical transition vectors. In addition, an inverse sixth order radial dependence is predicted.

Experiments conducted with $Fe(DBM)_3$ and $Cr(DBM)_3$ indicate that singlet quenching of benzophenone may be occurring in these systems. Discrepancies between the experimental results and those predicted on the basis of Förster's theory are apparent. As a possible account for these discrepancies, coupling of ketone and chelate singlet states through weak π-complex type interaction with the benzene solvent is considered. Substantial solvent effects are, therefore, predicted.

As an alternative explanation of the singlet quenching results, long-range dipole coupling between the donor and quencher under resonance conditions is considered. This process has been discussed in detail by Robinson (59), describing singlet energy migration between molecules with identical excited-state energies in the solid phase. The rate of energy transfer is predicted to be directly proportional to the concentration of quencher by this mechanism. Since no solvent interaction is necessary here, no substantial solvent effect on the rate is predicted. Experiments which may demonstrate possible solvent effects, and therefore support or reject either of the proposed explanations given above, have not yet been run.

A general mechanism for triplet energy transfer in solution has been developed. This mechanism involves the formation of a weak excited-state complex between the donor and quencher molecule. Complex formation permits spin exchange between partners in the complex which is necessary to satisfy the spin conservation requirement for the overall transfer process. If the lifetime of the complex is long compared to the time necessary for non-radiative partitioning of energy between states of the complex, the reaction is expected to follow a predictable rate given approximately by equation 161. When the time required for the partitioning of energy between complex states becomes slow compared to the lifetime of the complex, the rate-limiting factor

in the energy-transfer mechanism becomes the rate at which energy may be partitioned between states of the complex. Under these conditions, the rate of energy transfer is described by equation 142.

The general mechanism has been applied to the experimental results obtained for the transition-metal chelates. These compounds are considered to quench excited triplet states of benzophenone through energy transfer rather than by any "paramagnetic" effect. Interaction between benzophenone and the chelate is felt to occur between proper ketone orbitals and the π-orbital system of the chelates. These π-orbitals are formed from the interactions of ligand π-orbital systems with particular metal atomic orbitals. These interactions have been considered in the section on molecular orbital calculations.

Interaction between the ketone orbitals and the inner σ-bonding and non-bonding orbitals of the chelates is considered to be negligible compared to the interaction with the π-orbital system. The quenching results are in accord with this conclusion. A correlation was obtained between the energies of the π-π^* states of the chelates and their quenching efficiencies. No correlation was found between the quenching efficiencies and the energies of the low-lying π-σ^* and π-n^* transitions. Further evidence for this conclusion was demonstrated by the results with $Fe(Cl)_3$ and $Fe(DPM)_3$ in t-butyl alcohol. The ferric chloride salt did not have any measurable quenching effect, while the dipivaloylmethide chelate served as a good quencher in this system.

Direct consideration of chelate quenching by the proposed triplet energy transfer mechanism is complicated by the spin-statistical factor. Ideally, only certain complexes formed between the paramagnetic chelates and triplet benzophenone may decompose into product. These complexes have been called "deactivating" complexes. The number of "deactivating" complexes is determined by the spin-statistical factor (see page 125), and is expected to be approximately 1/3 for the low-energy π-π^* states of the chromium and iron chelates. However, all complexes incapable of decomposing directly into product, because of improper spin requirements, are excited states of complexes with proper spins for product formation. Therefore, direct formation of the lower energy "deactivating" complexes is expected to be the most favorable path for the reaction to take. In addition to the possibility of direct formation of "deactivating" complex states as described above, strong spin-orbit interactions within the chelates may be expected to significantly mix the possible complex states of improper spin with "deactivating" states. Under the conditions given here, the rate may be expected to exceed the maximum value predicted purely on the basis of the spin statistics.

With the exception of the dibenzoylmethide chelates, which apparently quench by a different mechanism than all other chelates, the best chelate quencher found in this investigation was ferric acetylacetonate. It was found to have a k_q/k_r quenching ratio of 540. This

ratio is close to the value expected for a diffusion-controlled quenching rate where energy transfer occurs on every collision. The largest quenching ratio found in this work, 580, was for dibenzoylmethane. This compound has a triplet state that is significantly lower than the lowest triplet state of benzophenone. The spin-statistical factor for energy transfer to this compound is unity, as seen from Table XIII. The energetic and statistical conditions are such that every collision with an excited benzophenone should result in the transfer of energy. Therefore, it is felt that the maximum diffusion-controlled quenching rate for compounds of this size may be expected to be somewhere in the vicinity of 600.

Moore (12) has obtained a value of 550 for the quenching ratio for naphthalene. This compound is also expected to quench triplet benzophenone with a diffusion-controlled rate and is in agreement with the value of 600 given above. Leermakers (9), on the other hand, has estimated that the quenching ratio for naphthalene was 750. This latter value is subject to question, however.

The chromium acetylacetonate chelate has a k_q/k_r ratio of 380. This ratio, therefore, is slightly greater than one-half of the expected diffusion-controlled rate. Both the $Fe(AA)_3$ and $Cr(AA)_3$ chelates are more effective than expected purely by the spin-statistical factor. The experimental results described above do not show any correlation between the spins of the unexcited quenchers and their

quenching ability. This is in agreement with the proposition that the regulating factor in the deactivation of the donor through energy transfer is the energetic availability of excited π-π^* states of the quencher.

A further complication to the application of the proposed mechanism to the chelate problem is introduced by the relative rates of the partitioning of energy between possible states of the complex. The partitioning of energy between states which are close together in energy may be expected to be considerably faster than the partitioning of energy between states that are very far separated. This effect is also demonstrated by the experimental data.

Energy transfer to vibrationally-excited levels of the ground electronic state of the paramagnetic chelates is allowed by spin conservation rules. Therefore, all paramagnetic chelates should be expected to be equally efficient quenchers if the internal conversion process is very efficient. However, a correlation is obtained only between the energies of the higher electronic states of the chelates and not with the spins of their ground states. This result is in agreement with the proposition that the partitioning of energy between electronic states of the exchange complex with energies that are in the neighborhood of the triplet-state energy of benzophenone is expected to be fast compared to the lifetime of the complex, while conversion to the lower electronic states of the complex is slow.

The steric effect observed with the chelates may also be explained by the proposed general mechanism. It is felt that this effect is dependent on several factors which have each been described earlier.

Dissipation of energy after transfer to the chelate is considered to proceed through a non-radiative decay process involving inter-system crossing, internal conversion, and vibrational relaxation. This is evidenced from a failure to observe induced emission from samples containing quencher and from the destruction of chelates capable of accepting excitation energy from benzophenone.

Support for the proposed general triplet energy transfer mechanism is obtained from the experiments concerning the quenching of biacetyl phosphorescence reported by Bäckstrom (6). These data are in exact agreement with the results predicted by equation 161 for the series of compounds studied.

It is felt that the mechanism of triplet energy transfer described here is general and may be applied to most systems in which this process occurs. If conditions are right, the same complex as that involved in energy transfer can serve as the intermediate which undergoes photochemical reaction between donor and acceptor, destroying both with the formation of product.

An example of this is the photoaddition reactions of olefins. Competition between energy transfer and addition exists, and whichever process is energetically most favorable will take precedence over the other. If donor and acceptor excited state energies are identical or very close, and the stability of the complex is sufficient, it may have an ample lifetime to allow radiative decay from it directly. Whereupon, the complex will decompose into ground state molecules. Such radiation would be found at longer wavelengths than found for non-complexed molecules. This has been observed in solutions containing high concentrations of scintillators. In this case donor and acceptor are the same molecule; the complex is called an excimer, and the emission is called excimer emission.

FIGURES VI - XXV

Figure VI. π-State Energies for the ML_3 Chelates

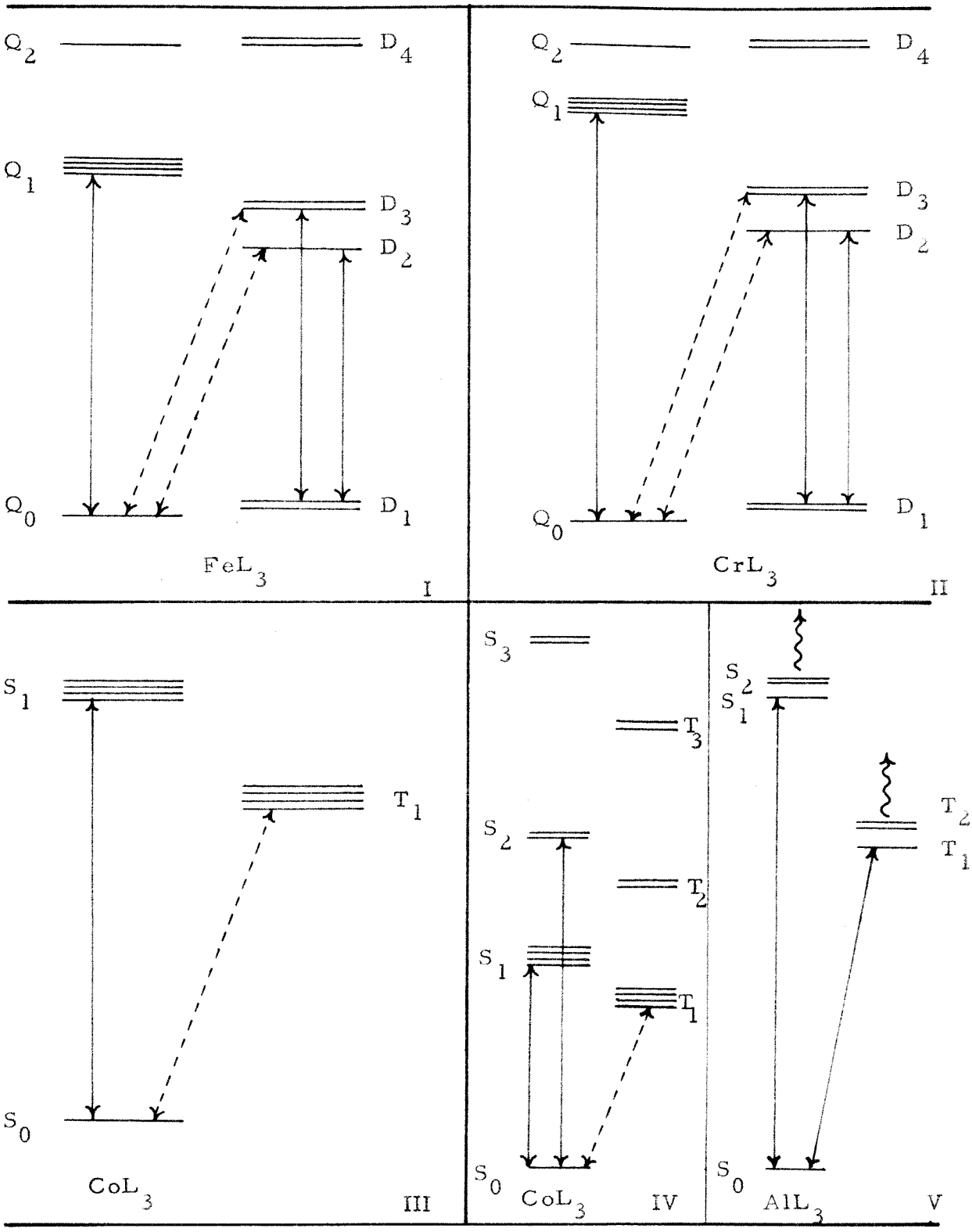

Figure VII. General ML_3 Chelate D_3-π and E_g-σ Orbitals--Ground State Configuration

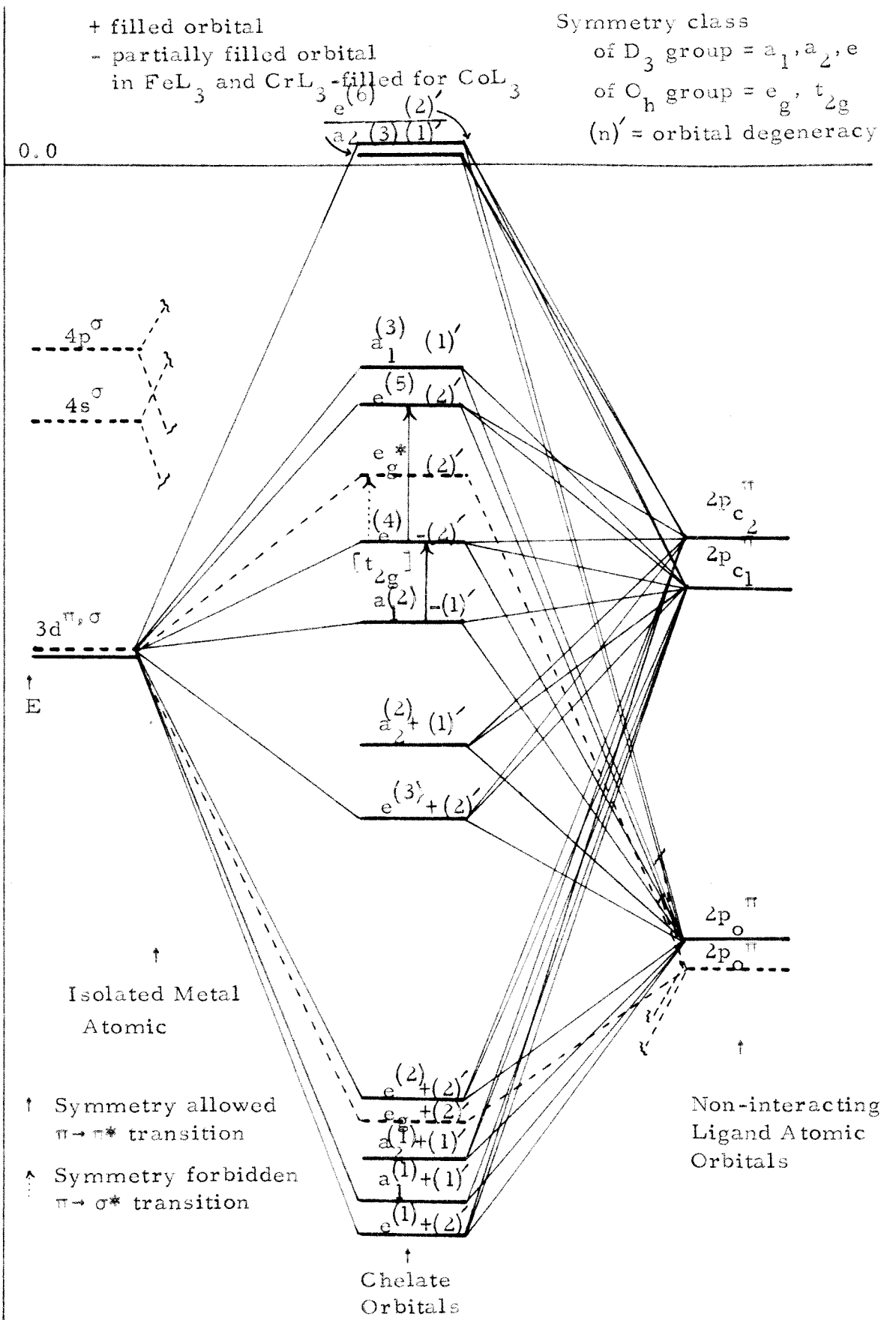

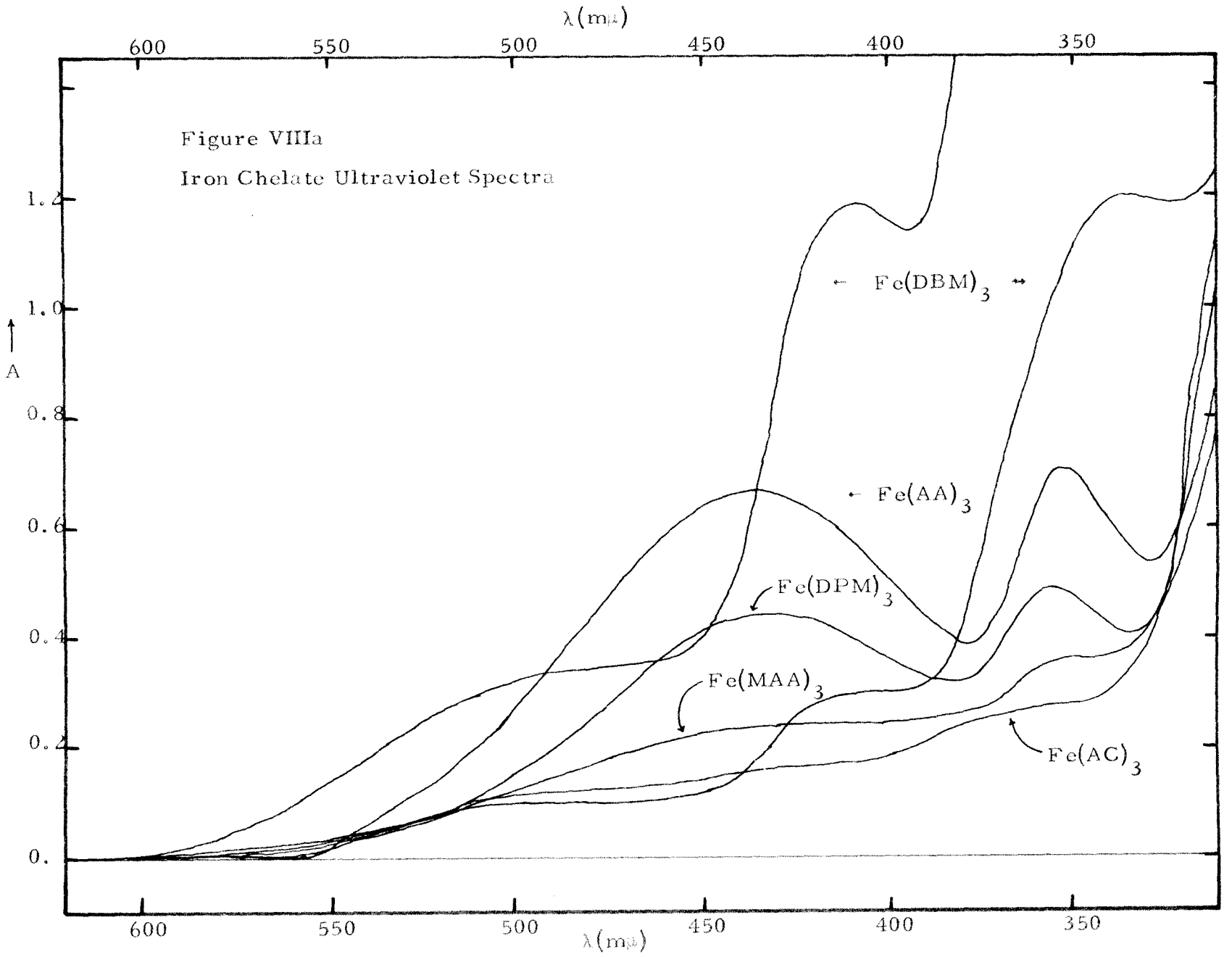
λ(mμ)
600
550
500
450
400
350
Figure VIIIa
Iron Chelate Ultraviolet Spectra
1.2
1.0
A
0.8
0.6
0.4
0.2
0.
← Fe(DBM)3 →
← Fe(AA)3
Fe(DPM)3
Fe(MAA)3
Fe(AC)3
600
550
500
450
400
350
λ(mμ)

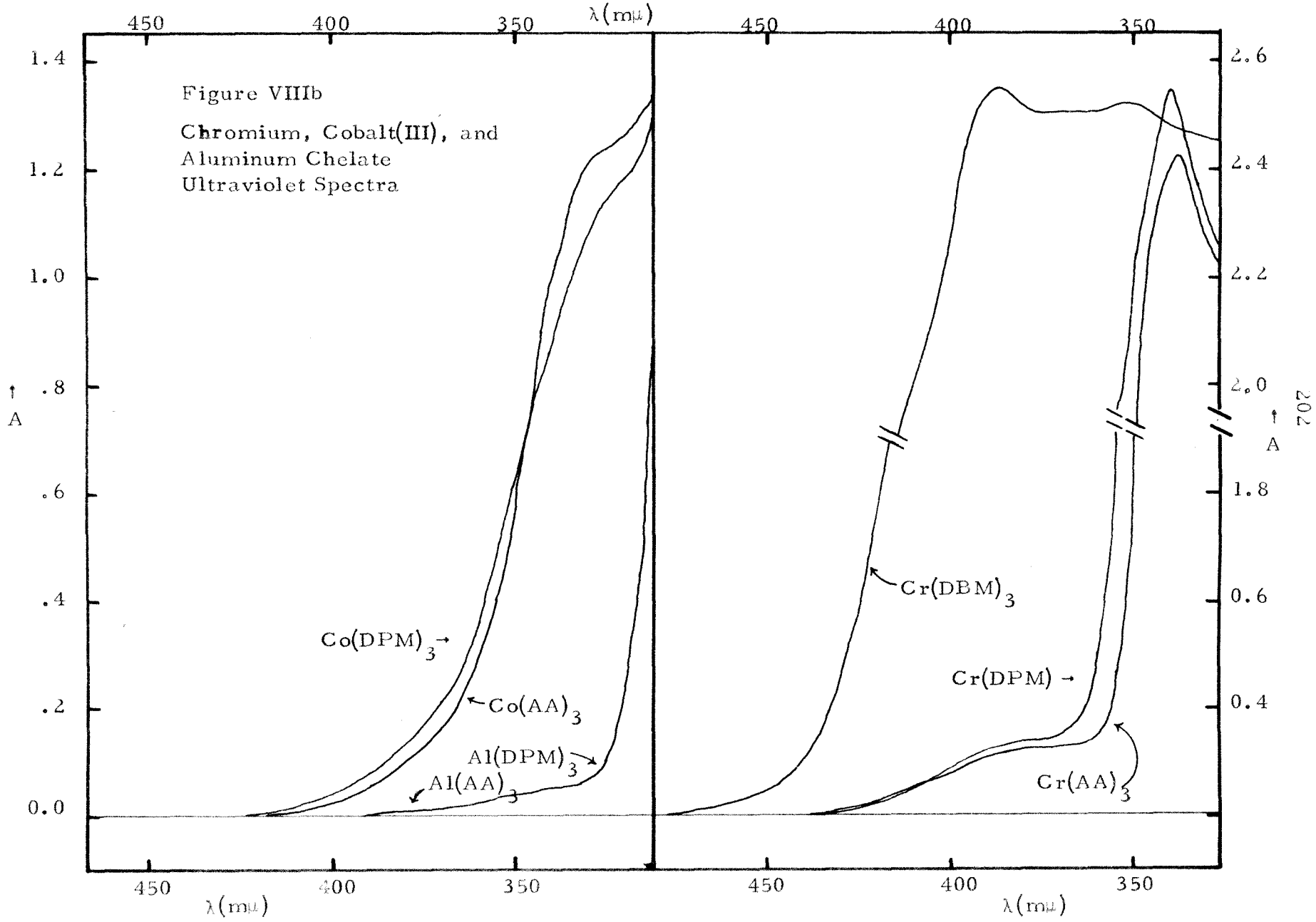
Figure VIIIb
Chromium, Cobalt(III), and
Aluminum Chelate
Ultraviolet Spectra
λ(mμ)
450
400
350
A
1.4
1.2
1.0
.8
.6
.4
.2
0.0
Co(DPM)3
Co(AA)3
Al(DPM)3
Al(AA)3
Cr(DBM)3
Cr(DPM)
Cr(AA)3
2.6
2.4
2.2
2.0
1.8
0.6
0.4
202

Figure IX. General ML_2 Chelate D_{2h}-π and B_{1g}-σ Orbitals--Ground State Configuration

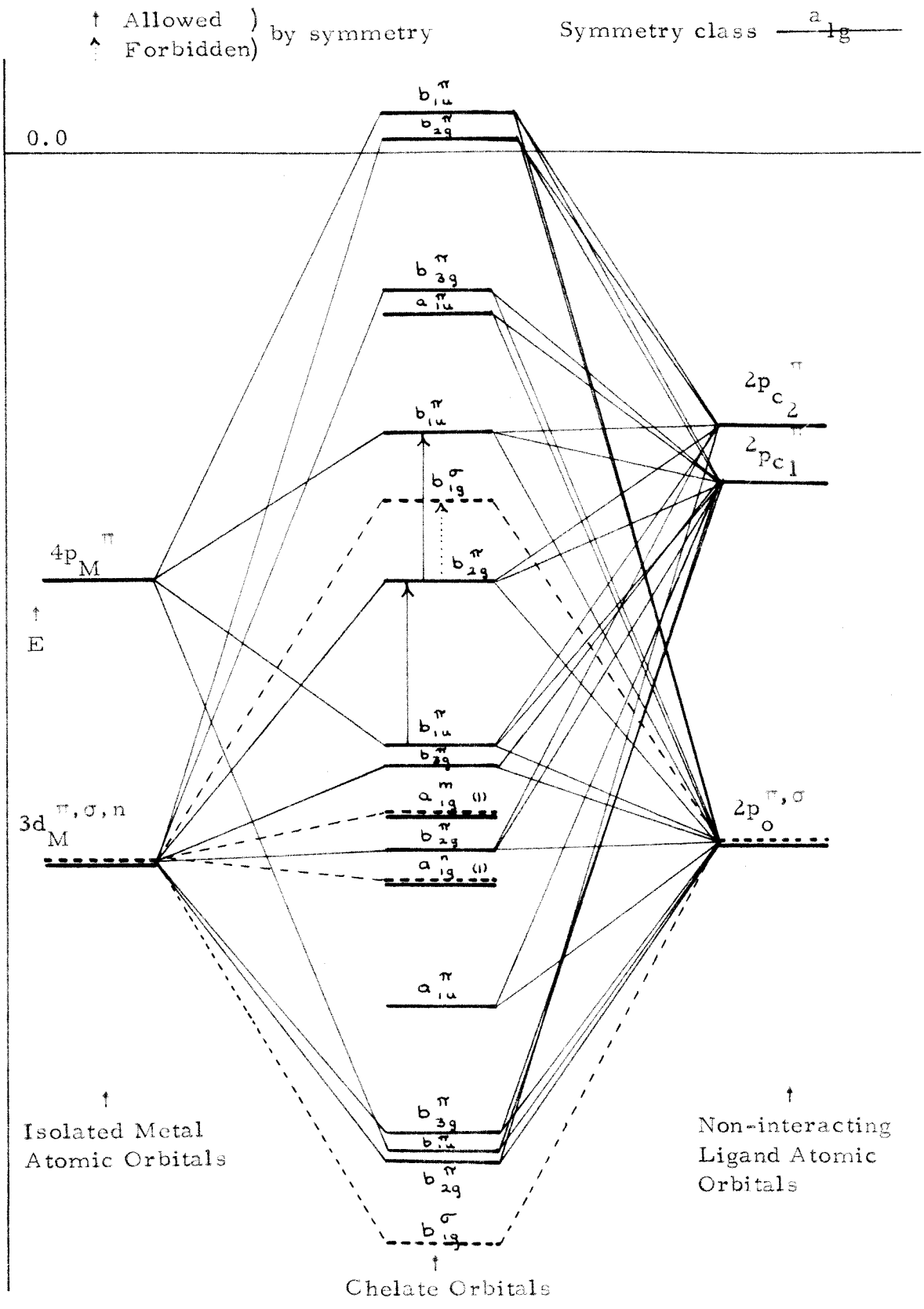

Figure X.

Quenching of the Photoreduction of Benzophenone by Benzhydrol in Benzene

Figure XI

Quenching of the Photoreduction of Benzophenone by Benzhydrol in Benzene

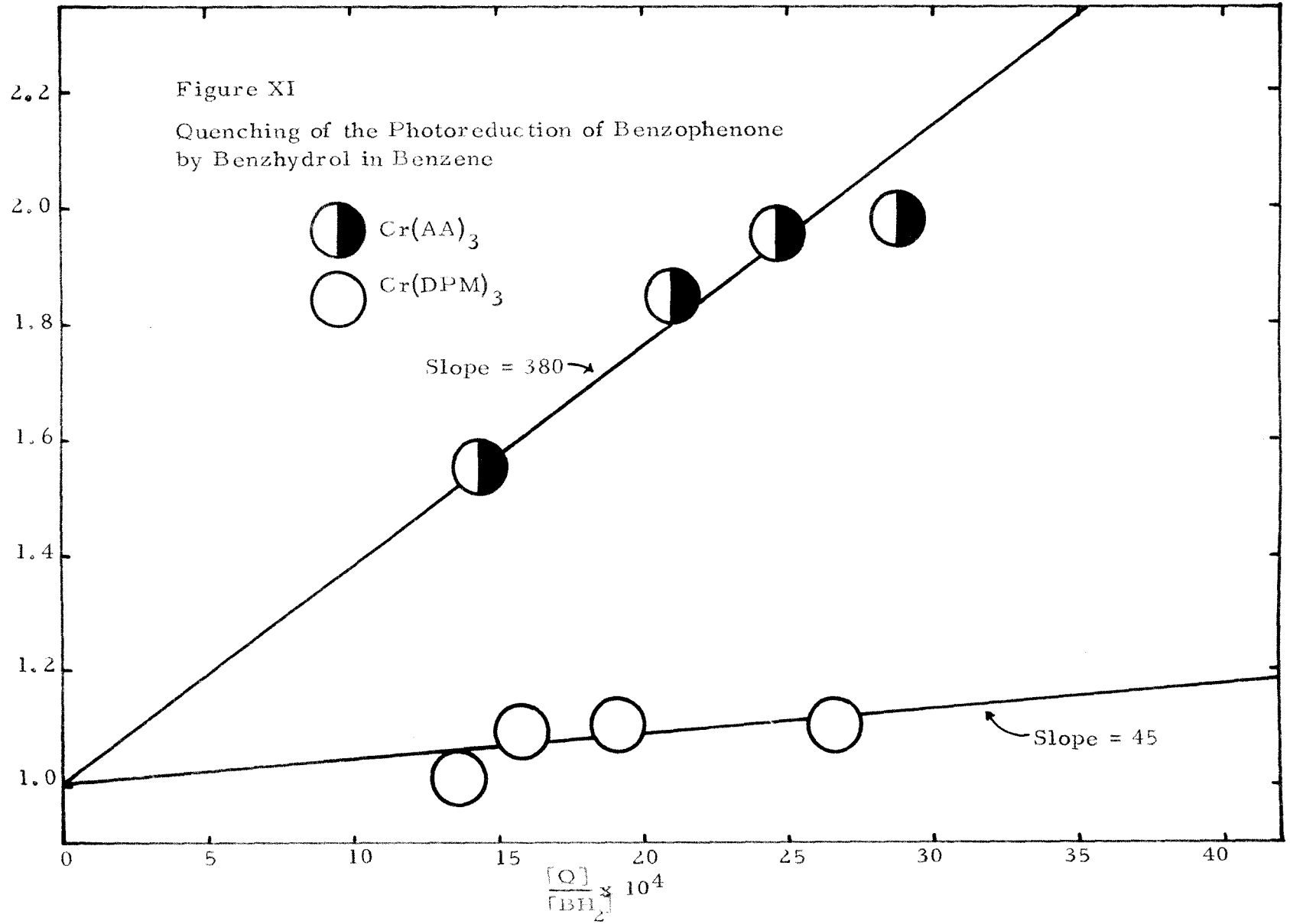

Figure XII

Quenching of the Photoreduction of Benzophenone by Benzhydrol in Benzene

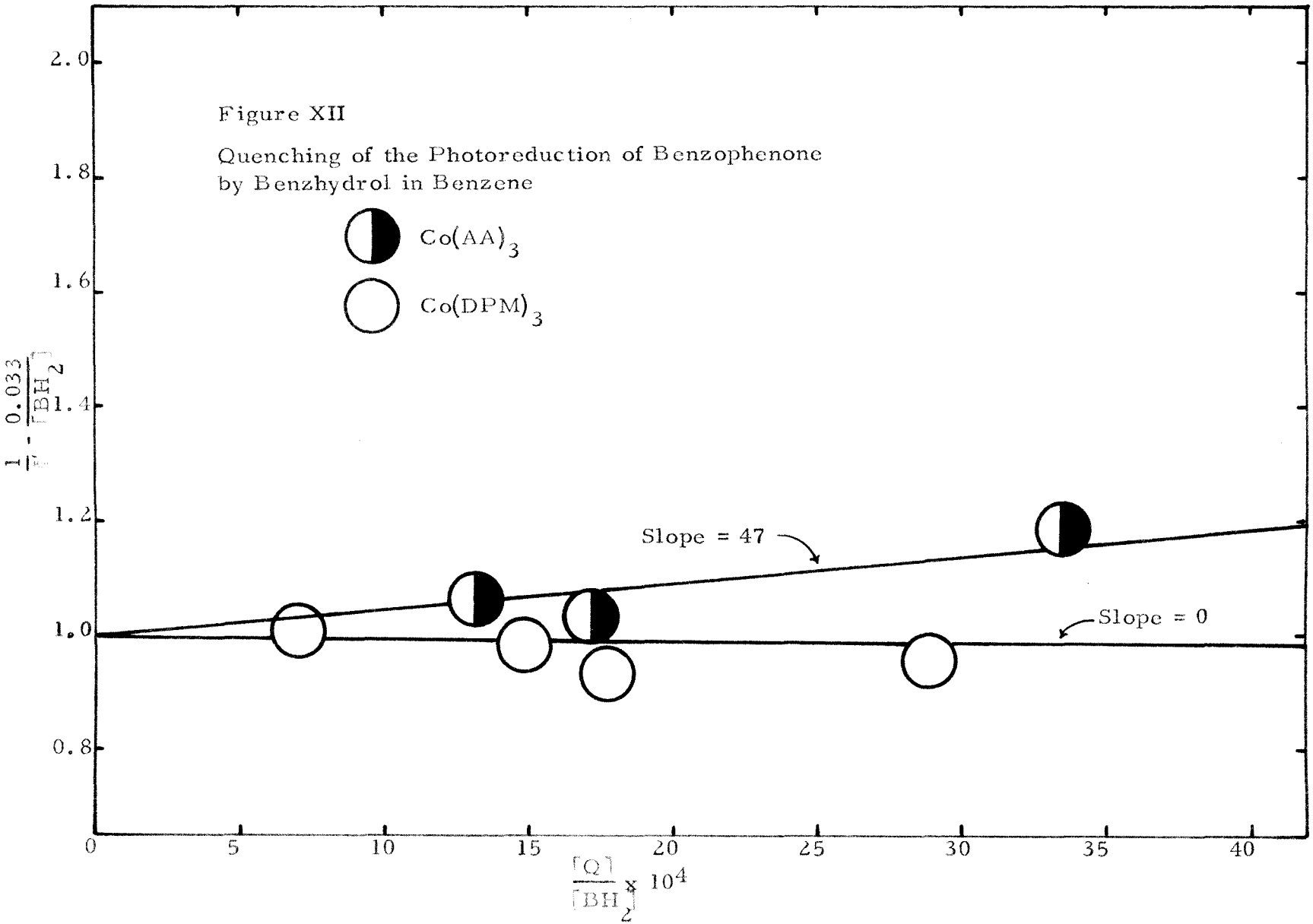

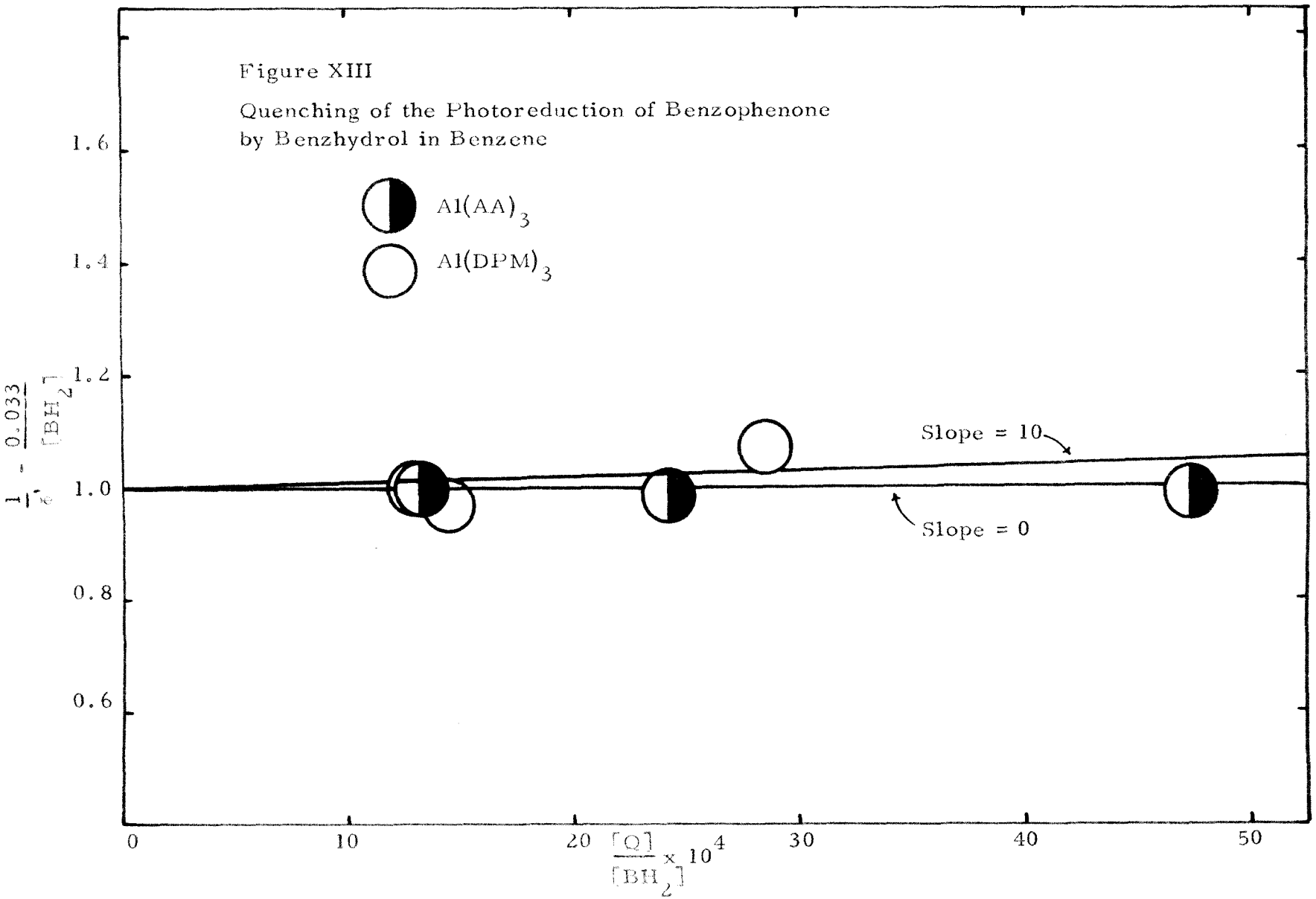
Figure XIII
Quenching of the Photoreduction of Benzophenone by Benzhydrol in Benzene
Al(AA)3
Al(DPM)3
Slope = 10
Slope = 0
1.6
1.4
1.2
1.0
0.8
0.6
0
10
20
30
40
50
$\frac{1}{\phi} - \frac{0.033}{[BH_2]}$
$\frac{[Q]}{[BH_2]} \times 10^4$

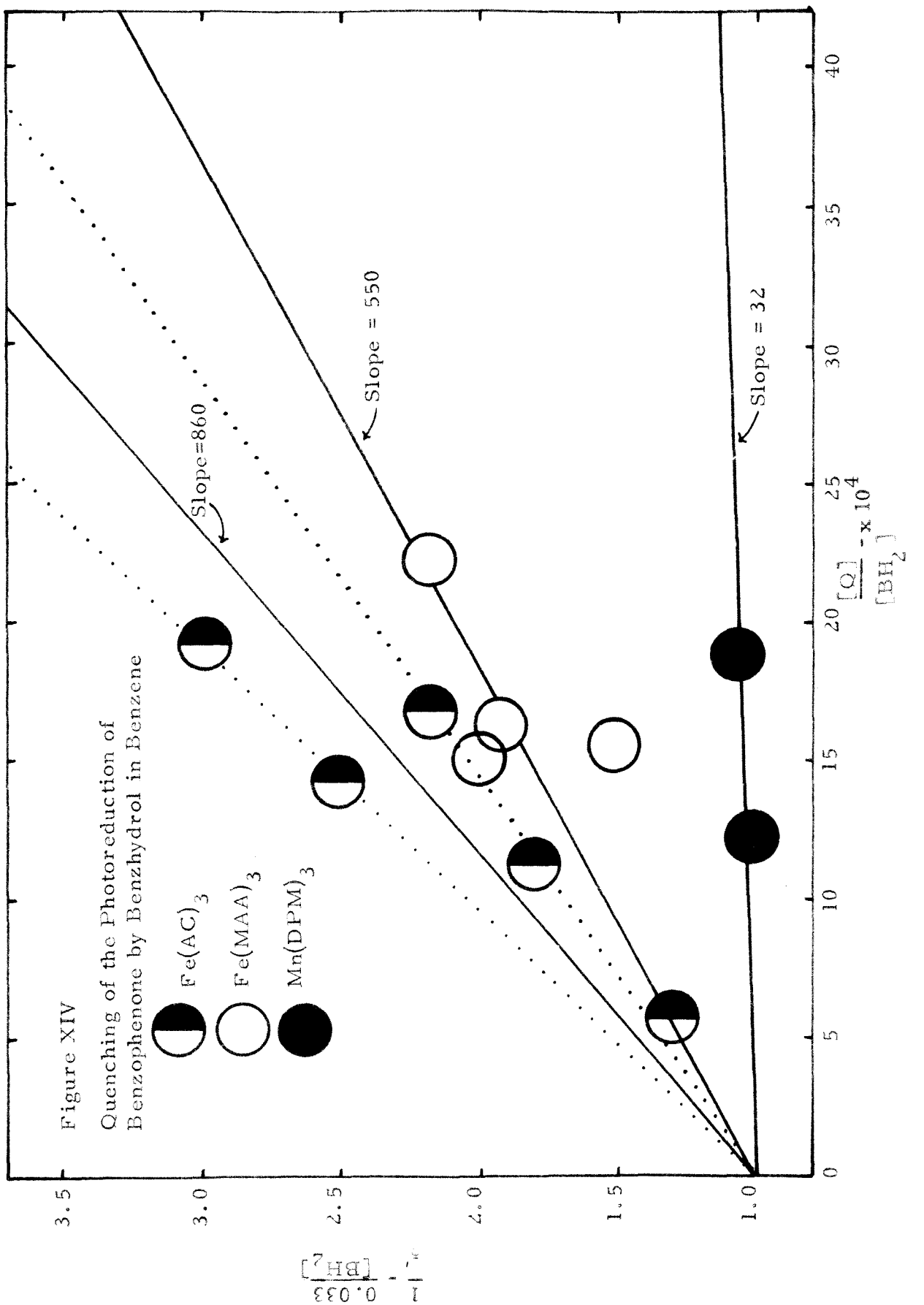
Figure XIV
Quenching of the Photoreduction of
Benzophenone by Benzhydrol in Benzene
Fe(AC)3
Fe(MAA)3
Mn(DPM)3
Slope=860
Slope = 550
Slope = 32
3.5
3.0
2.5
2.0
1.5
1.0
0
5
10
15
20
25
30
35
40
[Q] / [BH2] - x 10^4
1/φ - 0.033 [BH2]

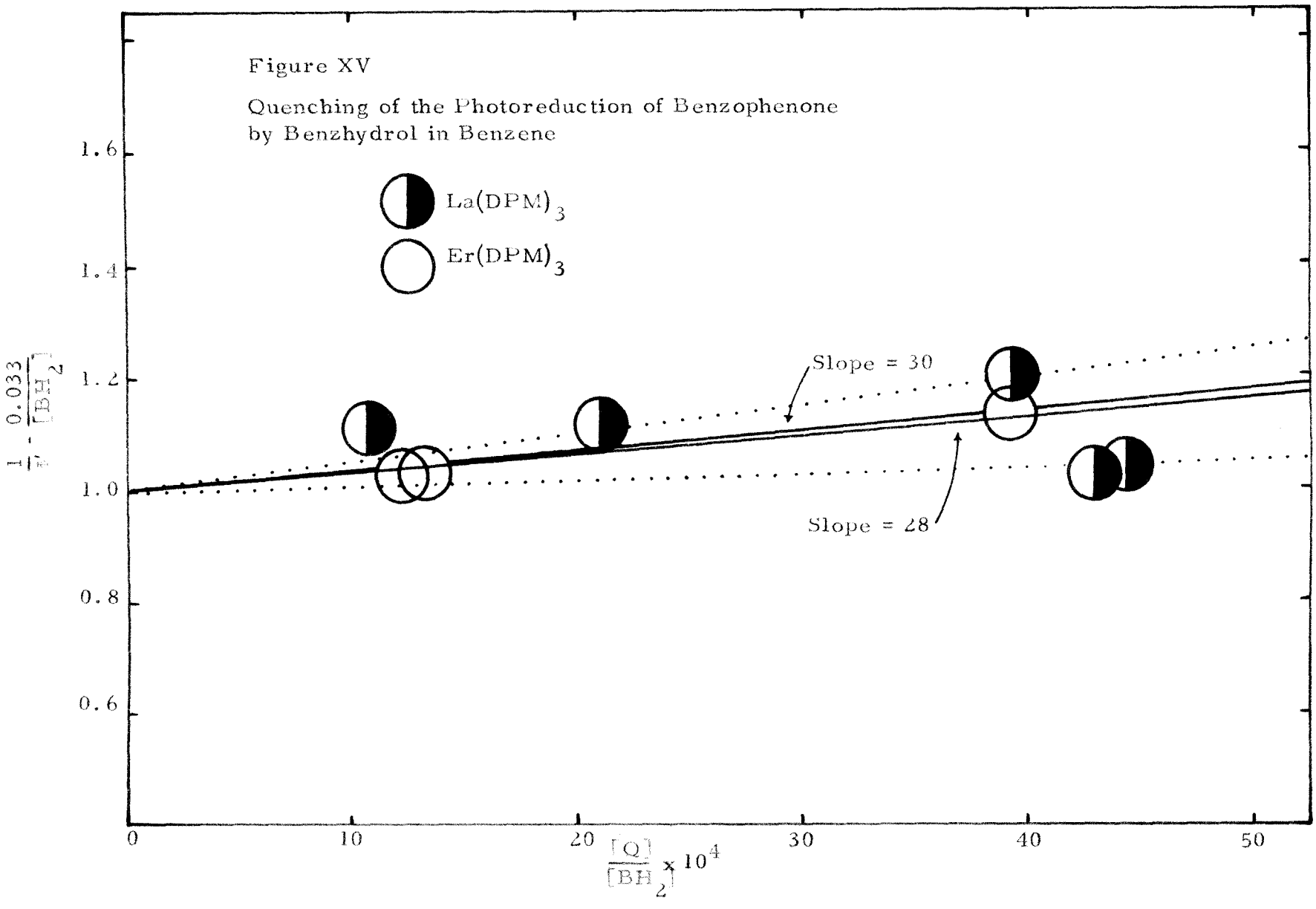
Figure XV
Quenching of the Photoreduction of Benzophenone by Benzhydrol in Benzene
La(DPM)3
Er(DPM)3
Slope = 30
Slope = 28
1.6
1.4
1.2
1.0
0.8
0.6
0
10
20
30
40
50
$\frac{1}{\Phi} - \frac{0.033}{[BH_2]}$
$\frac{[Q]}{[BH_2]} \times 10^4$

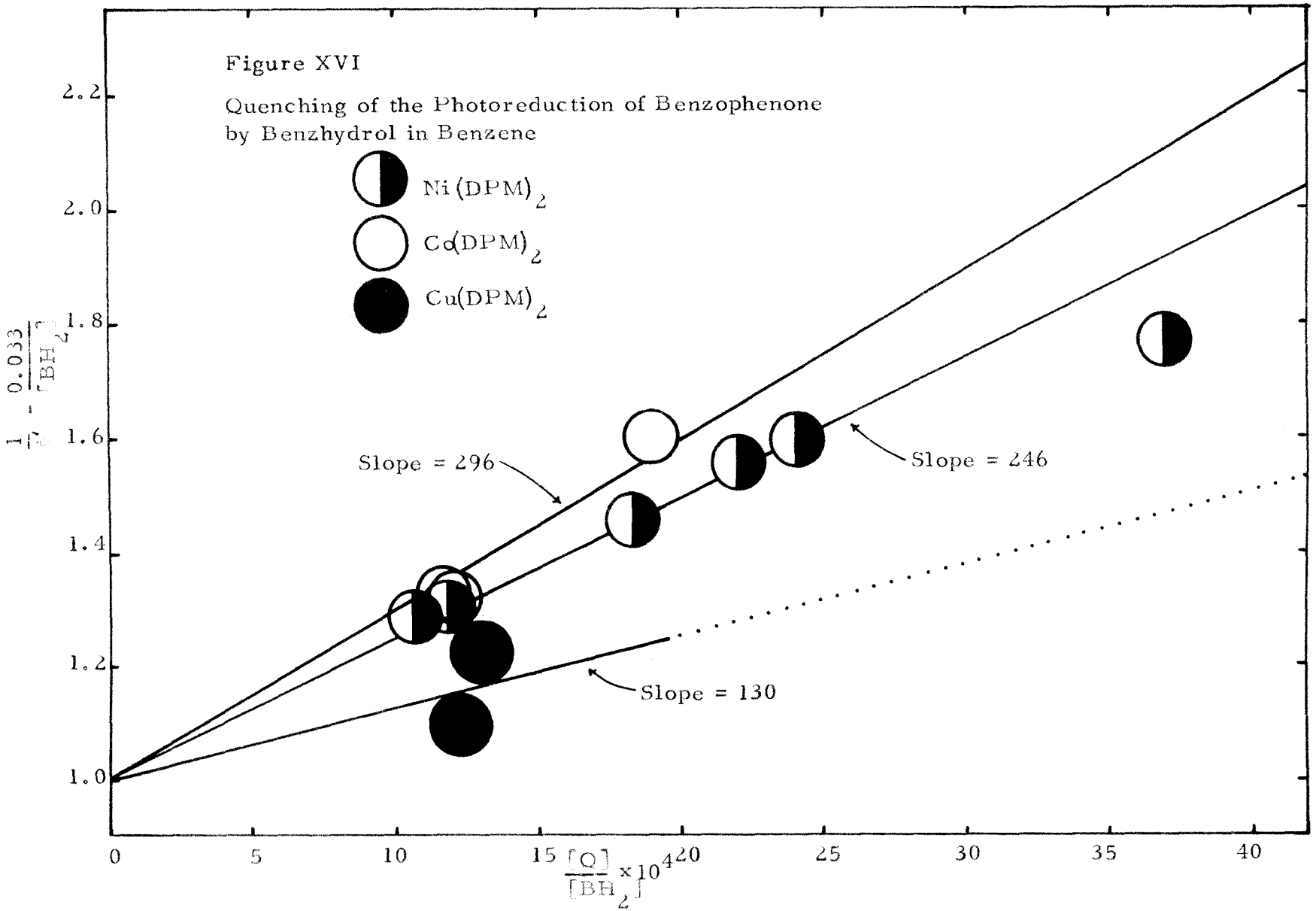
Figure XVI
Quenching of the Photoreduction of Benzophenone by Benzhydrol in Benzene
Ni(DPM)2
Co(DPM)2
Cu(DPM)2
Slope = 296
Slope = 246
Slope = 130
2.2
2.0
1.8
1.6
1.4
1.2
1.0
0
5
10
15
20
25
30
35
40
$\frac{1}{\Phi} - \frac{0.033}{[BH_2]}$
$\frac{[Q]}{[BH_2]} \times 10^4$

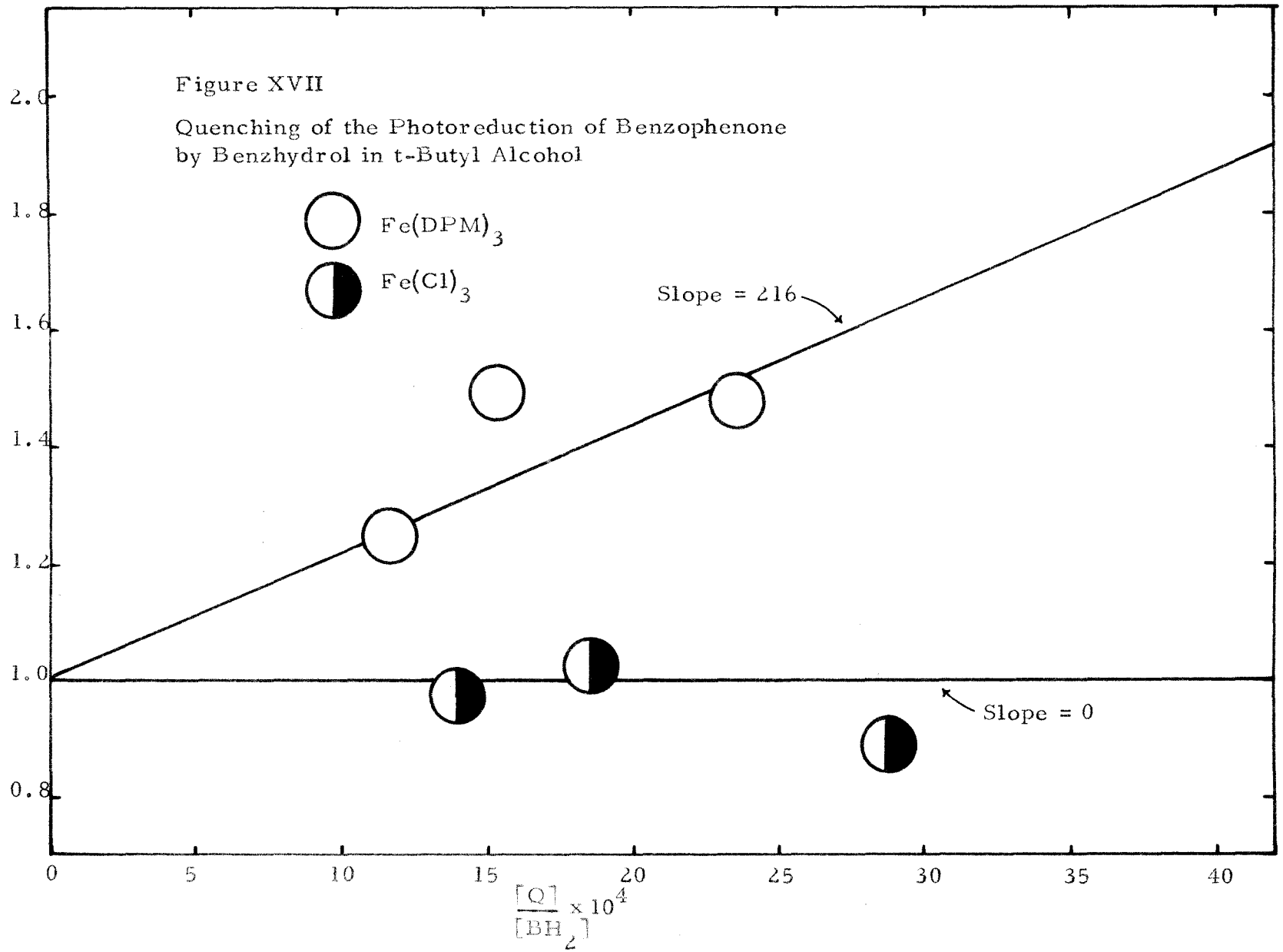
Figure XVII
Quenching of the Photoreduction of Benzophenone by Benzhydrol in t-Butyl Alcohol
Fe(DPM)3
Fe(Cl)3
Slope = 216
Slope = 0
2.0
1.8
1.6
1.4
1.2
1.0
0.8
0
5
10
15
20
25
30
35
40
1/φ - 0.0616/[BH2]
[Q]/[BH2] x 10^4

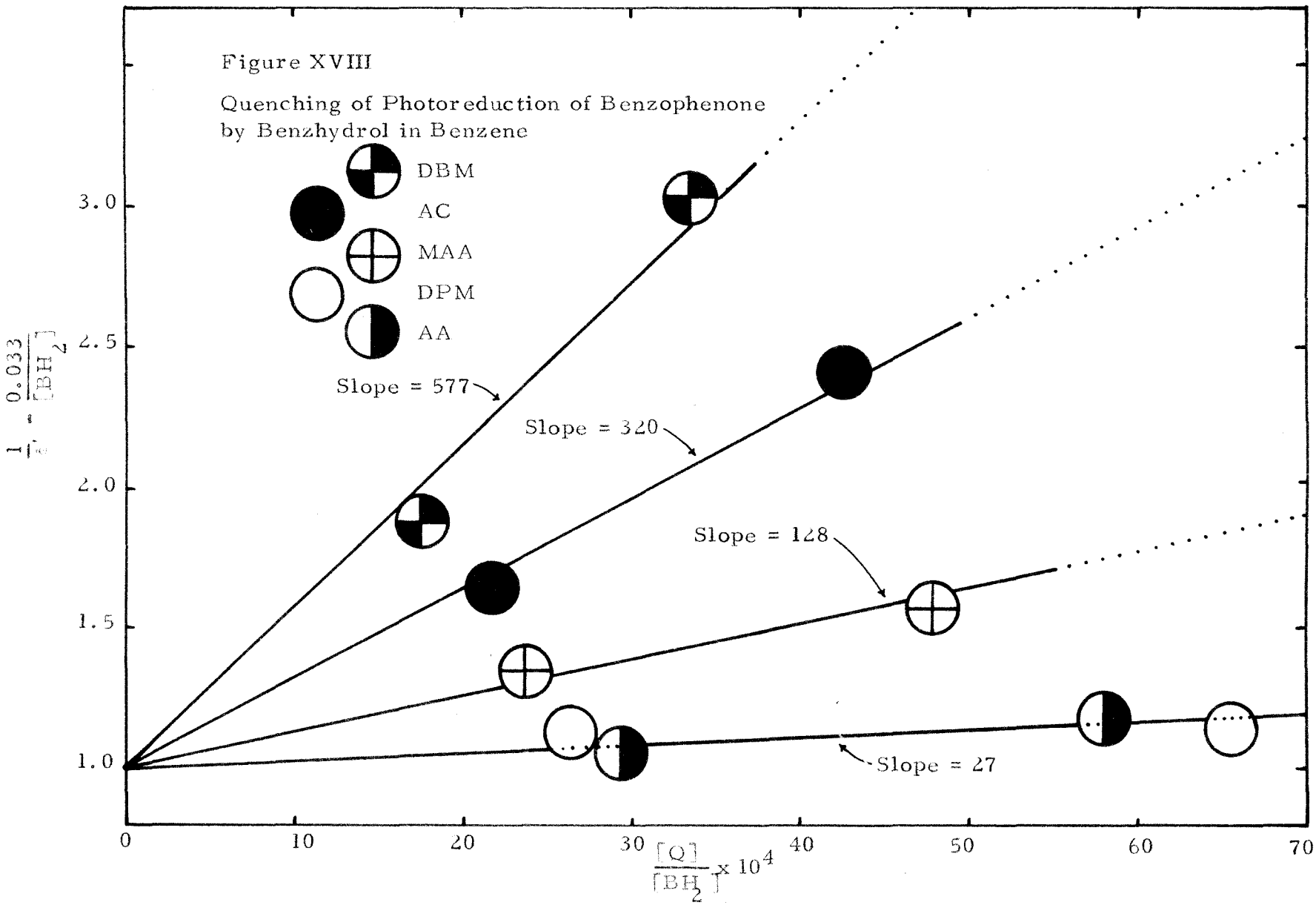
Figure XVIII
Quenching of Photoreduction of Benzophenone by Benzhydrol in Benzene
DBM
AC
MAA
DPM
AA
Slope = 577
Slope = 320
Slope = 128
Slope = 27
3.0
2.5
2.0
1.5
1.0
0
10
20
30
40
50
60
70
$\frac{1}{\phi} - \frac{0.033}{[BH_2]}$
$\frac{[Q]}{[BH_2]} \times 10^4$

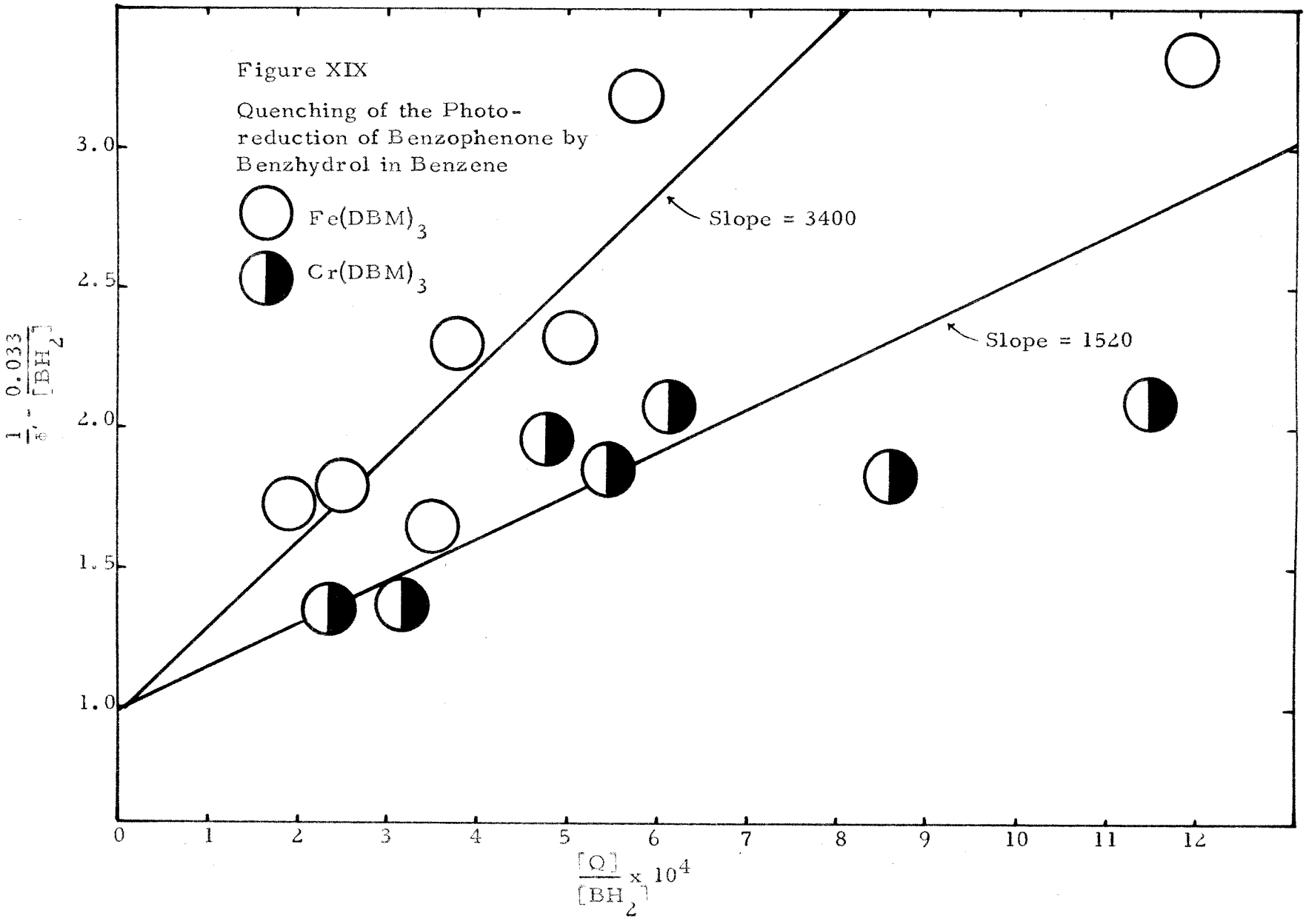
Figure XIX
Quenching of the Photo-reduction of Benzophenone by Benzhydrol in Benzene
Fe(DBM)3
Cr(DBM)3
Slope = 3400
Slope = 1520
3.0
2.5
2.0
1.5
1.0
0
1
2
3
4
5
6
7
8
9
10
11
12
1/Φ' - 0.033/[BH2]
[Q]/[BH2] x 10^4

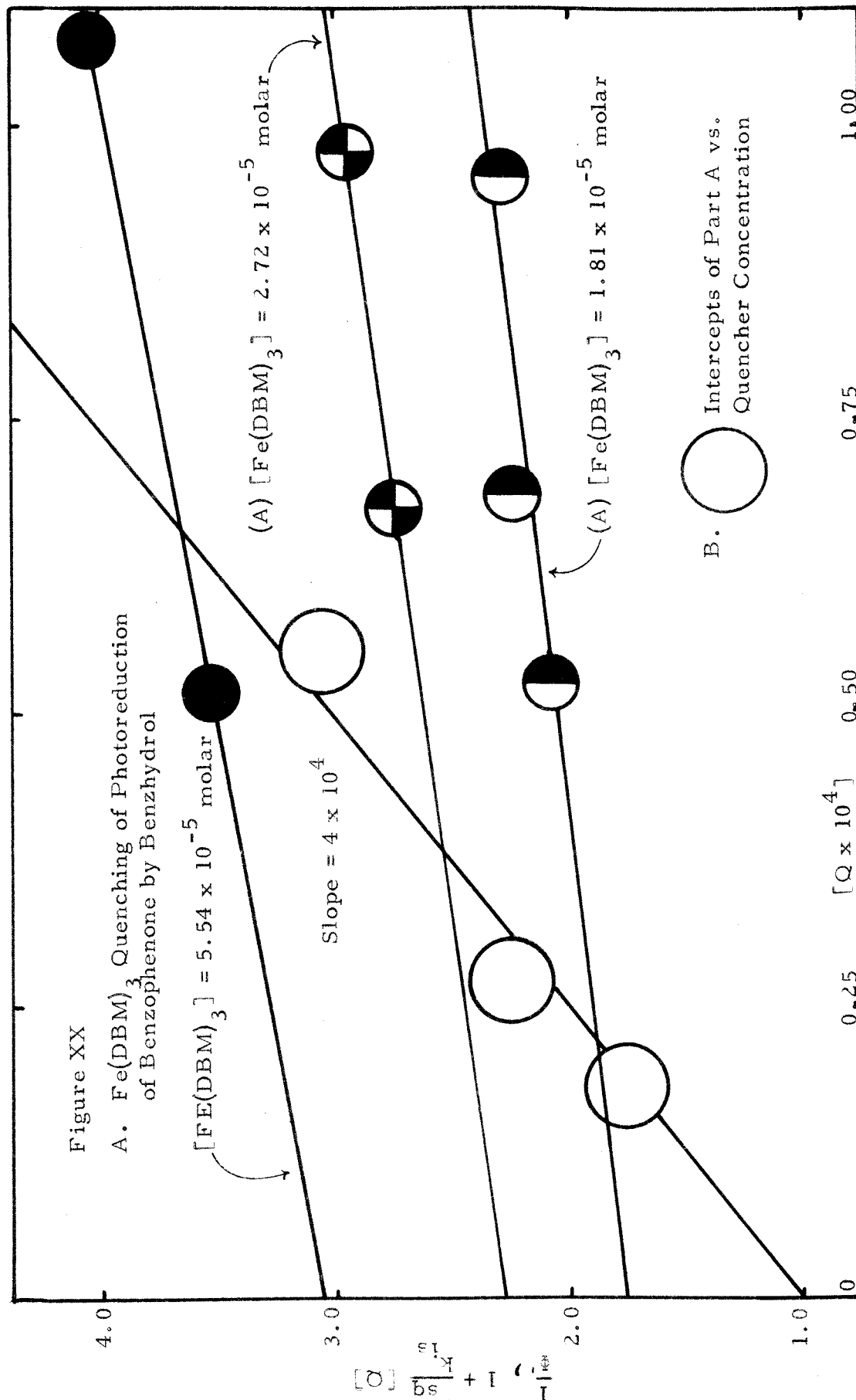
Figure XX
A. Fe(DBM)3 Quenching of Photoreduction of Benzophenone by Benzhydrol
[FE(DBM)3] = 5.54 x 10-5 molar
(A) [Fe(DBM)3] = 2.72 x 10-5 molar
(A) [Fe(DBM)3] = 1.81 x 10-5 molar
Slope = 4 x 10^4
B. Intercepts of Part A vs. Quencher Concentration
4.0
3.0
2.0
1.0
0
0.25
0.50
0.75
1.00
5
10
15
20
[Q x 10^4]
1/[BH2]

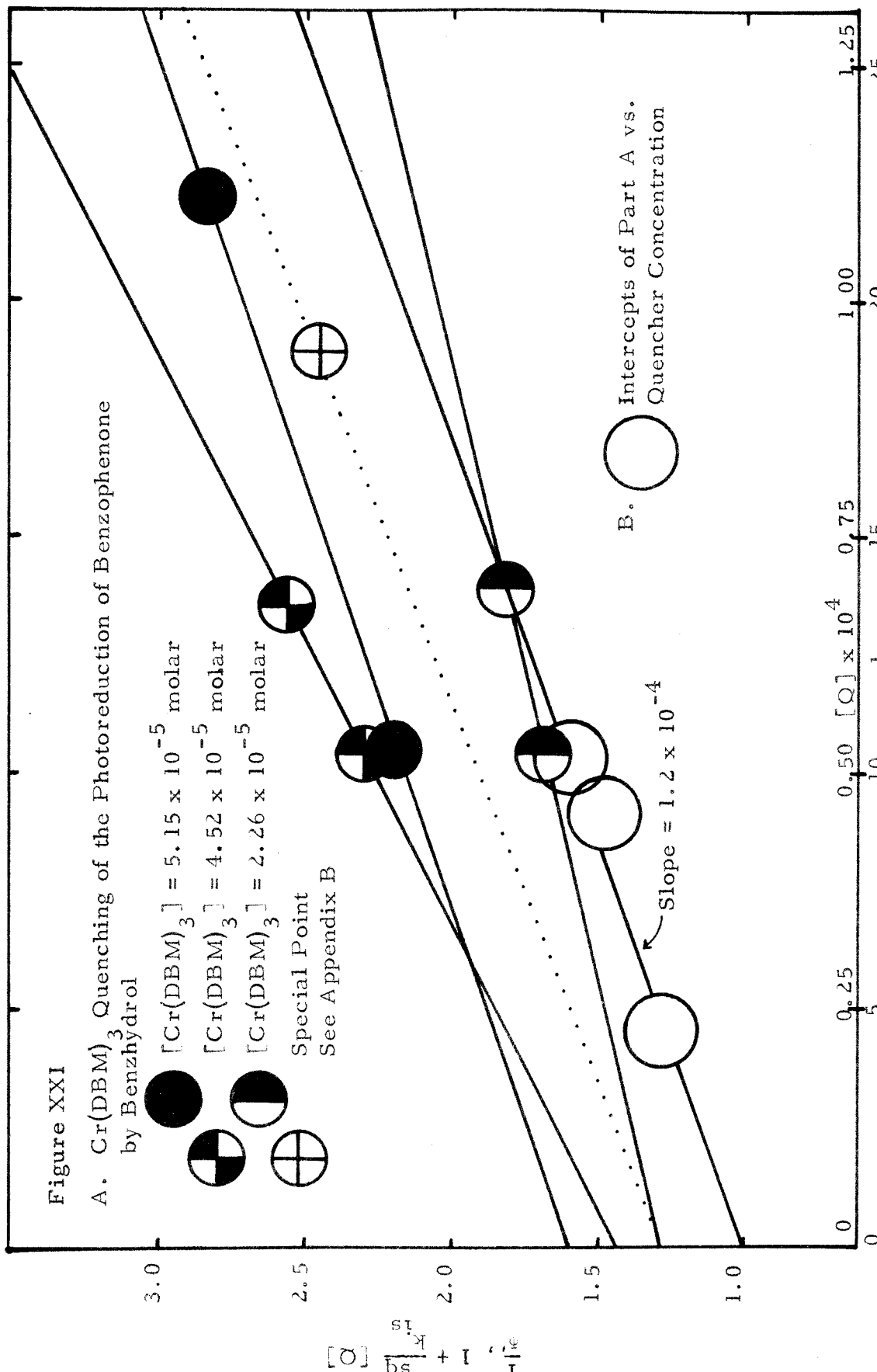
Figure XXI
A. Cr(DBM)3 Quenching of the Photoreduction of Benzophenone by Benzhydrol
[Cr(DBM)3] = 5.15 x 10-5 molar
[Cr(DBM)3] = 4.52 x 10-5 molar
[Cr(DBM)3] = 2.26 x 10-5 molar
Special Point See Appendix B
B. Intercepts of Part A vs. Quencher Concentration
Slope = 1.2 x 10-4
3.0
2.5
2.0
1.5
1.0
0
0.25
0.50
0.75
1.00
1.25
5
10
15
20
25
[Q] x 10^4
1/[BH2]

Figure XXII

Energy Level Diagram for the Electronic States for Three Triplet Transfer Intermediate Complexes as a Function of the Intermolecular Distance

(subscript 1 = bonding, subscript 2 = antibonding)

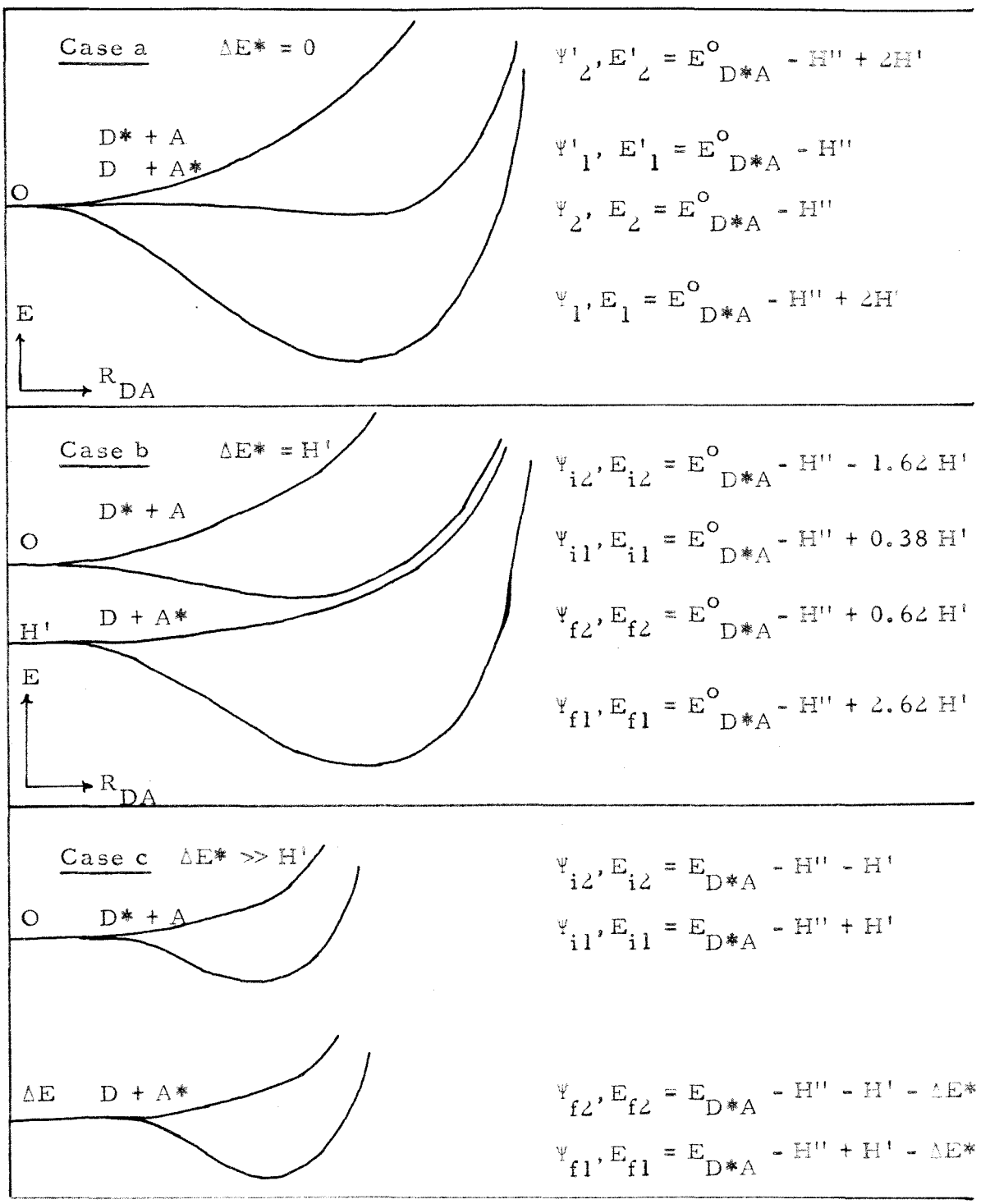

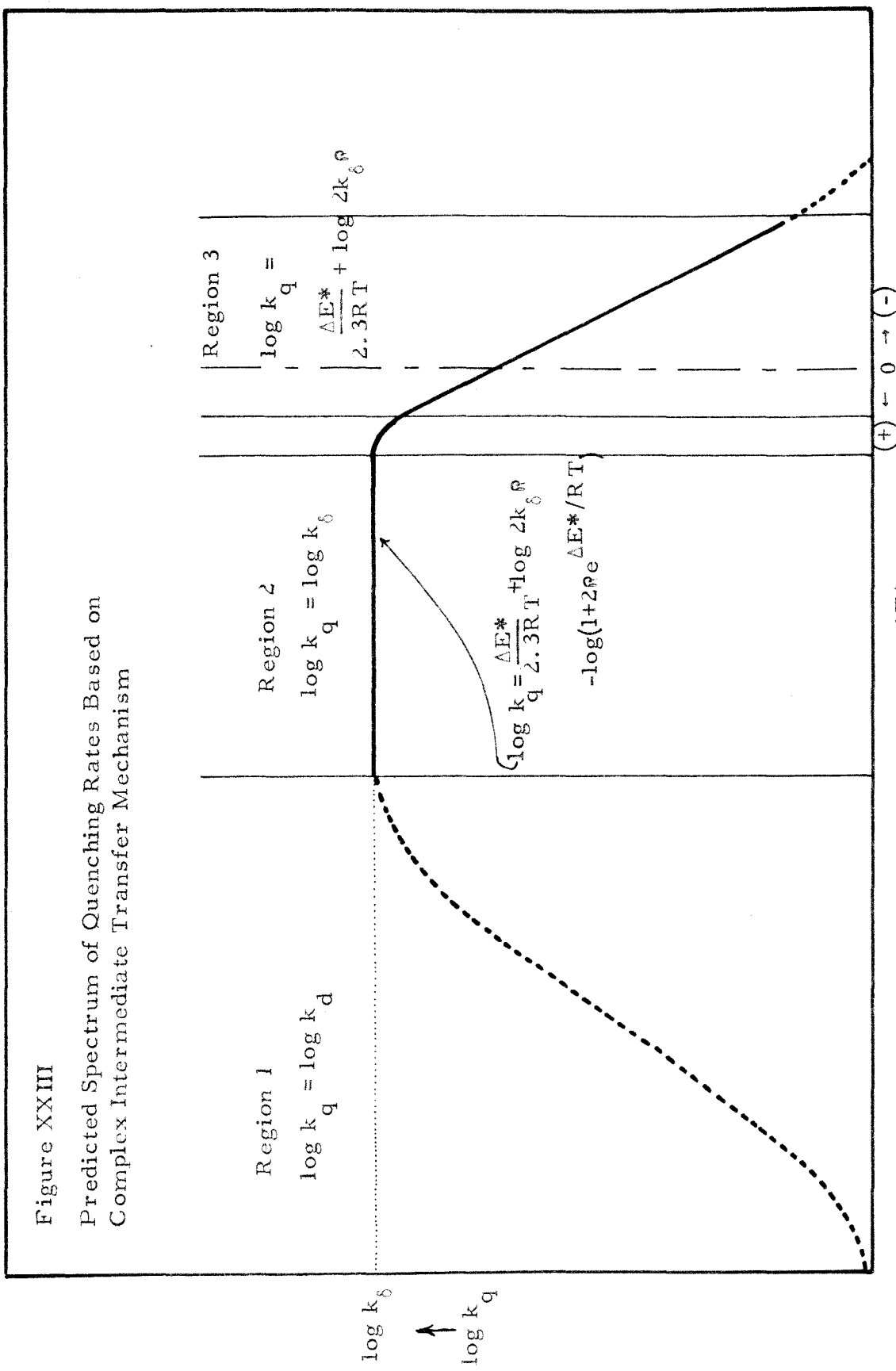

Figure XXIII

Predicted Spectrum of Quenching Rates Based on Complex Intermediate Transfer Mechanism

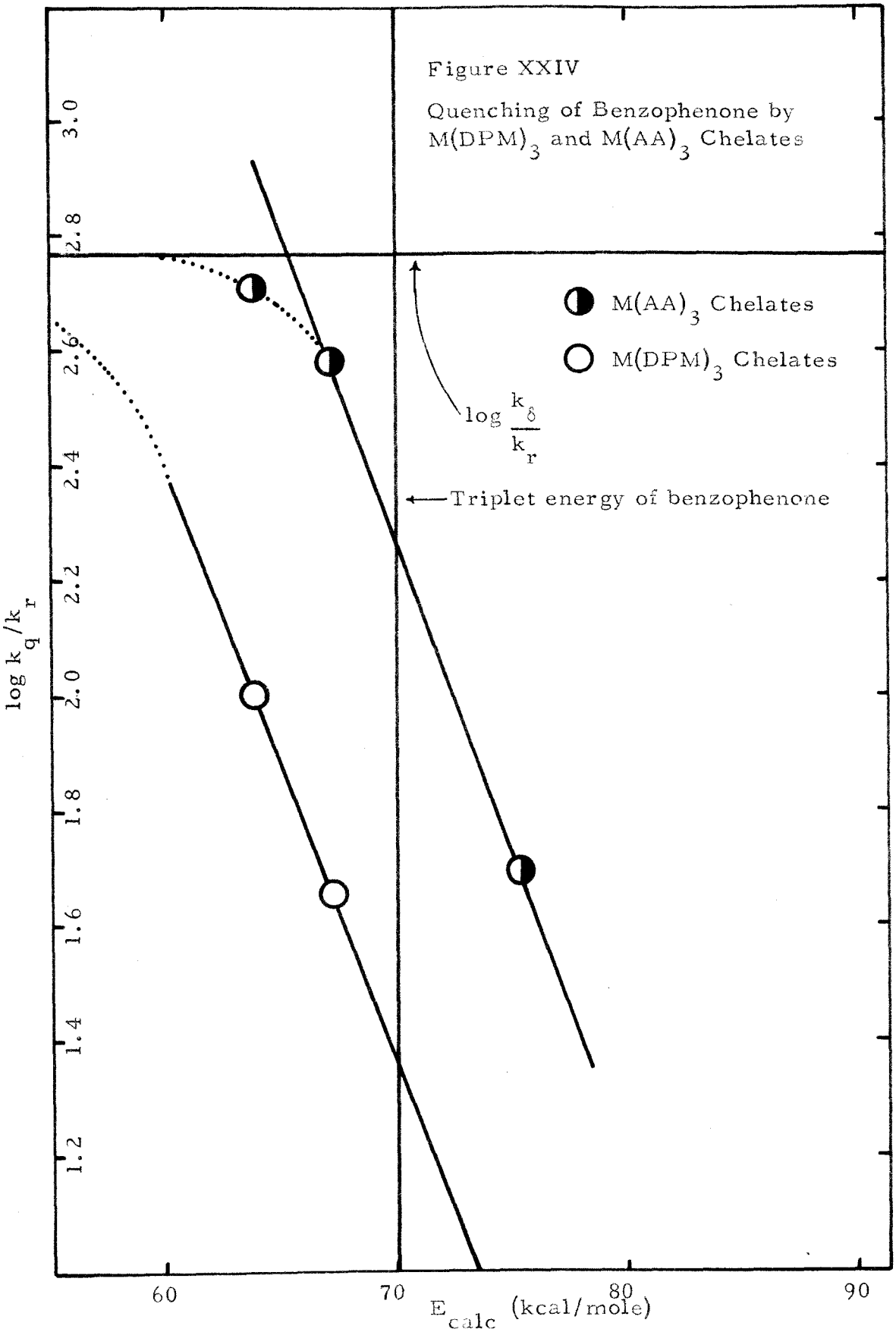
Figure XXIV
Quenching of Benzophenone by M(DPM)3 and M(AA)3 Chelates
M(AA)3 Chelates
M(DPM)3 Chelates
log kδ/kr
Triplet energy of benzophenone
log kq/kr
3.0
2.8
2.6
2.4
2.2
2.0
1.8
1.6
1.4
1.2
60
70
80
90
Ecalc (kcal/mole)

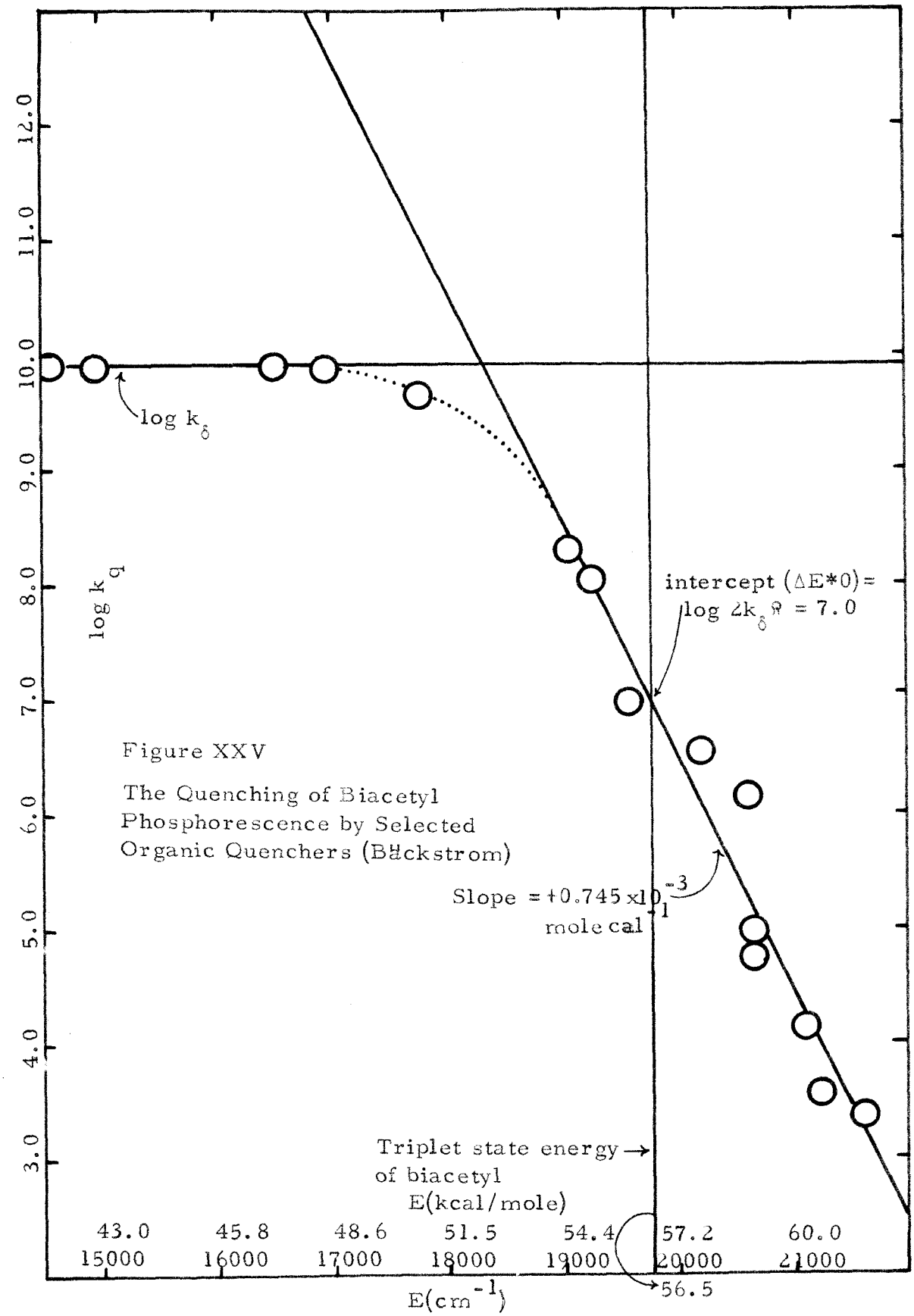

Figure XXV

The Quenching of Biacetyl Phosphorescence by Selected Organic Quenchers (Bäckstrom)

APPENDIX A

COMMON ATOMIC INTEGRALS USEFUL FOR CHELATE PROBLEMS

Table 1

Kinetic Energy and Nuclear Attraction Integrals.

Evaluated in Terms of Regular and Quasi Overlap Integrals

---

1. $(2p\pi_a | -\tfrac{1}{2}\nabla^2 | 2p\pi_b) = -\tfrac{1}{2}\zeta^2(1+\tau)^2 \left[(2p\pi_a | 2p\pi_b) - \frac{4}{\sqrt{3}}(1p\pi_a | 2p\pi_b)\right]$

2. $(2p\pi_a | -\tfrac{1}{2}\nabla^2 | 3d\pi_b) = -\tfrac{1}{2}\zeta^2(1+\tau)^2 \left[(2p\pi_a | 3d\pi_b) - \frac{4}{\sqrt{3}}(1p\pi_a | 3d\pi_b)\right]$

3. $(2p\sigma_a | -\tfrac{1}{2}\nabla^2 | 3d\sigma_b) = -\tfrac{1}{2}\zeta^2(1+\tau)^2 \left[(2p\sigma_a | 3d\sigma_b) - \frac{4}{\sqrt{3}}(1p\sigma_a | 3d\sigma_b)\right]$

4. $(2p\pi_a | -\tfrac{1}{2}\nabla^2 | 4p\pi_b) = -\tfrac{1}{2}\zeta^2(1+\tau)^2 \left[(2p\pi_a | 4p\pi_b) - \frac{4}{\sqrt{3}}(1p\pi_a | 4p\pi_b)\right]$

5. $(2S_a | -\tfrac{1}{2}\nabla^2 | 3d\sigma_b) = -\tfrac{1}{2}\zeta^2(1+\tau)^2 \left[(2S_a | 3d\sigma_b) - \frac{4}{\sqrt{3}}(1S_a | 3d\sigma_b) + \frac{2}{\sqrt{6}}(0S_a | 3d\sigma_b)\right]$

6. $(2p\pi_a | \frac{Z_a}{r_a} | 2p\pi_b) = \frac{1}{\sqrt{3}} Z_a\zeta(1+\tau)(1p\pi_a | 2p\pi_b)$

7. $(2p\pi_a | \frac{Z_a}{r_a} | 3d\pi_b) = \frac{1}{\sqrt{3}} Z_a\zeta(1+\tau)(1p\pi_a | 3d\pi_b)$

8. $(3d\pi_a | \frac{Z_a}{r_a} | 2p\pi_b) = \frac{2 Z_a\zeta(1+\tau)}{\sqrt{30}}(2d\pi_a | 2p\pi_b)$

9. $(2p\sigma_a | \frac{Z_a}{r_a} | 3d\sigma_b) = \frac{1}{\sqrt{3}} Z_a\zeta(1+\tau)(1p\sigma_a | 3d\sigma_b)$

10. $(3d\sigma_a | \frac{Z_a}{r_a} | 2p\sigma_b) = \frac{2}{\sqrt{30}} Z_a\zeta(1+\tau)(2d\sigma_a | 2p\sigma_b)$

Table 1 (continued)

11. $(2p\pi_a \left| \frac{Z_a}{r_a} \right| 4p\pi_b) = \frac{1}{\sqrt{3}} (Z_a)\,\zeta\,(1+\tau)\,(1p\pi_a \left| 4p\pi_b\right)$

12. $(4p\pi_a \left| \frac{Z_a}{r_a} \right| 2p\pi_b) = \frac{1}{\sqrt{14}} Z_a\zeta(1+\tau)\,(3p\pi_a \left| 2p\pi_b\right)$

13. $(2S_a \left| \frac{Z_a}{r_a} \right| 3d\sigma_b) = \frac{1}{\sqrt{3}} Z_a\zeta(1+\tau)\,(1S_a \left| 3d\sigma_b\right)$

14. $(3d\sigma_a \left| \frac{Z_a}{r_a} \right| 2S_b) = \frac{2}{\sqrt{30}} Z_a\zeta(1+\tau)\,(2d\sigma_a \left| 2S_b\right)$

Z_a = effective nuclear charge on atom a

$\zeta = \frac{1}{2}(\zeta_a + \zeta_b)$; $\zeta_a = (1+\tau)\zeta$

$\tau = \frac{(\zeta_a - \zeta_b)}{(\zeta_a + \zeta_b)}$; $\zeta_b = (1-\tau)\zeta$

$\zeta_a = \frac{Z_a}{n}$, n = principal quantum number

$\rho = \zeta R$, R = internuclear distance

Table 2

Regular and Quasi Overlap Integrals Evaluated in Terms of Incomplete Gamma Functions

1. $$(2p\pi_a \mid 2p\pi_b) = \frac{R^5 \zeta_a^{5/2} \zeta_b^{5/2}}{32} [A_0(B_2-B_4)+A_2(B_4-B_0)+A_4(B_0-B_2)]$$

2. $$(2p\pi_a \mid 2p\pi_b)_{\tau=0} = \frac{\rho^5}{120} [5A_4 - 6A_2 + A_0]$$

3. $$(1p\pi_a \mid 2p\pi_b) = \frac{\sqrt{3}\, R^4 \zeta_a^{3/2} \zeta_b^{5/2}}{16} [A_o(B_1-B_3)+A_1(B_2-B_0)+ A_2(B_3-B_1)+A_3(B_0-B_2)]$$

4. $$(1p\pi_a \mid 2p\pi_b)_{\tau=0} = \frac{\sqrt{3}}{16} \rho^4 [\frac{4}{3} (A_3 - A_1)]$$

5. $$(2p\pi_a \mid 3d\pi_b) = \frac{R^6}{32\sqrt{6}} \zeta_a^{5/2} \zeta_b^{7/2} [A_0(B_2-B_4)+A_1(B_5-B_3)+A_2(B_4-B_0) +A_3(B_1-B_5)+A_4(B_0-B_2)+A_5(B_3-B_1)]$$

6. $$(1p\pi_a \mid 3d\pi_b) = \frac{R^5}{32\sqrt{2}} \zeta_a^{3/2} \zeta_b^{7/2} [A_0(B_1-B_3)+A_1(B_4-B_0)+A_3(B_0-B_4) +A_4(B_3-B_1)]$$

7. $$(2d\pi_a \mid 2p\pi_b) = \frac{\sqrt{5}}{32} R^5 \zeta_a^{5/2} \zeta_b^{5/2} [A_0(B_1-B_3)+A_1(2B_2-B_0-B_4) +A_2(2B_3-2B_1)+A_3(B_0+B_4-2B_2)+A_4(B_1-B_3)]$$

8. $$(2p\pi_a \mid 4p\pi_b) = \frac{R^7}{128\sqrt{105}} \zeta_a^{5/2} \zeta_b^{9/2} [A_6(B_0-B_2)+2A_5(B_3-B_1) +A_4(B_2-B_0)+2A_3(B_1-B_5)+A_2(B_6-B_4)+2A_1(B_5-B_3) +A_0(B_4-B_6)]$$

Table 2 (continued)

9. $$(2p\sigma_a \mid 3d\sigma_b) = \frac{\sqrt{2}}{192} R^6 \zeta_a^{5/2} \zeta_b^{7/2} [A_0(B_4-3B_2)+A_1(B_3+B_5) + A_2(3B_0+B_4)+A_3(-B_1-3B_5)+A_4(-B_2-B_0)+A_5(3B_3-B_1)]$$

10. $$(1p\sigma_a \mid 3d\sigma_b) = \frac{1}{32} \frac{2}{3} R^5 \zeta_a^{3/2} \zeta_b^{7/2} [A_0(B_3-3B_1)+A_1(3B_0-B_4) + A_3(-B_0-3B_4)+A_4(3B_3-B_1)]$$

11. $$(2d\sigma_a \mid 2p\sigma_b) = \frac{R^5}{32} \sqrt{\frac{5}{3}} \zeta_a^{5/2} \zeta_b^{5/2} [A_0(B_3-3B_1)+A_1(3B_0-2B_2-B_4) + A_2(2B_1+2B_3)+A_3(3B_4-2B_2-B_0)+A_4(B_1-3B_3)]$$

12. $$(2p\sigma_a \mid 2p\sigma_b) = \frac{R^5}{16} \zeta_a^{5/2} \zeta_b^{5/2} [B_2(A_0+A_4)-A_2(B_0+B_4)]$$

13. $$(2S_a \mid 2p\sigma_b) = \frac{R^5}{16\sqrt{3}} \zeta_a^{5/2} \zeta_b^{5/2} [A_3(B_0-B_2)+A_1(B_4-B_2) + B_1(A_2-A_4)+B_3(A_2-A_0)]$$

$$A_n = A_n(\rho) = \int_1^\infty \xi^n e^{-e\xi} d\xi = e^{-e} \sum_{i=1}^{n+1} [n!/e^i (n-i+1)!]$$

$$B_n = B_n(|\tau e|) = \int_{-1}^{1} \eta^n e^{-e\tau\eta} d\eta = -A_n(\tau e)-(-1)^n A_n(-\tau e)$$

$B_n(0) = 2/(n+1)$ for n even; = 0 for n odd.

Table 2 (continued)

$$\rho = \zeta \mathcal{R}, \quad \tau = \frac{[\zeta_a - \zeta_b]}{[\zeta_a + \zeta_b]}, \quad \zeta_i = \frac{Z_i}{n}, \quad \zeta = \tfrac{1}{2}(\zeta_a + \zeta_b)$$

n = principal quantum number

$\mathcal{R}$ = internuclear distance

Table 3

Coulombic Nuclear Attraction Integrals Evaluated in Terms of Incomplete Gamma Functions

1. $$(2p\pi_a \left| \frac{1}{r_b} \right| 2p\pi_a) = \frac{R^4}{16} \zeta_a^5 [A_o(B_3-B_1)+A_1(B_2-B_0)+A_2(B_1-B_3)+A_3(B_0-B_2)]$$

2. $$(3d\pi_a \left| \frac{1}{r_b} \right| 3d\pi_a) = \frac{R^6}{96} \zeta_a^7 [A_0(B_3-B_1)+A_1(2B_4-B_2-B_0)+A_2(B_5-B_1)+A_3(B_0-B_4)+A_4(2B_1-B_3-B_5)+A_5(B_2-B_4)]$$

3. $$(2p\sigma_a \left| \frac{1}{r_b} \right| 2p\sigma_a) = \frac{R^4}{8} \zeta_a^5 [A_0B_1+A_1(B_0+2B_2)+A_2(2B_1+B_3)+A_3B_2]$$

4. $$(3d\sigma_a \left| \frac{1}{r_b} \right| 3d\sigma_a) = \frac{R^6 \zeta_a^7}{576} [A_0(9B_1-6B_3+B_5)+A_1(9B_0+18B_2-7B_4)+A_2(18B_1+28B_3-6B_5)+A_3(18B_4+28B_2-6B_0)+A_4(9B_5+18B_3-7B_1)+A_5(9B_4-6B_2+B_0)]$$

5. $$(3d\delta_a \left| \frac{1}{r_b} \right| 3d\delta_a) = \frac{R^6 \zeta_a^7}{384} [A_0(B_5-2B_3+B_1)+A_1(B_4-2B_2+B_0)+A_2(4B_3-2B_1-2B_5)+A_3(4B_2-2B_0-2B_4)+A_4(B_1-2B_3+B_5)+A_5(B_0-2B_2+B_4)]$$

$A_n = A_n(\zeta_a R)$ $\qquad$ $B_n = B_n(\zeta_a R)$

$\zeta_a = \frac{Z_a}{n}$, n = principal quantum number

R = internuclear distance

APPENDIX B

DIFFUSION GRADIENTS AND EFFECTS ON EXPERIMENTAL RESULTS

A calculation was made in order to show the approximate variation between the measured and actual benzhydrol concentration in the region of the photolysis cell where photoreduction was taking place. A diagram of this hypothetical situation is shown in Figure 1. It is assumed that the average benzhydrol concentration, within the region where the reaction occurs, is constant. It is also assumed that the concentration gradient within the cell is constant.

The average benzhydrol concentration measured is that concentration which is obtained from analysis of unreacted benzophenone and, therefore, will be the total average benzhydrol concentration in the cell. Ninety-eight percent or essentially complete light absorption occurs within a 1.85 mm. penetration layer of the cell if the benzophenone concentration is 0.08 molar. The distance is 1.33 mm. if the benzophenone concentration is 0.10 molar. Throughout irradiation the benzophenone concentration varies between the limits given above.

Assuming that the diffusion gradient within the solution remains constant, the equation describing the rate of change of benzhydrol concentration $[BH_2]$ with respect to time is given by the Fick equation (63).

$$\frac{\partial[BH_2]}{\partial t} = -AD\frac{\partial[BH_2]}{\partial x} \qquad (1')$$

A is the cross section area of the incident light beam, and D is the diffusion constant determined by Stoke's equation (64)

$$D = \frac{kT^\circ}{6\pi\eta r} \qquad (2')$$

The value of D calculated for benzhydrol in benzene at $T^\circ = 300^\circ K.$ is 0.975×10^{-4} $cm^2/sec.$ The molecular radius (r) for benzhydrol was taken to be 4 Å, k is Boltzmann's constant, and η is the viscosity of the solvent benzene at $300^\circ K.$

The reaction sequence described on page 85 may be represented by the rate law

$$-\frac{d[BH_2]}{dt} = \frac{k_{is}\, k_r\, I_a\, [BH_2]}{[k_{is} + k_{sq}[Q]]\,[k_d + k_q[Q] + k_r[BH_2]]} \qquad (73)$$

For small conversions between mixing intervals, the right side of equation 77 may be represented approximately as a constant by the expression

$$I_a K \cong \frac{I_a}{\left(1 + \frac{k_{sq}}{k_{is}}[Q]\right)\left(1 + \frac{k_d + k_q[Q]}{k_r[BH_2]_o}\right)} \qquad (3')$$

The activity factor K is made up of two quantities. The first is the efficiency factor (e) for the formation of triplet states (see page 86), and the second is the reactivity factor for the destruction of triplets given by

$$w = \frac{1}{1 + \frac{k_d + k_q[Q]}{k_r [BH_2]_o}} \qquad (4')$$

The solution of equation 73 is, therefore,

$$[BH_2]_{t, x=0} = [BH_2]_{o, 0} - KI_a t \qquad (5')$$

Since the benzhydrol concentration within the reaction region is considered constant for this analysis, x = 0 is taken at a mean distance 1.0 mm. inside the front surface of the cell. Ninety percent of the photochemical reaction is occurring within this distance of light penetration. Conditions at x = 0 are given by equation 5'.

Solutions of the Fick equation (1') for the boundary conditions of the reaction system are

$$[BH_2]_{x, t} = [BH_2]_{o, 0} - KI_a \left(t - \frac{x}{AD}\right), \quad t > \frac{x}{AD} \qquad (6')$$

$$[BH_2]_{x, t} = [BH_2]_{o, 0}, \quad 0 < t < \frac{x}{AD} \qquad (7')$$

The average benzhydrol concentration measured experimentally will be

$$[BH_2]_{av}\Big|_{measured} = \frac{1}{TL}\int_o^T \left[\int_o^{DAt} [BH_2]_{(x,t)}\,dx + \int_{DAt}^{L} [BH_2]_{o,o}\,dx\right] dt \qquad (8')$$

Integration over the limits yields

$$[BH_2]_{av}\Big|_{measured} = \frac{1}{L}\left[[BH_2]_{o,o}\,L - \frac{1}{6}\,KADT^2 I_a\right] \qquad (9')$$

The average benzhydrol concentration actually encountered within the reaction volume near the front surface of the cell will be given approximately by

$$[BH_2]_{av}\Big|_{actual} = \frac{1}{T}\int_o^T [BH_2]_{o,t}\,dt = [BH_2]_{o,o} - \frac{1}{2}\,KTI_a \qquad (10')$$

The experimentally measured average benzhydrol concentration is related to the actual benzhydrol concentration within the reaction region approximately by the equation

$$[BH_2]_{av}\Big|_{measured} = \frac{6[BH_2]_{o,o}L - KADT^2 I_a}{6[BH_2]_{o,o}L - 3LKTI_a}\,[BH_2]_{av}\Big|_{actual} \qquad (11')$$

where L is the length of the cell, T is time interval between mixing, and where all other terms have been previously defined.

The diffusion effect is calculated for several different experimental conditions. The results of these calculations are given in Table 1. The results are plotted in Figure 2. The calculations demonstrate two effects. The first is that encountered when actinometric runs are made in parallel with quenching experiments. The second occurs when the intensity has been accurately evaluated prior to quencher runs,and quenching experiments are then carried out without sufficient mixing.

When actinometer and quencher samples are run simultaneously, two situations may arise. The first includes cases where the efficiency factors (e) of both sample and actinometer are the same, such as with most triplet energy transfer processes where singlet quenching is not significant. When both actinometer and sample are irradiated over the same time intervals, the reactivity factors may differ due to quenching by an added acceptor in the sample solution. The overall result is that the activity factor $\underline{K}$ will be smaller in the sample containing quencher than in the actinometer.

The second situation encompasses experiments where, in addition to different reactivity factors, dissimilar efficiency factors are also involved in actinometer and test solutions. This may arise when singlet quenching is possible, as is the case with dibenzoylmethide chelates of iron and chromium. Here, as in the former situation, the

activity factor (K) for the sample containing quencher will be less than that for the actinometer. However, in the present case the effect is larger than in the first, due to larger contributions to K from the efficiency factor (e) than from the reactivity factor (w).

If the solutions are not mixed frequently enough, the actual benzhydrol concentration in the reactive region is less than that measured. This effect is most pronounced for the actinometer sample where the reaction rate is largest. The value of $1/\varphi'$ calculated for the actinometer sample by equation 15 will be underestimated. By using the intensity value corresponding to $1/\varphi'$ which is calculated in this manner, the quantum yield for the destruction of benzophenone in the sample containing quencher will be overestimated. Since the reaction rate in the sample containing the quencher is less than or equal to that of the actinometer, the prescribed kinetic treatment will give an apparent k_q/k_r value which is less than the actual value. If measurable quenching occurs, the actual average benzhydrol concentration in the quencher sample is more closely approximated by the measured average benzhydrol concentration than in the actinometer sample.

If efficiency factors are identical but reactivity factors differ, when a less efficient quencher is used the limiting slope corresponding to $k_d/k_r + k_q(Q)/k_r$ (from the plot of $1/\varphi'$ against $1/(BH_2)$) will approach the value of 0.033 which corresponds to k_d/k_r. When the

efficiency factor and reactivity factor are smaller for the sample containing quencher than in the actinometer, the contribution to the slope which corresponds to $k_d/k_r + k_q(Q)/k_r$ can take values less than 0.033.

It is estimated that the effects described above are reduced to insignificance when mixing frequency less than 1000 secs. is used. However, when mixing intervals exceed 1000 secs., the effect becomes significant and should be considered.

The mixing effects were demonstrated by experiments using ferric acetylacetonate as quencher where mixing was conducted at 600 and 4000 second intervals. The results are plotted in Figure 3. A value of 380 was found for k_q/k_r during the 4000 second mixing cycle as compared to 540 for the 600 second interval.

In the experiments with $Fe(DBM)_3$ and $Cr(DBM)_3$ as quenchers, the efficiency factors for the formation of triplets were less than unity when compared to those for the actinometric samples. Ordinate intercept values are the same regardless of what mixing frequency is used. Apparent values for $k_d/k_r + k_q(Q)/k_r$ determined for different quencher concentrations and shown in Figures XX and XXI may be less than the k_d/k_r value of 0.033 determined in the absence of quencher. This result is found for experiments with $Fe(DBM)_3$ and $Cr(DBM)_3$ in which the mixing frequency was varied between 2000 and 4000 seconds. The value for k_d/k_r calculated by equations 11' and 71 , for a 2000

second mixing cycle and with an efficiency factor of 2.0, is about 0.020. A value of 0.017 was found experimentally. A decrease in slopes was expected and found as the frequency of mixing was decreased.

With the exception of two experiments using $Cr(DBM)_3$ as quencher, all dibenzoylmethide chelate experiments were irradiated using 2000 to 4000 second mixing intervals. A value of 525 was obtained for the k_q/k_r ratio for two particular $Cr(DBM)_3$ samples where mixing was conducted every 500 to 600 seconds. This value approximates that expected for a diffusion-controlled quenching rate. The ordinate intercept from the above plot fits the linear relationship of intercept with quencher concentration for the particular quencher concentration used for these experiments. Experiments using $Cr(DBM)_3$ had efficiency factors closer to that of benzophenone and benzhydrol with no quencher than corresponding experiments using $Fe(DBM)_3$.

Extended mixing periods of 2000 to 4000 seconds gave values of $k_d/k_r + k_q(Q)/k_r$ for the chromium chelates which approached the value of 0.033 which corresponds to k_d/k_r.

When lamp intensity is accurately known from independent measurements, values for k_q/k_r are overestimated if there is insufficient mixing during runs with quenching samples. Early experiments using cells of the type I described on page 19 demonstrated this effect. Insufficient mixing for $Fe(DBM)_3$ experiments gave values

for k_q/k_r approximately equal to 250 as compared to values of 100 where there was sufficient mixing and when the reaction was run in cells of type III. (See Fig. 4 .)

Mixing intervals of 500 to 600 seconds were used for all quenching experiments, with the exception of those with the dibenzoylmethide chelates and with other specific selected $Fe(AA)_3$ samples.

Table 1

Effect of Mixing on Measured Quantum Yields

No.	$[BH_2]_{o,o}$ moles/liter	t sec.	f	$\frac{1}{\Phi}$	$\frac{1}{[BH_2]_{Act}}$	$\frac{1}{[BH_2]_{Mea}}$
1[a]	0.1	10^3	1.08	1.330	10	9.26
2[a]	0.1	$2x10^3$	1.17	1.330	10	8.55
3[b]	0.1	$1x10^3$	1.026	1.330	10	9.75
4[b]	0.1	$2x10^3$	1.035	1.330	10	9.65
5[a]	0.08	$1x10^3$	1.11	1.413	12.5	11.27
6[a]	0.08	$2x10^3$	1.224	1.413	12.5	10.21
7[b]	0.08	$1x10^3$	1.032	1.413	12.5	12.11
8[b]	0.08	$2x10^3$	1.061	1.413	12.5	11.79
9[a]	0.06	$1x10^3$	1.148	1.550	16.66	14.50
10[a]	0.06	$2x10^3$	1.323	1.550	16.66	12.59
11[b]	0.06	$1x10^3$	1.043	1.550	16.66	15.98
12[b]	0.06	$2x10^3$	1.082	1.550	16.66	15.40

a = efficiency factor e = 1 (triplet quenching only)

b = efficiency factor e = 0.327 (DBM chelates)

$I_a = 10^{16}$ quanta/sec.

$D = 0.975 \times 10^{-4}$ cm^2/sec.

$A = 1$ cm^2

$L = 1.3$ cm

$$f = \frac{6[BH_2]_{o,o}}{6[BH_2]_o} \frac{L - KADT^2 I_a}{L - 3LKT I_a}$$

Figure 1

Hypothetical Diffusion Gradient in Reaction Cells

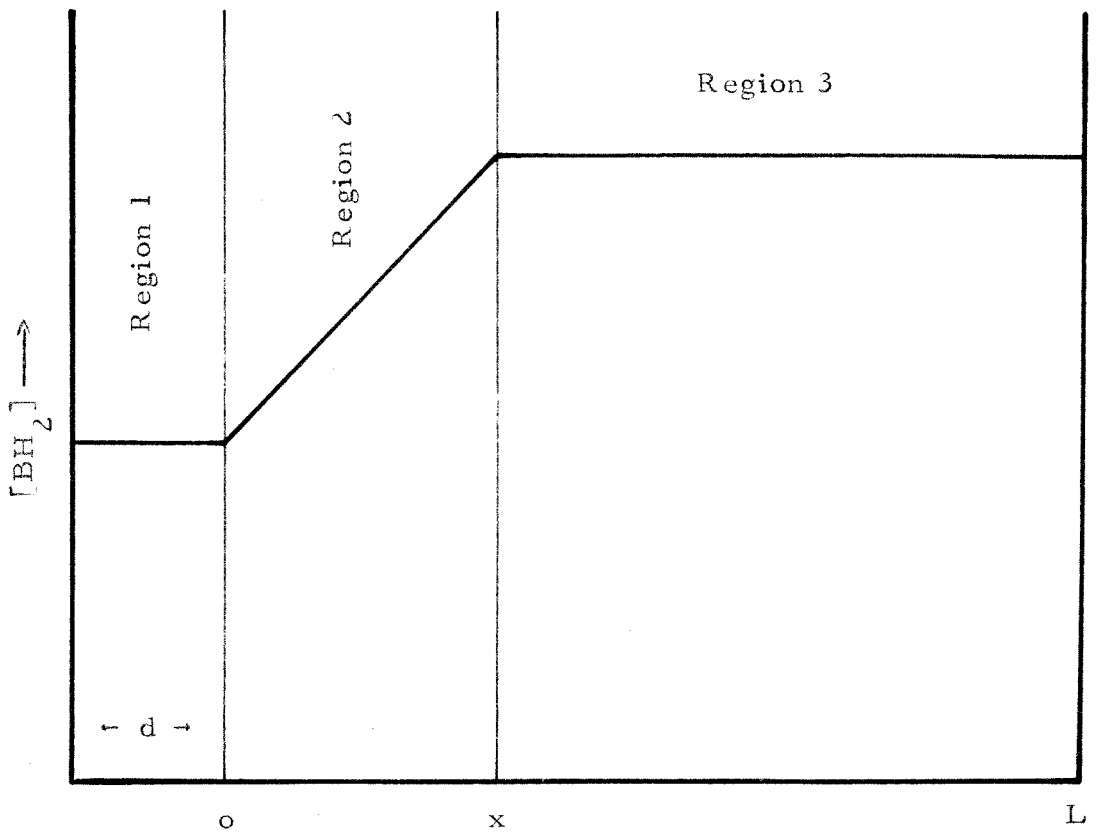

Region 1. Region in which reaction takes place of thickness d. $[BH_2]$ assumed constant throughout this region at any time t - $[BH_2]_t = [BH_2]_{o,t} - KI_a t$

Region 2. $[BH_2]_{x,t} = [BH_2]_{o,o} - KI_a \left(t - \frac{x}{AD}\right)$

Region 3. $[BH_2]_{x,t} = [BH_2]_{o,o}$

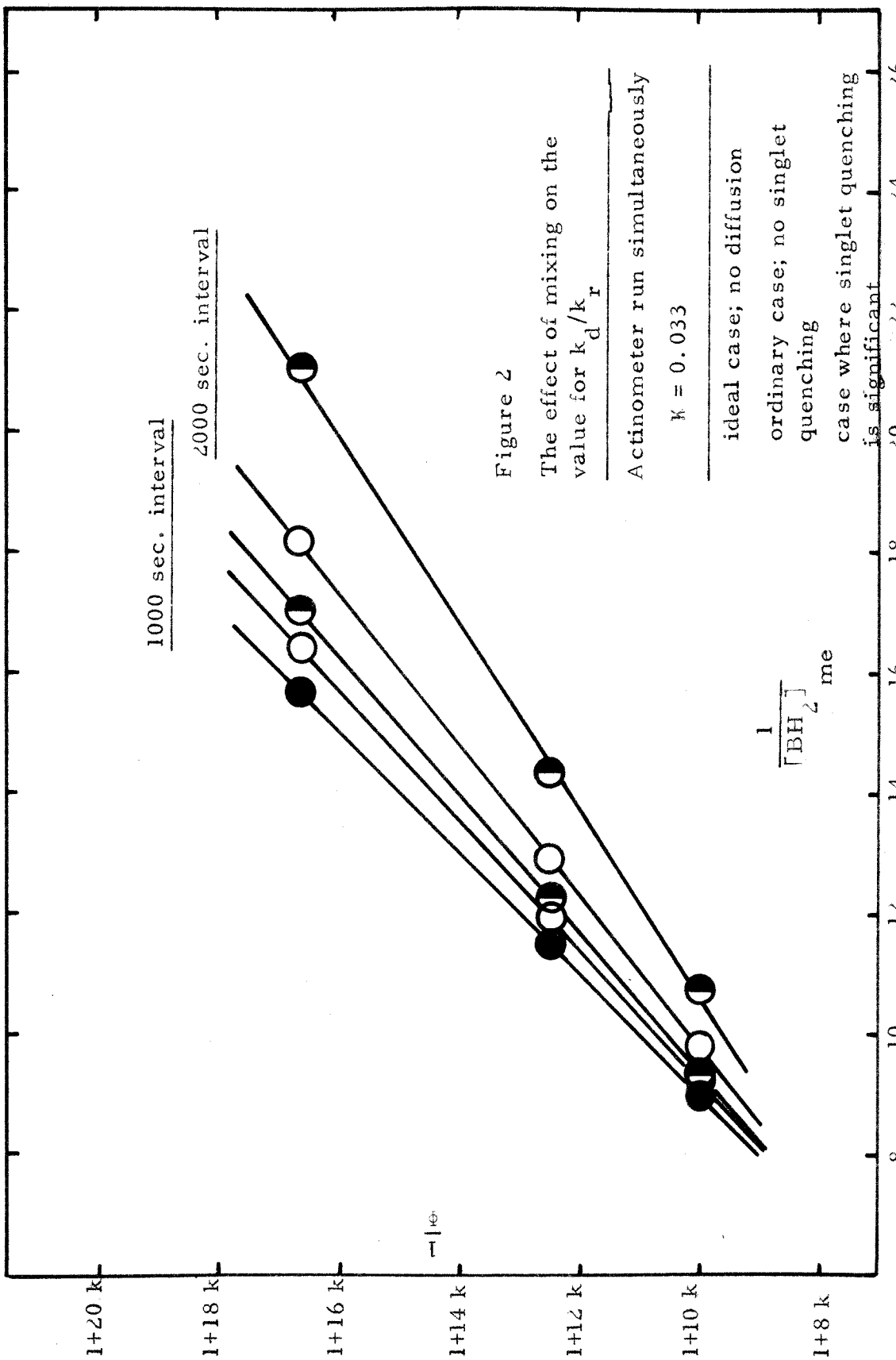

Figure 2

The effect of mixing on the value for k_d/k_r

Actinometer run simultaneously

$K = 0.033$

ideal case; no diffusion

ordinary case; no singlet quenching

case where singlet quenching is significant

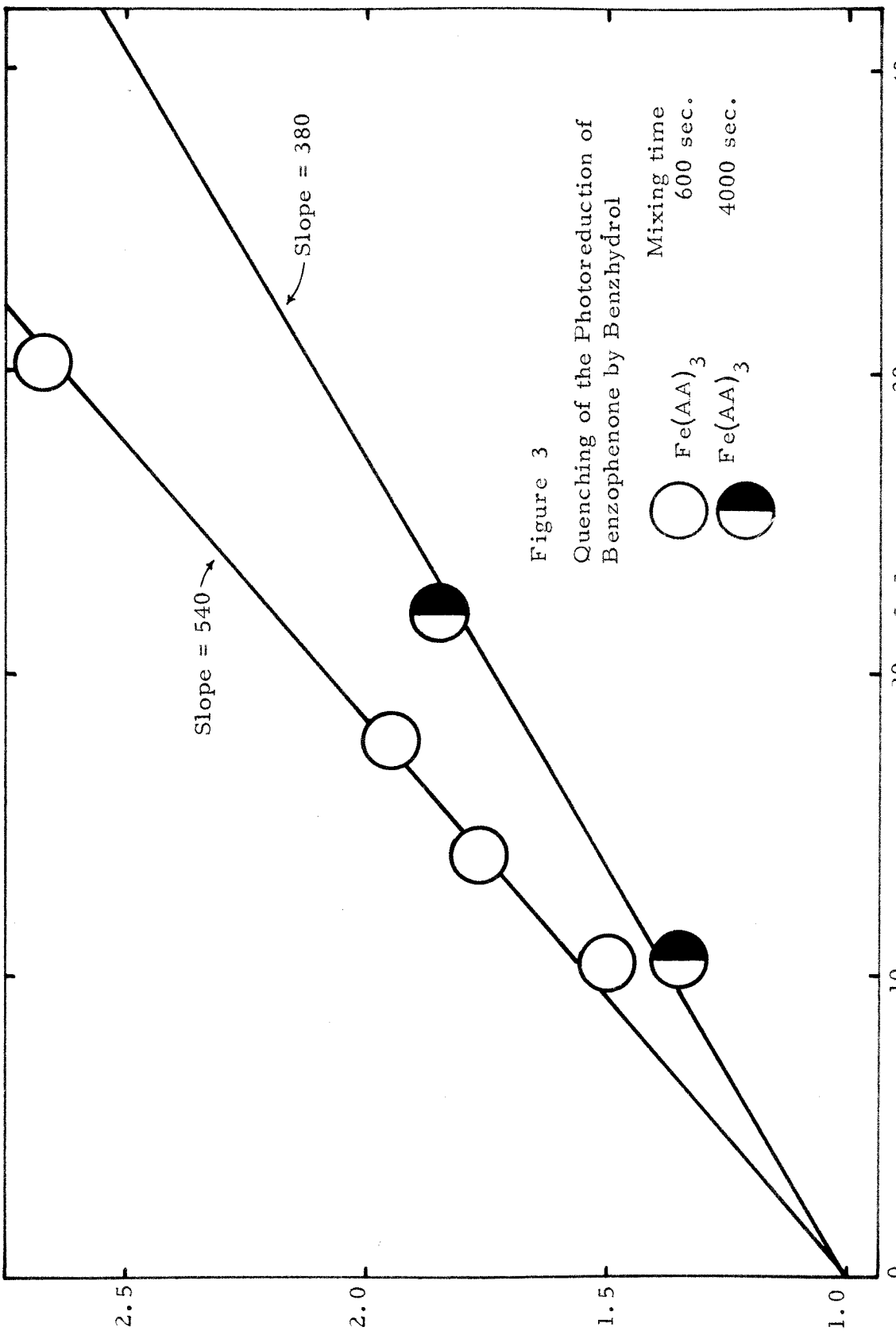

Figure 3

Quenching of the Photoreduction of Benzophenone by Benzhydrol

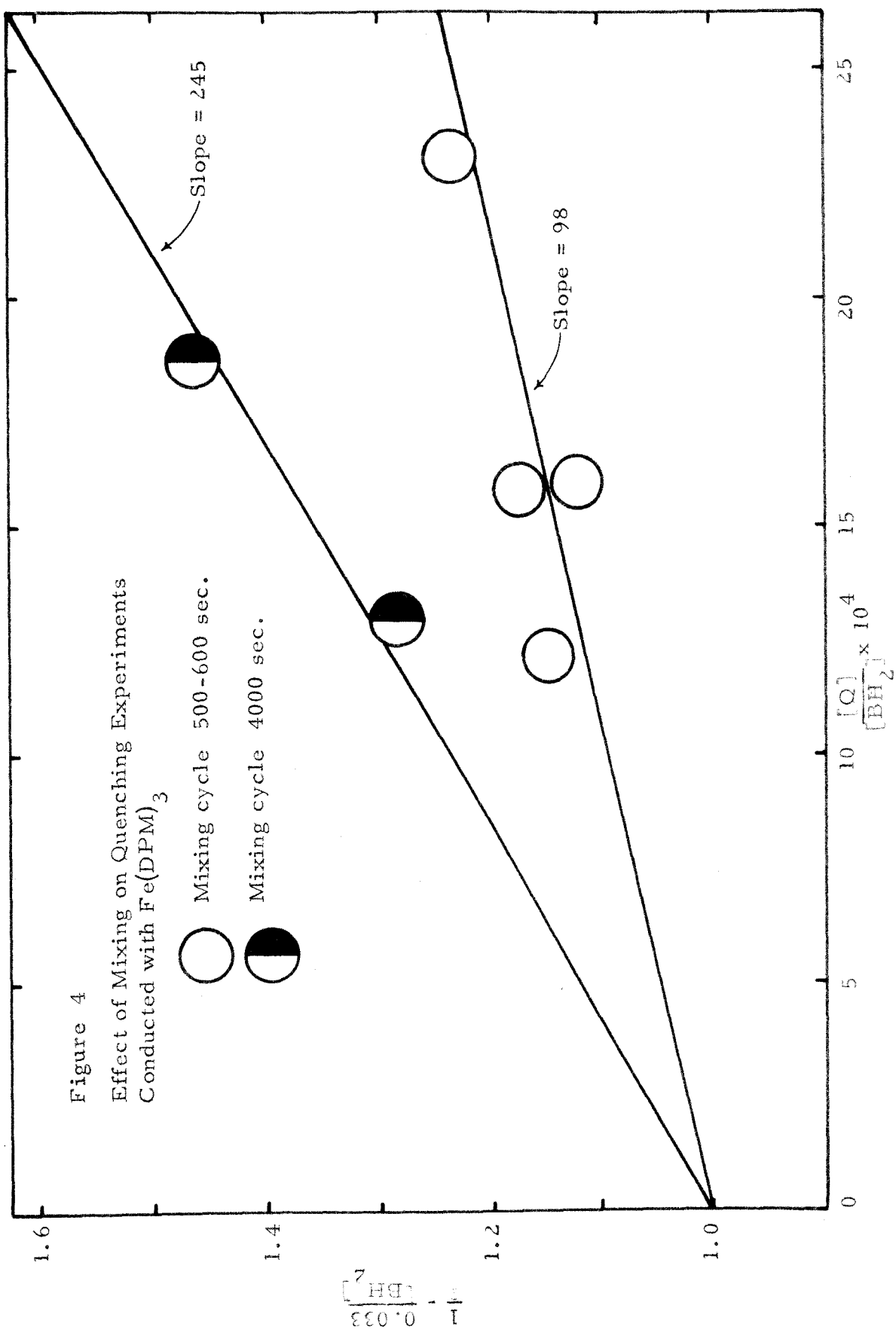

Figure 4

Effect of Mixing on Quenching Experiments Conducted with $Fe(DPM)_3$

REFERENCES

1. T. Förster, Naturwiss., 33, 166 (1946).
2. T. Förster, Disc. Faraday Soc., 27, 7 (1959).
3. A. Terenin and V. Ermolaev, Trans. Faraday Soc., 52, 1049 (1956).
4. H. L. J. Bäckstrom and K. Sandros, Acta Chem. Scand., 12, 8 (1958).
5. H. L. J. Bäckstrom and K. Sandros, Acta Chem. Scand., 14, 48 (1960).
6. K. Sandros and H. L. J. Bäckstrom, Acta Chem. Scand., 16, 958 (1962).
7. G. Porter and M. P. Wright, J. Chem. Phys., 55, 705 (1958).
8. G. Porter and F. Wilkinson, Proc. Roy. Soc. A., 264, 1-18 (1961).
9. G. S. Hammond and P. A. Leermakers, J. Phys. Chem., 66, 1148 (1962).
10. G. S. Hammond and W. M. Moore, J. Am. Chem. Soc., 81, 6334 (1960).
11. W. M. Moore, G. S. Hammond, and R. P. Foss, J. Am. Chem. Soc., 83, 2789 (1961).
12. W. M. Moore and M. Ketchum, J. Am. Chem. Soc., 84, 1368 (1962).

13. T. Walsh, private communication and unpublished observations.

14. J. Saltiel, private communication and unpublished observations.

15. G. S. Hammond, N. J. Turro, and P. A. Leermakers, J. Phys. Chem., 66, 1144 (1962).

16. H. L. J. Bäckstrom, A. Steneryr, and P. Perlman, Acta Chem. Scand., 12, 8 (1958).

17. G. Porter and M. P. Wright, Disc. Faraday Soc., 27, 18 (1959).

18. H. Linschitz and K. Sarkanen, J. Am. Chem. Soc., 80, 4826 (1958).

19. H. Linschitz and L. Pekkarienen, J. Am. Chem. Soc., 82, 2411 (1960).

20. W. M. Moore, G. S. Hammond, and R. P. Foss, J. Chem. Phys., 32, 1594 (1960).

21. H. M. McConnell, J. Chem. Phys., 20, 1043 (1952); 23, 2440 (1955).

22. G. S. Hammond, W. P. Baker, and W. M. Moore, J. Am. Chem. Soc., 83, 2795 (1961).

23. J. H. Van Vleck, Theory of Electric and Magnetic Susceptibilities, The Clarendon Press, Oxford, 1932.

24. G. A. Crosby, R. E. Whan, and R. M. Alire, J. Chem. Phys., 34, 743 (1961).

25. H. Linschitz and C. Steel, J. Phys. Chem., 66, 2577 (1962).

26. C. Hausen and J. Adams, J. Am. Chem. Soc., 66, 347 (1944).

27. K. Kopecky, Postdoctoral Fellow, California Institute of Technology.

28a. Chin-Hua Wu, Research Associate, California Institute of Technology.

28b. G. S. Hammond, D. C. Nonhebel, and C.-H. S. Wu, Inorg. Chem., 2, 73 (1963).

29. J. N. Pitts, R. L. Letsinger, R. P. Taylor, J. M. Patterson, G. Recktenwald, and R. B. Martin, J. Am. Chem. Soc., 81, 1068 (1959).

30. E. H. Gilmore, G. E. Gibson, and D. S. McClure, J. Chem. Phys., 20, 829 (1952).

31. Ibid., 23, 1772 (1955).

32. W. Herkstroetter, private communication and unpublished observations.

33. W. C. Leighton and G. S. Forbes, J. Am. Chem. Soc., 52, 3139 (1930).

34. G. S. Hammond and P. A. Leermakers, J. Am. Chem. Soc., 84, 207 (1962).

35. T. Förster, Fluoreszenz Organischer Verbindungen Göttingen, Vanderhoeck and Ruprecht, 1951.

36. W. M. Moore, Ph. D. Thesis, Iowa State University (1959).

37. M. Born and J. R. Oppenheimer, Ann. Physik, 84, 457 (1927).

38. C. C. J. Roothaan, Revs. Modern Physics, 23, 69 (1951).

39. R. Daudel, R. Lefebvre, and C. Moser, Quantum Chemistry, Interscience Publishers, Inc., New York, 1959.

40. J. C. Slater, Phys. Rev., 36, 57 (1930).

41. J. Belluque and R. Daudel, Rev. Sci., 84, 541 (1946).

42. W. Gordy and W. Thomas, J. Chem. Phys., 24, 439 (1956).

43. E. S. Gould, Inorganic Reactions and Structure, Henry Holt and Co., New York, 1955, p. 139.

44. R. S. Mulliken, J. Chem. Phys., 46, 497 (1944).

45. C. C. J. Roothaan, J. Chem. Phys., 19, 1445 (1951).

46. N. Rosen, Phys. Rev., 38, 255 (1931).

47. M. Kotani, A. Amemiya, and T. Simose, Proc. Phys. Math. Soc. Japan, 20, 1 (1938); 22, 1 (1940).

48. R. S. Mulliken, C. A. Rieke, D. Orloff, and H. Orloff, J. Chem. Phys., 17, 1248 (1949).

49. R. B. Roof, Acta Cryst., 9, 781 (1956).

50. Compiled by H. J. M. Bowen et al., Tables of Interatomic Distances and Configuration in Molecules and Ions, The Chemical Society, Burlington House, London, 1958.

51. L. Cambi and L. Szego, Ber., 64, 2591 (1931).

52. C. H. Johnson, Trans. Faraday Soc., 28, 845 (1932).

53. D. Hume and H. Stone, J. Am. Chem. Soc., 63, 1200 (1941).

54. R. H. Holm and F. A. Cotton, J. Am. Chem. Soc., 80, 5658 (1958).

55. H. Hartmann, J. Inorg. Nucl. Chem., 8, 430 (1958).

56. J. P. Fackler and F. A. Cotton, J. Am. Chem. Soc., 82, 5005 (1960).

57. F. A. Cotton and R. Holm, J. Am. Chem. Soc., 82, 2979 (1960).

58. F. A. Cotton and J. P. Fackler, J. Am. Chem. Soc., 83, 2818 (1961).

59. G. W. Robinson and R. P. Frosch, J. Chem. Phys., 38, 1187 (1963).

60. G. W. Robinson and R. P. Frosch, J. Chem. Phys., 37, 1962 (1962).

61. L. Pauling and E. B. Wilson, Introduction to Quantum Mechanics, McGraw-Hill, New York, 1935, pp. 95, 275, 294.

62. B. Stevens and E. Hutton, Symposium on Reversible Photochemical Processes, (Preprints of Papers) U. S. Army Research Office, Durham, N. C., page 10 (1962).

63. E. A. Moelwyn Hughes, Physical Chemistry, Pergamon Press, New York, 1957, p. 1167.

64. Ibid., p. 16.

PROPOSITION 1

The photopolymerization and photoreduction of benzaldehyde is considered. The polymerization is felt to result from a singlet state inner complex rearrangement. The ordinary reduction process is felt to proceed through a triplet intermediate. A mechanism for the above processes is proposed. In addition, experiments for testing the mechanism are given. Since most of the background material for this proposition was obtained in these laboratories, the first part of the following discussion will be devoted to it.

The photoreduction of ketones has received much recent attention and its mechanism is well understood. On the other hand, the photoreduction of aromatic aldehydes has not been studied in much detail. This is probably due to the occurrence of interfering side reactions in the aldehyde systems.

Benzophenone and acetophenone undergo clean reductions in the presence of alcohols and other compounds containing labile hydrogen atoms (1, 2, 3, 4). Major products from reactions involving the use of alcohols usually consist of pinacol mixtures which are dependent on the alcohol used. Moore (3) and Baker (4) have studied the photoreduction of benzophenone with several hydrogen donors.

Investigation of product composition was conducted in order to determine if there was any evidence that a "cage" mechanism might be playing a significant role in the combination of radicals produced during the hydrogen abstraction step. No evidence of this nature was found. Statistical distributions of products were obtained which indicated that no cage mechanism was important in radical recombination in these systems.

Photochemical reactions of benzaldehyde have been investigated by several workers (5, 6, 7, 8). Buchi and co-workers studied the photoaddition of benzaldehyde to 2-methyl-2-butene (7). Analysis of the major product, a four-membered cyclic ether, showed that the aldehyde oxygen had become attached to the olefin at the least hindered position. The product obtained from the irradiation of a solution of n-butyraldehyde with the same olefin had the oxygen adjacent to the most hindered olefin carbon atom.

The benzaldehyde result is in accord with a mechanism involving a chemically reactive $n-\pi^*$ excited state of the aldehyde. This excited state is probably a triplet. Benzaldehyde has a triplet state which is 72 kcal/mole above the ground singlet state (9). This excited triplet state is known to be formed in solution because benzaldehyde has been used successfully as a sensitizer for reactions requiring its existence (10). The mechanism for the addition reaction involving the aliphatic aldehyde may be explained by a mechanism proposed by Kharasch (8).

Hydrobenzoin has been identified as a product of the photolysis of benzaldehyde in various alcohols (5, 11). In addition, investigators have reported finding a yellow resin in the product mixture.

Ciamician and Silber isolated some polymer and determined its formula to be $(C_7H_6O)_9$ (11). Later these same authors reported the isolation of a benzaldehyde tetramer and suggested that it was (5)

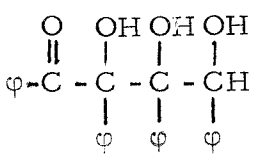

Neither of these articles contained information about the experimental technique used in product analysis. In addition, little experimental data was given regarding the reaction conditions.

An investigation was initiated in our laboratories in order to elucidate the mechanism for the photoreduction and photoaddition reactions of benzaldehyde in solution. Background evidence suggested that a chemically reactive triplet state was probably involved as an intermediate in these reactions. The problem never developed beyond the photoreduction stage, however. Instead, considerable time was spent on the isolation and identification of the polymer side-product.

Product analysis and other subsequent results lead to an interesting mechanism for the reaction. Evidence is obtained that suggests that polymerization proceeds by a singlet mechanism while photoreduction proceeds by a triplet mechanism.

Benzyl alcohol was chosen to serve as the hydrogen donor for the reduction work. This choice of alcohol was made since only one reduction product, hydrobenzoin, would be expected. In addition, disproportionation between ketyl radicals would produce only benzaldehyde and benzyl alcohol. The solvent used was benzene.

Reactions were run in degassed quartz cells, and in an immersion reactor where the solutions were flushed with nitrogen before and during irradiation. When the aldehyde concentration was kept low and the alcohol concentration kept high, the primary reaction product was hydrobenzoin. In addition to this product, a yellow substance was formed. An increase in the amount of yellow product accompanied an increase in the benzaldehyde concentration.

In addition to reactions run with benzyl alcohol, control reactions using only benzaldehyde in benzene were made. The same yellow polymer product was obtained for control reactions as was obtained for samples where benzyl alcohol was present. The product mixture of the control reaction did not contain an isolatable amount of hydrobenzoin.

The melting range for the polymer was very broad. A softening usually started at about 125°, but no sharp fusion point was observed.

Product analysis indicated that the major polymerization product was probably a mixture of the following substances.

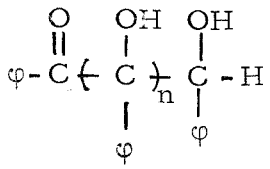

(A)

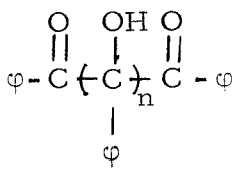

(C)

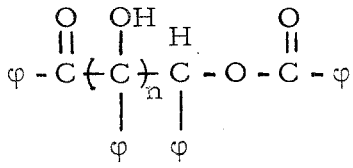

(B)

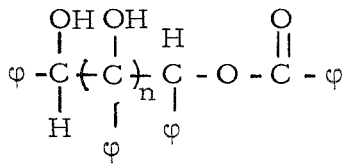

(D)

Identification of the polymer mixture was effected through the following information. Infrared spectra of the polymer indicated the presence of hydrogen bonded OH; two different carbonyls, one corresponding to a keto-group and the other to an ester-group; aromatic CH; and tertiary CH. In addition, aromatic absorption bands corresponding to mono-substituted benzene were observed.

The polymer was found to be relatively stable in acid but the ester linkage was readily hydrolyzed in base. Hydrolysis gave benzoic acid as one of the products. The other hydrolysis product retained the keto-carbonyl absorption band and other bands characteristic of the original polymer.

The molecular weight of the polymer was determined by cryoscopic methods and seemed to vary with the time of irradiation.

Long irradiation periods gave higher molecular weight polymer than was obtained for short irradiation periods. Elemental analysis indicated that the carbon and hydrogen composition of the polymers was very close to that for benzaldehyde.

Several compounds were prepared which were felt to be similar to the polymer molecules. These compounds were hydrobenzoin dibenzoate, hydrobenzoin monobenzoate, benzoin benzoate, benzoin, and hydrobenzoin. The infrared spectra of these compounds were studied in order to identify characteristic absorptions corresponding to groups felt to be contained in the polymer. The spectra of the polymer and the compounds given above are very similar. A mixture of the above compounds gave an infrared spectrum that accounted for every absorption band obtained for the polymer. No absorption band in either spectrum did not have a corresponding band in the other. The shapes of corresponding bands were similar but did show differences in intensities. Some of the intensity differences could be altered by varying the composition of the known compound mixture. However, the comparisons were so good that it was felt that the same groups were present in both mixtures.

The major products given earlier cannot account for the apparent yellow color of the polymer. No evidence for benzil was found. The color is due to a small quantity of phenyl dibenzoylmethane which is probably formed from the trimer of type (A) by the reaction

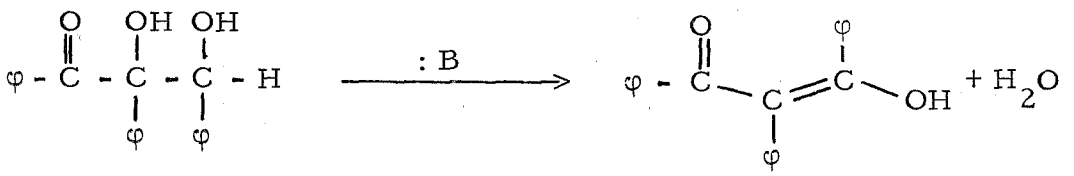

Phenyl-dibenzoylmethane enol is a brilliant red compound when isolated. It is acidic and was isolated from the product mixture by extraction with dilute sodium hydroxide. In addition, it may be separated from remaining polymer by passing the mixture through a basic alumina column. Identification of this compound as one of the reaction products was effected by comparison with a sample prepared by condensation of phenol benzoate with desoxybenzoin in the presence of sodium hydride (13).

It was of interest to see if the production of free benzoyl radicals could induce a non-radiative polymerization in solutions of benzaldehyde. The thermal decomposition of benzoylperoxide in benzaldehyde has been reported to give a quantitative yield of hydrobenzoin dibenzoate and benzoic acid (14). This reaction was repeated and verified. Free benzoyl radicals combine with benzaldehyde molecules to form only

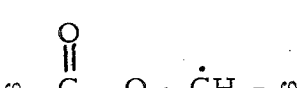

(E)

radicals. These radicals are sufficiently stable that they are unable to abstract hydrogen from another benzaldehyde molecule. Therefore, they can only couple with another similar radical to form the dibenzoate product.

With this information and results from the product analysis, the following mechanism for the photopolymerization of benzaldehyde was proposed.

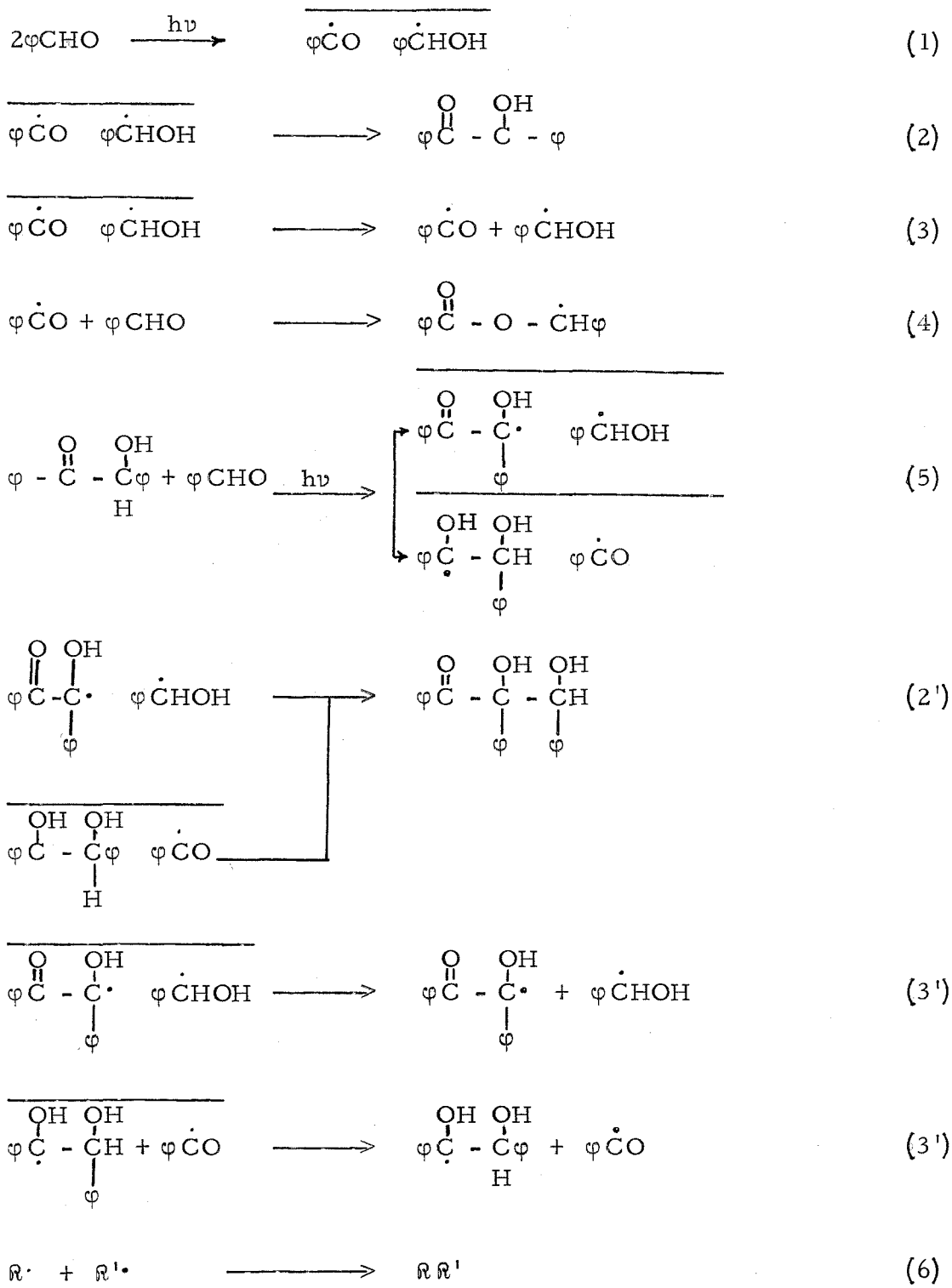
2φCHO hν φ·CO φ·CHOH (1)
φ·CO φ·CHOH → φC(=O) - C(OH) - φ (2)
φ·CO φ·CHOH → φ·CO + φ·CHOH (3)
φ·CO + φCHO → φC(=O) - O - ·CHφ (4)
φ - C(=O) - C(OH)φ + φCHO hν
φC(=O) - C·(OH)φ φ·CHOH
φC(OH) - ·CHφ φ·CO (5)
φC(=O) - C·(OH)φ φ·CHOH
φC(=O) - C(OH) - CH(OH)φ (2')
φC(OH) - C·φ φ·CO
φC(=O) - C·(OH)φ φ·CHOH
φC(=O) - C(OH)φ + φ·CHOH (3')
φC(OH) - ·CHφ + φ·CO
φC(OH) - CHφ + φ·CO (3')
R· + R'· → RR' (6)

The formation of polymer can be explained on the basis of this mechanism. However, it is felt that while being basically correct, the above mechanism is incomplete, since it does not consider the excited states involved.

The mechanism as written implies a formation of a radical pair in a solvent cage. These radicals may combine by reaction 2 or diffuse from the cage. Once outside of the cage, benzoyl radicals will add to benzaldehyde molecules by reaction 4. Polymer chains will be built up by cage recombinations of type 2. Reaction 6 shows the fate of stabilized radicals that are able to diffuse from a cage before recombination and which do not react with benzaldehyde. The mechanism suggests a dependence of the average polymer molecular weight on the time of irradiation and on the intensity of light.

Two questions still remain unanswered. What is the nature of the association between the two radicals in the cage, and why should benzaldehyde be different from benzophenone as far as allowing a cage mechanism for radical combination? The latter question is what provoked the proposal of a singlet mechanism for polymerization. The available experimental evidence seems to support this proposal. Many new experiments will have to be introduced in order to verify it, however.

The primary intermediate in the polymerization of benzaldehyde is felt to be a singlet eximer complex. The eximer may be formed

by either of the two ways given below.

$$A \xrightarrow{h\upsilon} A^* \xrightarrow{B} AB^* \qquad (7)$$

$$A + B \longrightarrow AB \longrightarrow AB^* \qquad (8)$$

The association between the two reacting molecules may occur either before or after the absorption of light. The latter process is favored. The excited complex AB^* then can undergo a simultaneous hydrogen migration and carbon-carbon bond formation similar to an intramolecular rearrangement. Process 7 requires the lifetime of the singlet state of A^* to be long enough to allow for collision with B to occur. Factors limiting the lifetime are fluorescent emission, internal non-radiative decay to ground state, and intersystem crossing to a triplet state. All three of these may be able to complete effectively with the rate of formation of AB^*. The most important competing factor is intersystem crossing. In dilute solutions and possibly in fairly concentrated solutions absorption of light by A will result in formation of a triplet before collision with B.

Process 8 allows the formation of complex AB before excitation. The reacting molecules may be oriented in a position favorable for reaction when the excited singlet state is formed. Complexing prior to light absorption will be favored in solutions rich in benzaldehyde.

In competition with the "rearrangement" within the singlet eximer complex is intersystem crossing to triplet eximer. The singlet eximer can allow simultaneous hydrogen migration and carbon-carbon bond formation resulting in a ground state product molecule. On the other hand, this simultaneous process is forbidden by spin multiplicity in a triplet eximer complex. An excited triplet state product molecule must be formed to conserve spin. In this latter case, hydrogen migration without carbon-carbon formation will result in the production of two radicals which can diffuse into and react with the surrounding environment.

A complete mechanistic diagram is given below.

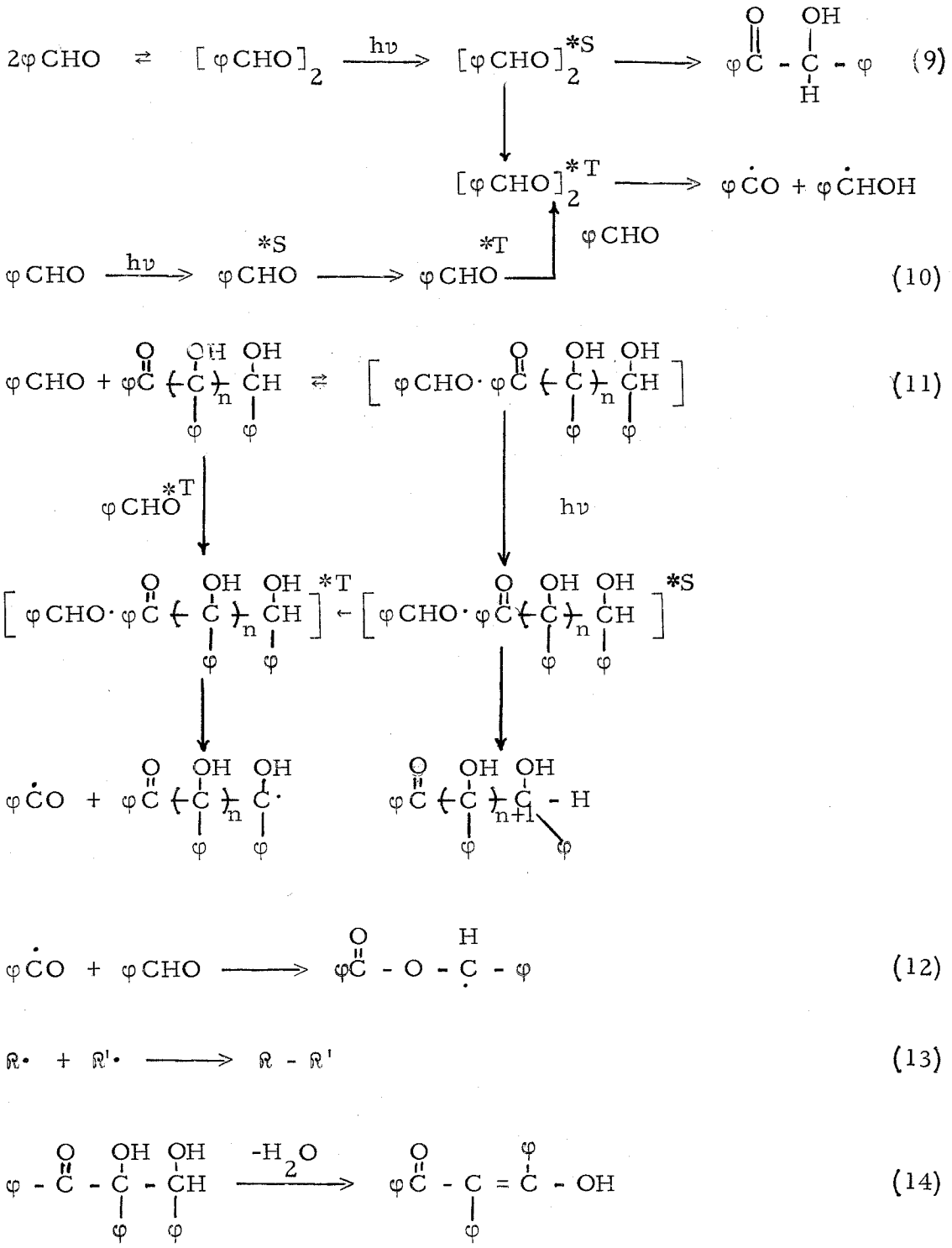

In addition to the reactions given above, there may also be others involving excited states of polymer molecules.

A proposed plan for testing the above mechanism is given below.

(1) The average molecular weight of the polymer should vary with the intensity of the incident light and with the time of irradiation. Using a constant light source, samples may be removed at regular intervals to test for this variation. The results from early experiments are in agreement with the predicted.

(2) Since benzoin is predicted to be the first dimer in the polymerization reaction, the irradiation of a solution containing benzoin and benzaldehyde in benzene should give the same polymer as obtained directly without benzoin added. The product mixture may not be identical, but the composition of the polymer molecules should be the same.

(3) In moderately dilute solutions where complexing between unexcited benzaldehyde is small, the addition of known triplet quenchers should decrease the amount of ester in the product relative to ketone. Also, a study of the effect on quantum yields for polymerization and photoreduction produced by introduction of triplet quenchers to solutions containing benzyl alcohol should be made. The photoreduction of benzaldehyde by the alcohol may be strongly affected by the addition of a triplet quencher while the polymerization will not be altered as drastically. This may have been demonstrated in early experiments,

but not enough data were obtained to make the results conclusive. The formation of phenyldibenzoylmethane during irradiation apparently had little or no effect on the rate of polymerization, even though it should be a good triplet quencher.

(4) The quantum yield for the formation of polymer might be expected to increase with an increase in the aldehyde concentration. At high aldehyde concentrations the relative amount of ester to ketone in the product would be expected to be less than in the product obtained at low benzaldehyde concentrations.

A single experimental result is in accord with the above prediction and was partially responsible for this proposal. When a sample of pure benzaldehyde was irradiated, a high yield of polymer was obtained. The irradiation was continued until the average molecular weight of the polymer was approximately six times the molecular weight of benzaldehyde.

An infrared spectrum of the polymer extracted from the above reaction mixture was made. It showed that the ratio of ester to ketone was less than obtained for a polymer of comparable molecular weight but formed by the irradiation of a more dilute (20% by volume) solution of benzaldehyde in benzene.

(5) A final study may be introduced using aliphatic substituted benzaldehydes. It would be of interest to see how steric hindering groups might effect the polymerization process. If the reaction is going

through an excited eximer as proposed, steric hindering groups might be expected to affect the stability and ease of formation of the aldehyde complex.

References

1. G. Ciamician and P. Silber, Ber., 44, 1280, 1554, 1558 (1911).
2. A. Schönberg and A. Mustafa, Chem. Revs., 46, 181 (1947).
3. W. Moore, G. Hammond and R. Foss, J. Am. Chem. Soc., 83, 2789 (1961).
4. G. Hammond, W. Baker and W. Moore, J. Am. Chem. Soc., 83, 2795 (1961).
5. G. Ciamician and P. Silber, Chemisches Zentralblatz, 80, 1557 (1909); Atti R. Accad. dei Lincei Roma [5], 18, 216 (1908).
6. P. A. Leighton, J. Phys. Chem., 42, 749 (1938).
7. G. Buchi, C. G. Inman and E. S. Lipinsky, J. Am. Chem. Soc., 76, 4327 (1954).
8. M. S. Kharasch, W. H. Urry and B. M. Kuderna, J. Org. Chem., 14, 248 (1949).
9. G. N. Lewis and M. Kasha, J. Am. Chem. Soc., 66, 2100 (1944)
10. G. S. Hammond, P. A. Leermakers and N. J. Turro, J. Am. Chem. Soc., 83, 2395 (1961); 83, 2396 (1961).
11. G. Ciamician and P. Silber, Atti R. Accad. dei Lincei Roma [5], 10, 92, 228-33 (1901).
12. R. E. Lutz and C. K. Dien, J. Org. Chem., 21, 551 (1956).
13. C. R. Hauser, B. I. Ringler, F. W. Swamer and D. F. Thompson, J. Am. Chem. Soc., 69, 2649 (1947).
14. F. R. Rust, F. H. Seubolt and W. E. Vaughan, J. Am. Chem. Soc., 70, 3258 (1948).

PROPOSITION 2

A new electrochemical technique is proposed for making continuous quantum yield measurements in irradiated solutions of benzophenone.

Recent studies have been made on photopotentials produced in alcoholic solutions of certain organic compounds. Two types of experiments have been performed in studying these potentials. The first involves the production of a photovoltic potential between two metallic electrodes placed in an alcoholic solution of the compound under investigation (1, 2, 3). One of the two electrodes is situated in the incident light beam. The other electrode is shielded from the light. Irradiation of the solution produces a gradual build-up of a potential difference between the two electrodes. When the light is turned off, the potential difference returns to zero.

Many compounds have been studied by this procedure. The results, even though being somewhat inconsistent, did seem to show certain trends. Alcohols were found to be inactive. The magnitude of the potential seemed to follow the same trend as the absorptivity of the compound. Both positive and negative potentials were observed. Positive potentials were generally obtained for compounds that

contained a carbonyl-like cyte of unsaturation. Negative photopotentials were observed for compounds that contained loosely attached electrons such as peroxides and similar substances.

The experimental results are inconclusive and should be repeated. Oxygen was not excluded during irradiation and in many instances intermediate reaction products were produced which established new potentials different from that produced by the original compound. The seat of the EMF was not determined in the above investigations.

It is felt here that light may perform two operations in the above solutions. The first is a photoelectric effect on the metal electrode exposed to the light. The second is the formation of excited state solute molecules.

The work function of the metal may be reduced sufficiently by the incident radiation that the electrode can become very sensitive to the electron affinity of molecules in the vicinity of the electrode. The electron affinity of excited state molecules would be expected to be considerably different from ground state molecules. In particular, excited ketones may exhibit considerable attraction for electrons if the lowest excited state is an $n-\pi^*$ state. This is reasonable since many ketones are able to abstract hydrogen atoms from alcohols. An electron attraction is evidence in ketone systems by the production of positive potentials.

A compound incapable of photoreducing may still have a significant affinity for electrons in its excited state. Therefore, one would expect the production of photopotentials by the above mechanism even though no radicals of the alcoholic oxidation type would be formed. This prediction is in accord with the observed results.

The second type of photopotential studies have involved the voltage produced between a platinum electrode immersed in an alcoholic solution containing an organic solute and a calomel reference electrode (4, 5). The reference electrode is connected to the reaction chamber by a salt bridge. Only the reaction chamber containing the platinum electrode is exposed to light.

Detailed investigations into the most probable processes responsible for the production of these potentials have been undertaken by certain researchers (4, 5). A mechanism for the photopotential produced in a solution containing anthraquinone has been proposed by Surash and Hercules (4). The mechanism was felt to be general and applied to other substances which gave photopotentials of the type described here.

The mechanism they proposed suggested that an anthraquinone molecule absorbed light and eventually formed a chemically active triplet state. The excited anthraquinone can then abstract a hydrogen atom from a solvent molecule. After sufficient time has elapsed,

a steady state radical and anthraquinone concentration was reached in the vicinity of the platinum electrode. The half cell potential for the reduction of the radical to anthraquinone is measured with reference to the normal calomel electrode.

If the above mechanism for the production of the potential difference is correct, then only substances capable of abstracting hydrogen from the alcohol solvent molecules should give this type of photopotential.

Pitts and co-workers investigated the process for several compounds that were known to photoreduce in alcohol (5). In addition, they tried other substances that were known not to undergo reduction in alcohol. They found that only the former compounds were able to give potentials, while the latter were inactive.

In both types of potential studies described above it was commonly observed that after the radiating source was turned off, the potential difference returned to zero. This is in accord with the notion that active radicals or other short-lived intermediates produced during the irradiation are responsible for the production of a photopotential.

In these laboratories, a frustration in measuring quantum yields for quenching experiments led to attempts in finding a new method for making these measurements. Among the various probing experiments made was one which involved the irradiation of a solution

of benzophenone and acetonitrile in an electro-conductivity cell. The cell was attached to a tube with a reservoir suitable for freezing and degassing the sample. Both electrodes were situated so that they were parallel to and within the light beam. The solution used for the experiment consisted of 0.02 molar benzophenone in freshly distilled, spectral-quality acetonitrile. The solution was placed in the photolysis cell and degassed using a freeze-thaw cycle. Filtered light was used for the irradiation. The filter system that was used allowed only the 3660 Å line of the mercury light source to be passed onto the cell.

Several different circuits were tried with the cell. The one showing the most interesting effect is described below. A Varian recording VTVM with a 100 mv. scan limit was connected across the terminals of the cell. A variable D.C. potential source was also attached between the terminals. A switch was provided so that the external potential source could be disconnected at any time.

No effect was observed when the cell was exposed to light before a potential had been impressed between the electrodes. However, an interesting change was observed when the electrodes had been charged prior to exposure to the light.

The cell was charged by impressing a potential between the electrodes. When the external circuit was disconnected, the cell retained the potential to which it had been charged. The potential difference between the electrodes did not decrease even after sitting

for several minutes. However, the introduction of an external circuit with variable resistance allowed an approximate exponential decay of the charge.

With only the VTVM connected to the cell and with a constant potential established between the electrodes, the solution was irradiated. A linear increase in the potential difference was observed. When the light source was removed, the cell potential again became constant; it did not drop toward its original value. Irradiation of the solution for additional time intervals continued to give linear increases in the cell potential. Removal of the light source after each interval allowed the potential to again become stationary. At no time was a decrease in potential observed unless an external decay circuit was provided.

It was of interest to see what effect changes in the light intensity had on the rate of increase of the cell potential. These initial experiments showed that the rate of increase was apparently linear with the intensity of the light source as measured by a thermopile coupled with a potentiometer.

By shorting the two electrodes with a piece of copper wire, most of the charge difference between the electrodes could be removed; however, this process took a long period of time. The bias on the electrodes could only be removed completely by washing with nitric acid.

It is felt that the processes responsible for the photo-induced

potential change in this system are not due to either a photovoltic or a photopotential effect of the types described earlier. It is proposed that the phenomenon observed here results from changes in electrode potentials produced by changes in the concentration of one or more of the original molecular species present in the solution during irradiation.

A potential impressed between the two electrodes prior to irradiation can cause the following electrode reactions to occur:

At the cathode: $$\varphi_2CO + H^+ + e \rightarrow \tfrac{1}{2}\varphi_2\text{-}\overset{OH}{\overset{|}{C}} - \overset{OH}{\overset{|}{C}}\varphi_2 \qquad (1)$$

At the anode: $$CH_3CN \rightarrow \tfrac{1}{2}NC\text{-}(CH_2)_2\text{-}CN + H^+ + e \qquad (2)$$

The products of the electrolysis may be plated onto the rough surfaces of the platinized electrodes.

Combining the electrode reactions 1 and 2, one obtains

$$2\varphi_2CO + 2CH_3CN \rightleftarrows \underline{\varphi_2\overset{OH}{\overset{|}{C}} - \overset{OH}{\overset{|}{C}}\varphi_2} + \underline{NC\text{-}(CH_2)_2\text{-}CN} \qquad (3)$$

where the underlined terms refer to substances that may be deposited on the electrode surfaces. The EMF of the above cell will be given by

$$\mathcal{E} = \mathcal{E}^\circ - \frac{RT}{\mathcal{F}} \ln \frac{[P]^{\frac{1}{2}}\,[SN]^{\frac{1}{2}}}{[\varphi_2CO]\,[CH_3CN]} \qquad (4)$$

where [P] is the activity of deposited benzpinacol, [SN] is the activity of deposited succinonitrile, and [φ_2CO] and [CH_3CN] correspond to the activities of solute benzophenone and solvent acetonitrile. $\mathcal{E}^\circ$ is the cell potential at unit activity and $\mathcal{F}$ is the Faraday constant.

As seen from equation 4, a decrease in benzophenone concentration will cause the cell potential to become more negative. After significant deposition of electrolysis product on the electrodes, the activities of these compounds should remain constant during small changes in the benzophenone concentration. The concentration of acetonitrile solvent will remain effectively constant throughout all other concentration changes within the cell. If the $\mathcal{E}^\circ$ of the cell is small or negative, a decrease in benzophenone concentration will produce an increase in the potential difference between electrodes.

Inspection of free energy tables and tables reporting heats of combustion shows that the changes in free energy and in heat content at unit activity for reaction 3 are nearly zero. Therefore, since $\Delta F \simeq 0$, then $\mathcal{E}^\circ \simeq 0$. The reaction described by equation 3 therefore probably has an equilibrium constant near unity. A high activation energy barrier between reactants and products prevents equilibrium from being established under normal non-radiative conditions.

Upon radiation the following sequence of reactions probably occurs:

$$\varphi_2CO \xrightarrow{h\upsilon} \varphi_2CO^{*S} \longrightarrow \varphi_2CO^{*T} \quad (5)$$

$$\varphi_2CO^{*T} + CH_3CN \longrightarrow \varphi_2\dot{C}OH + \dot{C}H_2CN \quad (6)$$

$$\varphi_2CO^{*T} \longrightarrow \varphi_2CO + E \quad (7)$$

$$2\varphi_2COH \longrightarrow \varphi_2\overset{OH}{\overset{|}{C}}-\overset{OH}{\overset{|}{C}}\varphi_2 \quad (8)$$

$$2CH_2CN \longrightarrow NC(CH_2)_2CN \quad (9)$$

$$\varphi_2\dot{C}OH + \dot{C}H_2CN \longrightarrow \varphi_2\overset{OH}{\overset{|}{C}} - CH_2CN \quad (10)$$

$$\mathfrak{R}'H\cdot + \mathfrak{R}\cdot \longrightarrow \mathfrak{R}' + \mathfrak{R}H \quad (11)$$

Equation 11 describes general disproportionation of radical products.

The overall reaction process given above is essentially the same as 3, but the products formed are not deposited on the electrodes. The concentrations of the plated substances are not significantly affected by the production of the photolysis products. The significant change in the electrolytic cell results from the decrease in the benzophenone concentration.

Equation 4 may be rewritten as

$$\mathcal{E} = K + \frac{RT}{\mathcal{F}} \ln [\varphi_2CO] \quad (12)$$

where K includes all constant terms in 4 in addition to the value for $\mathcal{E}^\circ$. For small irradiation intervals where the change in benzophenone concentration is not large, the change in cell potential can be given by

$$\Delta \mathcal{E} = - \frac{RT}{\mathcal{F}} \frac{\Delta [\varphi_2 CO]}{[\varphi_2 CO]_i} , \qquad (13)$$

where $[\varphi_2 CO]_i$ is the initial ketone concentration and $\Delta [\varphi_2 CO]$ is the change in concentration.

Since $\mathcal{E}_i$ is negative for the concentrations used in this experiment, a linear decrease in benzophenone concentration produces a linear increase in cell EMF. The rate of reduction of benzophenone is linear with the light intensity, therefore the change in EMF should vary as the intensity for small ketone conversions.

The effects described above are in agreement with experiment. The above treatment applies to the case where both electrolysis products are deposited on the electrodes. A similar treatment yielding the same conclusions can be applied to the situation where only one product is deposited on an electrode.

The process described suggests several interesting and useful experiments. The first and most important, however, must involve the proof of the reactions occurring within the system. A large-scale electrolysis should be run and the products deposited on the electrodes analyzed. Different solvents and solutes, both oxidizing and reducing, should be tried. Included in this phase of study would be reactions using selected solvent mixtures. One of the two solvents could be chosen so that it would be both electrolytically and photochemically

inert while the other is reactive. Next, the effect of quenchers on the rate of change in cell EMF should be investigated.

This reaction system or one similar to it may provide a way of easily following quenching reactions. A great advantage with this method is that it would allow quantum yield measurements to be made very quickly and easily. The above process is sensitive to less than 1% conversion of benzophenone.

References

1. I. Levin and C. E. White, J. Chem. Phys., 18, 417 (1950).

2. Ibid., 19, 1079 (1951).

3. Ibid., 21, 1654 (1953).

4. J. Surash and D. M. Hercules, J. Phys. Chem., 66, 1602 (1962).

5. J. N. Pitts, H. W. Johnson, and T. Kuwana, J. Phys. Chem., 66, 2456 (1962).

PROPOSITION 3

A slightly modified mechanism to the photo-oxidation and photo-reduction reactions of zinc tetraphenylchlorin and corresponding porphin is proposed. The mechanism is felt to be applicable to a large number of systems other than the two described. The mechanism uses a triplet-triplet reaction step which has significant applications to solution photochemistry in general. An expanded research program to study the mechanism in different systems is also proposed.

The photo-oxidation of zinc tetraphenylchlorin by 1,2-naphthoquinone has been studied in detail (1). The quantum yield of the reaction was found to be strongly dependent on the wave length of light used. A maximum value was obtained in systems exposed to 6225 Å radiation. This wave length corresponds to the location of the principal absorption band of the chlorin. Since this energy radiation produced the maximum quantum yields for the conversion of the chlorin to corresponding porphin, all studies made on the system were made at this wave length.

In addition to the experiments using 1,2-naphthoquinone as the oxidizing agent, other quinones were used in a further study of the photo-oxidation process. Both ortho- and para-quinones were used in these experiments. The results of this study indicated that the ortho-quinones were consistently better oxidizing agents than the corresponding para-quinones with identical oxidation potentials. A correlation between

the quantum yield for the reaction and the oxidation potential of the quinones was observed. A separate correlation was observed for the ortho-quinones and for the para-quinones.

When the paramagnetic copper tetraphenylchlorin was used as the reducing agent, the oxidation process was observed to become considerably less efficient than with the zinc chlorin. Oxygen was found to enhance the rate of the photo-oxidation of the zinc chlorin by para-quinones, but it inhibited the rate of oxidation by ortho-quinones (3).

A mechanism was offered in order to explain the above results. It was proposed that a triplet state of the chlorin was produced after the absorption of light. The energy of this triplet state was estimated from the phosphorescence measurements to be about 12500 cm^{-1}. This reactive triplet was then able to transfer protons to a quinone molecule on contact. The reactive excited state was required to be a triplet, since the times necessary for collisions between molecules of the different species were long compared to the lifetimes of the singlet states of the chlorins.

No dependence on the quinone concentration was found. This was accounted for by the fact that the triplet chlorin concentration was very small when compared to the concentration of the quinone. In general, the quinone concentrations were from ten to fifty times greater than the concentrations of the chlorin in the reaction systems.

The enhanced quantum yields for oxidation in solutions containing ortho-quinones over those containing para-quinones were suggested to result from the ortho-compounds being sterically favorable for the simultaneous removal of two hydrogens from the chlorin during a single encounter. The para-quinones present a less favorable steric situation and are probably unable to reorient during the lifetime of the activated complex to abstract both hydrogens simultaneously. Therefore, several collisions may be necessary before the reaction can take place.

The photo-reduction of zinc tetraphenylporphin to the corresponding chlorin has also been studied (4). The reducing agent that was used here was benzoin. It was found that the reaction would not go unless 3650 Å light was used during the irradiation. This energy radiation alone was sufficient to bring about the reduction of the porphin. However, if in addition to the 3650 Å light, equally intense radiation of a wave length suitable for absorption by the porphin was used, the quantum yield for the formation of the chlorin was enhanced significantly.

It was reported that the initial rate of the reaction was apparently proportional to the intensity of the 3650 Å radiation when only light of this wave length was used. However, when light of wave lengths where both the benzoin and quinone absorbed was used, the initial rate varied as a function of both light intensities.

The authors proposed that the reaction followed two parallel mechanisms. In the first, the rate was expected to be proportional to

the intensity of the light absorbed by the benzoin. In the second mechanism, the rate was expected to vary as the product of the light intensities absorbed by each separate compound. The light intensities and the concentrations of reactants in the solutions studied were such that long-lived triplet states of the reacting molecules must be involved. The proposed mechanism assumed that every collision between a triplet state benzoin and an unexcited porphin was not able to form an activated transition-state complex capable of decomposing into product. However, every collision between a benzoin and a chlorin which were both in an excited state was able to continue to the formation of product.

It is felt that the mechanism proposed for the photo-oxidation by Calvin and Dorough (1) is correct under the reaction conditions used. The mechanism for the photo-reduction of the porphins (4), however, is felt to be only partially correct. A modification of the earlier mechanisms will be given here. This new mechanism is applicable to both oxidation and reduction processes.

The mechanism may be written as:

$$D \xrightarrow{dI_D} D^* \qquad (1)$$

$$A \xrightarrow{aI_A} A^* \qquad (2)$$

$$D^* + A \xrightarrow{k_t} D + A^* \qquad (3)$$

$$A^* + D \xrightarrow{k_2} \text{Product} \qquad (4)$$

$$A^* + D^* \xrightarrow{k_1} \text{Product} \quad (5)$$

$$D^* \xrightarrow{k_d} D + E \quad (6)$$

$$A^* \xrightarrow{k_{d'}} A + E \quad (7)$$

In the above sequence of reactions, D represents the compound which has the highest triplet state energy. In the system described, D would therefore represent either the quinones or the benzoin. A represents the compound with the lowest triplet state energy in the reaction system, I_D and I_A are the intensities of light absorbed by both D and A. The efficiency factors d and a represent the fraction of singlet states formed upon the absorption of light which are converted to reactive triplets.

The destruction of A by the proposed reaction mechanism may occur by either of two possible steps. The first, described by reaction 4, involves the formation of a triplet transition state complex during the hydrogen migration process. If both hydrogens migrate within the same transition-state complex, then electron spin must be conserved in the overall reaction process. One of the products formed by this reaction must be a triplet as well as the intermediate complex.

The second process by which A may be destroyed, as shown by reaction 5, involves the reaction between two triplet-state molecules. This step is common to both the mechanism proposed here and that given by the above authors (4), and is the most interesting. The spins

of the two interacting excited-state molecules may add to give a transition-state complex with a spin of 2, 1, or 0. Preference is expected to be shown to the formation of the complex with the lowest spin, since this corresponds to the lowest electronic state of the transition-state complex.

If both hydrogen atoms simultaneously migrate within the same transition state, two triplets should be able to combine to form the transition-state complex with the lowest electronic energy. The combination of a triplet-state molecule with a singlet-state molecule requires the formation of a triplet transition-state complex. This triplet is an excited state of the lowest singlet-state complex that may be formed directly from the interaction of two triplets. This results in the possibility that the energy barrier offered to the overall hydrogen migration process is lower in the case of two triplets than in the case of a singlet and a triplet. Furthermore, a greater amount of activation energy may be obtained in the triplet-triplet reaction, because all of the excitation energy may be converted to thermal energy of activation. Both formation and decomposition of the singlet transition-state complex should be more rapid than the triplet-state complex.

A kinetic rate expression for the sequence of reactions described by equations 1-7 may be written as

$$\text{rate} = \frac{aI_A(k_t[A] + k_d) + k_t[A]dI_D}{(k_t[A] + k_d)(k_2(D) + k_d')} \left[\frac{k_1 dI_D}{k_t[A] + k_d} + k_2[D]\right] \quad (8)$$

Under the condition that

$$\frac{k_1 dI_D}{k_t[A] + k_d} << k_2[D]$$

and further assuming that $k_t[A] >> k_d$

$$\text{rate} = \frac{k_2[D](aI_A + dI_D)}{k_2[D] + k_d'} \quad (9)$$

These are the conditions under which the photo-oxidations of the zinc tetraphenylchlorin by quinones were considered. The effective intensity of light absorbed by the quinones was negligible. As seen by equation 9, the rate should be proportional to the intensity of absorbed radiation.

Since the quinones are good oxidizing agents, the activation energy gained from the triplet state of the chlorin was sufficient to account for the photo-catalytic effect of the light on the reaction.

It is expected, however, that the ground states of the quinones (in particular, the ortho-quinones) contain considerable triplet character. The triplet transition-state complexes in this case may first decay to lower singlets and finally decompose directly into singlet-state product. This is in agreement with the oxygen result.

It was found that the oxidation of the chlorin by oxygen correlated well with the oxidation results of the ortho-quinones. Oxygen, being paramagnetic, is expected to react by the lower singlet transition-state path.

Under the conditions used for the investigation of the photoreduction of zinc tetraphenylporphin,

$$\frac{k_1 \, dI_D}{k_t[a] + k_d} \gg k_2[D] \text{ and } k_2[D] \ll k_d'$$

This condition is implied, since light absorbed by the benzoin is necessary for the reaction to occur. The rate of the reaction between $\underline{A}^*$ and $\underline{D}$ to give product is apparently negligible. This may result because the triplet transition-state energy barrier is too great to be transversed with any small amount of activation energy gained from $\underline{A}^*$ during the conversion from the porphin triplet to the chlorin triplet.

The rate expression may be written as

$$\text{rate} = \frac{k_1 \, ad I_A I_D}{k_d'(k_t[A] + k_d)} + \frac{k_1 d^2 I_D{}^2 k_t[A]}{k_d'(k_t[A] + k_d)^2} \qquad (10)$$

Under the simplifying condition that $k_t[A] \gg k_d$, then

$$\text{rate} = \frac{dI_D \, k_1(aI_A + dI_D)}{k_d' k_t[A]} \qquad (11)$$

The available experimental data agree with equation 11, but more data are needed to verify the mechanism.

The mechanism from which equation 11 is obtained differs from that proposed by Calvin (4) in that all encounters between $\underline{D}^*$ and $\underline{A}$ result not in hydrogen migration, but in the transfer of energy to $\underline{A}$. Only collisions between $\underline{D}^*$ and $\underline{A}^*$ can lead to product. Energy transfer from benzoin to the porphin is expected to be very efficient, since more than one triplet state of the porphin with energy less than that of benzoin is expected. Exothermic triplet energy transfer should be diffusion-controlled and considerably more efficient than the abstraction or migration of two hydrogen atoms during an encounter.

The significance of this proposition is not primarily to give a new mechanism for the photo-oxidation and reduction of chlorins and porphins, but to point out the possibilities of a general study of triplet-triplet reactions. These reactions mentioned above are two important examples where kinetic evidence supports such a mechanism. Photo-induced oxidations of certain organic compounds by oxygen are another example. It is felt that a triplet-triplet reaction effect may be observed in any photochemical process where molecules with even numbers of electrons, rather than transient radicals, are produced directly from a single transition-state complex.

It is proposed that continued studies be made on chlorins using additional oxidizing agents such as benzil and other mono- and diketones. The effect of light absorbed by both compounds on the rate of oxidation should be studied.

The reduction of porphins by additional hydrogen donors with varying triplet-state energies may be investigated.

It is finally proposed that the study of the photo-induced oxidation and reduction of other organic compounds than the ones mentioned should be tried. An example might be the reduction of hydrobenzoins by benzils and other diketones. These systems are somewhat similar to the chlorin-quinone system. The products of the reaction here would be benzoins. Proper reaction conditions would have to be selected for each system.

REFERENCES

1. M. Calvin and D. D. Dorough, J. Am. Chem. Soc., 70, 699 (1948).

2. F. M. Huennekens and M. Calvin, J. Am. Chem. Soc., 71, 4024 (1949).

3. F. M. Huennekens and M. Calvin, J. Am. Chem. Soc., 71, 4031 (1949).

4. G. R. Seely and M. Calvin, J. Chem. Phys., 23, 1068 (1955).

PROPOSITION 4

A study of the ultraviolet absorption and emission spectroscopy and photochemical reactivity of aromatic vinyl ethers and esters is proposed. The investigation is designed to demonstrate the magnitude and nature of coupling between the electronic systems of the vinyl and aromatic parts of the molecules through the intermediate oxygen linkage. This interaction is expected to be dependent on the relative orientation of the two parts of the molecules with respect to each other. By the proper selection of compounds, the effect resulting from this interaction may be demonstrated.

The compounds that will be considered in this discussion and proposed research plan are

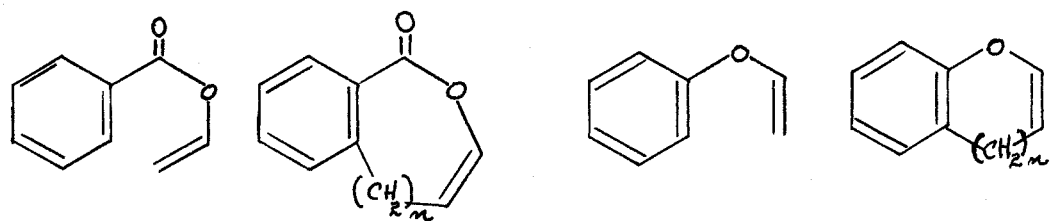

(A) (B) (C) (D)

where n = 1, 2, 3, . . .

If the atoms in the respective molecules contributing p-orbitals to the π-orbital system on either side of the oxygen are considered planar among themselves, it is seen that these systems may be oriented with respect to one another by any angle from 0° to 90° through the oxygen center. The p-orbitals on the oxygen are expected

to interact with both separate π-orbital systems. When the atoms composing the entire molecular π-orbital system lie in the same plane, then the two orbital systems are expected to be mixed most strongly with each other through the oxygen. On the other hand, when these systems are twisted a total amount of 90°, the interactions between π-systems are expected to reach a minimum since the orbital planes of symmetry are perpendicular to each other.

The ground state energies of these two limiting configurations are expected to be somewhat different, in that resonance stabilization through both π-orbital systems is expected in the planar molecule, and not in the perpendicular molecule. The lowest triplet state configuration, however, may belong to the perpendicular system. This may be expected to result since the lowest energy excited-electronic state in the perpendicular compound is formed from the promotion of a vinyloxy π-electron into the π-electronic system of the aromatic part of the molecule. Electron repulsion between electrons with parallel spins may be minimized when the molecule is in this configuration. Opposing this is the loss of possible resonance stabilization energy in twisting the molecule.

Simple molecular orbital calculations have been made on a compound which is similar to those described in this proposition. The calculations were made using a simple Hückel (1) approximation on isopropenyl acetate. Both planar and perpendicular forms of the molecule were considered.

At the time when calculations were made on isopropenyl acetate, no computer facilities were available; therefore, the calculations were made by hand. As a result, only the simplest compound similar to the type described for the study here, isopropenyl acetate, was considered. This compound is aliphatic, while those to be considered are aromatic. However, it seems reasonable that the results obtained using this compound may be intuitively extended to the more complex systems. The first project in any research program of the type proposed should include among the preliminary experiments more complete molecular orbital calculations on the electronic systems of the molecules described, using the most recent techniques for making the calculations.

The results of the calculations are shown in Figure 1. The coulomb integrals (α) which were used for each atom in the molecule are given in the figure. Resonance integrals used were β for the carbon-carbon bond and carbon-oxygen "single" bond, $\sqrt{2}\beta$ for carbon-oxygen double bond (2,3).

The results from the calculations indicate that the energy of both ground and excited states of the perpendicular compound are somewhat higher than the corresponding states of the planar compound, 0.336β and 0.182β, respectively. On the basis of these calculated results, which are admittedly very rough, the rotation of the two π-orbital systems with respect to each other around the oxygen-carbon

Figure 1. Results of M. O. Calculations on Isopropenyl Acetate

The carbon free valences ↑
and pertinent bond orders are given

Coulomb Integrals

Atom	α
1(c)	α
2(c)	$\alpha + 0.2\beta$
3(o)	$\alpha + 2\beta$
4(c)	$\alpha + 0.4\beta$
5(o)	$\alpha + 2\beta$

Planar Molecule

Ground State $E_\pi = 8\alpha + 16.746\beta$

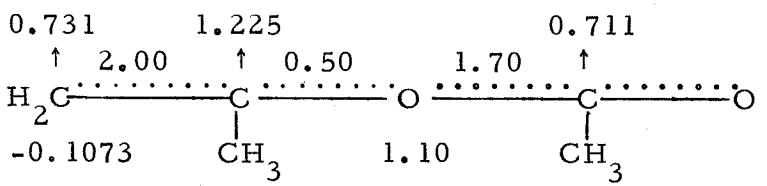

First Excited State $E_\pi = 8\alpha + 15.307\beta$

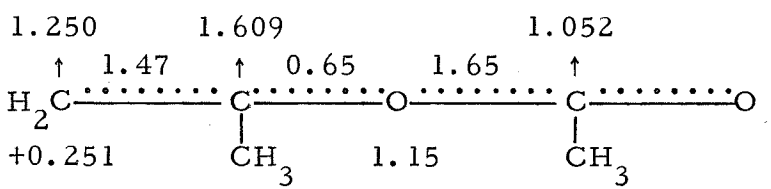

$\Delta E_\pi = 1.439\beta$

Perpendicular Molecule

$E_\pi = 8\alpha + 16.410$

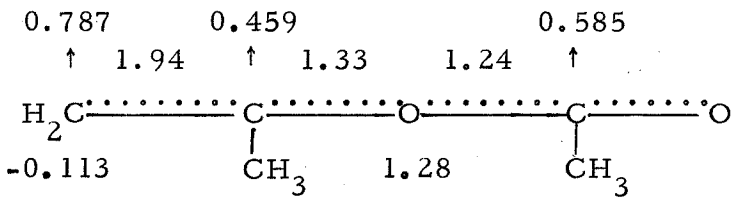

$E_\pi = 8\alpha + 15.125$

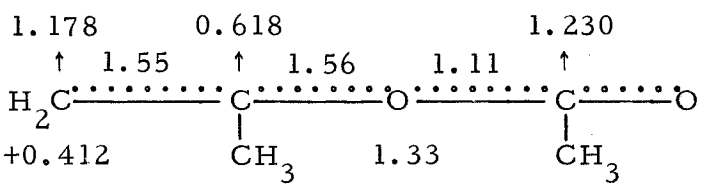

$\Delta E_\pi = 1.285\beta$

bonds is expected to be hindered significantly in both the ground and excited states, due to the significant energy change accompanying the conversion of the system from a planar to perpendicular configuration.

Through the use of a series of compounds of types B and D, the significance of the bonding between the two π-orbital systems may be studied by locking specific angles or angular limits between the two π-orbital systems through the selection of a proper number of methylene groups.

A red shift in the lowest energy absorption band is predicted to accompany the distortion of the molecule from the planar to the perpendicular configuration. In addition, the absorption maximum of the lowest energy transitions is expected to decrease during this shift, reaching a minimum value when the angle between π-systems is 90°. The transition is symmetry-forbidden under these conditions and is similar to an n-π* transition in ketones and aldehydes.

From the above calculations, it is seen that there is expected to be a significant increase in the free valence on the vinyl carbon atoms upon formation of the first excited state for both planar and perpendicular configurations. However, the positive charge density on the number 1 carbon atom (as numbered in Figure 1) is considerably greater in the perpendicular system than in the planar system. Therefore, it is felt that molecules locked in a perpendicular configuration should demonstrate a greater electron affinity in their excited state due to the larger

positive hole on the 1 carbon than on the planar molecule. The effects are expected to be greater in the aromatic systems than in the aliphatic system which is described.

The effect described may be demonstrated by studying the photo-reduction of the vinyloxy compounds with a good hydrogen donor such as tributyltin hydride. The study should consider the reaction rate as a function of the degree of distortion from the planar configuration introduced by the introduction of methylene groups in the compounds of type B and D. The planar system may not be expected to be as efficient a photo-oxidizing agent as the perpendicular molecules, and therefore, the rate of hydrogenation should be expected to increase as the system is distorted from planarity.

The effects described here, as predicted from the calculation on the simple molecule are expected to be better demonstrated in the larger aromatic systems, since here it is felt that the lowest energy, most stable excited-state will be formed from the promotion of a vinyloxy π-electron into the aromatic π-system in the perpendicular configuration. More complete M. O. calculations will be needed to support these predictions and experimental evidence to verify it.

References

1. E. Hückel, Z. Physik, 70, 204 (1931); 76, 628 (1932).

2. R. D. Brown, Quart. Revs., 6, 63 (1952).

3. G. W. Wheland and L. C. Pauling, J. Am. Chem. Soc., 57, 2086 (1935).

PROPOSITION 5

One of the largest problems encountered when making molecular orbital calculations on complex molecules is to properly account for electron correlation within the molecular orbital systems. The problem becomes especially difficult when considering molecules containing hetero-atoms. A very large amount of work has been done in order to improve molecular orbital calculation techniques for obtaining accurate descriptions of ground-state and excited-state energies and configurations for complex molecules. In most cases the complexity of the solution outweighs its usefulness; and unless the experimentalist has a big enough computer and proper programs available, it is useless to consider a problem in detail.

A procedure for making simple molecular orbital calculations on complex systems has been developed and used in this thesis for calculations made on transition metal chelates. This technique was developed in such a manner that some electron correlation in the systems could be accounted for. The method involved the evaluation of nuclear shielding parameters for each atomic center in the molecule. The shielding parameters consisted of two components. The first was concerned with shielding from inner σ- and non-bonding electrons, and the second was shielding from π-electrons. With these terms evaluated,

coulomb and resonance integrals which were functions of the electron charge distribution within the molecules could be determined. Since electron charge distributions are obtained from the solution of the secular matrix equation for the problem, new shielding parameters could be evaluated,and thus the entire process was reiterable until self-consistent.

One shortcoming of the technique described was that there was no distinguishability between electronic states of different spin multiplicity. It is proposed here that a correction to the calculation procedure may be effected by considering the π-electron shielding parameters on each atomic center as composed of two quantities: the first corresponding to electrons with spin parallel to the electron being considered, and the second corresponding to electrons with opposed spins. Each of these terms is expected to contribute a different amount to the general shielding constant for the effective nuclear charge.

Using the general "rule of thumb" that electrons with parallel spins cannot occupy the same spot at the same time, it seems reasonable to expect that the largest contribution to the shielding constant should result from electrons with opposite spin. Electrons with parallel spin should contribute a lesser amount to the shielding parameter.

In order to properly evaluate the shielding parameters, it must be remembered that each electron moves in the coulombic field of all other electrons in the molecule. Since the electrons are indistinguishable,

an average shielding parameter for each of them must be evaluated. The problem may be solved directly for each atomic nucleus where the contributions of electrons from each orbital are totaled, multiplied by the proper constant for opposed or parallel electrons, and then averaged to obtain the average shielding constant.

In the simple case where the electron density contributed to each nucleus by each orbital is the same, the following π-shielding constants may be obtained:

singlet $$\sigma_{\pi} = (a + b)\ \frac{n}{2} - a \qquad (1)$$

doublet $$\sigma_{\pi} = (a + b)\ \frac{n}{2} - a - \tfrac{1}{2}n(b - a) \qquad (2)$$

triplet $$\sigma_{\pi} = (a + b)\ \frac{n}{2} - a - \frac{2}{n}(b - a) \qquad (3)$$

quartet $$\sigma_{\pi} = (a + b)\ \frac{n}{2} - a - \frac{9}{2n}(b - a) \qquad (4)$$

In 1, 2, 3, and 4, a is the constant for electrons with parallel spin, b is the constant for electrons with opposed spin, and n is the total number of electrons in the π-orbital system.

The evaluation of the constants a and b may be undertaken in three different ways. The first is from the consideration of atomic spectra reported in standard spectroscopy tables. Transition energies may be evaluated in terms of the shielding parameters a and b. Then, an average value for each of these terms may be evaluated from the consideration of transitions within the same atom and in similar atoms.

A second method would be to solve simple molecular problems in terms of these constants, and then with available spectroscopic information, evaluate the constants a and b. Finally, the method of successive approximations may be tried in order to obtain the best set of constants to give the observed spectra of a set of compounds.